BAGHOUSE FINES IN ASPHALT MIXES

by

Douglas I. Hanson
L. Allen Cooley, Jr.

for

South Carolina Department of Transportation

November 1997

NATIONAL CENTER FOR ASPHALT TECHNOLOGY
211 Ramsay Hall
AUBURN UNIVERSITY, AL 36849-5354

Technical Report Documentation Page

1. Report No.	2. Government Accession No.	3. Recipient's Catalog No.
FHWA-SC-97-01		

4. Title and Subtitle	5. Report Date
BAGHOUSE FINES IN ASPHALT MIXES	November 1997
	6. Performing Organization Code
7. Author(s)	8. Performing Organization Report No.
D.I. Hanson and L. A. Cooley, Jr.	
9. Performing Organization Name and Address	10. Work Unit No. (TRAIS)
National Center for Asphalt Technology 211 Ramsay Hall Auburn University, AL 36849	11. Contract or Grant No.
12. Sponsoring Agency Name and Address	13. Type of Report and Period Covered
Research and Materials Division South Carolina DOT Box 191 Columbia, SC 29202	Final Report July 1994 to November 1997
	14. Sponsoring Agency Code

15. Supplementary Notes

Prepared in cooperation with the U.S. Department of Transportation, Federal Highway Administration

16. Abstract

This research study was accomplished to establish criteria for the reintroduction of baghouse fines into HMA mixtures.

Baghouse fines were obtained from a total of 18 HMA plants in South Carolina. These samples were subjected to a particle size analysis using a Coulter LS200 particle size analyzer and then tested using the modified Rigden's void test. Based on the results of this testing, ten plants were chosen to have samples combined to form ten combined baghouse fine samples. These ten combined samples were then added to asphalt binders and subjected to various mortar tests. Five of these combined baghouse fine samples were then selected to be added to asphalt binders and aggregate and subjected to various HMA tests.

Findings of this research indicate that a property derived from the modified Rigden's void test (percent bulk volume of a compacted dust) can be used to indicate the contribution of a mortar to a HMA's resistance to permanent deformation, fatigue cracking, and low temperature cracking. Based on the research, a critical value of 55 percent was found.

17. Key Words	18. Distribution Statement
Flexible pavements, asphalt cement, aggregates, baghouse fines, hot mix asphalt	Document is available to the U.S. public through the National Technical Information Service, Springfield, VA 22161.

19. Security Classif. (of this report)	20. Security Classif. (of this page)	21. No. of Pages	22. Price
Unclassified	Unclassified		

Form DOT F 1700.7 (8-72)

Reproduction of completed page authorized

TABLE OF CONTENTS

LIST OF TABLES

LIST OF FIGURES

CHAPTER 1: INTRODUCTION

1.1 PROBLEM STATEMENT

Dust collection systems on hot mix asphalt (HMA) facilities originated from a need to protect equipment from dust particles created during HMA production. However, once the Environmental Protection Agency set forth stringent emission standards on HMA facilities, dust collection systems became mandatory. Baghouses emerged as a popular form of dust collection system because they efficiently captured the dust particles created during HMA production. Dust particles captured by baghouses (baghouse fines) are reusable and are typically reintroduced back into the HMA production process.

The South Carolina Department of Transportation (SCDOT) is concerned about this reintroduction of baghouse fines because of the uncertainty that exists about the effects baghouse fines have on HMA mixtures. Baghouse fines are dependant on the source of parent aggregate. Research has shown that some baghouse fines stiffen asphalt binders, possibly leading to HMA pavements that are susceptible to thermal cracking problems. Baghouse fines that are smaller than the asphalt film coating aggregates within HMA can extend the volume of the asphalt binder. Because of this extending, HMA mixtures that contain baghouse fines can be susceptible to small

variations in asphalt binder content. Research has also shown that baghouse fines can affect the compactibility and moisture sensitivity of HMA mixtures. Therefore, a study was needed to evaluate how baghouse fines produced at South Carolina HMA producing facilities affect HMA mixtures.

1.2 OBJECTIVE OF STUDY

The research described in this report was conducted to establish criteria for the reintroduction of baghouse fines into HMA mixtures in South Carolina. This was accomplished by evaluating the variability in baghouse fines' physical properties, evaluating the effects of baghouse fines on baghouse fines/asphalt binder mortars, and evaluating the effects of baghouse fines on HMA mixtures.

1.3 SCOPE OF STUDY

This project involved obtaining samples of baghouse fines from HMA facilities in South Carolina. These baghouse fines were then tested to determine physical properties. Next, baghouse fines from ten HMA facilities were combined to produce ten combined samples for a detailed laboratory study of baghouse fine/asphalt binder mortars. Five of the ten combined baghouse fine samples were then selected to combine with the two asphalt binders and one aggregate for the evaluation of baghouse fines within HMA mixtures.

1.4 FORMAT OF REPORT

This report consists of chapters describing the research project, test results, data analysis, conclusions, and recommendations. Chapter 2 of this report provides a

literature review based on previous research performed on baghouse fines and the results of a survey conducted for the project. Chapter 3 presents the plan of study followed to accomplish the objectives of the study. This chapter also includes discussion of the different test methods utilized. Chapter 4 discusses the different materials and tests utilized during the study. Chapter 5 presents the results of laboratory testing and Chapter 6 discusses the analyses performed on these results. Chapter 7 describes the conclusions and recommendations developed from the analyses performed on the laboratory results.

CHAPTER 2: BACKGROUND

2.1 LITERATURE REVIEW

2.1.1 Dust Collection Systems

During the 1960's when there became a desire for higher HMA production rates, HMA facilities began installing exhaust fans in the place of steam ejector jets. This new technology brought about a new problem in that dust was being sucked out of the drum and was damaging the fan blades of the exhaust fan. Not only were the fan blades being damaged, but the plants were losing useful and expensive fine materials. The remedy was to install dust collection systems.

In 1970 Congress passed the Clean Air Act, from which the Environmental Protection Agency (EPA) was formed. In 1973, the EPA issued strict regulations to control the particulate emissions produced by the exhaust systems of HMA plants. Because of these strict regulations, all HMA facilities were required to have a dust collection system.

Several types of dust collectors are used in the United States: cyclones, knockout boxes, baghouses, and wet scrubbers are a few. Dust collection systems can be either one or two or more dust collectors used in conjunction with each other. Studies have shown that the most efficient way to capture the dust particles is with the use of primary

and secondary collectors. The larger sized particles are captured in the primary collector and the smaller sized particles are then collected in secondary collectors.

2.1.1.1 Primary Collectors

Two general types of primary collectors are used in HMA facilities: the knockout box and the cyclone (1). Knockout boxes (Figure 2.1) are expansion chambers where the cross-sectional area increases, thereby reducing the velocity of the exhaust gases. With the reduced velocity, the larger particles fall out of the air stream and accumulate at the bottom of the collector. Knockout boxes can be used to remove particles larger than about 40 microns (40μm) (2).

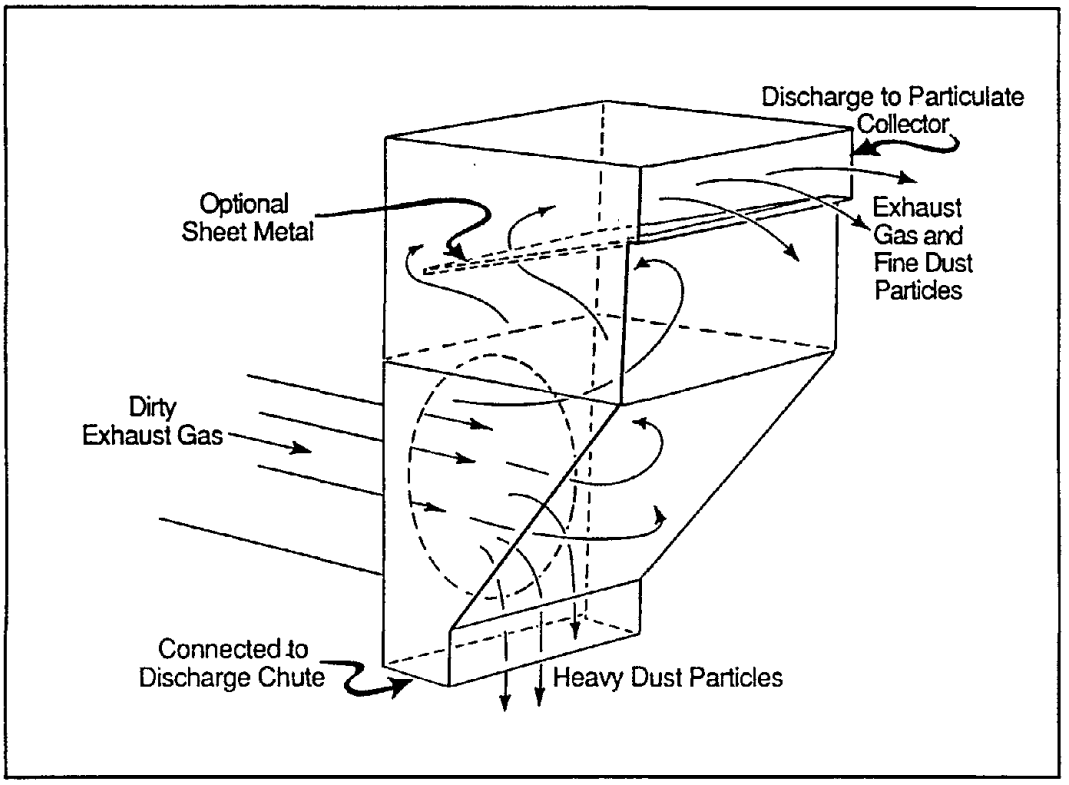

Figure 2.1: Knockout Box (2)

Cyclone collectors (Figure 2.2) act on three basic rules of physics: 1) anything in motion will continue to move at the same speed and in a straight line unless forced to change; 2) the heavier the object and/or the more drastic the change in motion, the greater the force required to keep the particle airborne; and 3) anything that is moving around a circular path of a given diameter and is forced to move around a smaller circular path will speed up in proportion to the size of the circular path (2). Once the gas stream enters the cyclone the gases continue turning as they are forced downward. Being heavier than the exhaust gases, the dust particles move to the outside wall of the collector and settle downward. The exhaust gas is then pulled up through the top of the cyclone by the exhaust fan and the dust particles pass through the bottom. The heavier the particle, the easier it is to remove from the exhaust gas. Individual cyclones can be used or they may be used in multicone configurations. Single cyclone collectors can be used to remove dust particles down to 30 μm (2).

2.1.1.2 Secondary Collectors

Typically two different types of secondary dust collectors are used in the United States today: baghouses and wet collectors. Both types of collectors are very efficient at collecting particles sizes down to 10 μm (2). Wet collectors are generally used as secondary collectors, but can also be used as the only collector. They can typically be classified by one of two methods of dust capture: particle wetting or particle impingement (2). The latter method is not common to HMA facilities (2) and therefore will not be discussed. The particle wetting method employs four principles in capturing

the airborne dust including: impaction, interception, diffusion, and electrostatic attraction (2). The efficiency of this system depends on the ability of the wet scrubber to generate droplets fine enough to capture the fine particles, and the ability of the scrubber to remove the droplets from the gas stream. These types of wet collectors are generally efficient at capturing particles to a size of 5μm (2).

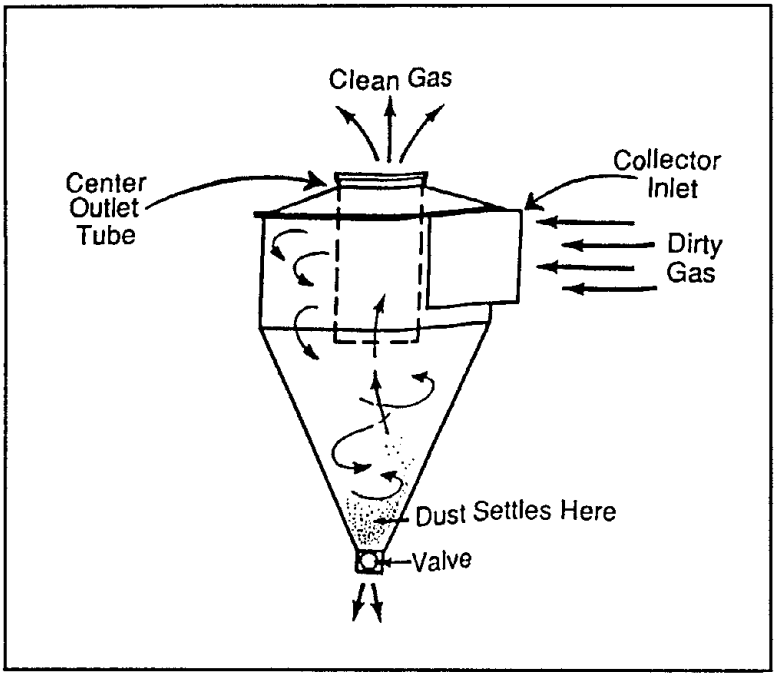

Figure 2.2: Cyclone Dust Collector (2)

The idea for baghouse dust collection systems is simple. Dust laden exhaust gases enter the baghouse from the drying unit or primary collector and are drawn through a series of fabric filter bags (Figure 2.3). Fibers within the filter bags capture the dust particles on the outside, or "dirty side", of the bag and allow the clean air to pass through the inside, or "clean side". As the dust particles build up on the dirty side of the filter bag, they form dust cakes. The presence of these dust cakes is essential to

the proper functioning of the baghouse (2). As the dust cakes build up on the filter bag, the filtering efficiency of the filter bag increases as finer and finer dust particles can be trapped. Eventually though, the dust cakes will have trapped so many fine dust particles that the flow of air across the filter bag is almost completely stopped. Therefore, the filter bags must be cleaned. The maximum thickness of the dust cake is determined by the frequency of cleaning the filter bag goes through. If the cake is not allowed to build up enough, fine dust particles can pass through the filter bag and leave with the gases through the stack.

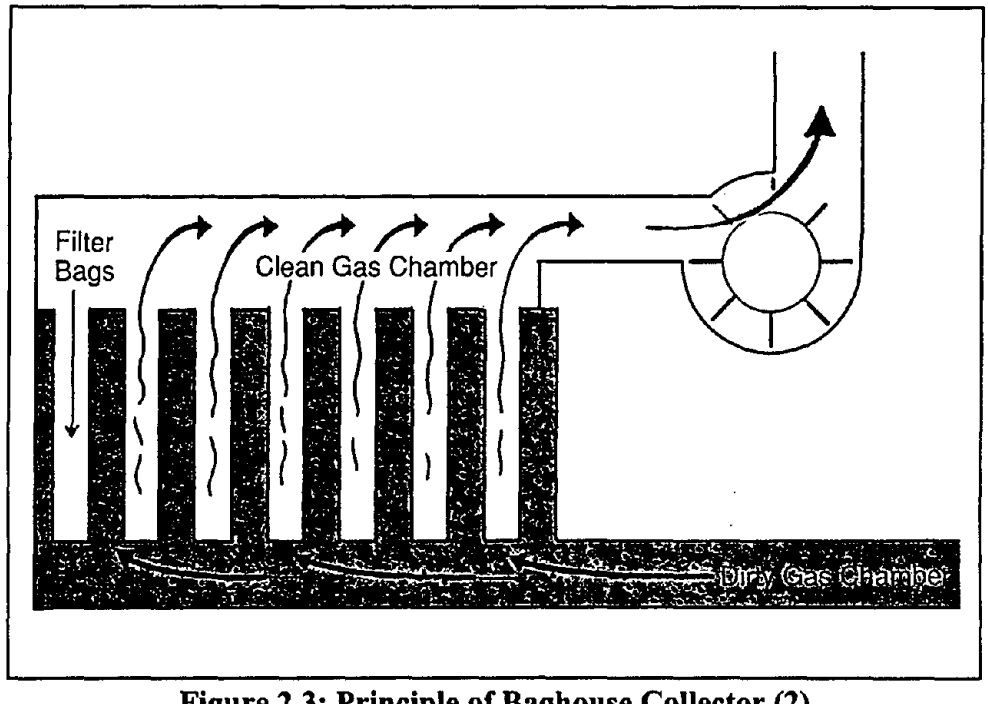

Figure 2.3: Principle of Baghouse Collector (2)

The frequency of the cleaning cycle will vary depending on the amount and shape of the dust particles entering the baghouse. Typically, the filter bags are cleaned in groups (called compartments). The cleaning method can be either by reverse air or by pulse jet. Reverse air consists of sending a jet of air into the bag through the clean side of the filter bag, which causes the dust particles on the dirty side to fall off into the hopper at the bottom of the baghouse. For the pulse jet method, a shockwave is sent through the bag causing the dust particles to fall into the hopper at the bottom of the baghouse.

In a reverse air cleaning baghouse, the cleaning cycle generally takes a few seconds, during which time the filter bags are not collecting dust. This is called "off-stream." In a pulse jet baghouse, a shockwave of very short duration does the cleaning, hence there is very little off-stream time. The net result of these cleaning cycles is that one compartment of the baghouse is always off-stream. This means that at any given time the baghouse will have some filter bags that have just been cleaned, some that are being cleaned, and some that are about to be cleaned. This process allows the baghouse to maintain a constant degree of efficiency.

A large area of filter fabric is needed to adequately clean the large amount of exhaust gases entering the baghouse from the drying process. The most popular filter bag shape is a cylinder, open on one end and closed on the other. This shape of filter bag allows the largest cloth surface area in a closed compartment and is therefore the most efficient (2). Within the baghouse, the cylinder filter bags are typically

mounted or fitted over a metal cage to prevent the bags from collapsing during the filtering process.

Nearly all particles coarser than 10μm can be trapped in a well-maintained baghouse (2). The collection efficiency of a baghouse for particles between 10μm and 1μm in diameter decreases to between 75 and 99 percent (3). The efficiency depends on the particle size, size distribution, the exhaust air-to-cloth ratio, and the weave and thickness of the filter fabric.

Important keys to the effectiveness of a baghouse are the type of fabric used for the filter bag, the ratio of the volume of exhaust gases to the exposed area of the filter fabric, and the condition of the filter bags. The filter bags must be able to withstand several abusive factors: high temperatures, high humidity, and abrasive dust particles. Temperatures within a baghouse can reach 350°C, so the filter bags must be heat resistant. The exhaust gases entering the baghouse may contain more than 50 percent water vapor and therefore must not degrade. The abrasive properties of the dust particles can have a major impact on the longevity of the filter bags. Dust particles that have sharp edges or particles that are difficult to remove from the filter cloth require more frequent cleaning. Repeated flexing of the cloth during the cleaning cycle can affect the useful life of the filter fabric of the bag.

Baghouses are dry collectors, therefore offer several advantages over wet collectors. As new and stricter EPA regulations are being enforced, concerns are growing about the waste water and waste soil disposal accompanying the use of wet

collectors. An advantage the baghouse has over many wet scrubbers is its lower energy requirement. The development and improvement of the fabrics used for filter bags has made the baghouse the most popular dust collection system. Also, the requirement for higher efficiencies and the conservation of energy and space has resulted in the increased use of baghouses.

2.1.2 Handling of Baghouse Fines

HMA facilities can have either an open or closed dust collection system. In an open system, the plant wastes all or part of the collected fines. Wasted fines can be stored onsite for future use, returned to the quarry, sold, and/or sent to a settling pond. The first two options would be strictly regulated by environmental agencies. Installing a settling pond would result in the same types of difficulties and costs associated with wet collection systems.

In a closed system, all of the fines are reintroduced into the mixing process. The method of handling the fines is extremely important, because it affects the uniformity of the fines entering the mixing process and may result in a mixture that is dry, stiff, susceptible to asphalt binder fluctuations, or difficult to compact. Processes for reintroducing the dust back into the mix are quite different for batch and drum plants.

2.1.2.1 Batch Plants

In a batch plant, the baghouse fines can be returned to the HMA production process in the hot elevator, a hot bin, or the weigh box. The term "No. 1 hot bin" is generally used to indicate the hot bin in which finer particles are located. The simplest

method is to return them to the hot elevator, but the best location is probably the weigh box. Baghouse fines can be fed to the hot elevator through a duct by gravity or by a screw conveyor from the collector to the hot elevator. An alternative method would be to use a small surge bin on or near the hot elevator. The surge bin could be fed by gravity, a screw conveyor, or pneumatically. The fines are then removed from the surge bin by a rotary air lock and fed to the hot elevator by gravity or a screw conveyor (4).

Baghouse fines can be returned to the No. 1 hot bin by blowing them pneumatically into the bin. The dust would have to exit the baghouse through a rotary air lock to prevent "false air" from entering the baghouse. The fines would then be blown directly to the No. 1 hot bin (4). This method can be detrimental because dust slides can occur along the walls of the bin and cause a surge of fines into the weigh box.

Dust added back via the weigh box should be routed through a storage silo to prevent dust surges. This can be done by one of three methods. First, the dust can be added as a separate material and added to the batch ticket. Alternatively, the dust may also be weighed on a separate scale before being added to the weigh box. The final option would be to add the baghouse fines along with the material from the No. 1 hot bin. This can be accomplished by having a screw conveyor running from the storage silo to the weigh box. The conveyor would add the dust in proportion to the weight of the material in the No. 1 hot bin (4).

2.1.2.2 Drum Mix Plant

In a drum mix plant, the baghouse fines have to be added back to the cold feed conveyor or back into the drum. The best method of introduction is back into the drum. When returning the fines to the drum, a method that returns them in a controlled manner should be employed. Several methods can be utilized. They can be added back at the drum entrance, the drum discharge, or the point where the asphalt is introduced (5). The introduction of the fines where the asphalt is introduced is felt to be the best location. This is because the asphalt hinders the reentrainment of the fines into the system gas and provides a good distribution of the dust in the coating zone of the drum. If the drum plant has a coating unit, the fines can also be added at this point to ensure an adequate coating of asphalt binder onto the fines. An important point to be made is that no matter which method is used for the reintroduction of fines, the fines should be returned in a uniform manner. (6)

Several systems can be used to return the fines to any point of the mixing process. Figure 2.4 shows a simple pneumatic device that can be effective. It collects the dust at a constant rate that varies only with the production rate or changes to the job mix formula. Being pneumatic it also prevents dust slugs from forming. With this system, the cleaning of the baghouse and the rotary airlock system are interlocked with the drum rotation. When the drum stops, the fines recycling also stops (7).

Some states require the addition of a surge bin between the baghouse and the reintrainment point (Figure 2.5). With this system, dust surges due to the change in the

rate of production or changing job mix formulas can be diverted. This system uses screw conveyors to feed the fines to the surge bin. From there, the dust is metered to the drum by a rotary airlock or auger. When the hopper is full, the excess dust can be wasted to another storage container or to a truck. (7)

Another method, shown in Figure 2.6, blows the fines from the baghouse to a storage silo from which the dust can be metered into the drum. Excess dust can be held in the silo until the silo becomes full. Once the silo is full, a truck or a waste container can be used to waste the excess dust.

To increase repeatability, weighing the amounts of dust being returned to the drum may be necessary. This can be done by adding a weigh hopper to the bottom of the silo (Figure 2.7). The fines can then be weighed before they are added back to the drum. This method should be satisfactory for normal plant operations, but if closer tolerances are needed another weigh hopper may be needed (Figure 2.8). Very seldom will this method be economically feasible.

2.1.3 Variability of Baghouse Fines

Several factors can affect the quantity, properties, and size distribution of fines collected within a dust collection system. These include the type and characteristics of the parent aggregate, the type and operating characteristics of the drying unit, and the configuration of the dust collection system.

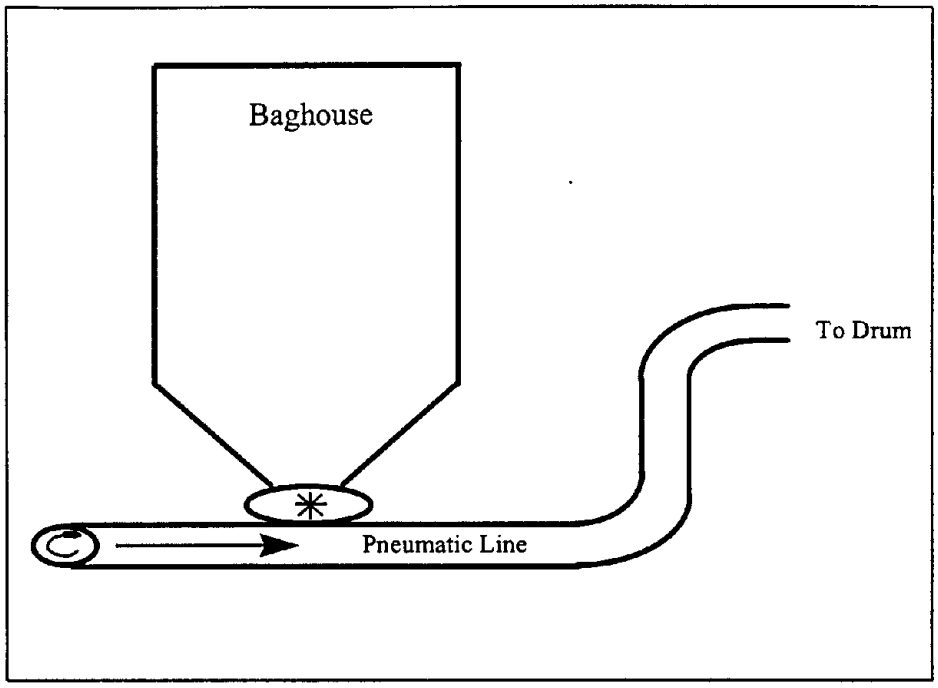

Figure 2.4: Fines Return System (7)

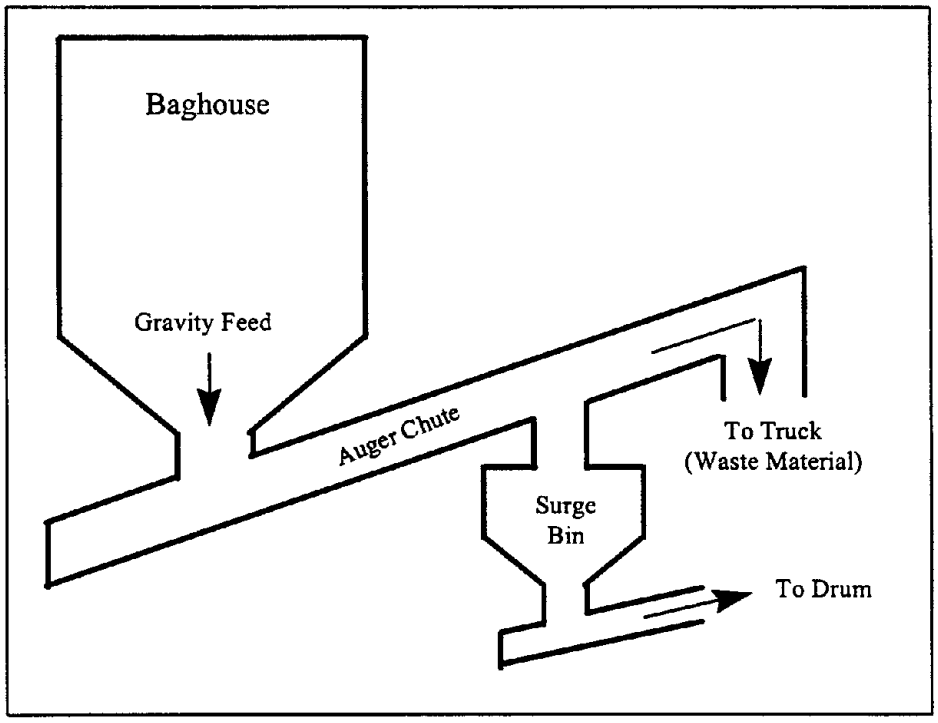

Figure 2.5: Surge Bin Between Baghouse and Reintrainment Point (7)

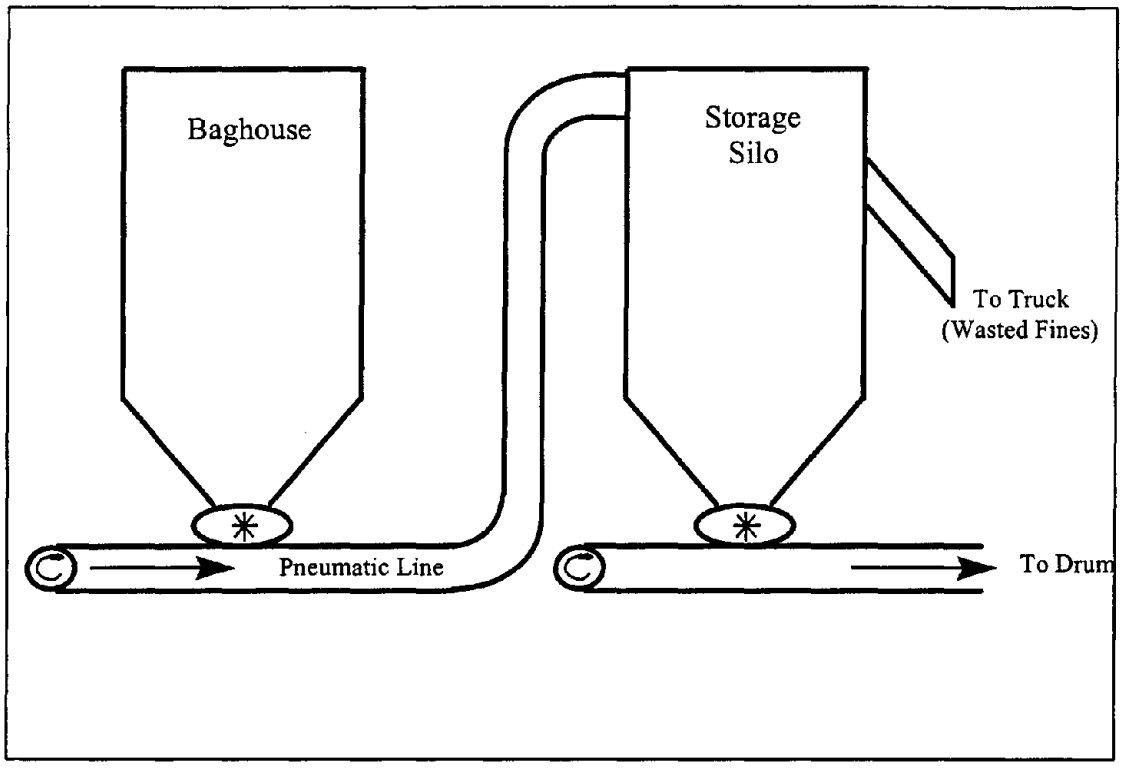

Figure 2.6: Storage Silo Between Baghouse and Reintroduction (7)

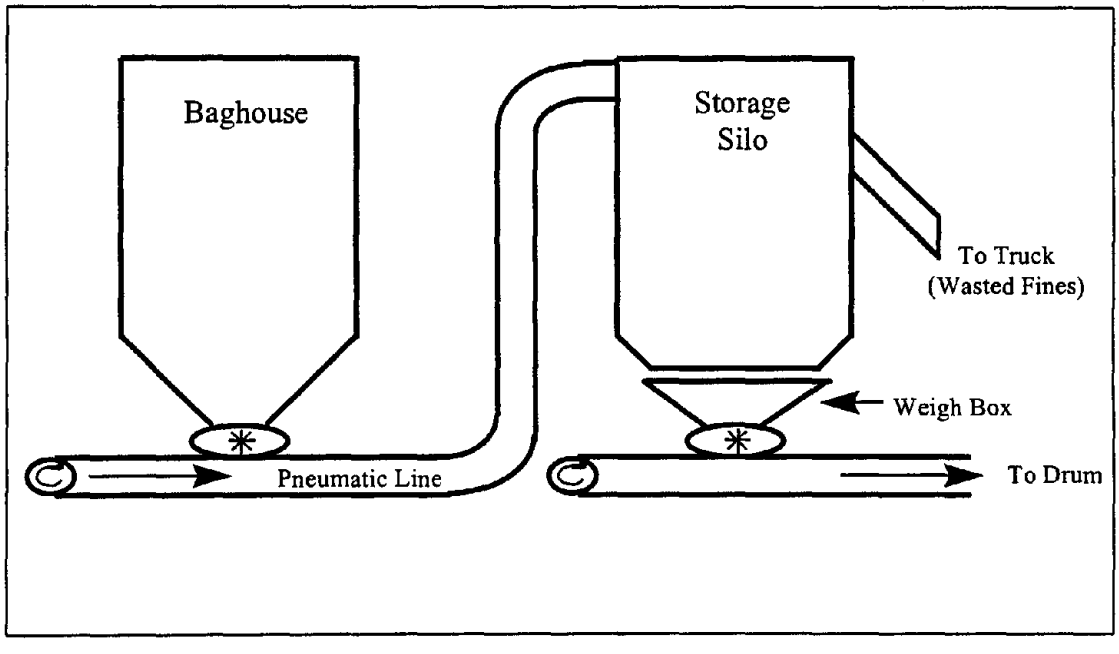

Figure 2.7: Single Weigh Hopper System (7)

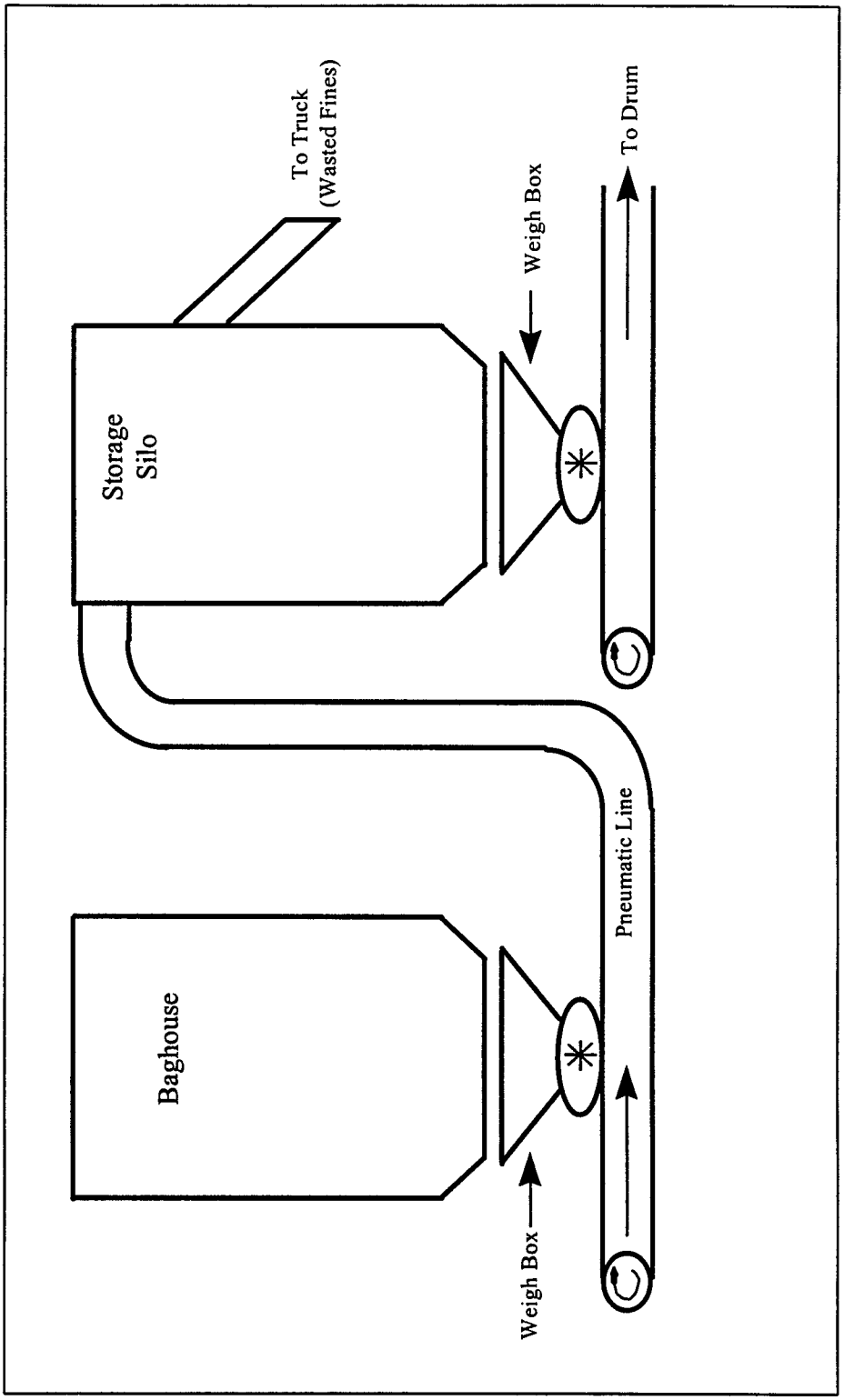

Figure 2.8: Double Weigh Hopper System (7)

Research has shown considerable variations in the fineness of baghouse fines from different aggregate sources. These variations have been attributed to the natural characteristics of the aggregate and the processing methods used by the aggregate supplier. For instance, the fineness of the dust can be directly influenced by the amount of fine particles adhered to the coarse aggregate. Degradation of the coarse aggregate within the drying process can also influence the fineness of the dust. Natural aggregates may have large amounts of clay particles coating the aggregate (e.g., gravels). This can have a large impact on the fineness of the dust. Consequently, plants with identical equipment and operating conditions but using different aggregates produce baghouse fines of different quantity, properties, and size distributions.

Brock (8) suggested that the size of particles that become airborne during the drying process varies depending on the velocity of the gases passing through the drum. Drum gas velocity is the velocity at which the gases move through the drum. It can be defined as the exhaust gas flow rate divided by the area of the drum (3). Drum gas velocities that exceed a particle's terminal velocity will cause the particle to be picked up into the airstream. Terminal velocity is defined as the velocity at which a specific dust particle becomes airborne and is dependent on the particle's size, density, and shape. The larger the particle, the higher the velocity that will be required to pick the particle up into the airstream. Batch plants typically have a drum gas velocity of 800 feet per minute (fpm) while drum plants can have drum gas velocities of 1,000

fpm or more (8). These drum gas velocities are such that all particles smaller than a 75μm (No. 200 sieve) can become airborne.

The type and configuration of dust collection systems are also important to the quantity and size-distribution of the fines captured by the baghouse. A primary collector present before the baghouse can have significant effects on the size of the particles captured by the baghouse. The more efficient the primary collector, the less variability in the characteristics of the baghouse fines.

If a HMA plant has only a baghouse as its dust collection system, the range of particle sizes can range from material as coarse as 700μm down to 1μm (8). With no primary collector to remove the larger size particles, the baghouse has to capture all of the fines generated by the drying process, and therefore the quantity and size-distribution can be affected by the type and gradation of the aggregate.

Anderson and Tarris (4) showed that there is considerable plant-to-plant variability in baghouse fines. After randomly sampling 33 plants in 12 states, they suggested that this variability is related mainly to the efficiency of the primary dust collection system and the nature of the cold feed aggregate. Also, at a single HMA plant, the greatest day-to-day and within-day variability in the fineness of the baghouse fines occurs in the coarse fraction of the dust, 50 to 75μm. They also stated that this day-to-day and within-day variability in the fineness of the baghouse fines is largely dependent on the efficiency of the primary dust collector. The more efficient the primary collector, the less variable the fineness of the baghouse fines.

2.1.4 Definition of Mineral Fillers

The primary components used to produce HMA mixtures are asphalt binder and mineral aggregate. Mineral aggregate can be subdivided into three groups: 1) coarse aggregate; 2) fine aggregate: and 3) mineral filler. When added back to the HMA production process, baghouse fines fall into the category of mineral filler and much of the research done on mineral fillers can be used to describe the effect baghouse fines have on hot mix asphalt. (9)

The exact definition or description of suitable mineral filler has not been agreed upon by researchers. ASTM D242 (10) defines mineral filler as:

> "Mineral filler shall consist of finely divided mineral matter such as rock dust, slag dust, hydrated lime, hydraulic binder, fly ash, loess, or other suitable mineral matter."

This definition is inadequate because it leaves the acceptability of the mineral filler to the discretion of the engineer without a provision for testing to determine the suitability of the filler.

Warden, Hudson, and Howell (11), describe a suitable filler as one that is non-critical in the completed mix. This means that the variations in the filler content over a normal plant operating period do not cause detrimental effects in the final pavement. They suggest that suitable fillers have the following characteristics in the completed pavement:

1) The pavement surface must be durable over a wide range of temperatures and over an extended amount of time,

2) the filler must not decrease the resistance to water or the bond of the asphalt binder to the aggregate, and

3) The filler must not decrease the durability through loss of flexibility.

In 1962, Tunnicliff (12) suggested that a mineral filler should be defined in terms of what is being filled, what does the filling, and why the filling is being done. He offers two definitions that satisfy these criterion of mineral filler: "filler is that portion of the mineral aggregate generally passing the 0.075 mm (No. 200) sieve which occupies void space between the coarser aggregate particles in order to reduce the size of these voids and increase the density and stability of the mass" and "filler is the mineral matter which is in colloidal suspension in the asphalt binder and which results in an asphalt binder with a stiffer consistency." This second definition has been the subject of many research studies and will be discussed in detail in this review.

Tunnicliff (13) followed in 1967 by saying that for mixture design practices, filler is that portion of the aggregate that will pass through a 0.075 mm sieve, which will perform satisfactorily in the presence of water, and which has been found by experience to produce successful pavements.

Based on the definition of mineral filler in ASTM D242, baghouse fines can be classified as mineral filler. However, based on the other definitions provided, baghouse fines should not decrease the resistance of a HMA pavement to moisture and must not

decrease the durability of a HMA pavement through the loss of flexibility (i.e., stiffen the mixture). In addition, HMA mixtures containing baghouse fines should be durable over a wide range of temperatures and over an extended amount of time.

2.1.5 Effect of Baghouse Fines on Mortars

The mixture of asphalt binder and mineral filler particles comprise a mortar that binds the larger particles of mineral aggregate. The stiffening effect that Tunnicliff spoke about relates to this mortar, and has been called the key to the performance of a pavement (9). Traxler (14) has shown that the stiffening effect cannot be reliably predicted from the mineral filler's physical properties alone. He considered particle size, grain-size distribution, and shape as the fundamental physical properties in that they affect the void content and average void size of the compacted filler.

Several researchers have shown that there exists a stiffening effect when fines are added to asphalt binder. In a study conducted by Warden, Hudson, and Howell (11) on several commercial fillers, they showed that as filler/asphalt binder ratios increased, the penetration values at 77° F with a 100-gram mass for 20 seconds decreased, the softening point temperature increased, and the ductility at 77° F at five centimeters per minute (cm/min) decreased for the mortar. All three of these tests show that the addition of fillers stiffens the asphalt, forming a mortar that closely resembles a higher consistency grade of asphalt binder (9).

Puzinauskas (15) again proved that changes occur with the addition of filler to asphalt binder. He also used commercial fillers (limestone dust, kaolin clay, fuller's

earth, and short-fiber asbestos). Puzinauskas showed that the physical properties of the asphalt binder (ductility, penetration, and viscosity) similarly changed with the addition of mineral filler. These changes even occurred at filler/asphalt binder ratios lower than is commonly used in paving mixtures.

In another study performed on baghouse fines by Anderson (16), it was apparent that different types of baghouse fines stiffen asphalt binders differently. Figure 2.9 shows four of the ten baghouse fines he studied at different concentrations of fines to asphalt binder (F/A ratio) plotted versus viscosity measurements at 140° F. Anderson used the same asphalt binder to fabricate each of these mortars. This figure clearly shows that each of the four fines reacts differently with the same asphalt binder.

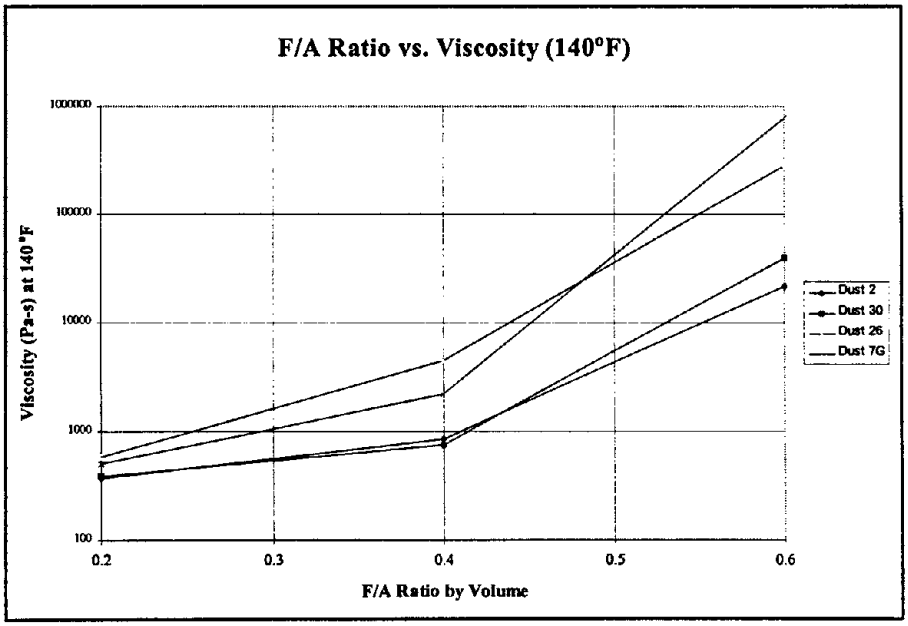

Figure 2.9: Fines to Asphalt Binder Ratio (F/A) by Volume versus Viscosity at 140°F (16)

A typical method presented in the literature for determining the stiffening effect of fines was to measure the viscosities of a neat asphalt binder and for the same asphalt binder with the fines added to it (mortar). By dividing the viscosity of the mortar by the viscosity of the neat asphalt binder, a stiffening ratio is obtained (16). This stiffening ratio can be used to correlate the stiffening effect of fines with a number of tests or particle properties. An important point to be made is that the stiffening ratio increases with an increase in dust content. Several researchers have shown that as the F/A ratio increases, the stiffening ratio also increases. Referring back to Figure 2.9, it can be seen that as the F/A ratio increases, the viscosity of the mortar also increases. Therefore, as the viscosity of the mortar increases, the stiffening ratio also increases.

Another method of measuring the stiffness of a mortar presented in the literature was with the softening point test. The purpose of this test is to determine the temperature at which a physical change occurs in the mortar. The property used to determine stiffness was actually the change in softening point temperatures which was calculated by subtracting the softening point temperature of the neat asphalt binder from the softening point temperature of the mortar. This test has been suggested as a quality control test for the stiffening effect of fines, because it has better test repeatability than the determination of a stiffening ratio (17).

Without giving statistics, it can be seen in Figure 2.10 that a relationship exists between the change in softening point temperatures and the stiffening ratio for different mortars. Each data point shown in the figure is the resulting stiffening ratio and change

in softening point temperature for a particular source of fines which was combined with the same asphalt binder (17). It should be noted that testing performed on mortars with a F/A ratio of 0.3 by volume and the viscosity tests were performed at 135°C (275° F).

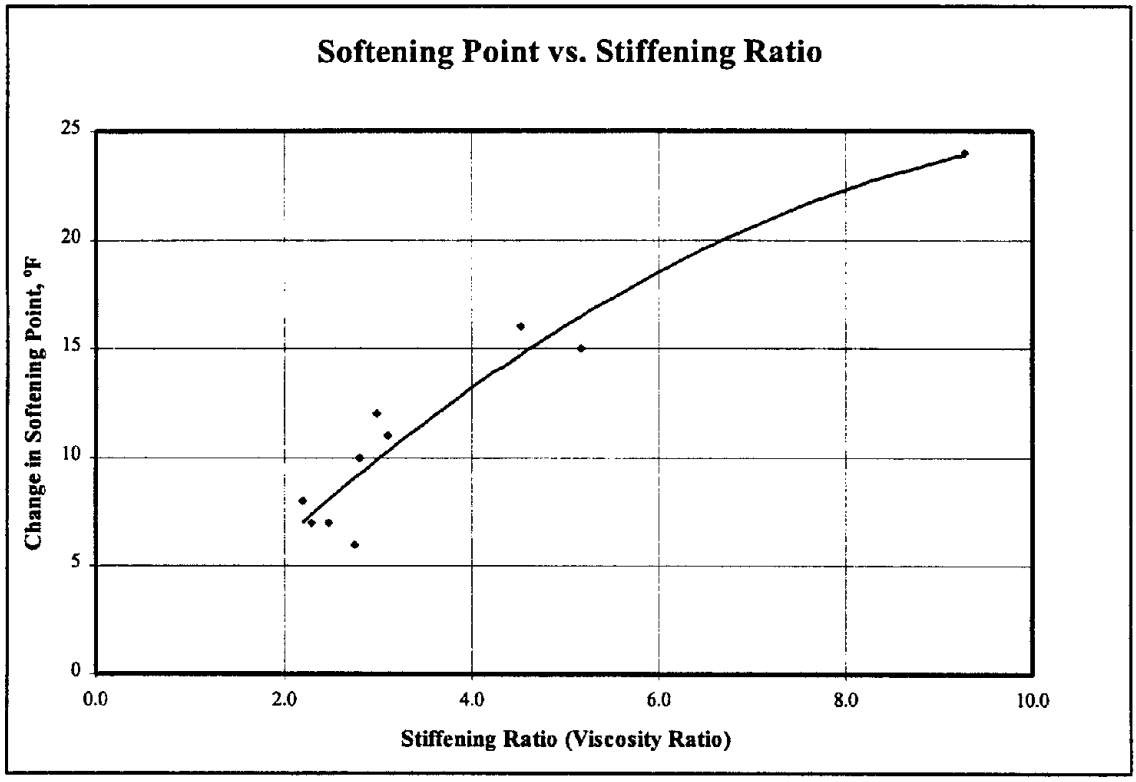

Figure 2.10: Change in Softening Point Temperature versus Stiffening Ratio (17)

Since it has been determined that different fines stiffen asphalt binders differently, a question that must now be asked is "Does a particular fine have the same stiffening effect on different asphalt binders?" Huscheck and Angst performed a study (18) using four different asphalt binders and four different fines. The fines included

limestone, siliceous limestone, Schist flour, and Bauxit residue. It can be seen from Figure 2.11 that the stiffening effects of these fines are asphalt specific. For this plot, three asphalt binders were combined with two of the fines. The x-axis of this plot shows the combinations between the fines and asphalt binders. AC1-F1 refers to asphalt binder number one and fine number one, AC2-F1 refers to asphalt binder number two and fine number one, and so forth. This nomenclature is taken from Huscheck and Angst's study. Each of these combinations have F/A ratios of one-to-one by weight.

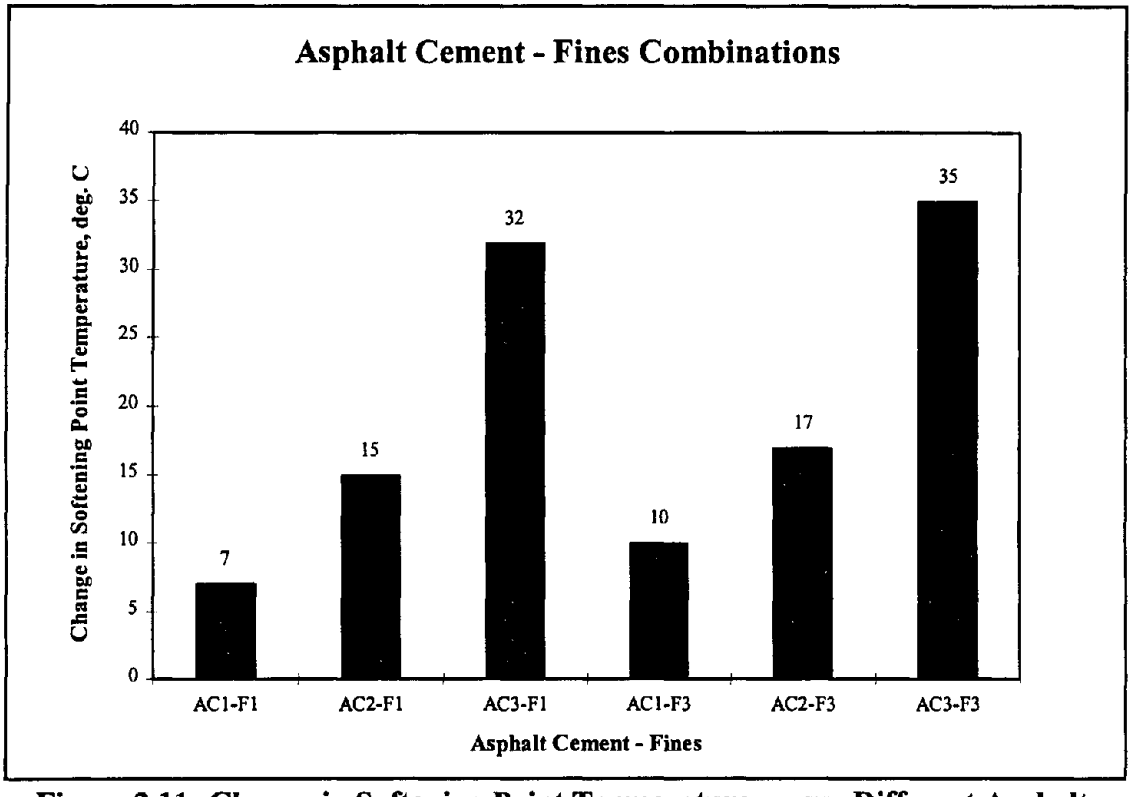

Figure 2.11: Change in Softening Point Temperature versus Different Asphalt Binder-Baghouse Fines Combinations (18)

It was shown in Figure 2.10 that the softening point test is a good indicator of the stiffening effect of fines. From Figure 2.11, it can be seen that for a single fine, the change in softening point temperatures was different for different asphalt binders. This suggests that the fines do have different stiffening effects on different asphalt binders.

As yet, a correlation between the physical properties of mineral fillers and the stiffening effect caused by these fillers has not been found. Research has shown though, that a test initially described by Rigden (19) and then modified by Anderson (16) can be correlated to the stiffening effects of filler. The test determines the volume of voids in a dry-compacted filler. Figure 2.12 illustrates the theory behind Anderson's modified Rigden's void test. When fillers are dry-compacted to their maximum density, the void content of the dust is at a minimum. If asphalt binder is then added to the compacted dust, the portion of asphalt binder needed to fill the voids is called "fixed" asphalt. Asphalt binder in excess of the fixed amount is called "free" asphalt. Rigden theorized that if a compacted dust was mixed with less asphalt binder than is required to fill its voids, a stiff dry mortar would occur. Referring to Figure 2.12, it can be visualized that as the amount of free asphalt binder decreases, the stiffness of the mortar increases.

Using Anderson's version of Rigden's voids test, several properties of the compacted dust can be calculated. These properties include bulk volume of the compacted dust (V_{db}) and the volume of voids in the compacted dust (V_{dv}). For fine/asphalt binder mixtures, the percent bulk volume ($\%V_{db}$) and percent free asphalt ($\%V_{af}$) can be calculated.

The volume of voids in the compacted dust, percent bulk volume of the compacted dust, and percent of free asphalt have all been used to correlate the effects a fine may have on an asphalt binder. For instance, Kandhal's study (17) showed a relationship between the percent bulk volume of fines in a specific HMA mixture and the stiffening effect the fines may have on a asphalt binder. He recommended a test methodology for a specific HMA mixture as:

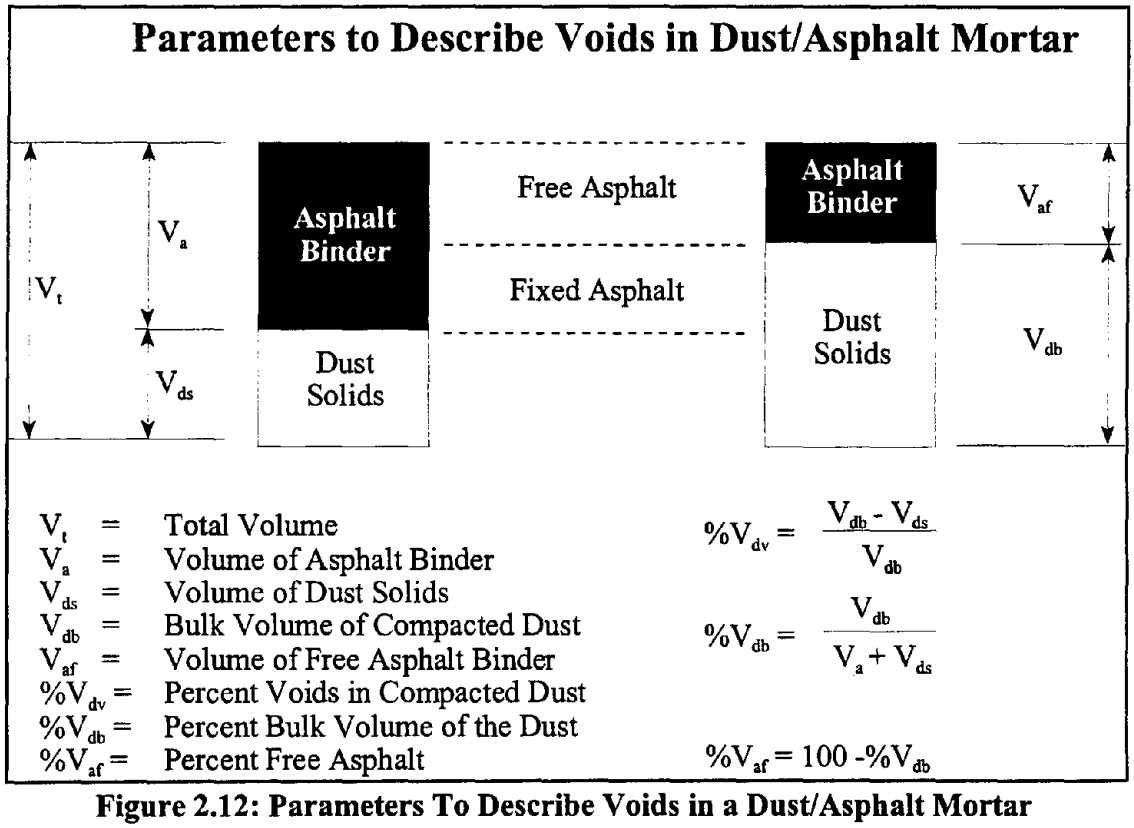

Figure 2.12: Parameters To Describe Voids in a Dust/Asphalt Mortar (18)

1) Perform the Rigden voids test;

2) Calculate the percent bulk volume;

3) If the percent bulk volume was equal to or less than 50 percent, the HMA is acceptable;

4) If the percent bulk volume was greater than 50 percent, measure the softening point (R&B) of the original asphalt binder and the fines/asphalt binder mortar; and

5) If the actual stiffening was less than 11 °C the concentration of fines was satisfactory, if not the stiffening effect of the fines was too pronounced and the mixture should be discarded.

Referring to Figure 2.12, it can be seen that percent bulk volume and percent free asphalt are inversely related. As percent bulk volume goes up, the percent free asphalt goes down. Kandhal's methodology could have read, "if the percent free asphalt is equal to or greater than 50 percent, the HMA is acceptable.

Kandhal's selection of 50 percent bulk volume seems sound. Huscheck and Angst (18) concluded that 60 percent should be the maximum allowable percent bulk volume based on tensile strength and elongation at failure criteria. Anderson (16) suggested a maximum allowable percent bulk volume of 45 percent. These values correspond to a stiffening ratio between 10 and 15 (16).

This relationship between the percent bulk volume (or percent free asphalt) and the stiffening ratio can be used to develop a design chart as shown in Figure 2.13. Bulk

densities and F/A ratios that plot in the right-hand portion of this chart will give stiffening ratios that are less than 10, which is acceptable. Bulk densities and F/A ratios that plot in the shaded portion of the chart ($\%V_{af}$ < 50 percent) would need either softening point testing or a determination of the stiffening ratio to be accepted.

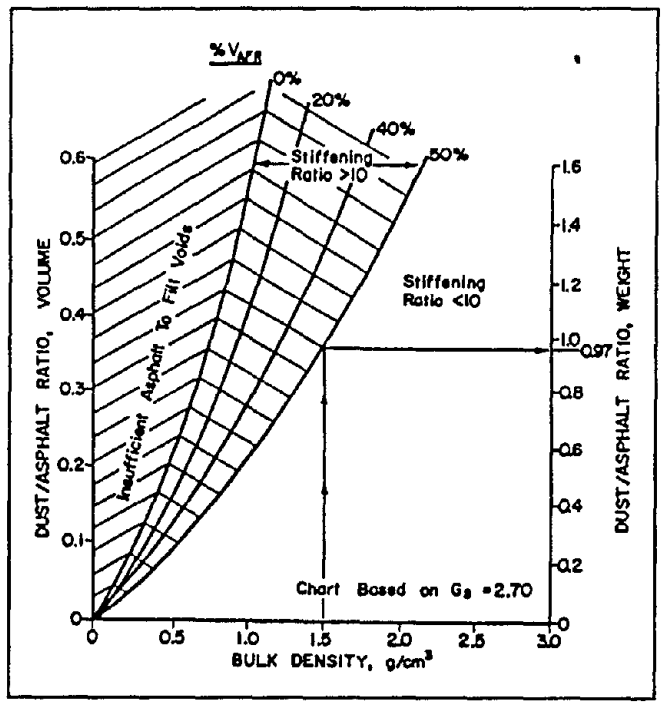

Figure 2.13: Design Chart Based on Bulk Density and Percent Free Asphalt (16)

2.1.6 Effect of Baghouse Fines on HMA Mixtures

HMA pavements consist of mineral aggregates, asphalt binder films, and air voids. For dense-graded mixtures the volumetric proportions of the components are approximately 79, 17, and 4 percent, respectively (15). The thickness of the asphalt

film coating the mineral aggregate will depend upon factors such as the gradation of the mineral aggregate, type mineral aggregate, surface area of the mineral aggregate, asphalt content, and degree of HMA compaction. Researchers have yet to agree on actual film thickness, but it can be assumed to be on the order of 10 to 100 μm (15). Anderson et. al. (20) suggest the film thickness is between 9 and 25 μm, depending on the type of mixture. Thus it seems logical that the portion of mineral aggregate that is smaller than the thickness of the asphalt film will become embedded in the asphalt binder. This would have the affect of increasing (extending) the asphalt binder volume. Conversely, if the diameter of the particle is greater than the thickness of the film, the particle will protrude through the film and act more as an aggregate particle. These fines may increase the voids in mineral aggregate (VMA) which will in turn will increase the demand for asphalt binder. These concepts are illustrated in Figure 2.14.

The asphalt film is critical to the durability of HMA mixtures. Without adequate film thickness, the asphalt binder can be oxidized faster, more easily penetrated by water, and decrease the tensile strength of the mixture (21). This is easily linked to the percentage of VMA in the mixture. VMA has two components: the volume of voids filled with asphalt binder and the volume of air voids remaining after compaction. If the VMA is too low, sufficient asphalt binder cannot be added to produce a durable mix. Mixes with low VMA are also sensitive to small changes in the asphalt binder content. If the VMA is too high, the mixture can have stability problems (21).

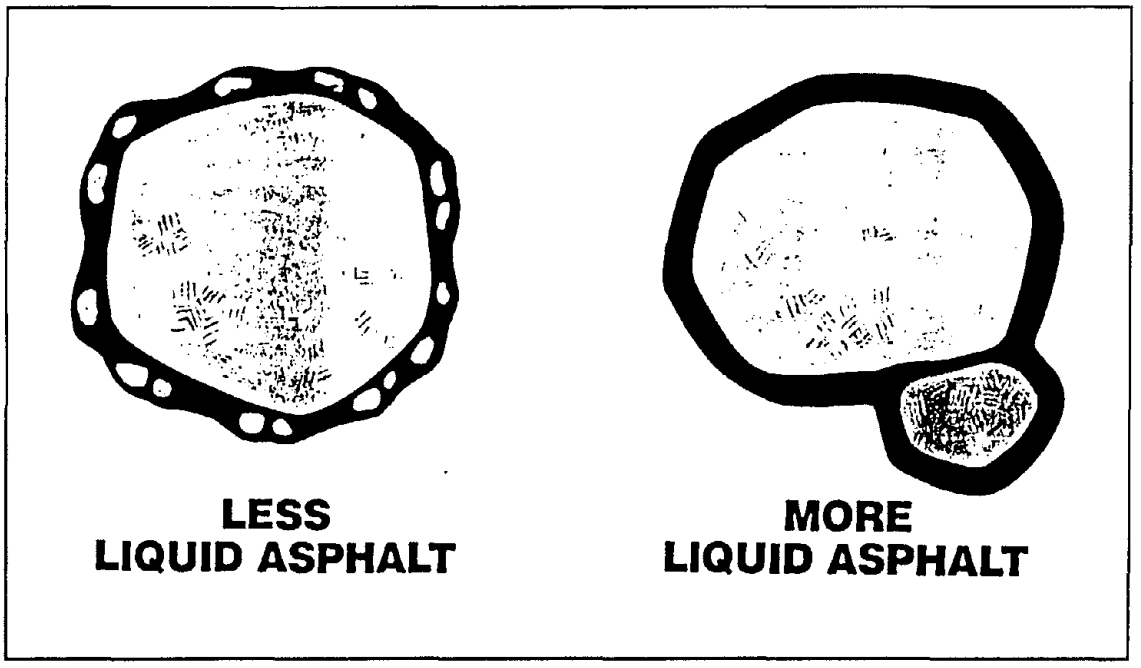

Figure 2.14: Decreasing and Increasing of Asphalt Binder Demand (16)

The literature has revealed five concepts for adding fines into mixtures. These concepts were: 1) replacing asphalt with dust while maintaining a constant volume of dust plus asphalt; 2) adding fines to the mixture while maintaining a constant asphalt content; 3) adding baghouse fines while maintaining a constant asphalt content and primary fines content; 4) interchanging ultra fine dust with coarse dust; and 5) increasing asphalt binder while maintaining a constant amount of fines.

In a study performed by Anderson, Tarris, and Brock (20), they replaced asphalt binder with baghouse fines and determined that fines with similar stiffening effects, as determined by the stiffening ratio, produced HMA mixtures with similar properties. They summarized that fine dust could apparently reduce the optimum asphalt content

but at the expense of increased mix sensitivity. The Marshall data they obtained did not reflect the excessive stiffening of the mixtures that resulted from increased dust content. These researchers suggested that some upper limit should be placed on the F/A ratio in the mixture rather than simply on the fine dust percentage (20).

Puzinauskas (15) also used this method for the introduction of fines into a mixture. He studied the compaction characteristics of sheet asphalt using a mechanical gyratory compactor. Samples were compacted to a constant volume and the number of gyrations required to achieve this constant volume were counted. The number of gyrations was used as an indication of the effort needed for compaction. Based on the results of this testing, as the F/A ratio increased, so did the compactive effort required to obtain the desired volume (15).

Testing also indicated that a relationship existed between the binder viscosity (or stiffness) and compactive effort. As the binder stiffness increased, the compactive effort required also increased. Puzinauskas concluded that a substantial increase in temperature may be needed when compacting paving mixtures with high viscosity mortars.

Increasing the dust content with a constant asphalt content can represent a typical field problem. For instance, at a drum mix plant the volume of baghouse fines being reintroduced into the drum is not uniform while a constant volume of asphalt is being added. Throughout the literature, this method of fine introduction was characterized by F/A ratios.

When Anderson et. al. (20) increased the fines content in their study, the mixture showed decreasing air voids and increasing flow, except for the coarsest fines. The effect was more pronounced for the finer dusts. For each fine, except the coarsest, the flow values increased as the stiffness of the mortar increased. This can only be explained if the increased amount of fines lubricates the mix and acts as an extender to the asphalt binder (20). High flow values typically indicate a plastic mix that will experience permanent deformation under traffic. They also concluded that the increase in flow was not related to the stiffening effect of the fines. Also, Marshall stability was not significantly affected by the amount or type of fines, which confirms the insensitivity of the stability measurements to the stiffness of the mortar.

Another study performed by increasing the dust content with a constant asphalt content was performed by Kandhal (17). He studied the effect of baghouse fines on compaction of HMA mixtures. For this study, he used two methods to evaluate the resistance to compaction: a) compacting the mixtures with the same compactive effort but at different temperatures and b) compacting at the same temperature but with different compactive efforts. For both methods he calculated a compaction factor. The compaction factor for method (a) was calculated as follows:

$$C = \frac{Volume\ of Specimen\ @\ 220^{\circ}F\ Compaction}{Volume\ of Specimen\ @\ 280^{\circ}F\ Compaction} \qquad \textbf{Eq: 2.1}$$

The compaction factor for method (b) was calculated as:

$$C = \frac{Volume\ of\ Specimen\ after\ 10\ Blows\ per\ side}{Volume\ of\ Specimen\ after\ 50\ Blows\ per\ side} \qquad \textbf{Eq: 2.2}$$

Kandhal used these compaction factors along with the bulk volume of fines in the mixture to determine that the resistance to compaction increases as the bulk volume of fines in mix also increases. The compaction factor based on compaction at the same temperature but with different compactive efforts illustrated this best. Results obtained from Kandhal and the aforementioned Puzinauskas study support the notion that the addition of fines to a HMA mixture affect the compatibility of the mixture.

Besides studying the compactibility of mixtures, Kandhal (17) also looked at the moisture susceptibility of mixtures. The Idaho test was used to measure the moisture susceptibility (this method later became known as the Lottman test). This procedure consists of compacting samples to approximately the same density as the pavement just after construction (8% voids) and then subjecting the specimens to freeze-thaw cycles. He used two different F/A ratios for his testing, 0.3 and 0.5 by volume. In order to quantify the effects of moisture on mixture properties, Kandhal used the tensile strength ratio (TSR). Figure 2.15 illustrates the results of his testing.

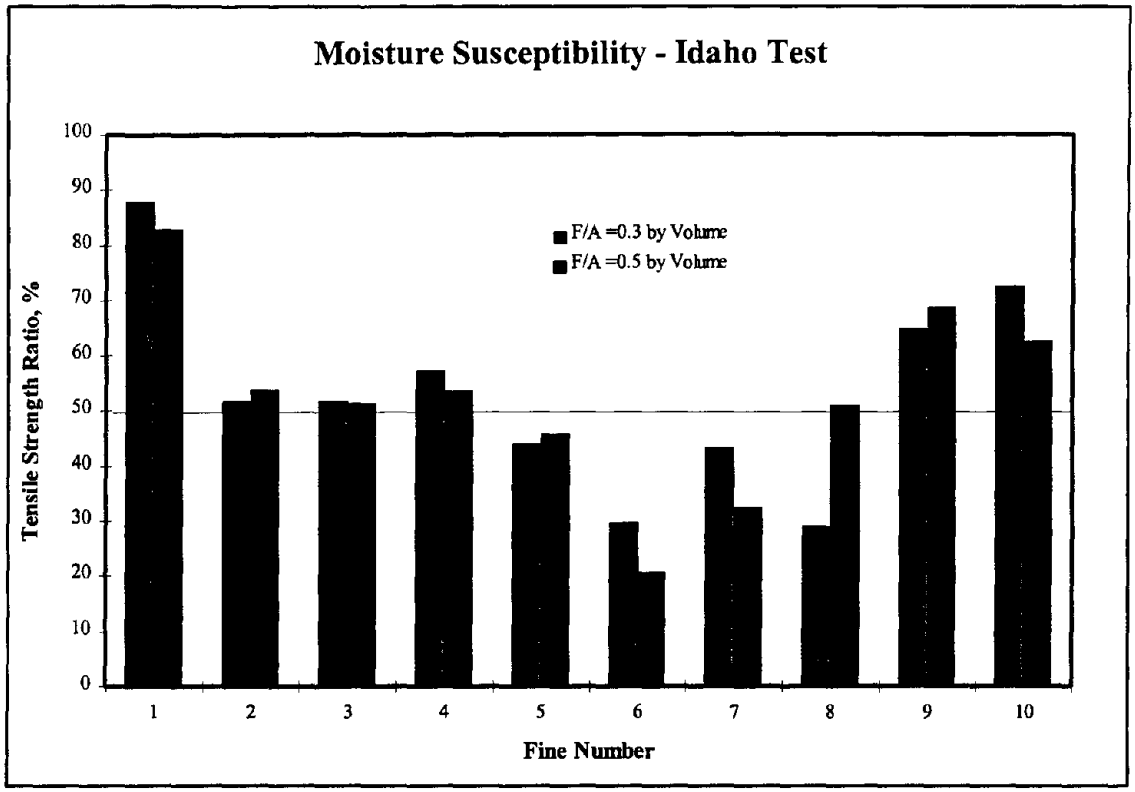

Figure 2.15: Results of Idaho Moisture Susceptibility Tests (17)

TSR is calculated by dividing the tensile strength of a conditioned sample by the tensile strength of an unconditioned sample. At the time of Kandhal's study, the accepted minimum value of TSR was 70 percent. Kandhal suggested that this may be too high. He suggested a minimum value of 50 percent. Today this value varies from state to state. It can be seen from Figure 2.15 that at a minimum TSR value of 50 percent three of the ten fines fail at both concentrations of F/A and one failed at F/A equal to 0.3 by volume. It should be noted that the three samples which failed were mixtures which contained baghouse fines from plants which used slag as the aggregate.

In a study performed by Anderson (16), he showed that as the percentage of fines increased in a mixture, the resilient modulus also increased. The resilient modulus test is a measure of mixture stiffness. Figure 2.16 presents the results of testing performed by Anderson. Resilient modulus testing occurred at 39 °F and the percentage of fines were taken as a percentage of total mineral aggregate in the mixture.

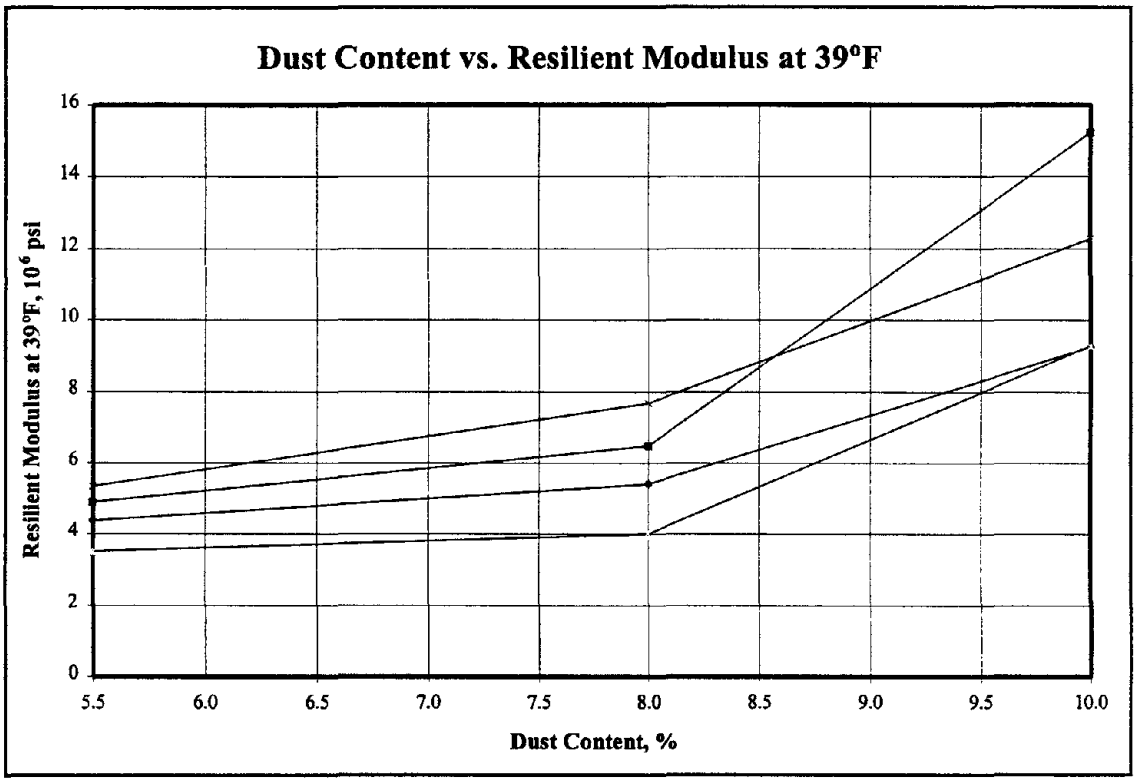

Figure 2.16: Dust Content versus Resilient Modulus (16)

Anderson (16) also performed tensile strength testing that showed increases in tensile strength with increasing stiffening ratios of the mortar. However, the failure strain decreased with increasing stiffening ratios. The trends of these relationships were

only slight but were consistent with a more brittle behavior of the mixture with increasing stiffening ratios of the mortar.

The third study approach entails adding fine dust to a mixture with a constant percentage of coarse dust. This represents a typical field problem. The primary collector fines content is under control, but a wet system collector is replaced by a baghouse and the collected baghouse fines are added back to the production process. By increasing the amount of fine dust, there is little effect on Marshall stability, but there is a significant effect on flow and air voids (20). An increase of only one percent in baghouse fines can cause a mixture to fall out of specifications with respect to air voids. Therefore, Anderson et. al. (20) summarized that the fine dust can extend asphalt binder in a mixture. Flow values were also sensitive to increases in the percentage of the baghouse fines and could be used to monitor the introduction of excess fines at the plant (20).

The fourth method of introducing fines was to replace part of the primary collector dust with the finer baghouse fines. Anderson et. al. (20) concluded that flow and stability were very sensitive to changes in asphalt binder content in mixtures with high contents of fine dust. An important point they made was that many other properties of the mixtures are being altered when the fines content is changed. These properties were not reflected in the Marshall design properties but they may have had an influence on other types of mixture behavior, such as creep, fatigue, and thermal cracking.

The final method of introduction was by increasing asphalt binder while maintaining a constant amount of fines. Puzinauskas (15) used this method to show the influence of fillers on water sensitivity, he compacted the mixtures at different asphalt contents and then measured the TSR using the Marshall Immersion-Compression test. Figure 2.17 illustrates the effects increasing asphalt contents have on TSR. It can be seen that as the asphalt content increases, so does the TSR. This should be expected. As the amount of asphalt binder increases, the waterproofing of the mixture also increases. Interestingly though, the fine illustrated in Figure 2.17 yielded an optimum asphalt content of 9 percent when subjected to Marshall mix design methods. This corresponds on the figure to a TSR value of approximately 56 percent, which, depending on the criteria, could be construed as failure. It takes an additional two and a half percent of asphalt binder to waterproof the mixture completely. Thus, with the results of this study and Kandhal's study (17) it can be seen that the type and amount of fines do influence the water sensitivity of HMA mixtures.

2.2 SURVEY OF STATE DEPARTMENT OF TRANSPORTATION'S

A survey of State Departments of Transportation (DOT) was conducted to develop background information on how other states treat baghouse fines. The questionnaire was sent to the Materials Engineer of each state and the District of Columbia (total of 51 questionnaires were sent). This survey inquired as to the dust-to-asphalt binder specification of each agency, whether this dust-to-asphalt binder

specification was by weight or volume, and whether baghouse fines are thought to be detrimental to an HMA mixture. Results of this survey are presented in Appendix A.

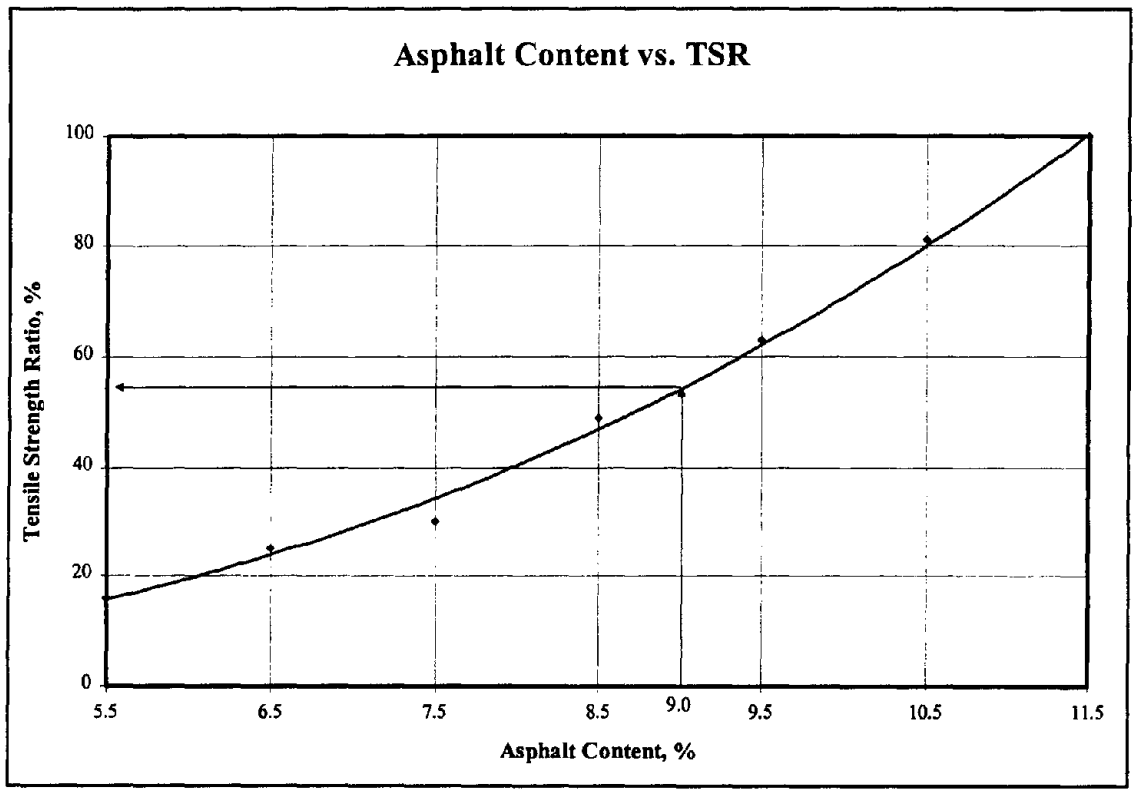

Figure 2.17: Asphalt Binder Content versus Tensile Strength Ratio (15)

Of the 51 questionnaires sent for the survey, 42 states responded. If these 42 responses are considered to be a representative sample of all DOT's, several conclusions can be assumed, some of which are the following:

1. Half (21 of those responding) of the State DOT's have a dust-to-asphalt binder specification;

2. Twenty of the 21 with dust to asphalt ratio specifications use the percent material finer than 0.075 mm (No. 200 sieve) and percent asphalt binder (total or effective) with the percentages based on weight to determine the dust-to-asphalt binder ratio;

2. The other state uses percentages based on volume in their dust-to-asphalt binder specifications;

3. Of those 20 that use percentages based on weight, three use the percent of effective asphalt binder to determine the dust-to-asphalt binder ratio;

4. Those that use percentages based on the total asphalt binder content have dust-to-asphalt binder specification ratios of 0.0 to 1.2, with the majority being 0.6 to 1.2. This range of 0.6 to 1.2 is also the recommended values of Superpave.

2.3 Review of Background Information

Dust collection systems originated from a need to protect a HMA facilities' exhaust system. However, once the EPA set forth the stringent emission standards, dust collection systems became required. Industry began to turn toward baghouses because of the reusable resource (dry fines) that they captured. Fines that are captured can be reintroduced into an HMA production process in a number of ways at both batch and drum plants. The method in which the fines are reintroduced is of major importance. Therefore, fines should be reintroduced in a controlled, uniform manner.

When added to an asphalt binder, baghouse fines combine with the asphalt binder and can form a mortar which may resemble a stiffer grade of asphalt binder. Several tests can be used to measure this stiffening effect. Based on the literature the softening point test seems to be the best indicator. Subtracting the softening point temperature of the neat asphalt binder from the softening point temperature of the mortar produces the change in softening point temperature. A good correlation has been shown in the literature between the change in softening point temperature and the stiffening effects of fines.

Viscosity measurements have also been found to be good indicators of stiffening. Dividing the viscosity of the mortar by the viscosity of the neat asphalt binder, yields what is called a stiffening ratio. By limiting the stiffening ratio to below 10, the stiffening effect of a fine on an asphalt binder has been shown to be acceptable.

The literature has also shown that dust particles which are smaller than the asphalt film coating the aggregate will extend the asphalt binder volume. This was illustrated by increasing the amount of fine dust in an HMA mixture and measuring flow and percent air voids. However, the literature did not suggest a critical particle size in which the particle would act as an extender.

Baghouse fines have also been found to affect the compactibility of HMA mixtures. This was proven using both a gyratory compactor and the Marshall hammer. As the amount of fines increase in a mixture the compactibility of the mix decreases.

This could necessitate a substantial increase in temperature when compacting HMA in the field.

Previous research studies have shown that baghouse fines can affect the moisture susceptibility of an HMA mixture. The addition of baghouse fines to an HMA mixture can produce tensile strength ratios less than 50% even at design asphalt binder contents.

CHAPTER 3: PLAN OF STUDY

The objective of this research was to establish criteria for the reintroduction of baghouse fines into HMA mixtures. In order to accomplish this objective the study was divided into five main tasks. These are illustrated on Figure 3.1 in the form of a flow diagram. The first task was presented as Chapter 2. Tasks 2 through 4 are discussed in this chapter while task 5 is presented in Chapter 7.

3.1 Field Sampling of Baghouse Fines - Task 2

Field sampling at HMA producing facilities in South Carolina was accomplished to collect the baghouse fines necessary to perform this research project. These fines were used in each of the three remaining tasks in this study.

Ninety to ninety-five percent of the HMA facilities in South Carolina use a granite or granite-gneiss aggregate, therefore sampling was limited to HMA facilities that use this type of aggregate. Eighteen facilities were selected for sampling and a representative of NCAT traveled to each facility to obtain baghouse fine samples. While at each facility, sampling locations and plant equipment and operations were documented.

A minimum of 24 samples were taken over a minimum of five production days at each facility. For plants with only a baghouse as the dust collection system, only a

baghouse fine sample was obtained per sampling interval. For plants with a primary collector, it was attempted to obtain samples directly from both the primary collector and baghouse. If the primary collector could not be sampled directly, a combined sample containing both the primary fines and baghouse fines was obtained.

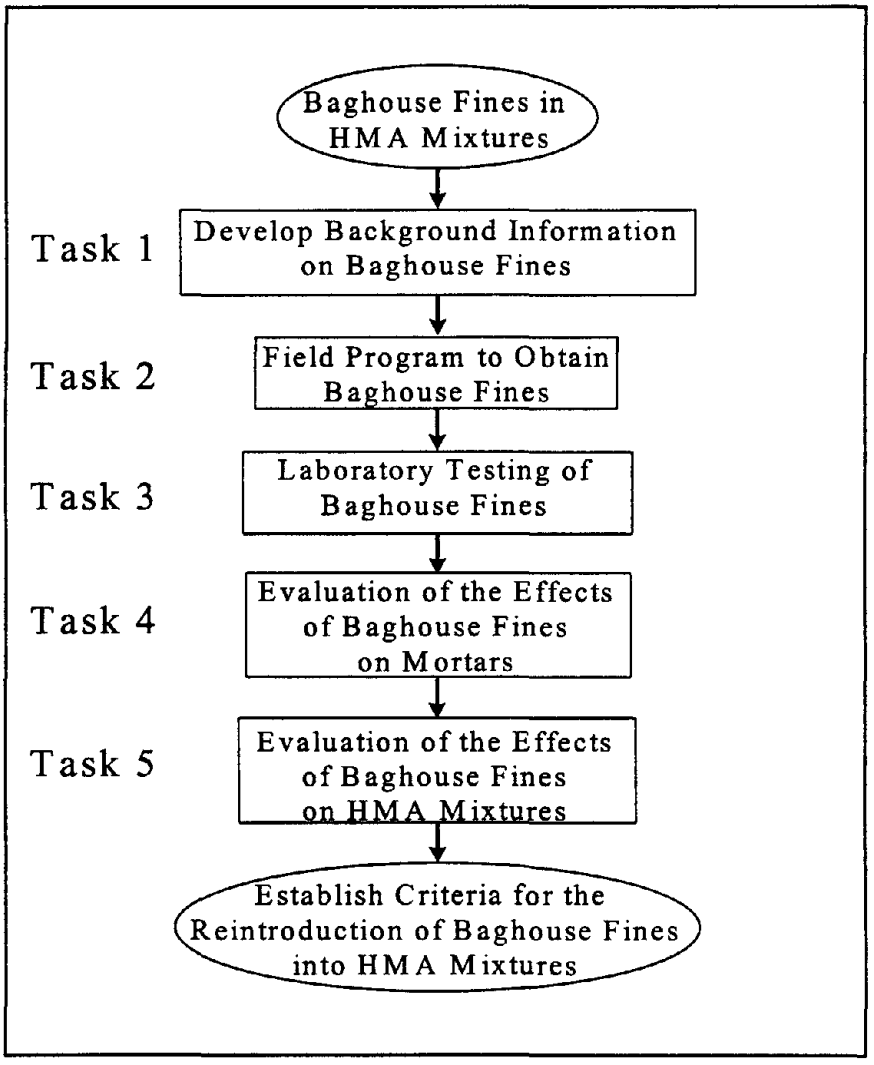

Figure 3.1: Flow Diagram for Overall Research Study

Each sample consisted of 20 to 30 pounds of baghouse fines. Documentation of the times, temperature, production rate, type fuel being burned, and other pertinent information was obtained for each period of sampling. The sample form utilized during this phase for each sample obtained is presented in Figure 3.2. Table 3.1 shows a typical field sampling plan for five production days; however, this plan was not always followed due to weather and variations in HMA production.

A secondary objective of this task was to determine the rate at which baghouse fines were being reintroduced into HMA mixtures. This consisted of determining the weight of baghouse fines leaving the baghouse in a given time period. The weight (in tons) and time (in hours) were then used to determine the rate of baghouse fines reintroduction in tons per hour (tph).

3.2 Laboratory Testing of Baghouse Fines

Laboratory testing of the baghouse fines obtained during the field sampling program consisted of the following tests:

1. Laser diffraction particle size analyses;
2. Mechanical particle size analyses;
3. Modified Rigden's void test;
4. Methylene Blue test; and
5. Specific gravity test.

PLANT DATA TO BE OBTAINED

Contractor: _____

Plant Location: _____

Mix Type: _____ Aggregate Type: _____

Plant Type: _____

Plant Manufacturer: _____

Date: _____ Time Sample Being Taken: _____

TEMPERATURES:

Temperature of Material leaving Dryer: _____

Dryer exhaust temperature: _____

Stack exhaust temperature: _____

Moisture Conditions (determine the moisture content and attach the data)

Moisture Content of material on cold feed: _____

Moisture Content of mix being produced: _____

Other Information

Rated Capacity of the plant: _____

Tons per hour being produced: _____

Type fuel being used: _____

Describe the dust collection system: _____

_____

What is the damper setting on the exhaust fan: 100% 75% 50% Other ____

What percentage of primary dust is being returned to the plant: _____

What percentage of baghouse dust is being returned to the plant: _____

Figure 3.2: Sampling Form Used During Field Program

Table 3.1: Typical Plant Sampling Schedule

Time of Day	Day				
	1	2	3	4	5
Start-up		X		X	
AM		X		X	X
AM	X	X	X	X	
AM	X	X		X	X
PM		X	X	X	
PM		X	X	X	
PM	X	X		X	X

3.2.1 Laser Diffraction Particle Size Analyses

A particle size analysis using an automated particle size analyzer was conducted on samples obtained during the field program. This was accomplished to study the variations in particle size for the baghouse fines. No ASTM or AASHTO standardized procedure was found to perform this test. Therefore, the manufacturer's instructions were utilized.

The automated particle size analyzer (PSA) is a Coulter LS 200 analyzer, that uses laser diffraction to determine the particle size distribution. Figure 3.3 shows the instrument. The PSA measures particles with diameters from 0.37 μm to 2000 μm. This corresponds to Standard sieve sizes of No. 999 to No. 10, respectively. Calculations by the PSA assume that the particles are rotating at a high speed in the

system fluid as they pass through the instrument. Therefore, it calculates the particle sizes as if the particles are spherical.

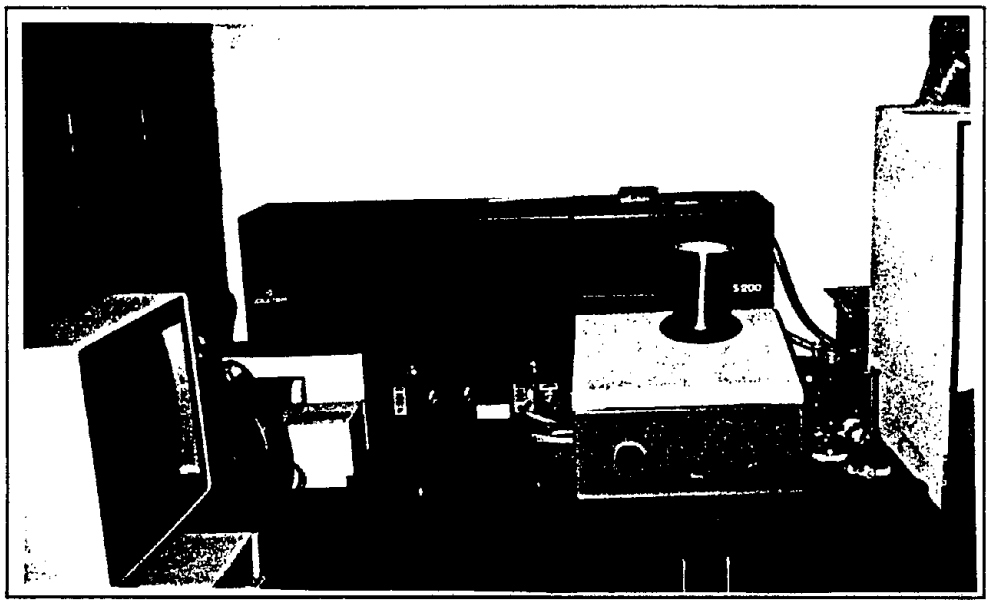

Figure 3.3: Coulter LS200 Laser Diffraction Particle Size Analyzer

Output from the PSA consists of a particle size distribution based on percent volume versus particle diameter. Typical output from the PSA is presented in Figure 3.4. While this is not a "standard" particle size distribution as would be obtained from a mechanical sieve analysis or hydrometer analysis (based on percent by mass), it was used because of the large quantity of samples obtained for this research study. Testing time for a single sample using the PSA is approximately two minutes per test. With three replicates for each sample tested to improve consistency of results, the PSA was very time effective.

The PSA particle size distribution was used to calculate the fineness modulus and uniformity coefficient for each sample. Both of these properties are normally calculated from mass based particle size distributions of an aggregate. In addition, the PSA was used to calculate other properties of the particle size distribution such as: the mean particle size, D_{10}, D_{30}, D_{60}, and percent clay (material finer than 2μm).

Volume	100.0%		
Mean:	108.8 um	95% Conf. Limits:	0-401 um
Median:	65.10 um	S.D.:	149 um
Mode:	116.3 um	C.V.:	137%
Specific Surf. Area	5776 cm^2/ml	Skewness:	4.29 Right skewed
		Kurtosis:	28.8 Leptokurtic

% <	10	30	50	60	90
Size um	4.130	24.71	65.10	92.18	256.3

Size um	ASTM	Cum. < Volume %	Size um	ASTM	Cum. < Volume %
0.37	999	0.00	250	60	89.43
0.5	998	0.26	300	50	93.11
1	997	1.88	355	45	95.73
2	996	5.21	425	40	97.55
5	995	11.40	500	35	98.41
10	994	17.29	600	30	98.78
20	635	26.58	710	25	98.94
25	500	30.20	850	20	99.12
32	450	34.59	1,180	16	99.60
38	400	37.92	1,400	14	99.84
45	325	41.42	1,700	12	99.99
53	270	45.03	2,000	10	100.00
63	230	49.18	2,360	8	100.00
75	200	53.84	2,800	7	100.00
90	170	59.26	3,350	6	100.00
106	140	64.48	4,000	5	100.00
125	120	69.84	4,750	4	100.00
150	100	75.60			100.00
180	80	81.03			
212	70	85.47			

Figure 3.4: Typical Output From Coulter LS200 PSA

The mean particle diameter is defined as the average particle size of the distribution and is calculated as follows:

$$\bar{x} = \frac{\Sigma (\bar{x_c} \times n_c)}{\Sigma n_c} \qquad \textbf{Eq.: 3.1}$$

where:

$\bar{x}$ = mean particle diameter, microns

$\bar{x}_c$ = average particle size for a given size interval, microns

n_c = percent material retained within a given size interval, percent

D_{10} is defined as the particle diameter through which 10 percent of the material was passing. Likewise with the D_{30} and D_{60}. The percent clay (the percent material finer than 2 μm) was also determined.

The uniformity coefficient, C_u, was calculated as follows:

$$C_u = \frac{D_{60}}{D_{10}} \qquad \textbf{Eq.: 3.2}$$

The coefficient of uniformity is used to define the range that the particles extend. If C_u is large, the particle distribution extends over a large range.

The fineness modulus for each sample was calculated based on Anderson's "Guideline on the Use of Baghouse Fines" (16). This calculation consisted of summing the percent coarser than 75, 53, 32, 20, 10, 5, 2, and 1 μm and dividing by 100.

3.2.2 Mechanical Analysis of the Baghouse Fines

To determine if a correlation existed between the Coulter LS200 PSA and the "standard" mechanical analysis, ten baghouse fine samples were randomly selected for testing by both mechanical means and the Coulter LS200 PSA. Each of the ten samples were tested three times to form three replicates. The mechanical analysis consisted of dry-sieving each sample over a 2.0 mm (No. 10), 0.425 mm (No 40), and 0.075 mm (No. 200) sieve to determine the percentage passing. In addition, the portion passing the 0.075 mm sieve was subjected to a particle size analysis using the hydrometer test. This mechanical analysis of the baghouse fines was performed by the Alabama Department of Transportation. The manufacturer's instructions were used for testing with the Coulter LS200.

3.2.3 Modified Rigden's Void Test

The modified Rigden's void test was also performed on the baghouse fine samples obtained during the field sampling phase. Testing was accomplished in accordance with a test standard outlined in Anderson's "Guidelines on the Use of Baghouse Fines" (16). This test method is a modified form of Rigden's voids test (19) with the primary difference being the equipment used for testing.

The test procedure entails compacting a small amount of fines in a mold to determine the percentage of voids in the compacted fines. Figure 3.5 presents a schematic of the equipment needed to perform this test. Appendix B presents the actual test standard developed by Anderson.

The specific gravity of the dust must be known to determine the parameters. Specific gravities were not determined for each of the samples obtained in the field program. Five samples from each plant were randomly selected for specific gravity tests. However, if more than one type of sample was obtained for a plant, five specific gravity tests were performed for each type of sample. An average specific gravity value was then used to determine the different parameters.

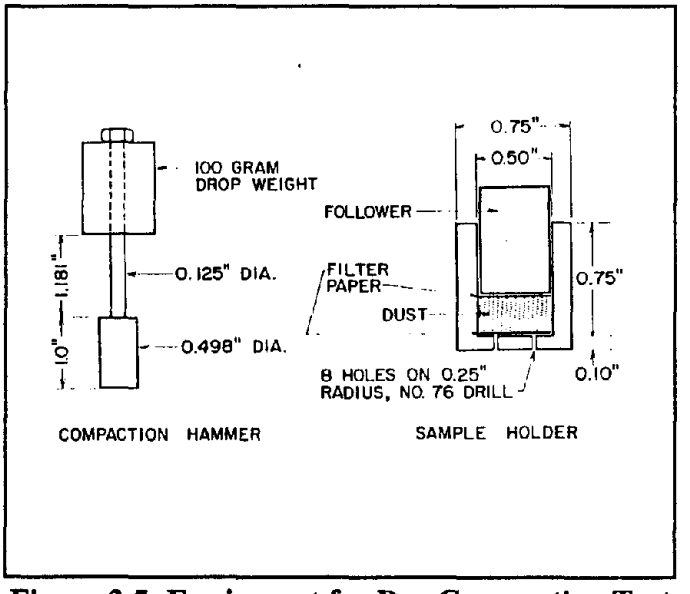

Figure 3.5: Equipment for Dry Compaction Test (16)

Figure 3.6 illustrates the theory for additional properties derived from the modified Rigden's void test. A mortar is comprised of three components: fines, air, and asphalt binder. If the fines are compacted to the densest packing state (bulk volume of the dust), a certain percentage of the fines' bulk volume will be air voids. The volume

of asphalt binder required to fill these voids is referred to as "fixed" asphalt. Any asphalt binder in excess of the fixed asphalt is called "free" asphalt. Equations used to calculate these parameters are also presented on Figure 3.6.

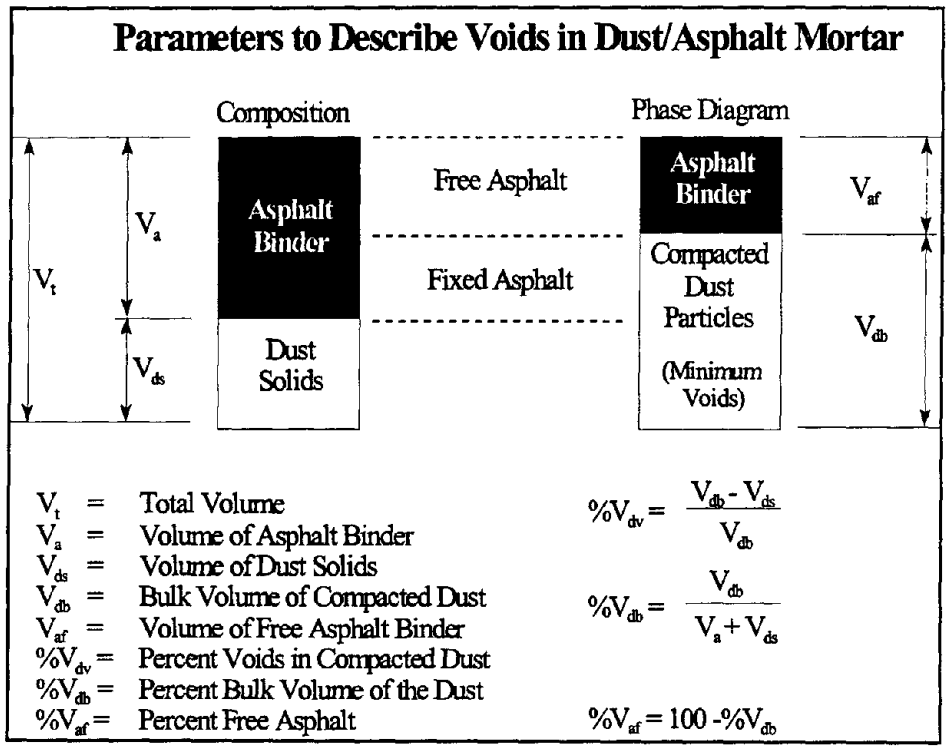

Figure 3.6: Theory of Modified Rigden's Void Test (18)

3.2.4 Methylene Blue Testing

This test is used to quantify the amount of harmful clays in a material passing the 0.075 mm (No. 200) sieve by measuring the surface activity of the material. Material that has a high surface activity is less moisture susceptible than material with low surface activity (22). The test method used was the International Slurry Surfacing Association's Technical Bulletin No. 145 (23) which is presented in Appendix C.

As will be discussed in Section 3.3, baghouse fine samples were combined for each of ten plants to perform mortar and mixture laboratory testing. The Methylene Blue test was conducted on these ten combined baghouse fines samples.

3.2.5 Specific Gravity Testing

As alluded to in Section 3.2.2, the specific gravity of the different fines is needed to calculate the percent air voids in a compacted dust (modified Rigden's void test). Testing was accomplished as outlined in AASHTO T 100-90 "Specific Gravity of Soils."

3.3 Laboratory Testing of Asphalt Binder/Baghouse Fine Mortars - Task 3

Based on the information obtained from the particle size analysis and modified Rigden's void testing, ten plants were selected to have samples combined. Samples from each of the ten plants plant were combined, resulting in ten baghouse fine combined samples. The properties used for selection were the mean particle diameter and the percent air voids in a compacted dust. The samples were combined so that enough material would be available for testing in this task and the subsequent mixture evaluation task. Figure 3.7 illustrates the process by which the different combined samples were combined. These ten combined samples were sequentially numbered from Fine 1 to Fine 10.

Two different asphalt binders used in South Carolina were selected for this task. These asphalt binders were a Citgo AC-20 and a Shell AC-20. The Citgo AC-20 was a Venezuelan crude, while the Shell AC-20 was from Wood River, Illinois. These asphalt

binders were also numbered: the Citgo AC-20 was designated Asphalt Binder No. 1 and the Shell AC-20 was designated Asphalt Binder No. 2. Using the numbering system used for the ten baghouse fine combined samples and the two asphalt binders, a nomenclature was formulated to designate the different mortars tested. This nomenclature is presented in Table 3.2.

During this task four different baghouse fines/asphalt binder concentration levels (F/A ratio) were evaluated. These F/A ratios were 0.2, 0.3, 0.4, and 0.5. They were calculated as the volume of baghouse fines divided by the volume of asphalt binder. If a specific gravity of a particular fine were 2.65, this would result in a F/A ratio (based on weight) range of between 0.7 and 1.3. This range is above and within the Superpave requirements of 0.6 to 1.2 (based on weight).

Table 3.2: Nomenclature for Mortar Testing

Asphalt Binder	Fine	Mortar Designation	Asphalt Binder	Fine	Mortar Designation
1	1	AC1F1	1	6	AC1F6
2	1	AC2F1	2	6	AC2F6
1	2	AC1F2	1	7	AC1F7
2	2	AC2F2	2	7	AC2F7
1	3	AC1F3	1	8	AC1F8
2	3	AC2F3	2	8	AC2F8
1	4	AC1F4	1	9	AC1F9
2	4	AC2F4	2	9	AC2F9
1	5	AC1F5	1	10	AC1F10
2	5	AC2F5	2	10	AC2F10

The test matrix for this phase consisted of 80 combinations of asphalt binder, Fines, and F/A ratios (10 fines * 2 asphalt cements * 4 F/A ratios). Testing of these mortars consisted of performing tests on the original mortars before any aging, after aging by the Thin Film Oven Test (TFOT), and further aging in the Pressure Aging Vessel (PAV). Tests conducted on the original, unaged mortars included: Viscosity measurements using the Brookfield Viscometer (BV); Softening Point Test (SP); and the Dynamic Shear Rheometer (DSR). The DSR was performed on the TFOT aged mortars. After additional aging of the mortars with the PAV, the DSR and Bending Beam Rheometer (BBR) tests were performed. The following sections describe both the aging techniques and tests used to evaluate the mortars, while Figure 3.8 illustrates the steps followed.

Two statistical designs were utilized for the testing of the mortars. First, testing of the original, unaged mortars was accomplished on each of the baghouse fine/asphalt binder combinations. This was assumed as a completely randomized experimental design. In such a design, the resulting data are viewed as a random sample from a normal distribution. Because each mortar was prepared and tested identically, this assumption was correct.

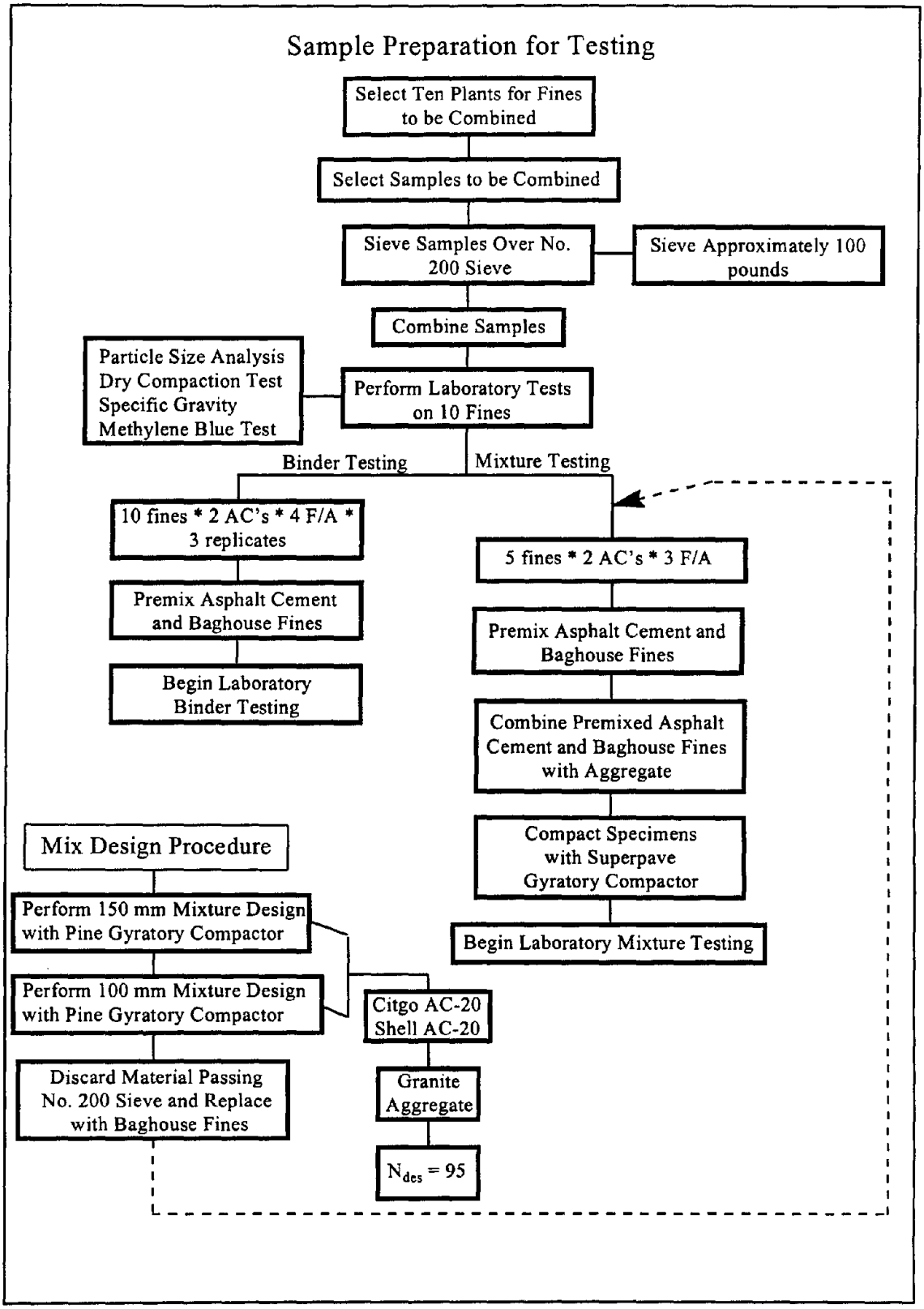

Figure 3.7: Flow Diagram for Sample Preparation

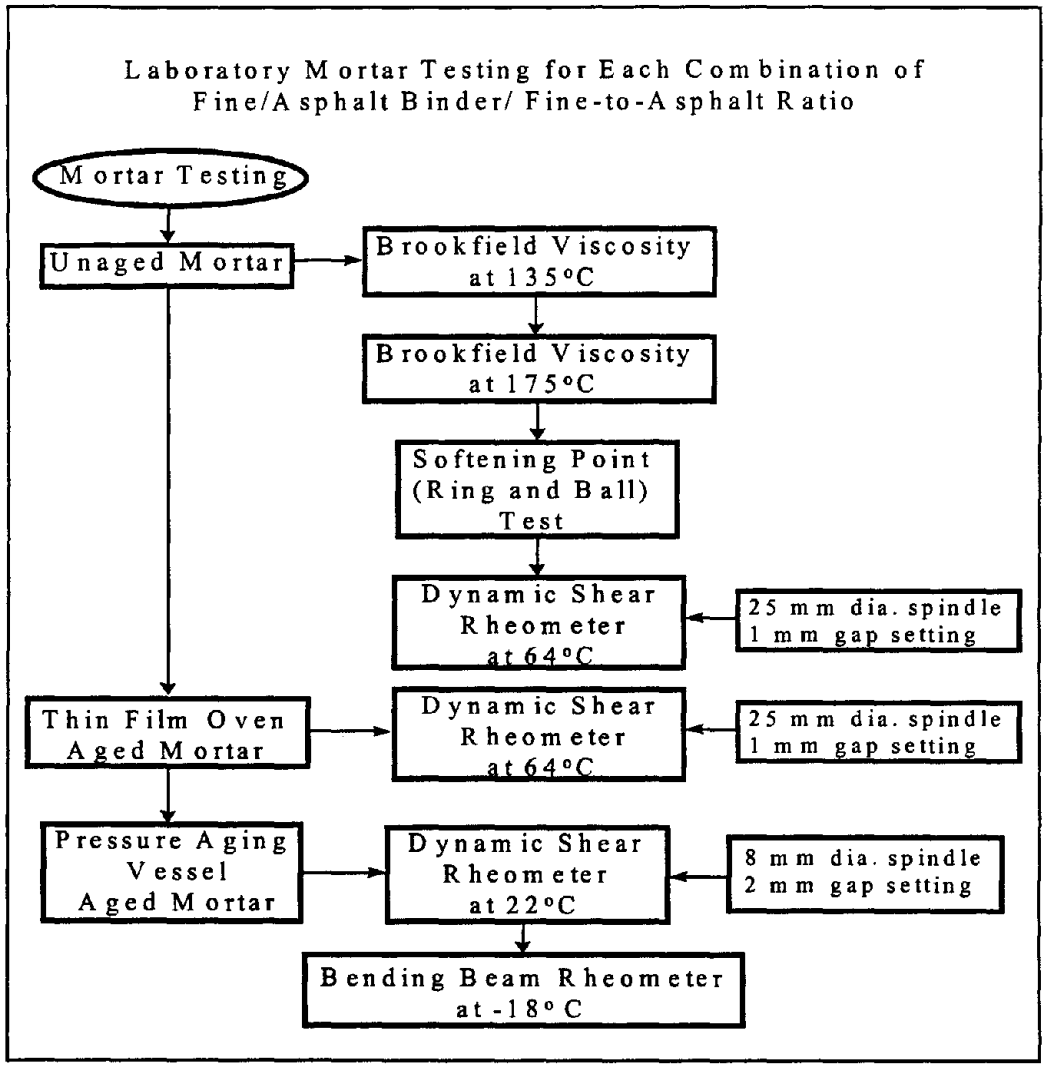

Figure 3.8: Flow Diagram for Mortar Evaluation Phase

Testing of the TFOT and PAV aged mortars was based on a one-half fractional factorial design. This statistical design allowed for the testing of only half of the baghouse fine/asphalt binder combinations while maintaining statistical integrity. The process of designing this experiment consisted of "sacrificing" a high order interaction that was considered insignificant. Based on this statistical design, there were three main

effects: asphalt binder, baghouse fine combined samples, and F/A ratios. The asphalt binder had one degree of freedom, the baghouse fine combined samples had nine degrees of freedom, and the F/A ratios had three degrees of freedom. For this experiment the high order interaction that was sacrificed included one degree of freedom from both the F/A ratio and the ten combined baghouse fine samples. Therefore, two degrees of freedom remained for the F/A ratios and eight remained for the combined baghouse fine samples. This high order interaction is referred to as a generator. The generator was then used to divide the experiment into two blocks. Testing by this design consisted of performing all tests associated with one of the two blocks.

This statistical design was utilized because of the time needed to perform the TFOT and subsequent PAV aging. The TFOT aging procedure requires 5 hours and the PAV aging procedure requires 20 hours. For each mortar combination, two TFOT and two PAV aging procedures were needed to provide enough material for testing. Therefore three working days were required for each combination. Since 80 different combinations were tested, this would have resulted in 240 working days (or 48 working weeks) to perform the required aging procedures. Therefore, because of the statistical integrity of the one-half fractional factorial design, it was determined to utilize this statistical design.

3.3.1 Mortar Preparation

There is no standard for blending of asphalt binders and baghouse fines (or mineral fillers) to produce mortars. To produce mortars of equal uniformity, the following procedure was used for this project:

1. Determine the specific gravity for both the asphalt binder and baghouse fine sample.
2. Calculate the mass of asphalt binder needed to give the proper F/A ratio based on volume for a given mass of baghouse fines of 100 grams.
3. Prepare the baghouse fines sample by drying to a constant weight at 110 ± 5 °C.
4. Place one quart of neat asphalt binder into a 165 ± 5°C oven. The binder should remain in the oven until it reaches a uniform temperature of 165 ± 5 °C. Occasional stirring may be needed.
5. Weigh 100 grams of dried baghouse fine sample into a 8 ounce sample tin and place in a 175 ± 5 °C oven. This sample tin and baghouse fine sample should remain in the oven for a minimum of 30 minutes.
6. After preheating the asphalt binder and baghouse fine sample, remove each from their respective oven.
7. Place the sample tin containing the baghouse fine sample onto a balance with a 2 kg. capacity and sensitive to 0.1 gram and tare.

8. Weigh the appropriate amount of asphalt binder into the sample tin to the nearest 0.1 gram.
9. Place the sample tin on an electric hot plat set to a temperature of approximately 165°C and hand-mix with a spatula. Care must be exercised to prevent loss of the baghouse fine sample during mixing.
10. When the mortar (blended asphalt binder and baghouse fine) visually appears homogeneous, the mixture is ready for testing.

This procedure was used for each mortar tested during this project.

3.3.2 Aging of Mortars

Asphalt binders age due to two mechanisms: volatilization of light oils present in the asphalt binders and oxidation by reacting with the oxygen in the environment. Blending and mixing within the heated environment of a HMA producing facility and the subsequent lay-down process ages an asphalt binder due to the heat and air flow involved with these processes. After laydown, aging continues as oxidation occurs on the roadway. (24)

The TFOT (AASHTO T 179-93) procedure simulates both of the above aging mechanisms. This method was selected over the Rolling Thin Film Oven Test (RTFOT) because preliminary work performed in the laboratory showed that the mortars had a tendency to "crawl" out of the RTFOT bottles during the test. The RTFOT method uses a horizontally mounted rack that rotates vertically about its axis.

Bottles are placed in the rack horizontally. When the mortars were introduced into the bottles and the rack was rotating, the mortars would crawl out of the bottles.

The TFOT procedure utilizes a horizontal rotating shelf mounted on a vertical shaft. This rotating shelf is located within the Thin Film Oven. Cylindrical flat-bottom pans with an inside diameter of 140 mm and a depth of 9.5 mm are used to hold the samples during the test. This horizontal rotating shelf and the flat-bottom pans eliminated the mortars from crawling.

The procedure for the TFOT consisted of placing enough mortar into the cylindrical pans to create a film thickness of 3.2 mm. The pans were then placed on the rotating shelf in the Thin Film Oven for five hours at 163 °C. The rotating shelf rotates within the oven at a rate of 5.5 revolutions per minute. At the completion of the test, the mortar was assumed to be in a condition similar to the condition it would be in after the mixing process and laydown.

In order to obtain the 3.2 mm film thickness in the cylindrical pans, the specific gravity of the mortar had to be assumed. By knowing the specific gravities of the asphalt binder and the filler and the F/A ratio, the specific gravity of the mortar could be assumed. Once this was determined, the mass of the mortar to fill the volume needed for a 3.2 mm film thickness could be determined.

Enough mortar per combination of asphalt binder/baghouse fine was aged using the TFOT procedure for all testing at this aged condition and for the subsequent aging in the PAV conditioning device.

The PAV conditioning device (AASHTO PP1) subjects the material to high pressure and temperature for 20 hours to simulate long-term (5 to 10 years) aging (24). Because an asphalt binder that is in-service has been through the mixing and lay-down processes, the PAV procedure was performed on the mortars already aged in the TFOT.

The PAV conditioning device consists of a pressure aging vessel and a forced draft oven. A sample rack that can hold ten sample pans is placed within the pressure aging vessel. For this study, 50 grams of mortar was placed in each sample pan. The sample pans were then placed on the sample rack. The sample rack was placed in the pressure aging vessel and both were placed in the forced draft oven to preheat to 100°C. Once preheated, a pressure of 2.1 MPa was applied via a regulated compressed air bottle. After the pressure was applied, the mortars were allowed to age for 20 hours before removing. Enough mortar per combination of asphalt binder/baghouse fine was aged to perform testing at this aged condition.

3.3.3 Brookfield Viscometer (BV)

The BV is a rotational viscometer used to measure an asphalt binder's viscosity (or resistance to flow). ASTM D 4402 defines the procedures for using the BV. This viscometer was selected over other viscometers (kinematic and absolute) because rotational viscometers have larger clearances between components, thus making it more applicable to mortars (24). For this project, two test temperatures were utilized: 135°C (275°F) and 275°C (347°F).

The rotational viscometer determines viscosity by measuring the torque required to maintain a constant rotational speed of a cylindrical spindle while submerged in an asphalt binder sample at a constant temperature (24). This is illustrated in Figure 3.9. Depending on the particle sizes of the materials in the mortar, different spindles can be used. For this project a No. 27 spindle was utilized to ensure adequate clearance between the spindle and the sample chamber.

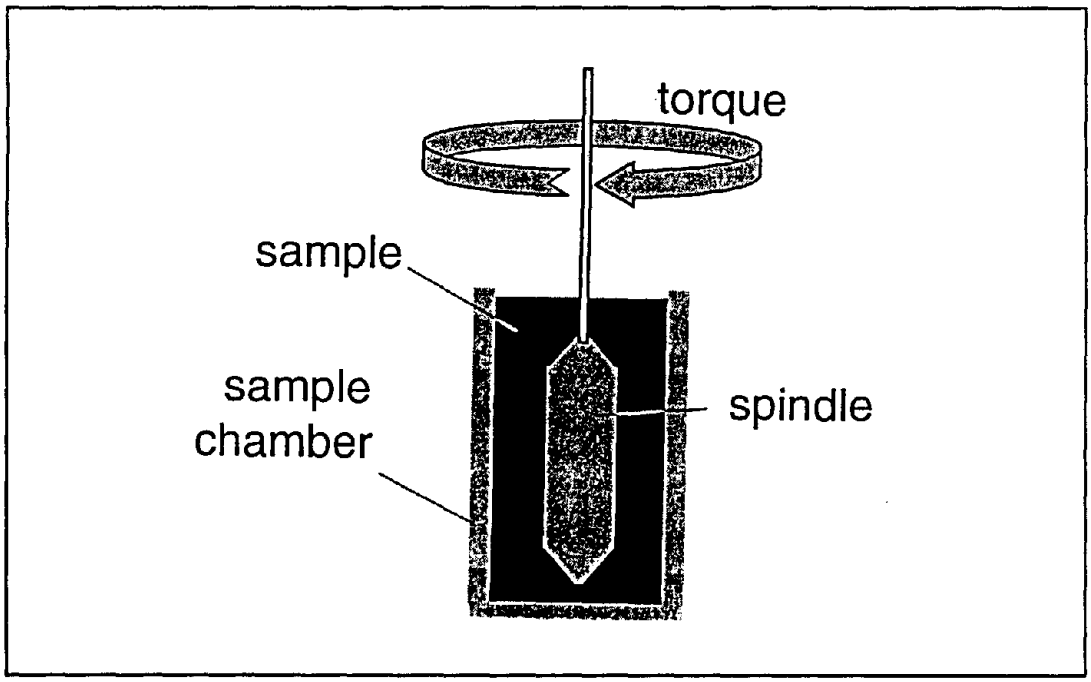

Figure 3.9: Rotational Viscometer Operation (24)

3.3.4 Softening Point Test (SP)

The SP is used to determine the temperature at which an asphalt binder cannot support the weight of a standard steel ball. This temperature defines the temperature at

which a phase change from solid to liquid occurs in the asphalt binder. (21). This test method is defined in AASHTO T 53-92 and illustrated in Figure 3.10.

The test consisted of taking two brass rings filled with asphalt binder (or mortar) and suspending the rings in a beaker filled with water or glycol. A steel ball of standard dimensions and mass was then placed in the center of each ring, on top of the binder sample. The steel ball, brass ring, and asphalt binder sample were all placed in the beaker and heated at a controlled rate of 5°C (41°F) per minute. When the asphalt binder softens, the steel balls and asphalt binders sink toward the bottom of the beaker. The temperature is recorded the instant the steel balls and asphalt binder sink one-inch. (21)

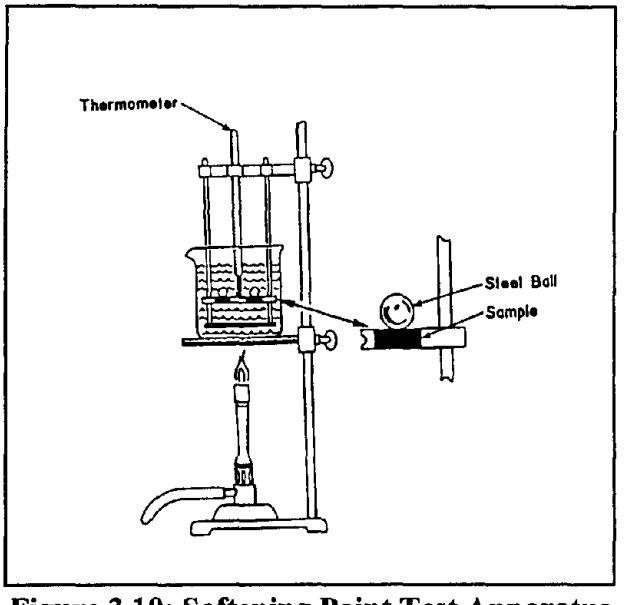

Figure 3.10: Softening Point Test Apparatus (21)

3.3.5 Dynamic Shear Rheometer (DSR)

The DSR is used to characterize the viscous and elastic behavior of asphalt binders (or mortars). This is accomplished by measuring the complex shear modulus (G*) and the phase angle (δ) of the asphalt binder. The complex shear modulus is a measure of the total resistance of a material to deformation when it is repeatedly sheared.

This test procedure is outlined in AASHTO TP5. It consisted of pouring a mortar into a rubber mold in the shape of a disk and allowing to cool. The binder disk was then sandwiched between a fixed plant and an oscillating disk (spindle) on the DSR apparatus. The thickness of the sandwiched disk was carefully controlled. This was accomplished by adjusting the gap between the fixed plate and spindle. The thickness of the gap was dependent on the test temperature. Tests performed at 64°C had a gap of 1 mm while tests at 22°C had a gap of 2 mm. Spindle size also depended upon test temperature, with a 25 mm diameter spindle used at the 64°C test temperature and an 8 mm diameter spindle used at 22°C.

Once the binder disk was properly mounted and loaded for testing, the temperature of the sample was allowed to equalize. After temperature equilibrium, the spindle begins oscillating back and forth. This is illustrated in Figure 3.11. The spindle starts at point A and moves to point B. From point B, the spindle moves back through point A to point C. This process comprises one cycle. The frequency of oscillation is the length in time for one cycle to occur, and one complete cycle is called one hertz

(Hz). The DSR test was performed at 1.59 Hz. The oscillation process was performed in a constant strain mode. This means that the spindle rotated through a fixed distance, regardless of stress.

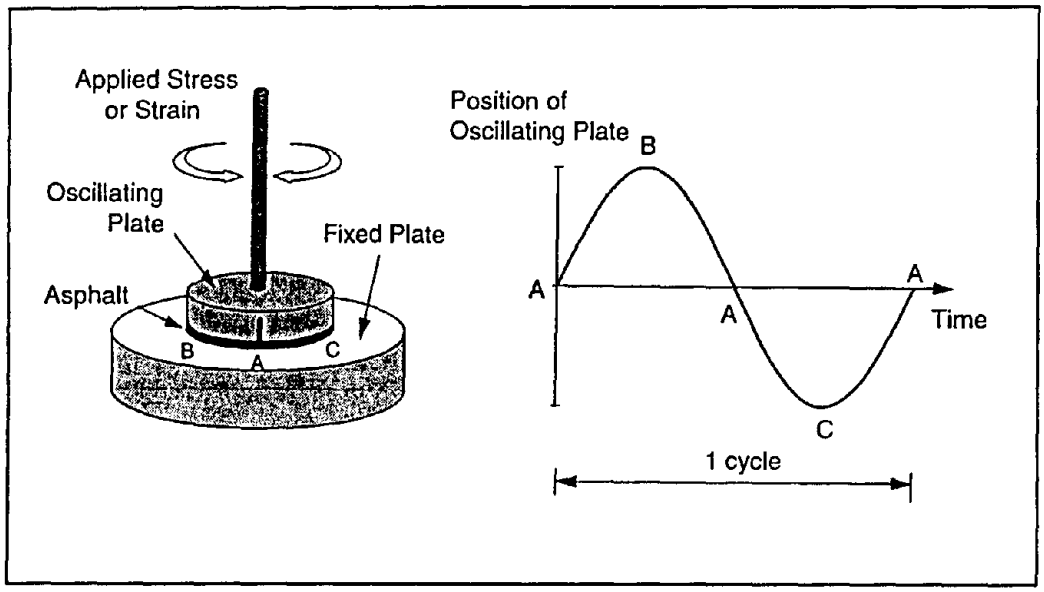

Figure 3.11: DSR Oscillation (24)

The complex shear modulus and phase angle are dependant on the magnitude of the shear strain within the specimen. Both decrease with increasing shear strain. (AASHTO TP5). Testing with the DSR should be performed at small strains where the modulus is relatively independent of shear strain. This linear region is defined as the range in strains where the complex shear modulus is 95 percent or more of the zero strain value (AASHTO TP5). Determination of the linear region is accomplished by performing a linearity sweep in which G* and δ are measured at different levels of shear strain. For each strain level, the value of G*Cos(δ) is calculated and plotted against the

strain value. For this project a linearity sweep was performed on two samples to determine if G* and δ were actually being measured in the linear region. Figures 3.12 and 3.13 present the results of these linearity sweeps. Figure 3.12 presents the sweep for the original, unaged mortar AC1F2-0.3. This nomenclature references Asphalt Binder No. 1, Fine 2, and a F/A ratio of 0.3. Actual testing for this combination occurred between 7 and 8 percent strain, which is within the linear range. Figure 3.13 presents the sweep for the original, unaged mortar AC1F5-0.5. Actual testing for this combination occurred between 6 and 7 percent strain, which is within the linear range. This testing shows that the DSR can be used to evaluate the stiffness of mortars.

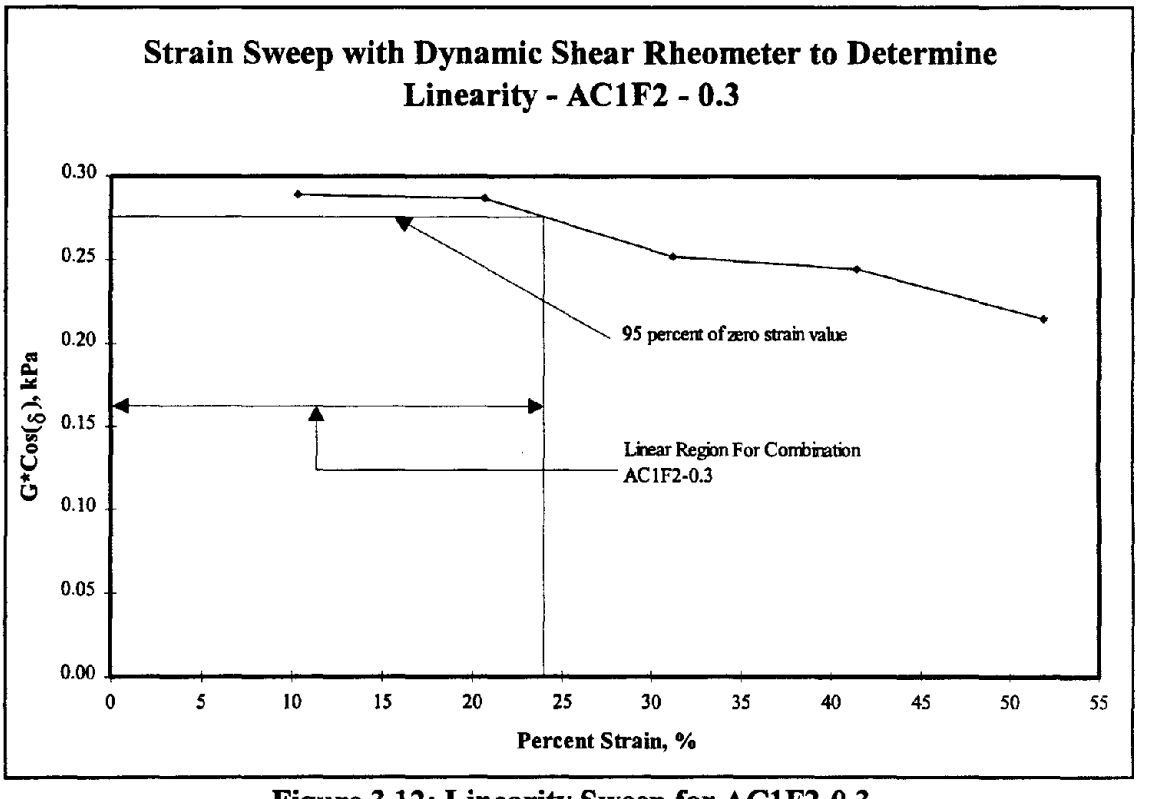

Figure 3.12: Linearity Sweep for AC1F2-0.3

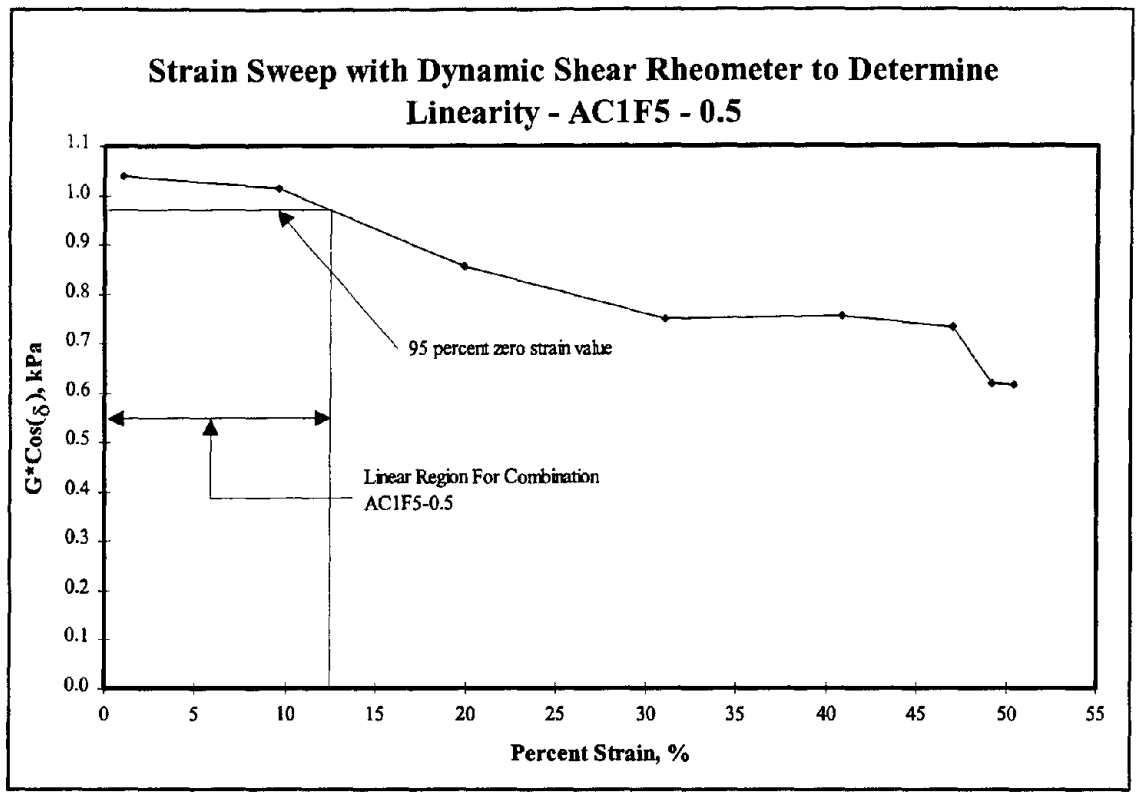

Figure 3.13: Linearity Sweep for AC1F5-0.5

This test method was used for this study to give an indication of the mortar's elastic and viscous characteristics. Also, because of the two testing temperatures and different aging conditions, this test will give an indication of the mortars high temperature and intermediate temperature characteristics. Test results at 64°C were used for high temperature characteristics and results at 22°C indicate the mortars intermediate temperature characteristics.

3.3.6 Bending Beam Rheometer (BBR)

The BBR is another test method adopted by SHRP researchers for the characterization of asphalt binders. Superpave has also adopted this test in the

performance graded binder specification. This test method is used to measure the low temperature properties of an asphalt binder. It measures the stiffness (S) of a simply supported asphalt binder beam loaded with a constant load of 980±50 mN. Since the time dependency of asphalt binders vary, the shape of the stiffness curve is also important. The slope of this stiffness curve (m) is determined and shows the rate of stress relaxation of the beam.

This test procedure is outlined in AASHTO TP1. To perform this test, beams were molded for the neat asphalt binder and mortars. The beams were 6.35±0.05 mm thick, 12.70±0.05 mm wide, and 127±0.05 mm long. Standard beam molds were utilized to ensure proper specimen dimensions. Once the beams were molded, they were allowed to cool to room temperature. Prior to testing, the beams were further cooled to -5±5◦C for 5 to 10 minutes to aid in demolding. Once the beams were demolded, they were placed in the BBR apparatus fluid bath that had been brought to the test temperature of -18◦C. The beams were then conditioned in the fluid bath at the test temperature for 60±5 minutes. After conditioning, the beams were tested by placing a single beam on the testing supports and using a preloading sequence in order to seat the specimen. Following beam seating, the test load of 980±50mN was applied and held constant to ±5mN for 240 seconds. The computer recorded the continuous deformation of the beam and reports the beam stiffness. A schematic of the equipment needed to perform the BBR test is presented in Figure 3.14.

The BBR tests asphalt binder beams at low temperatures and therefore indicates a binder's propensity for thermal cracking. Thermal cracking can occur from one thermal cycle where a pavement's temperature reaches a critical low. Cracking caused by a single thermal cycle is related to the asphalt binder's stiffness at the temperature at which cracking occurs.

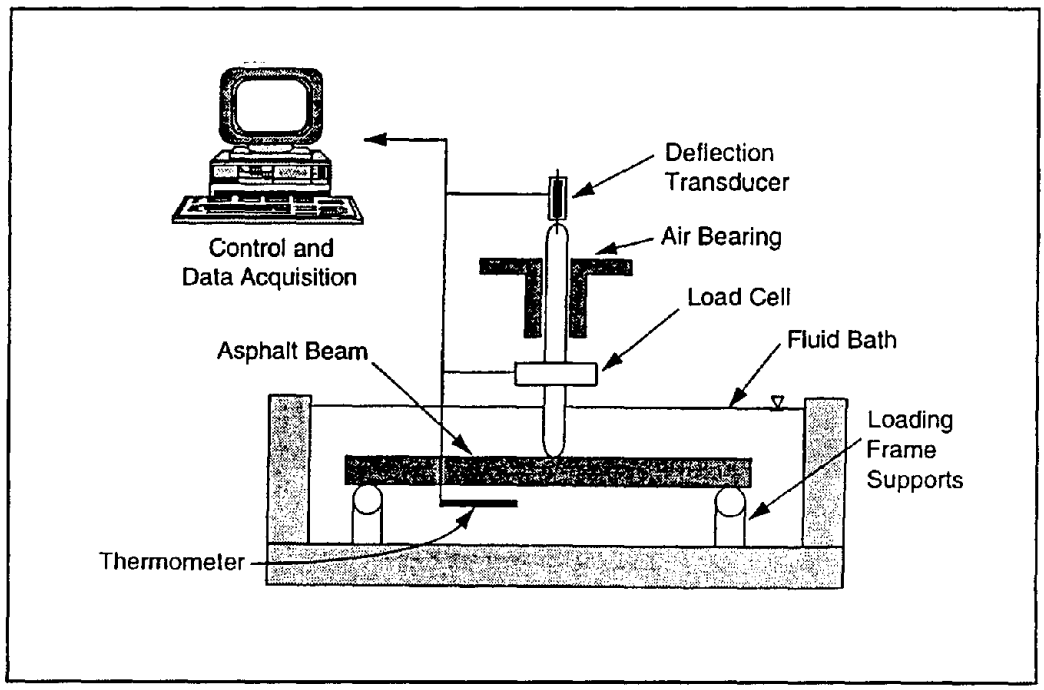

Figure 3.14: Bending Beam Rheometer Test Equipment (24)

3.4 Laboratory Testing Program for HMA Mixtures - Task 4

The mixture study was performed to evaluate the effects of baghouse fines on HMA mixtures. A granite-gneiss aggregate obtained from a quarry near Spartanburg, South Carolina was utilized. Again, the Citgo AC-20 and Shell AC-20 were used for this task.

Mixture designs were developed using a SCDOT Type 1B gradation. This is a dense-graded mixture designed for high traffic volumes. Mix designs were conducted using a Superpave Gyratory Compactor (SGC). The design number of gyrations (N_{des}) for this project was selected to be 95 gyrations. This corresponds to an initial number of gyrations (N_{ini}) of 8 and a maximum number of gyrations (N_{max}) of 150. The optimum asphalt content for each of the mixtures was selected as the asphalt content at which the voids in total mix (VTM) was four percent at N_{des}.

Five of the ten fines used in the mortar evaluation phase were selected for this task (Fines 1,2, 4, 5, and 9). These fines were selected based on percent air voids in a compacted dust (modified Rigden's void test) and mean particle diameter. Three different F/A ratios were evaluated: 0.3, 0.4, and 0.5. The test matrix for this phase consisted of 30 different combinations (5 fines * 2 asphalt cements * 3 F/A ratios). Figure 3.7 illustrated the procedures by which each combination was prepared. Figure 3.15 presents a flow diagram that illustrates the testing accomplished during this phase..

Three separate compactive efforts were utilized. Initially, twelve specimens of each combination were compacted to 95 gyrations with the SGC. Three of these twelve specimens were tested using the Indirect Tensile Test (IDT) and three were tested using the confined repeated load deformation test. Compactibility of each combination was also determined using the results of compaction for each of the twelve specimens.

The second compactive effort was utilized with the Root-Tunnicliff Moisture Susceptibility Test. Six specimens for each combination were compacted to between 6 and 8 percent voids in total mix (VTM).

The final compactive effort also used 95 gyrations with the SGC. However, each specimen was subjected to a short-term aging procedure prior to compaction. This short-term aging procedure was part of the Superpave Long-Term Aging procedure (AASHTO PP2).

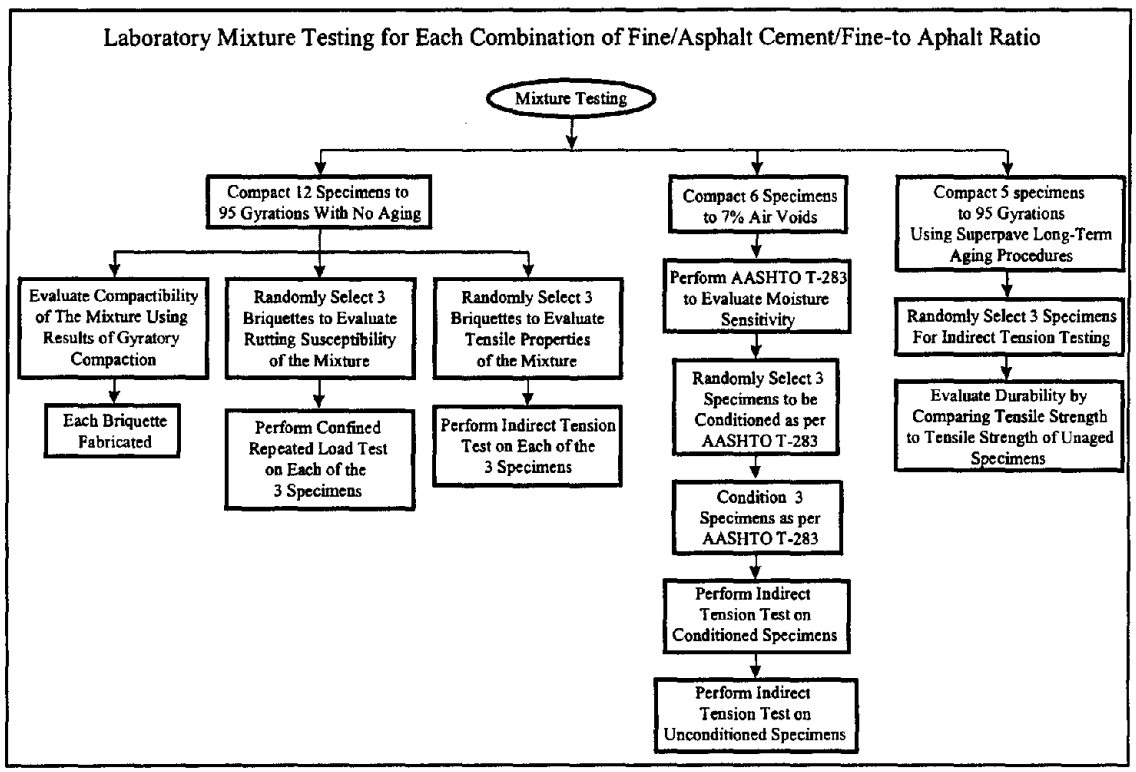

Figure 3.15: Flow Diagram for HMA Program

3.4.1 Mixture Designs

Two mix designs were performed using each asphalt binder. One mix design was conducted utilizing a 150 mm mold and one utilizing a 100 mm mold. Superpave

requires mixture designs to be performed with 150 mm molds. However, each of the tests performed during the HMA testing program, requires 100 mm specimens. Therefore, both asphalt binders were subjected to mixture designs with the two different molds.

Each mix design was conducted using the SGC. The objective of these mix designs was to determine the asphalt binder content at which the mixture exhibited 4.0 percent air voids at N_{des}. This was referred to as the optimum asphalt binder content.

3.4.2 Sample Preparation

For this study, HMA mixtures were defined by three constituents: mineral aggregate, filler (baghouse fine combined samples), and asphalt binder. Based on a study performed prior to fabricating test specimens, the filler and asphalt binder were premixed to comprise a mortar and then added to the mineral aggregate. This side-study is presented in Appendix D.

The premixing procedure for the mortars was identical to that used in the mortar evaluation task. However, for this task the volume of asphalt binder was held constant. This volume of asphalt binder was based on the optimum asphalt binder content determined during the mixture designs. Based on the volume, baghouse fines were added to produce the proper F/A ratio.

Mixing of the HMA specimens consisted of preheating both the mortar and mineral aggregate to a temperature of 160°C. Once this temperature was achieved, the mortar was added to the mineral aggregate and mixed for a minimum of 90 seconds

with an automated mixer. After mixing, the loose, uncompacted mixture was placed in an oven set at 170°C to bring the specimen back up to the compaction temperature of 150°C. The specimens were then compacted with the SGC.

Lime was only added to the mineral aggregate for the control mixture (Fine 9). Lime was introduced by pre-wetting the aggregate and then adding 1 percent lime by mass of total aggregate.

3.4.3 Indirect Tensile Test (IDT)

The IDT provides two properties used to characterize an HMA mixture: the tensile strength and the tensile strain at failure. Even though the IDT is not a true tensile test, it is commonly used to characterize HMA mixtures. It was developed to indirectly determine the tensile strength of an HMA specimen. The theory behind the IDT is based on mechanics of materials principles. A single compressive load is applied by two loading plates to a cylindrical specimen parallel and along the specimen's vertical diametral plane. This loading subjects the center plane between the loading plates to a near uniform tensile stress acting perpendicular to the center plane, hence the name "indirect" tensile test (Figure 3.16).

This test was performed as outlined in ASTM D4867 except no preconditioning was conducted. A test temperature of 25°C (77°F) was selected. To perform this test, a load was applied via two loading plates at a constant deformation rate of 2 in. per minute until failure. The ultimate load and amount of vertical deformation was recorded for each specimen. The tensile strength was calculated as follows:

$$S_t = \frac{2\ P}{\pi\ t\ d} * 6.895 \qquad \textbf{Eq.: 3.3}$$

where:

S_t = tensile strength, kPa

P = ultimate load, lb.

t = thickness of the specimen, in.

d = diameter of the specimen, in.

6.895 = conversion from psi to kPa.

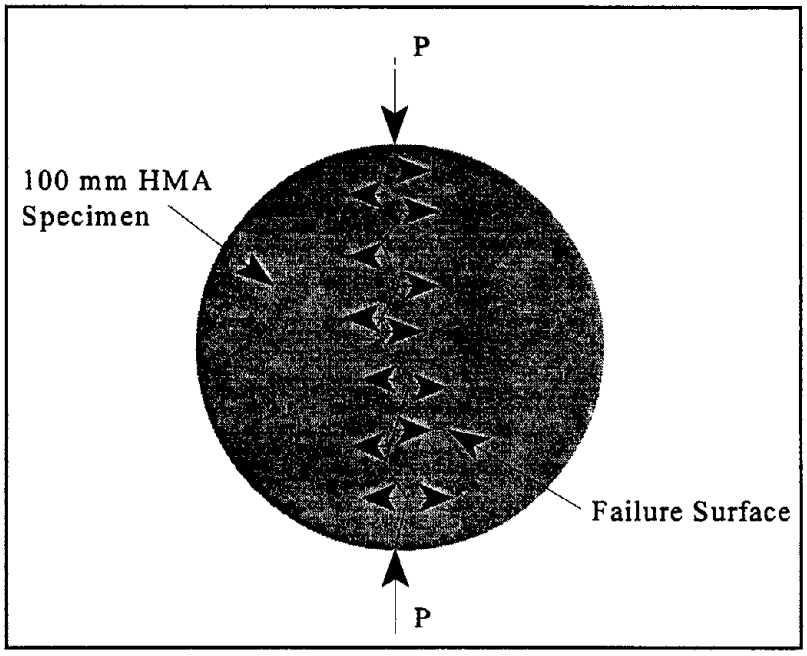

Figure 3.16: Schematic of Indirect Tensile Test

Tensile strain at failure values are typically determined as follows:

$$\varepsilon_t = 0.52 * H \quad (21) \qquad \textbf{Eq.: 3.4}$$

where:

ϵ_t = strain at failure, in./in.

H = horizontal deformation, in./in.

However, IDT tests were performed using Marshall stability equipment with a specially designed breaking head to measure tensile strength. This method of testing does not measure horizontal deformation. This equipment does however provide the vertical deformation. Therefore, an equation was derived to determine ϵ_t in terms of vertical deformation.

Based on the mechanics of materials and Poisson's ratio, an equation was derived to use the vertical deformation data. Poisson's ratio relates the horizontal and vertical strain of a material. A typically accepted value of Poisson's ratio for HMA is 0.35 (25). The derivation is as follows:

$$\mu = 3.59 * \frac{H}{V} - 0.27 \quad (21) \qquad \textbf{Eq.: 3.5}$$

where:

μ = Poisson's ratio

H = horizontal deformation

V = vertical deformation

Equation 3.5 estimates Poisson's ratio for a 4-in. cylindrical specimen. Substituting the assumed value of Poisson's ratio into Equation 3.5 and solving for the horizontal deformation, the resulting equation is as follows:

$$H = 0.173 * V \qquad \textbf{Eq.: 3.6}$$

Substituting Equation 3.6 back into Equation 3.4 yields the derived equation for tensile strain at failure based on vertical deformation, and is as follows:

$$\varepsilon_t = 0.090 * V \qquad \textbf{Eq.: 3.7}$$

Equation 3.7 was utilized for calculating tensile strain at failure for each tested specimen for this project.

3.4.4 Confined Repeated Load Deformation Test

This test method was selected to provide an indication of the rutting potential of the different asphalt binder-baghouse fine HMA mixtures. Currently no ASTM (or otherwise) test standard exists for this test. Therefore, a brief discussion follows.

A 100 mm diameter specimen that had been compacted to 95 gyrations using the SGC was placed in a rubber membrane. The specimen was then placed in a triaxial cell. This triaxial cell was similar to cells used in soil testing laboratories. Once in the triaxial cell, the cell and specimen were placed in a temperature control chamber having a temperature of 60°C. After reaching temperature equilibrium, a confining pressure of 137.9 kPa was applied to the specimen. A seating load (compressive) of 68.9 kPa was

then applied. Once seated, the specimen was repeatedly loaded with an 827.4 kPa compressive pulse load. This load was applied for 0.1 seconds and then removed for 0.9 seconds, thereby producing a 1 second loading cycle. Loading cycles were continued for 3,600 seconds (1 hour). After the hour of loading cycles, the specimen was allowed to recover for 15 minutes. Figure 3.17 illustrates the non-linear strain accumulation typical of this confined repeated load test.

During the test, deformation measurements are recorded through a data acquisition system. These deformation measurements were then used to determine strain. The strain value of interest is the maximum strain accumulated in the specimen. Maximum strain was defined as the strain at the end of the 1 hour loading cycle.

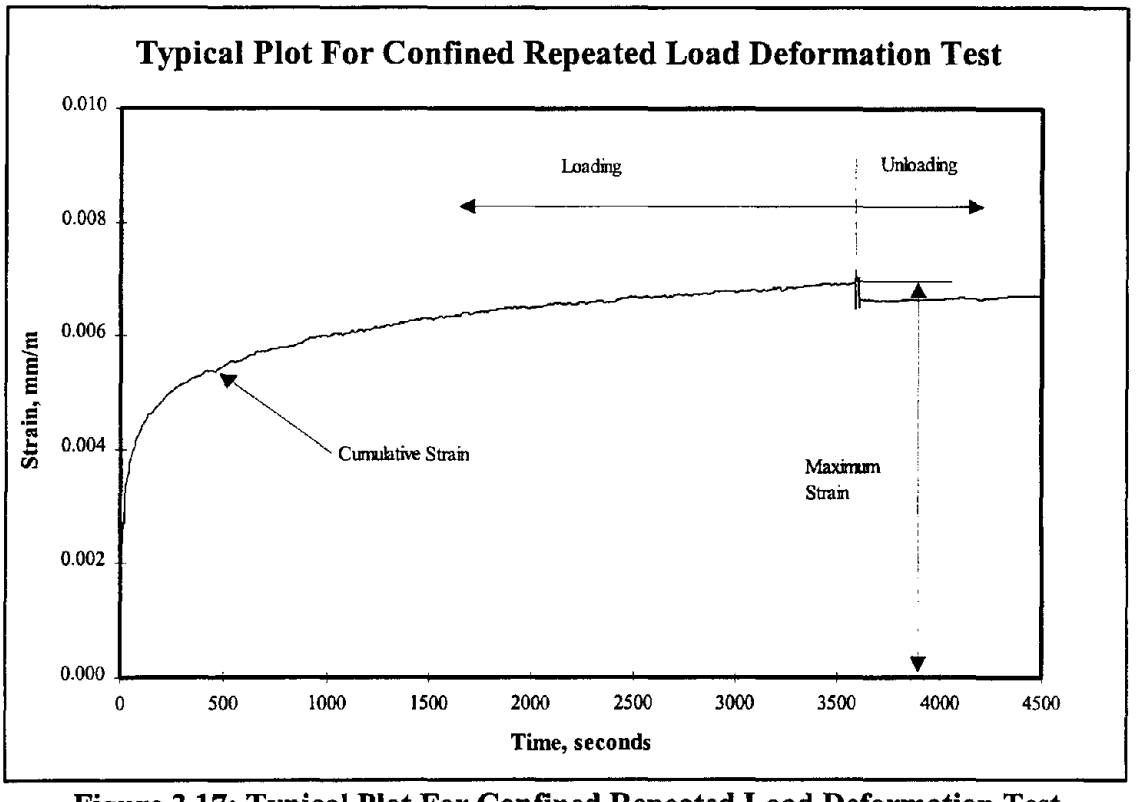

Figure 3.17: Typical Plot For Confined Repeated Load Deformation Test

3.4.5 Moisture Susceptibility

The Root-Tunnicliff (AASHTO T-283) method of determining a mixture's moisture susceptibility was selected for this project. Moisture susceptibility of a HMA mixture is the potential for deterioration of the mixture due to the detrimental influences of water. Stripping is a term used to describe the effects of moisture damage. Stripping produces a loss in strength through the weakening of the bond between the asphalt binder and aggregate. In effect, stripping causes the loss of cohesion in the mixture that leads eventually to distresses.

The Root-Tunnicliff method requires that six specimens be compacted to between 6 and 8 percent voids in total mix (VTM). After compaction, three specimens were partially saturated to between 55 and 80 percent using a vacuum system. The partially saturated specimens (conditioned samples) were then placed in a 60 °C water bath for a 24 hour period. After this time, the specimens were placed in a 25 °C water bath for 2 more hours and subsequently tested by the IDT. The remaining three specimens (unconditioned samples) were tested by the IDT in an unsaturated state at a temperature of 25 °C. Results of the three IDT for the conditioned and unconditioned samples were then averaged and the Tensile Strength Ratio (TSR) determined. The TSR is the ratio (expressed as a percentage) between the unconditioned average tensile strength and the conditioned average tensile strength. The lower the TSR, the more susceptible the HMA is to stripping.

3.4.6 Long-Term Aging

In order to evaluate the durability of the asphalt binder-baghouse fines HMA mixtures, each combination was subjected to Superpave Long-Term Aging procedures. The SHRP researchers developed this procedure to simulate in-service aging in the field. AASHTO PP2 outlines this procedure. However, some modifications were made to this procedure. These are discussed in the following paragraphs.

This procedure actually involves aging in two stages. A short-term aging procedure is performed on a loose, uncompacted HMA specimen. This procedure was developed to simulate the aging that occurs during field plant mixing operations. After short-term aging, the specimen is compacted using normal compacting procedures. Once compacted, the specimen undergoes further aging using the long-term aging procedures. This procedure simulates the in-service aging of HMA after field placement and compaction.

In order to accomplish the short- and long-term aging procedures, a HMA specimen's aggregate and mortar were preheated to the desired mixing temperature. These constituents were than mixed to produce a loose, uncompacted mixture. Next, the mixture was placed in a baking pan and spread to an even thickness of approximately 21 to 22 kg/m^3. The baking pan was then placed in a forced draft oven for 4 hr ± 5 minutes at a temperature of 135 °C ± 1 °C. Short-term aging is completed at the end of this 4 hr. period. After the 4 hr, the mixture was removed from the 135 °C oven and placed in a 170 °C oven to bring the mixture up to compaction temperature.

The mixture was then compacted to 95 gyrations using the SGC. Once compacted, the specimen was extruded from its mold and placed in a 60°C forced draft oven for 2 hr. After the 2 hr in the 60°C oven, the specimen was allowed to cool to room temperature. The specimen was then placed on a rack in a 85°C forced draft oven for 120 hr. After 120 hr, the forced draft oven was turned off and the door left ajar to allow the specimen to cool to room temperature. Long-term aging was completed once the specimen reached room temperature.

To evaluate durability, three specimens of each asphalt binder/baghouse fine combination were prepared using the short- and long-term procedures. Each of these specimens were tested using the IDT to provide the tensile strength of the aged specimens. These values of tensile strength were then averaged to yield an average tensile strength. These average tensile strength values and the results of the IDT testing on unaged specimens (as outlined in Section 3.4.3) were used to calculate a Long-Term Ratio (LTR). The LTR was defined as the ratio of the tensile strength of the aged specimens to the tensile strength of the unaged specimens.

3.4.7 Compactibility

Relative compactibility of each specimen was determined from the data generated during compaction with the SGC. Output from the SGC consisted of a specimen's height for each gyration. Based on a specimen's height, the percent Theoretical Maximum Specific Gravity ($\%G_{mm}$) was calculated for each height. For this study, the $\%G_{mm}$ was determined for the following gyrations: 5, 8, 15, 20, 30, 40, 50,

60, 70, 80, 90, and 95. From this data, a compaction curve was generated for each specimen. Compaction curves were defined as $\%G_{mm}$ plotted versus the number of gyrations. When the number of gyrations were plotted on a logarithmic scale, these curves were essentially a straight line. A typical compaction curve is presented in Figure 3.18.

Compactibility was defined for a specimen as the slope of the compaction curve for that specimen. The slope was determined between 8 and 95 gyrations. These correspond to N_{ini} and N_{des} from the mixture design process. In general, mixtures having a steep slope are thought to be more resistant to rutting than mixtures with a flatter slope.

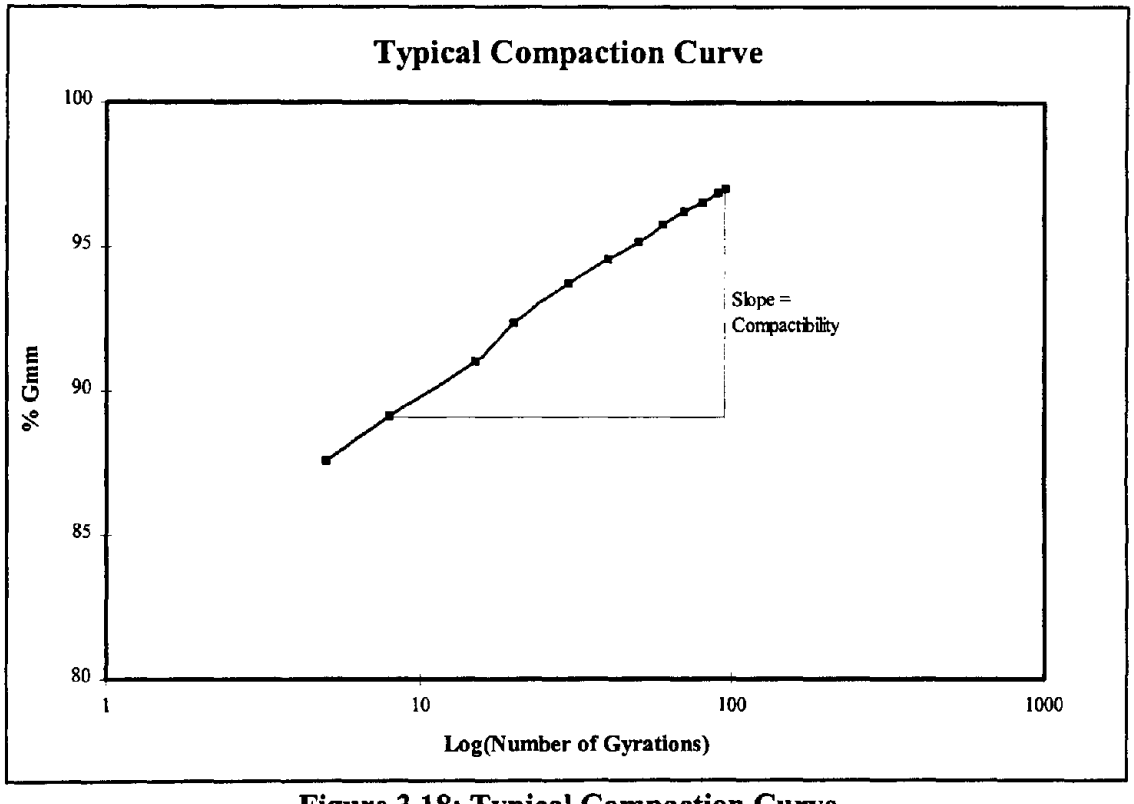

Figure 3.18: Typical Compaction Curve

Chapter 4 - Materials

Materials needed for this research study consisted of two asphalt binders, one source of aggregate, and baghouse fine samples. A total of ten different baghouse fines were used during the mortar and HMA mixture evaluation phases. All ten were used for the mortar evaluation, while five of the ten were used for the HMA mixture evaluation. Each of these materials are described in the following sections.

4.1 Asphalt Binders

This research study used two sources of one grade of asphalt binder (AC-20). This grade of asphalt cement was selected because it is considered a medium hard asphalt that would not hinder evaluation of the effects of the baghouse fines. The two asphalt cements were a Citgo AC-20 and a Shell AC-20. The Citgo AC-20 is a Venezuelan crude while the Shell AC-20 is from a Wood River, Illinois origin. The physical properties of these asphalt binders are presented in Table 4.1. Superpave testing was performed on these two asphalt binders. Results of these tests are presented in Chapter 5 (Table 5.6)

Temperature-viscosity charts for the Citgo AC-20 and Shell AC-20 are presented in Figures 4.1 and 4.2, respectively. These two charts were utilized to determine both the mixing and compaction temperatures for the HMA mixtures.

Mixing and compaction temperature was defined as the temperature at which the asphalt binder must be heated to produce a viscosity of 170 ± 20 cSt and 280 ± 30 cSt, respectively. Based on Figures 4.1 and 4.2, the mixing and compaction temperatures for both asphalt binders were selected as 160°C and 150°C, respectively.

Table 4.1: Physical Properties of Asphalt Binder Materials

Properties	Citgo AC-2O	Shell AC-2O
Viscosity - Absolute, 60° C, P	2252	1980
Viscosity - Kinematic, 135 ° C, cSt	490	390
Penetration - 25 ° C, 100g, 5 sec. 0.1 mm	84	64
Flash Point - Cleveland Open Cup, ° C	500	600
Solubility in Trichloroethylene - %	99.95	99.87

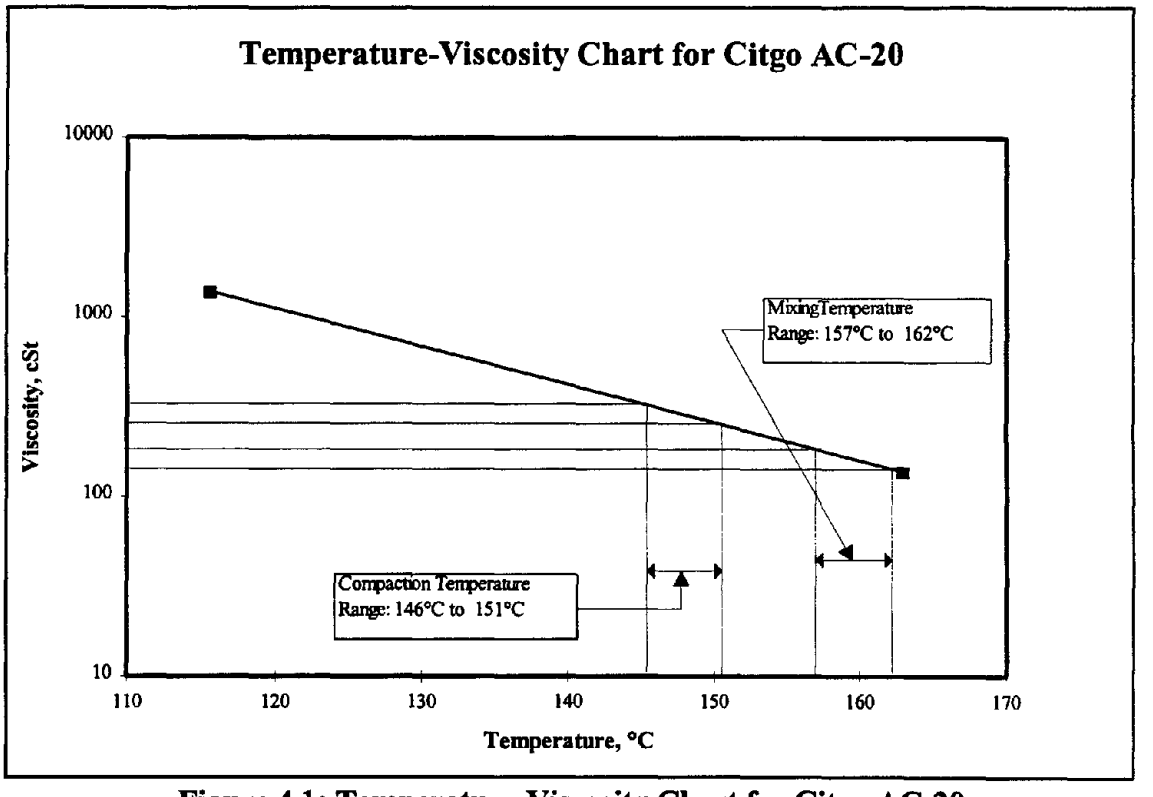

Figure 4.1: Temperature-Viscosity Chart for Citgo AC-20

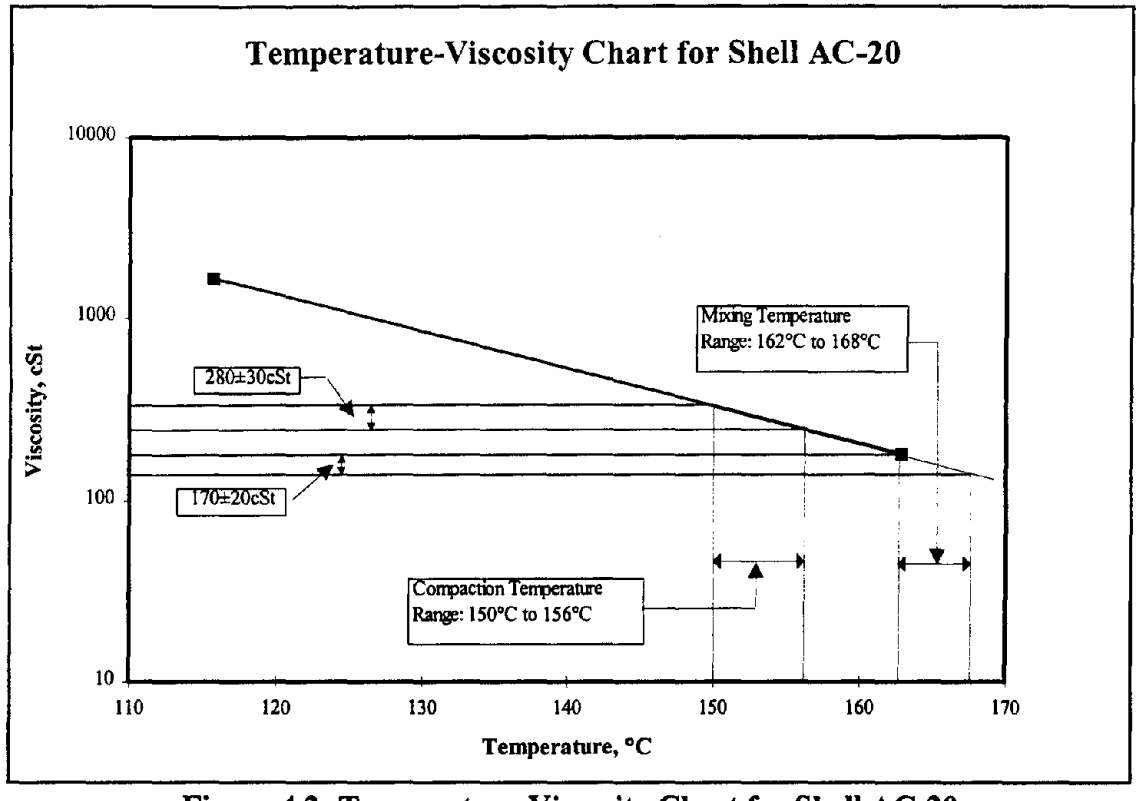

Figure 4.2: Temperature-Viscosity Chart for Shell AC-20

4.2 Aggregates

Only one source of aggregate, a quarried granite-gneiss obtained from a quarry near Spartanburg, South Carolina, was used for this project. Three different stockpiles of this aggregate were obtained for use in this research study. The stockpile designations were No. 6M, No. 789, and Regular Screenings. Aggregate from each stockpile was processed in the laboratory by screening the material into individual sieve sizes and then recombining to meet the gradation shown in Table 4.2. This is a dense-graded gradation used for high volume traffic pavements. Table 4.2 also shows that a 9.5 mm (3/8 in) sieve was added to the gradation specification. This was done because

of a discrepancy in the material retained on the 4.75 mm (No. 4) sieve between the No. 6M and No. 789 stockpiles. By adding this sieve, the fabricated gradations were more consistent. Figure 4.3 illustrates this gradation graphically on a 0.45 power gradation chart.

Table 4.2: SCDOT Type 1B Gradation Limits

Sieve Size, mm	Percent Passing (Specification Range)	Percent Passing (Project)
25.0	100	100
19.0	90-100	95
12.5	72-90	81
9.5	*	66
4.75	42-60	51
2.36	30-48	39
0.600	12-29	20.5
0.150	6-16	11
0.075	2-8	5

* Not in Specification

4.3 Baghouse Fines for Mortar and Mixture Evaluation

Baghouse fine samples from ten plants were selected and combined to produce ten baghouse fine combined samples which would represent an average of the five day production for each of the ten plants. Table 4.3 presents the plants from which the ten fines were obtained along with the configuration of the dust collection system for each plant.

Each baghouse fine combined sample was produced by sieving a plant's selected samples over a 0.075 mm (No. 200) sieve. Approximately 100 pounds of material was sieved for each combined sample. Once this amount was produced, the combined sample was thoroughly mixed to yield a uniform sample. Fine No. 9 in Table 4.3 was actually material minus the 0.075 mm (No. 200) sieve from the Regular Screenings stockpile. This fine constituted the control.

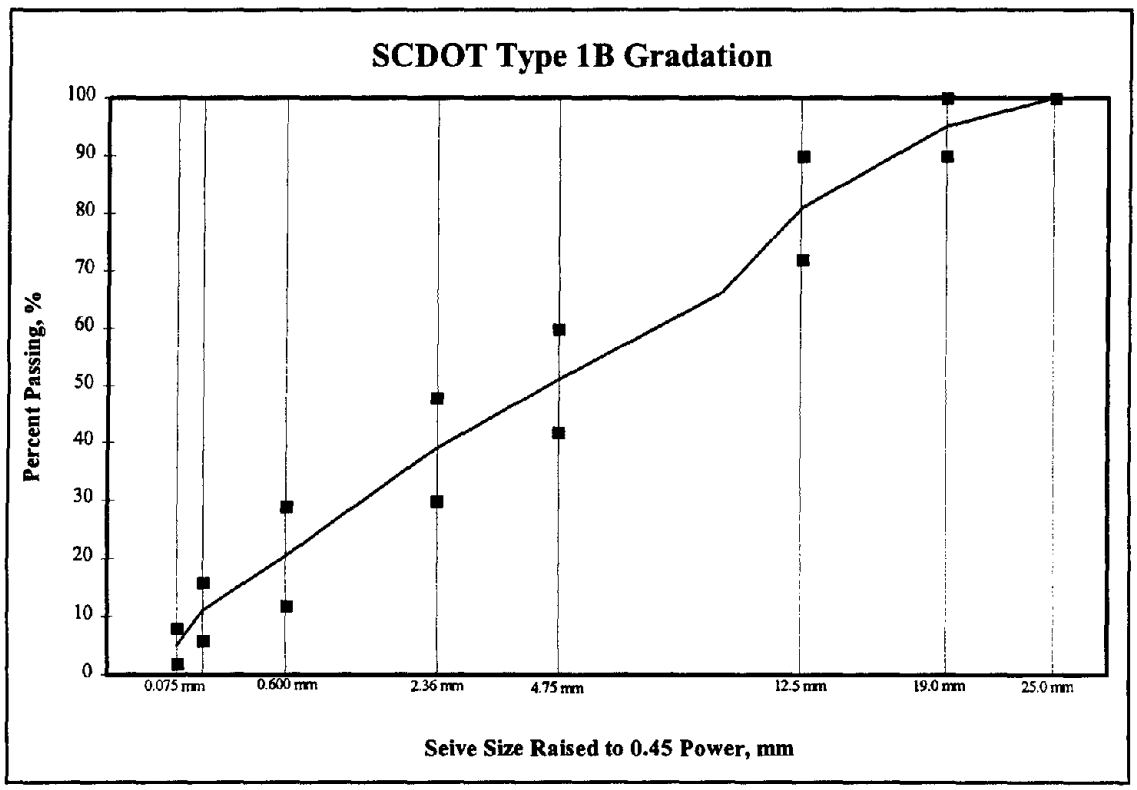

Figure 4.3: SCDOT Type 1B Gradation Used for Project

Table 4.3: Origin of Ten Baghouse Fine Combined Samples and The Configuration of the Dust Collection System.

Fine No.	Plant No.	Dust Collection System
1	6	Knockout Box and Baghouse
2	7	Baghouse
3	11	Baghouse
4	17	Baghouse
5	5	Cyclone and Baghouse
6	14	Knockout Box and Baghouse
7	15	Knockout Box and Baghouse
8	12	Baghouse
9	Control	N/A
10	1	Cyclone and Baghouse

CHAPTER 5: TEST RESULTS

The four main tasks outlined in the Plan of Study were conducted to establish a criteria for the inclusion of baghouse fines into HMA mixtures. Each of these tasks were designed to develop information to reach this objective. This chapter presents the results for each of these phases.

5.1 Results of Field Program

This section presents a discussion of the results of the field sampling program. Eighteen HMA producing facilities were sampled for baghouse fines. At each of these facilities, a representative of the National Center for Asphalt Technology obtained the baghouse fine samples. Actual documentation as to sampling times and each facility's equipment and operation is presented in Appendix D.

Another objective of the field sampling program was to determine the rate at which baghouse fines are reintroduced into the HMA mixing process. Of the 18 facilities sampled, only one had a configuration in which the rate could be determined. This plant utilized a surge bin between the baghouse and the reintroduction point. The dust collection system for this facility consisted of only a baghouse. The surge bin (Figure 5.1) allowed the full-flow of baghouse fines to be either reintroduced into the bin or wasted.

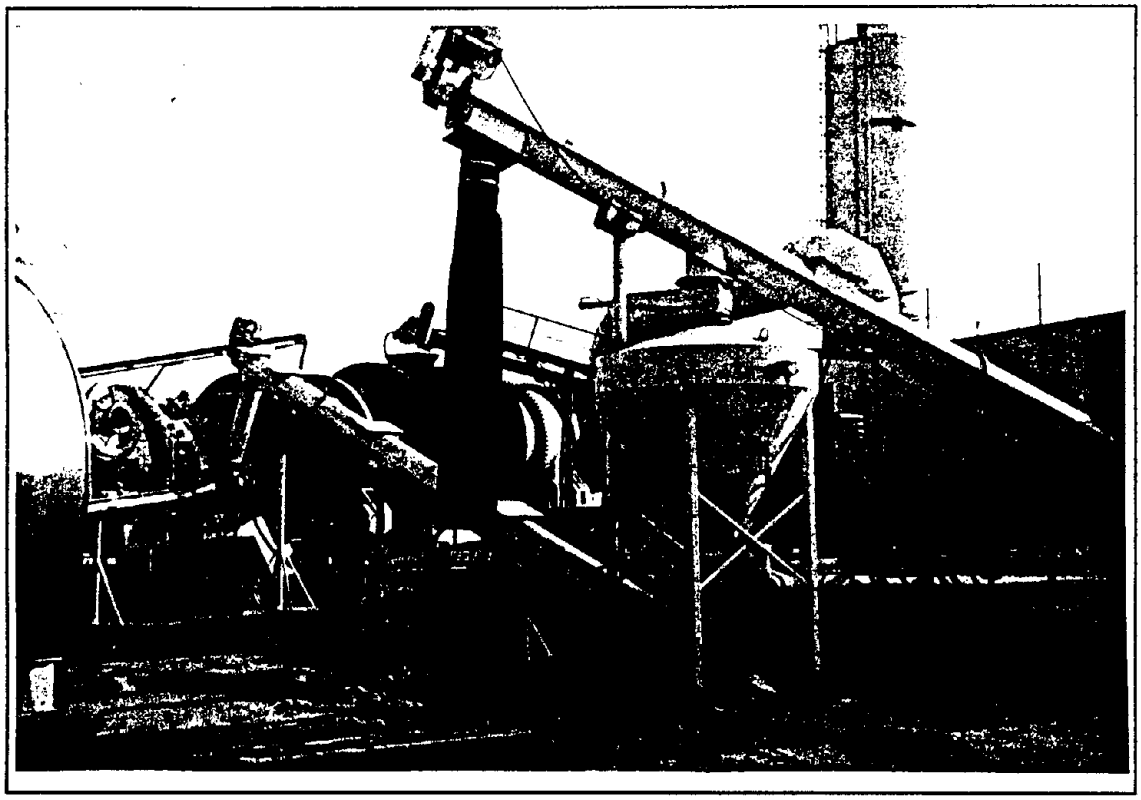

Figure 5.1: Surge Bin Utilized During Rate of Reintroduction Experiment

From Figure 5.1, it can be seen that the surge bin is fed by an auger chute incoming from the baghouse (right side of figure). Also, there is an auger chute leading from the bottom of the bin to the drum. This chute is utilized for the reintroduction of the baghouse fines into the HMA mixing process. A control valve is located at the top of the surge bin. If the control valve is closed, the full-flow of baghouse fines are sent over the surge bin to the wasting point located to the left of the bin.

In order to measure the rate of baghouse fines being reintroduced, the control valve on top of the surge bin was closed. A dump truck was tared on the scales located at the plant and placed under the wasting point. The baghouse fines were wasted into

the dump truck for a period of 20 minutes. Weighing the dump truck after the conclusion of wasting allowed the rate to be determined. Table 5.1 presents the results of this experiment. The rate of reintroduction was determined five times for this experiment.

Table 5.1: Results of Rate of Reintroduction Experiment

Property	Sample 1	Sample 2	Sample 3	Sample 4	Sample 5
Rate of Reintroduction of Baghouse Fines, tph	15.3	13.5	18.0	17.3	21.2
Rate of HMA production, tph	260	272	297	298	325
Percentage of Baghouse Fines in HMA Mixture, %	5.9	5.0	6.0	5.8	6.5
Percent of Baghouse Fines Finer Than 0.075 mm Sieve, %	50.2	52.0	51.1	52.1	55.0
Rate of Reintroduction of Baghouse Fines Finer Than 0.075 mm Sieve, tph	7.7	7.0	9.2	9.0	11.7
Percent of Mixture That Is Baghouse Fines Finer Than 0.075 mm Sieve, %	3.0	2.6	3.1	3.0	3.6
Job Mix Formula Specification for Percent Minus 0.075 mm Sieve, %	5.4	5.4	5.4	5.4	5.4
Percent of Material Finer Than 0.075 mm Sieve That are Baghouse Fines, %	55	48	57	56	67

The rate of reintroduction of baghouse fines ranged from 13.5 to 21.2 tons per hour (tph). During the rate of reintroduction testing, the plant operator monitored the rate of HMA production. The average values ranged from 260 to 325 tph. Based on these two quantities, the percentage of baghouse fines in the produced HMA mixture was determined. This quantity was calculated by dividing the rate of baghouse fines by

the rate of HMA production, expressed as a percentage. The percentage of baghouse fines in the HMA pavement ranged between 5.0 and 6.5 percent.

Samples were obtained each time the rate of reintroduction test was performed. For each of these samples, the percent material minus the 0.075 mm sieve was determined (washed). These values ranged from 50.2 to 55.0 percent passing.

Based on these values, the rate of baghouse fines finer than a 0.075 mm sieve being reintroduced was determined by multiplying the percent of baghouse fines finer than 0.075 mm and the overall rate of baghouse fines being reintroduced. These quantities ranged between 7.0 and 11.7 tph.

Using rate of baghouse fines finer than 0.075 mm and the average rate of HMA production, the percentage of the HMA mixture that was comprised of baghouse fines passing the 0.075 mm sieve was determined. This was accomplished by dividing the rate of minus 0.075 mm material and the rate of HMA production and expressing as a percentage. These values ranged from 2.6 to 3.6 percent.

The job-mix-formula for this project indicated that the actual percent material passing the 0.075 mm sieve should be 5.4 percent. By using this value and the percentage of baghouse fines smaller than 0.075 mm, the percentage of all material finer than a 0.075 mm sieve that was comprised of baghouse fines was determined. These values ranged from between 48 and 67 percent. The significance of these results is that more than 50 percent of the material passing the 0.075 mm (No. 200) sieve can come

from the baghouse fines. Therefore, changes in the properties of baghouse fines may have a significant effect on HMA mixtures.

5.2 Results of Baghouse Fines Laboratory Testing

This section presents the results of laboratory testing on the baghouse fines obtained during the field program. Appendix F presents the results for the particle size analyses performed on the samples obtained during the field sampling program. Based on these results, the mean particle diameter ranged from approximately 12 to 300 microns. This lower value of 12 microns was a baghouse sample from a plant that utilized a primary collector before the baghouse. The value of 300 microns also came from a plant with a primary collector, but this sample was a combined primary and baghouse fine sample.

Table 5.2 presents the results for the ten baghouse fine combined samples utilized for the mortar and HMA laboratory programs. Results are presented for the mean particle diameter, the D_{10} diameter, the D_{30} diameter, the D_{60} diameter, the Coefficient of Uniformity, the percent clay-sized particles, the Fineness Modulus, and the Specific Surface Area.

Based on Table 5.2, several observations can be made. First, Plant No. 3 had the lowest mean particle diameter at 16.1 μm. Interestingly though, this plant did not utilize a primary collector. Based on the literature and other data in the Table 5.2, plants that use a primary collector usually have finer baghouse fines. Next, the two samples that showed the largest range in particle sizes (as defined by C_u) were Plants

No. 4 and 7. Plant No. 4 used only a baghouse for the dust collection system, while Plant No. 7 had a knockout box before the baghouse. Reason would suggest that there would not be as large of variation in a baghouse fine with the presence of a primary collector before the baghouse.

Table 5.2: Results of Particle Size Analyses for the Ten Baghouse Fine Combined Samples

Fine No.	Mean Particle Diameter, μm	D_{10}	D_{30}	D_{60}	C_u	% Clay	FM	Specific Surface Area, cm^2/ml
1	20.5	1.51	4.89	18.27	12.14	14.2	3.06	14114
2	32.8	2.43	13.03	34.55	14.22	8.27	4.15	8901
3	16.1	1.12	2.74	9.32	8.32	22.17	2.34	20142
4	54.1	7.48	31.34	61.91	8.28	3.13	5.49	4296
5	25.3	2.19	8.79	24.44	11.15	9.01	3.57	10132
6	32.1	2.60	12.10	32.67	12.59	7.62	4.08	8621
7	38.4	2.13	12.30	37.75	17.76	9.41	4.28	9572
8	36.5	2.47	12.54	28.30	11.46	8.05	4.29	8729
9	41.0	3.43	16.54	33.49	9.75	5.92	4.63	6969
10	44.6	4.03	20.87	48.70	12.07	5.42	4.90	6313

Appendix G presents the results of the modified Rigden's voids test for the samples obtained during the field sampling task. Results are presented as the modified Rigden's percent voids. In addition, the results of the specific gravity tests performed are presented in these tables.

Table 5.3 presents the results of modified Rigden's voids test and specific gravity testing performed on the ten baghouse fine combined samples utilized for the

mortar and HMA laboratory tasks. Results in this table are presented for the modified Rigden's percent voids ($\%V_{dv}$), percent bulk volume ($\%V_{db}$), and the percent free asphalt in an asphalt binder/baghouse fine mortar ($\%V_{af}$). These latter two properties were calculated based on F/A ratios (volume) of 0.2, 0.3, 0.4, 0.5. Also presented in Table 5.3 are the results of the specific gravity tests for each of the ten combined samples.

Table 5.3: Results of Modified Rigden's Void Test and Specific Gravity Testing for the Ten Baghouse Fine Combined Samples

Baghouse Fine Combined Sample No.	F/A Ratio	$\%V_{dv}$	$\%V_{db}$	$\%V_{af}$	Specific Gravity
1	0.2	55.8	37.7	62.3	2.736
	0.3		52.2	47.8	
	0.4		64.6	35.4	
	0.5		75.4	24.6	
2	0.2	44.5	30.0	70.0	2.646
	0.3		41.6	58.4	
	0.4		51.5	48.5	
	0.5		60.1	39.9	
3	0.2	50.9	34.0	66.0	2.654
	0.3		47.0	53.0	
	0.4		58.2	41.8	
	0.5		67.9	32.1	
4	0.2	50.8	33.9	66.1	2.629
	0.3		46.9	53.1	
	0.4		58.1	41.9	
	0.5		67.8	32.2	

Table 5.3: Results of Dry Compaction and Specific Gravity Testing for the Ten Baghouse Fine Combined Samples

Baghouse Fine Combined Sample No.	F/A Ratio	% V_{dv}	%V_{db}	%V_{af}	Specific Gravity
5	0.2	62.6	44.5	55.5	2.701
	0.3		61.6	38.4	
	0.4		76.3	23.7	
	0.5		89.0	11.0	
6	0.2	49.8	33.2	66.8	2.728
	0.3		45.9	54.1	
	0.4		56.9	43.1	
	0.5		66.3	33.7	
7	0.2	55.2	37.2	62.8	2.750
	0.3		51.5	48.5	
	0.4		63.7	36.3	
	0.5		74.3	25.7	
8	0.2	46.7	31.3	68.7	2.757
	0.3		43.3	56.7	
	0.4		53.6	46.4	
	0.5		62.6	37.4	
9	0.2	39.5	27.6	72.4	2.648
	0.3		38.2	61.8	
	0.4		47.3	52.7	
	0.5		55.1	44.9	
10	0.2	53.1	35.6	64.4	2.763
	0.3		49.3	50.7	
	0.4		61.0	39.0	
	0.5		71.1	28.9	

The control Fine (Fine 9) had the lowest modified Rigden's percent voids. This would indicate that as the percentage of manufactured fines are increased in a HMA mixture, the modified Rigden's percent voids should decrease.

Methylene Blue testing was conducted on the ten baghouse fine combined samples. Table 5.4 presents the results of this testing. Results are presented as the Methylene Blue Value.

Table 5.4: Results of Methylene Blue Testing for the Ten Baghouse Fine Combined Samples

Baghouse Fine Combined Sample	Methylene Blue Value
1	2.8
2	3.0
3	11.0
4	0.5
5	1.0
6	0.5
7	0.5
8	0.8
9	0.5
10	0.5

Based on the study performed by Aschenbrener (22), only Fine 3 would be marginal. Each of the other baghouse fine combined samples would be expected to perform excellent with respect to moisture susceptibility. Aschenbrener stated that excellent fillers have a Methylene Blue Value of less than 6.

Results of the 30 particle size analyses (10 fines * 3 replicates) performed by mechanical means are presented in Table 5.5. Recall that mechanical particle size analysis encompasses both the use of sieves and hydrometer testing and was conducted by the Alabama Department of Transportation. This table also presents the particle size analyses for each of the 30 samples using the Coulter LS200 Particle Size Analyzer. These values were utilized to determine if a correlation exists between these two methods of particle size analysis.

Table 5.5: Results of Mechanical and Laser Diffraction Particle Size Analysis on 30 Samples

Sample	Rep.	Mechanical Analysis				Coulter LS200 Analysis			
		Percent Passing				Percent Passing			
		2000μm	420μm	75μm	2μm	2000μm	420μm	75μm	2μm
1	1	100.0	98.5	33.4	6.6	100.0	95.4	28.8	2.8
	2	100.0	99.1	35.3	7.1	100.0	96.5	30.7	3.0
	3	100.0	98.8	34.3	6.7	100.0	96.7	29.2	2.9
2	1	100.0	99.7	96.6	20.9	100.0	100.0	94.1	7.0
	2	100.0	100.0	97.7	23.6	100.0	100.0	93.1	7.0
	3	100.0	99.9	97.4	24.1	100.0	100.0	87.0	6.0
3	1	100.0	99.9	75.5	7.8	100.0	100.0	89.8	11.8
	2	100.0	100.0	74.2	1.4	100.0	100.0	81.0	10.7
	3	100.0	100.0	75.8	9.8	100.0	100.0	86.6	11.5
4	1	100.0	98.8	85.1	28.3	100.0	100.0	95.1	22.3
	2	100.0	99.7	86.3	27.4	100.0	100.0	100.0	26.8
	3	100.0	100.0	85.9	27.4	100.0	100.0	95.9	22.6

Table 5.5: Results of Mechanical and Laser Diffraction Particle Size Analysis on 30 Samples

Sample	Rep.	Mechanical Analysis Percent Passing				Coulter LS200 Analysis Percent Passing			
		2000μm	420μm	75μm	2μm	2000μm	420μm	75μm	2μm
5	1	100.0	99.8	98.7	2.3	100.0	100.0	98.8	14.6
	2	100.0	99.9	99.4	4.9	100.0	100.0	99.4	14.7
	3	100.0	99.9	99.2	2.1	100.0	100.0	99.9	15.6
6	1	100.0	99.8	96.5	10.3	100.0	100.0	53.7	3.8
	2	100.0	99.9	85.7	9.8	100.0	100.0	70.7	5.3
	3	100.0	99.9	86.9	7.9	100.0	100.0	86.9	5.8
7	1	100.0	97.7	26.6	5.2	100.0	93.1	23.0	1.3
	2	100.0	98.3	25.4	5.0	100.0	92.9	23.3	1.2
	3	100.0	97.4	26.2	5.0	100.0	91.7	22.8	1.2
8	1	100.0	87.8	38.7	7.2	100.0	97.1	46.6	3.9
	2	100.0	98.4	49.7	6.0	100.0	97.8	46.8	4.0
	3	100.0	98.8	49.5	6.6	100.0	88.9	44.3	3.7
9	1	100.0	98.6	17.4	6.4	100.0	93.4	16.6	1.7
	2	100.0	98.3	18.3	5.5	100.0	93.9	17.8	1.8
	3	100.0	99.1	17.8	6.5	100.0	94.9	18.9	1.7
10	1	100.0	88.3	52.7	4.8	100.0	71.5	52.9	5.3
	2	100.0	88.3	56.0	4.7	100.0	76.1	62.5	6.4
	3	100.0	88.8	59.0	3.0	100.0	89.7	46.6	4.0

Based on Table 5.5, for the coarser sieve sizes it looks like both methods are similar. However, below the 420μm size, there are differences in the data and it does not seem to be consistent.

5.3 Results of Mortar Testing

As stated previously, mortar testing completed on the TFOT and PAV aged mortars was conducted based on a one-half fractional factorial statistical design. Results of all mortar testing are presented in Appendix H. Cells within this table that are blank indicate no testing was performed. Results of testing on the neat asphalt binders is presented in Table 5.6. Based on the results of this testing of the neat binders, it appears that the Citgo AC-20 would be a PG 64-28 and the Shell AC-20 would be a PG 64-22.

Table 5.6: Results of Testing on the Two Neat Asphalt Binders

Aged State	Test		Asphalt Binder No. 1	Asphalt Binder No.2
Original, Unaged	SP, °C		47.7	48.9
	BV @ 135 °C, cP		487	412
	BV @ 175 °C, cP		108.3	104
	DSR @ 64 °C	G*, kPa	1.304	1.135
		δ	84.6	85.4
TFOT Aged Binder	DSR @ 64 °C	G*, kPa	3.177	2.892
		δ	79.7	81.0
TFOT and PAV Aged Binder	DSR @ 22 °C	G*, kPa	4741	6492
		δ	46.8	39.5
	BBR @ -18 °C	S, Mpa	268	327
		m-value	0.336	0.283

5.4 HMA Laboratory Testing

Five of the ten Fines were combined with mineral aggregate and asphalt binder to produce HMA mixtures. Fines 1, 2, 4, 5, and 9 were utilized during the HMA laboratory testing. To maintain similar nomenclature, the Fine numbers presented in this section correspond to the same Fine numbers utilized during the mortar test results. Therefore, AC1F1 similarly corresponds with a mortar comprised of Asphalt Binder No. 1 and Fine 1.

As stated previously, four mix designs were performed. Both asphalt binders were added to the granite-gneiss aggregate and mix designs were performed using both a 150 mm and 100 mm mold. The optimum asphalt binder content was defined as the asphalt binder content that yielded 4.0 percent air voids in total mix at the design number of gyrations. Results of these four mixture designs are presented in Table 5.7.

Table 5.7: Results of Mixture Designs

Asphalt Binder	Mold Size, mm	Optimum Binder Content
Asphalt Binder No. 1	150	4.1
Asphalt Binder No. 1	100	4.3
Asphalt Binder No. 2	150	4.3
Asphalt Binder No. 2	100	4.5

Based on Table 5.7, the particular gradation and two asphalt binders used for this project, the mold size did not influence the optimum binder content. In addition, the mix designs using both asphalt binders yielded similar optimum asphalt binder

contents. For this reason, an optimum asphalt binder content of 4.3 percent was chosen for both asphalt binders.

Indirect Tensile Tests (IDT) were performed on three specimens per combination of asphalt binder/baghouse fine/fine-to-asphalt ratio. Results for this testing are presented in Table 5.8. This table presents the average tensile strength (S_t) and tensile strain at failure (ϵ_t) per combination. Therefore, each value is the average of three specimens.

Table 5.8: Results of Indirect Tensile Testing

Asphalt Binder/Fine Combination	F/A Ratio	S_t, kPa	ϵ_t, mm/mm	Asphalt Binder/Fine Combination	F/A Ratio	S_t, kPa	ϵ_t, mm/mm
AC1F1	0.3	1138.5	0.00621	AC2F4	0.3	952.6	0.00675
	0.4	1245.4	0.00591		0.4	992.8	0.00660
	0.5	1284.1	0.00570		0.5	1024.4	0.00663
AC2F1	0.3	1176.3	0.00615	AC1F5	0.3	1117.3	0.00642
	0.4	1201.5	0.00591		0.4	1209.1	0.00636
	0.5	1321.8	0.00588		0.5	1229.0	0.00627
AC1F2	0.3	1088.3	0.00681	AC2F5	0.3	1114.1	0.00669
	0.4	1223.0	0.00624		0.4	1114.4	0.00621
	0.5	1205.0	0.00645		0.5	1284.7	0.00627
AC2F2	0.3	1146.1	0.00612	AC1F9	0.3	1032.4	0.00600
	0.4	1252.9	0.00591		0.4	1029.0	0.00639
	0.5	1255.1	0.00606		0.5	1029.6	0.00624
AC1F4	0.3	962.5	0.00645	AC2F9	0.3	1062.5	0.00627
	0.4	1008.7	0.00666		0.4	1189.6	0.00636
	0.5	836.7	0.00687		0.5	1176.8	0.00600

The lowest tensile strengths and highest strains at failure presented in Table 5.8 were for Fine 4. This particular fine had a large portion of mica. Mica is a soft elastic material and may explain why this particular fine had the lower tensile strengths and highest strains at failure.

Confined Repeated Load tests were performed on three specimens per combination of asphalt binder/Fine/fine-to-asphalt ratio combination. Results for this testing are presented in Table 5.9. This table presents the average Creep Stiffness and Creep Strain Rate per combination. Therefore, each value is the average of three specimens.

Confined repeated load deformation test data for two combinations are not presented (AC1F4 at a F/A ratio of 0.5 and AC2F4 at a F/A ratio of 0.3). The results for these two combinations were on the order of ten times higher than other test results for this fine. For this reason, the results were not reported.

Root-Tunnicliff Moisture Susceptibility tests were performed on six specimens per combination of asphalt binder/Fine/fine-to-asphalt ratio. Three specimens were tested in an unconditioned state and three were tested after vacuum saturating and a subsequent conditioning in a water bath at 60°C for 24 hours. Each of the six specimens were tested by the IDT test to determine tensile strength. For each combination, the results of the tensile strengths for the three unconditioned and three conditioned specimens were averaged. A tensile strength ratio (TSR) was then determined for each combination by dividing the average tensile strength of the

conditioned specimens by the average tensile strength of the unconditioned samples. The results for this testing are presented as TSR values for each combination in Table 5.10.

Table 5.9: Results of Confined Repeated Load Testing

Asphalt Binder/Fine Combination	F/A Ratio	Maximum Strain, mm/mm	Asphalt Binder/Fine Combination	F/A Ratio	Maximum Strain, mm/mm
AC1F1	0.3	0.0205	AC2F4	0.3	******
	0.4	0.0146		0.4	0.0250
	0.5	0.0154		0.5	0.0403
AC2F1	0.3	0.0194	AC1F5	0.3	0.0221
	0.4	0.0215		0.4	0.0131
	0.5	0.0390		0.5	0.0131
AC1F2	0.3	0.0438	AC2F5	0.3	0.0197
	0.4	0.0486		0.4	0.0625
	0.5	0.0254		0.5	0.0255
AC2F2	0.3	0.0250	AC1F9	0.3	0.0160
	0.4	0.0274		0.4	0.0235
	0.5	0.019		0.5	0.0235
AC1F4	0.3	0.0221	AC2F9	0.3	0.0252
	0.4	0.0347		0.4	0.0247
	0.5	******		0.5	0.0233

A typical requirement for a TSR value is 70 percent. Based on Table 5.10, approximately 70 percent of the combinations would pass this requirement. This can probably attributed to the fact that South Carolina requires lime to be added to HMA mixtures as an anti-stripping agent. Because of its particle size, the lime is probably

being picked up into the exhaust gas stream and taken to the baghouse. This would explain the high TSR values.

Table 5.10: Results of Root-Tunnicliff Moisture Susceptibility Testing

Asphalt Binder/Fine Combination	F/A Ratio	TSR, %	Asphalt Binder/Fine Combination	F/A Ratio	TSR, %
AC1F1	0.3	73.3	AC2F4	0.3	77.3
	0.4	72.6		0.4	75.8
	0.5	82.2		0.5	84.4
AC2F1	0.3	81.8	AC1F5	0.3	65.6
	0.4	76.0		0.4	80.9
	0.5	76.5		0.5	81.4
AC1F2	0.3	53.5	AC2F5	0.3	66.6
	0.4	64.6		0.4	67.8
	0.5	72.8		0.5	69.1
AC2F2	0.3	65.3	AC1F9	0.3	75.6
	0.4	69.4		0.4	83.6
	0.5	70.7		0.5	77.0
AC1F4	0.3	82.7	AC2F9	0.3	83.1
	0.4	72.6		0.4	82.8
	0.5	78.7		0.5	81.1

Long Term Aging procedures were performed on three specimens per mixture combination. Subsequent to the Long Term Aging procedures, each specimen was tested by the IDT test to determine the tensile strength. The tensile strengths for the three specimens of a given combination were then averaged. In addition, the results of the tensile strengths for the same combination as determined on the unaged specimens

during IDT testing were averaged. From these two averages a Long Term Ratio (LTR) was determined by dividing the average tensile strength of the aged specimens by the average tensile strength of the unaged specimens. Table 5.11 presents the results of this testing as LTR values.

Interestingly, Table 5.11 shows that some mixture combinations lost tensile strength and some gained tensile strength after the long term aging procedure. Combination AC2F1-0.5 lost approximately half of its tensile strength, while combination AC1F4-0.3 gained 30 percent after long term aging.

Table 5.11: Average Results of Long Term Aging Testing

Asphalt Binder/Fine Combination	F/A Ratio	LTR	Asphalt Binder/Fine Combination	F/A Ratio	LTR
AC1F1	0.3	0.79	AC2F4	0.3	0.92
	0.4	0.77		0.4	0.92
	0.5	0.85		0.5	1.15
AC2F1	0.3	0.75	AC1F5	0.3	1.02
	0.4	0.90		0.4	1.02
	0.5	0.56		0.5	1.08
AC1F2	0.3	0.91	AC2F5	0.3	1.13
	0.4	0.75		0.4	1.28
	0.5	0.78		0.5	0.97
AC2F2	0.3	0.78	AC1F9	0.3	0.94
	0.4	0.71		0.4	0.99
	0.5	1.08		0.5	1.03
AC1F4	0.3	1.30	AC2F9	0.3	1.00
	0.4	0.92		0.4	1.04
	0.5	1.11		0.5	1.13

Recall from the Plan of Study that twelve specimens per combination were compacted to 95 gyrations. Volumetric properties were determined for these twelve specimens. These properties included percent air voids in total mix (VTM), voids in mineral aggregate (VMA), and voids filled with asphalt binder (VFA). Volumetric properties for each combination are presented in Table 5.12. Values in this table represent the average volumetric property based on the twelve specimens compacted.

Table 5.12: Average Volumetric Properties for Each Combination Based on Twelve Specimens

Asphalt Binder/Fine Combination	F/A Ratio	VTM, %	VMA, %	VFA %	Asphalt Binder/Fine Combination	F/A Ratio	VTM, %	VMA, %	VFA, %
AC1F1	0.3	3.9	16.5	76.5	AC2F4	0.3	5.0	17.0	70.5
	0.4	3.0	15.7	80.7		0.4	4.6	16.6	72.5
	0.5	2.8	15.4	81.9		0.5	4.5	16.5	72.8
AC2F1	0.3	4.5	16.9	73.4	AC1F5	0.3	2.8	15.1	81.2
	0.4	4.0	16.3	75.6		0.4	2.8	14.9	81.5
	0.5	3.4	15.7	78.7		0.5	2.9	14.9	80.3
AC1F2	0.3	4.1	16.5	75.4	AC2F5	0.3	3.5	16.1	78.0
	0.4	3.4	15.9	78.6		0.4	3.2	15.7	79.3
	0.5	3.2	15.7	79.3		0.5	3.4	15.7	78.7
AC2F2	0.3	4.4	16.8	74.0	AC1F9	0.3	3.7	15.8	76.5
	0.4	4.1	16.4	75.0		0.4	3.5	15.5	77.6
	0.5	3.8	16.1	76.7		0.5	3.2	15.2	78.8
AC1F4	0.3	4.5	16.5	72.7	AC2F9	0.3	3.8	16.0	76.3
	0.4	4.0	16.1	75.0		0.4	3.5	15.6	77.6
	0.5	4.3	16.3	73.6		0.5	3.5	15.6	77.5

Based on a preliminary observation of the data in Table 5.12, it appears that with an increase in the percentage of baghouse fines, the voids in total mix and percent voids in mineral aggregate both decrease, while the percent voids filled with asphalt increases. Recall that the optimum asphalt content was defined as the asphalt content at which the voids in total mix were 4.0 percent at N_{des}. Based on Table 5.12, it appears that the different fines do affect the optimum asphalt content. Some combinations begin above 4.0 percent and then drop to below 4.0 percent as the percentage of baghouse fines increases. However, for some combinations, the voids in total mix are below 4.0 percent at the lowest percentage of baghouse fines.

The twelve specimens compacted to 95 gyrations were used to measure the relative compactibility of HMA mixtures containing the five Fines. Compactibility was defined as the slope of a specimen's compaction curve between N_{ini} and N_{max}. Results of the relative compactibility are presented in Table 5.13. Values within the table constitute the average compactibility of the twelve specimens per combination.

As a mixture's resistance to compaction increases, the compactibility should also increase. Therefore, reason would suggest that Fine 9 should have the highest compactibility values because it is a 100 percent manufactured fine aggregate. However, this is not the case. Fine 1 seems to have the highest compactibility values.

Table 5.13: Average Compactibility Results for the Twelve Specimens Per Combination

Asphalt Binder/Fine Combination	F/A Ratio	Compactibility	Asphalt Binder/Fine Combination	F/A Ratio	Compactibility
AC1F1	0.3	6.93	AC2F4	0.3	6.44
	0.4	7.24		0.4	6.55
	0.5	7.22		0.5	6.31
AC2F1	0.3	7.05	AC1F5	0.3	6.93
	0.4	7.11		0.4	6.87
	0.5	7.02		0.5	7.00
AC1F2	0.3	6.65	AC2F5	0.3	6.82
	0.4	6.77		0.4	7.05
	0.5	6.81		0.5	7.02
AC2F2	0.3	6.84	AC1F9	0.3	6.61
	0.4	6.79		0.4	6.54
	0.5	6.88		0.5	6.58
AC1F4	0.3	6.37	AC2F9	0.3	6.76
	0.4	6.20		0.4	6.64
	0.5	6.07		0.5	6.58

CHAPTER 6: ANALYSIS OF LABORATORY TESTING

6.1 Statistical Analysis Procedures

6.1.1 One-Way Analysis of Variance (ANOVA)

An analysis of variance (ANOVA) was used to determine if significant differences occurred between groups of data. This method was utilized for each of the three main laboratory phases. Assumptions for the ANOVA consist of assuming that all populations conform to a normal distribution, all population variances are approximately equal, and that all samples from the populations are independent (26).

The null hypothesis (H_0) for the ANOVA was that all population means were equal, while the alternative hypothesis (H_a) was that at least one population mean differed significantly from the remaining means. In addition, the ANOVA procedure allows interactions between these main effects to be analyzed.

The ANOVA separates the total variability of a population into two groups: the variation between treatment groups (or treatment effects plus random variation) and the variation within treatment groups (or random variation). Based on these two groups of variation, a variance ratio is determined. This ratio is called the *F-ratio* and is determined as follows (26):

$$F\text{-}ratio = \frac{MST}{MSE} \qquad \textbf{Eq.: 6.1}$$

where,

MST = Variance Between Treatments; and

MSE = Variance Within Treatments.

The *F-ratio* is then compared to a critical F value, F_{crit}. If the *F-ratio* exceeds F_{crit}, the means for a given population are said to be significantly different (reject H_o). This F_{crit} value is based on the number of degrees of freedom for the MST and MSE and the level of significance selected for testing. All analyses performed during this project were accomplished at a level of significance (α) of 0.05.

6.1.2 Student's t-Test

The Student's t-test is similar to the ANOVA in that it tests for significant dif nces, however the Student's t-test is best suited to determine significant differences between two sample populations. Assumptions for the Student's t-test consist of the two sample populations are independent, the theoretical distribution of sample means follows a normal distribution, and that the variances of the two populations should be approximately equal (27).

The H_o for the Student's t-test was that both population means were equal, while the H_a was that the two populations were significantly different. Again, the level of significance utilized was 0.05.

The Student's t-test procedure consists of calculating a t_{stat} value from the observed data. The t_{stat} is calculated by the following equation (27):

$$t_{stat} = \frac{(\mu_\Theta - \mu_\theta)}{s_p \sqrt{(\frac{1}{n_\Theta} + \frac{1}{n_\theta})}} \qquad \textbf{Eq.:6.2}$$

where:

μ_1 = mean of sample population No. 1

μ_2 = mean of sample population No. 2

s_p = pooled standard deviation of the two sample populations

n_1 = sample size for population No. 1

n_2 = sample size for population No. 2

The absolute value of t_{stat} is then compared to a critical value of t, t_{crit}. If t_{stat} is greater than t_{crit} then H_o is rejected and H_a is accepted. T_{crit} is dependant on the degrees of freedom and level of significance.

6.1.3 Duncan's Multiple Range Test

Duncan's multiple range test (DMRT) was chosen as the multiple comparison test for this project. The DMRT is useful in comparing population means that are found significantly different with the ANOVA by ranking the different population means to show which are significantly different. Assumptions for the DMRT are identical to those for the ANOVA; however, this test is based on the sampling distribution of the range of sample means, not the variance of the sample means (26).

The range of sample means for a given set of sample populations is compared to a critical value based on the percentiles of the sampling distribution of the range. The critical value (r_α:p,f) is based on the number of means being compared (p) and number of degrees of freedom(f) at an α. Again, a level of significance of 0.05 was selected for this procedure.

In the procedure, the sample population means are ranked in order from the smallest to the largest and the range is tested. The range is considered to be significant if it exceeds the critical range. The critical range is calculated as follows (26):

$$Critical\ Range = \frac{s}{\sqrt{n}} * r_\alpha{:}p,f \qquad \textbf{Eq.: 6.3}$$

where:

s = standard deviation of sample populations

n = total number of observations

r_α:p,f = critical value

Beginning with the smallest and largest sample population means in the ordered list, the range between means are considered not significant if the range between the means does not exceed the critical range. If not significant, testing ceases. If the range is significant, the sample population means are declared not equal and assigned different letters. Next, the range of two sets of (k-1) sample population means is tested for significance, where k = the total number of sample populations being tested. Testing

continues until eventually pairs of adjacent means are tested. Finally, sample population means with differing letters are significantly different. Sample populations with the same letter are not significantly different.

6.1.4 Grubb's Test For Outlying Observations

The statistical procedure used to determine outliers is called the "Grubbs Test for Outlying Observations" (28). For a sample population, this procedure utilizes the average and standard deviation to statistically identify outliers. The procedure encompasses calculating a T-value as follows (28):

$$T = \frac{\bar{x} - x_i}{s} \qquad \textbf{Eq.: 6.4}$$

where:

$\bar{x}$ = Average value for a sample population

x_i = Value being tested as outlier

s = Standard deviation of sample population

The absolute value of this T-value is then compared to a critical value of T (T_{crit}). If the T-value is greater than T_{crit}, the observation x_i is said to be an outlier. This critical value is dependant on the number of observations and the level of significance in testing. For all analyses, the level of significance was selected as 0.05.

6.2 Analysis of Laboratory Testing of Baghouse Fine Samples

One of the primary objectives of this research project was to evaluate the variability in the physical properties of the baghouse fines obtained during the field program. The two tests performed to measure the physical properties of the baghouse fines were the particle size analysis using the Coulter LS200 PSA and the Modified Rigden's Voids test.

Additionally, an analysis was performed to determine if particle size analyses performed with both the Coulter LS200 and by mechanical means were statistically similar.

6.2.1 Analysis of the Coulter LS200 Particle Size Analyzer Data

Large amounts of data were accumulated as a result of the particle size analyses performed on the baghouse fine samples obtained during the field program. Recall that data such as mean particle diameter, D_{10} particle diameter, coefficient of uniformity, percent clay-size particles, etc. were generated based on these particle size analyses. To evaluate the variability in the particle sizes for the baghouse fines, the mean particle diameter (MPD) data was selected for analysis because it represents an average particle diameter within a baghouse fine sample.

The first step in the analysis of the MPD data was to develop frequency distribution charts for each plant sampled. This procedure consisted of dividing the data for a given plant into classes (or ranges) of equal width. The number of data that fell into each class was then counted. Based on the number of data within a given class and

the total number of data for the plant, the percentage of data that fell into each class was determined. This method of grouping was chosen because it readily illustrates the range of the MPD. Figures 6.1 through 6.18 present the frequency distribution charts for each of the 18 plants sampled.

An observation based on Figures 6.1 through 6.18 is that most of the plants using primary collectors showed MPD data that followed a normal distribution. Figure 6.13 is a good example. This could be a result of variations in the coarser fractions entering the dust collection system. If the primary collector captures these coarser fractions, the MPD data for baghouse fines would not show these variations.

Next, Grubb's Test for outlying observations was used to determine if outlying data existed for a given plant. Outliers indicate an individual data observation that is not indicative of the overall pattern of the data. The significance of outliers is that they indicate a test result is significantly different than a sample population. If a consistent cause for outliers can be distinguished, the cause can be corrected.

Plants No. 2, 5, 6, 8, 12, and 14 exhibited outliers in their data as illustrated on their respective frequency distribution charts. Figure 6.2 shows that the outlier for Plant No. 2 represents a MPD of 276.8 μm. This point is obviously outside the overall pattern of the data. Evaluation of the field sampling logs for this plant indicated a possible reason why this observation is an outlier. The sample was obtained as the plant started up in the morning. A sample obtained at start-up is dependent on whether:

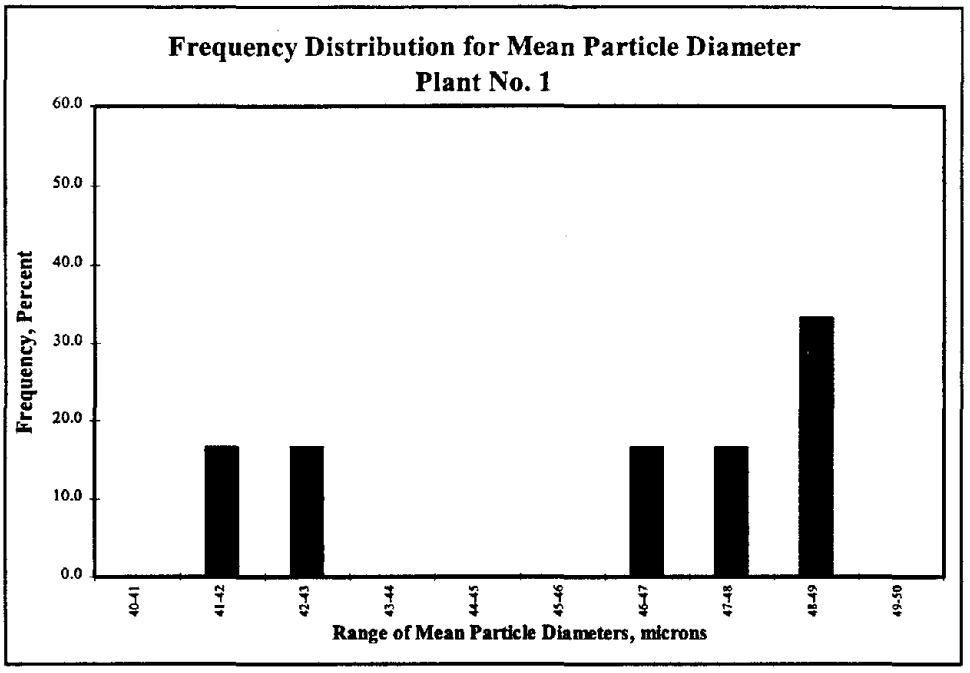

Figure 6.1: Frequency of MPD Data For Plant No. 1

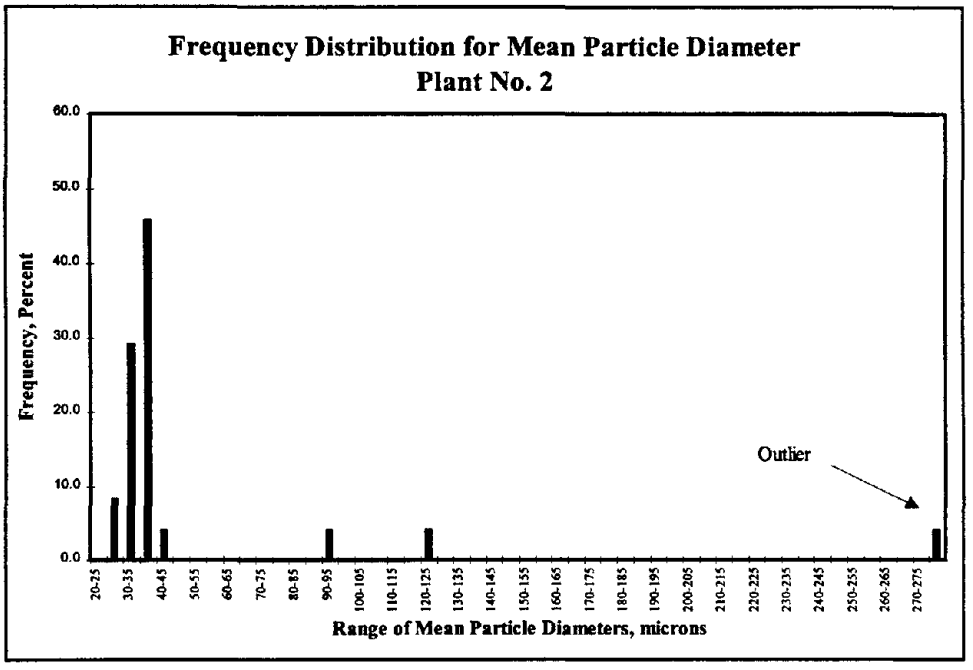

Figure 6.2: Frequency of MPD Data For Plant No. 2

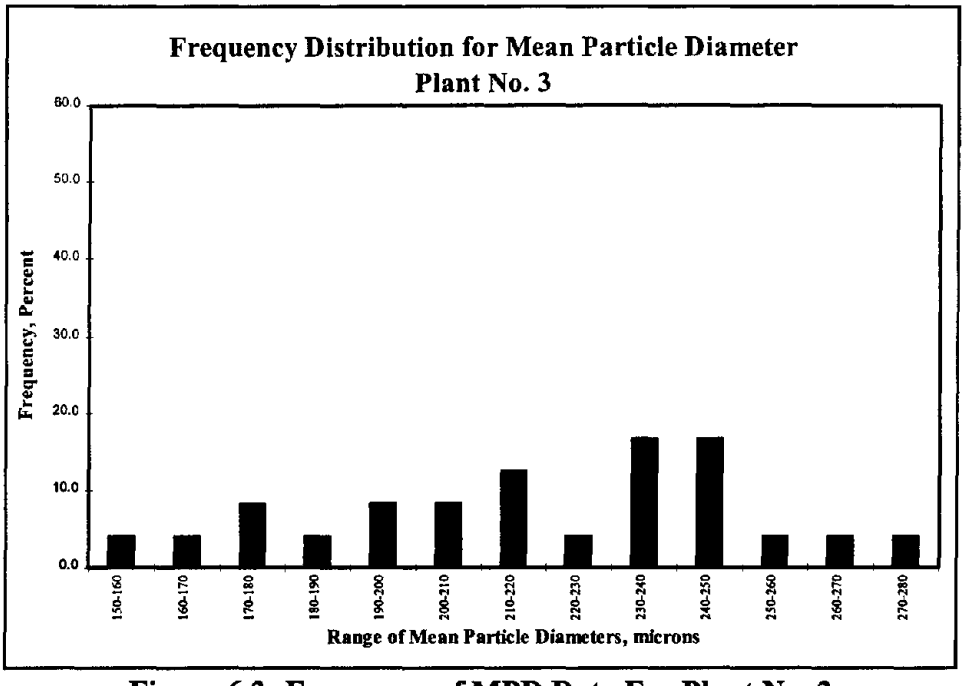

Figure 6.3: Frequency of MPD Data For Plant No. 3

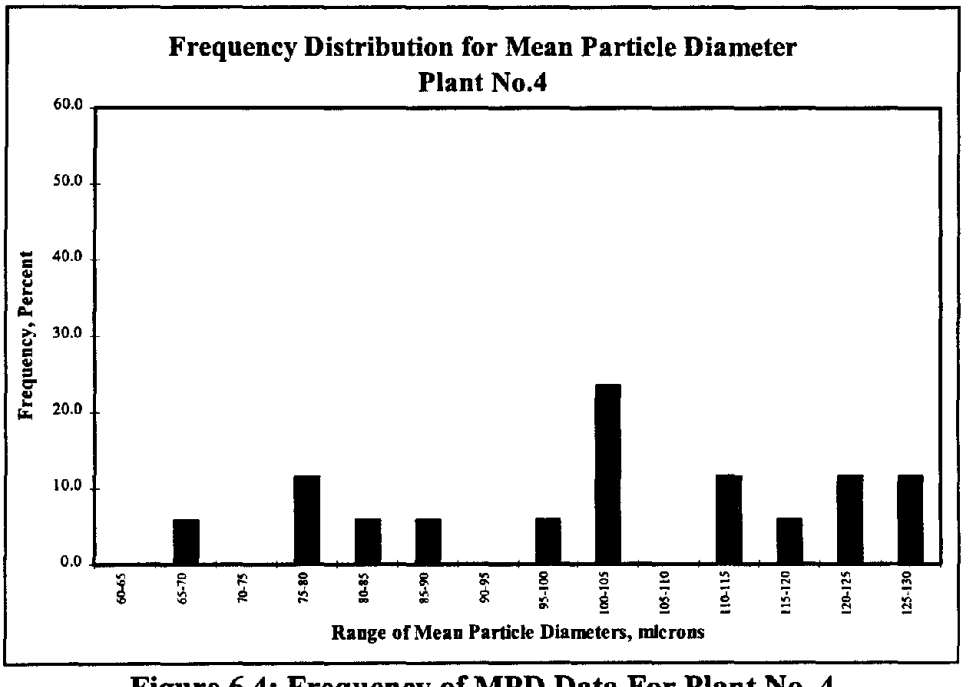

Figure 6.4: Frequency of MPD Data For Plant No. 4

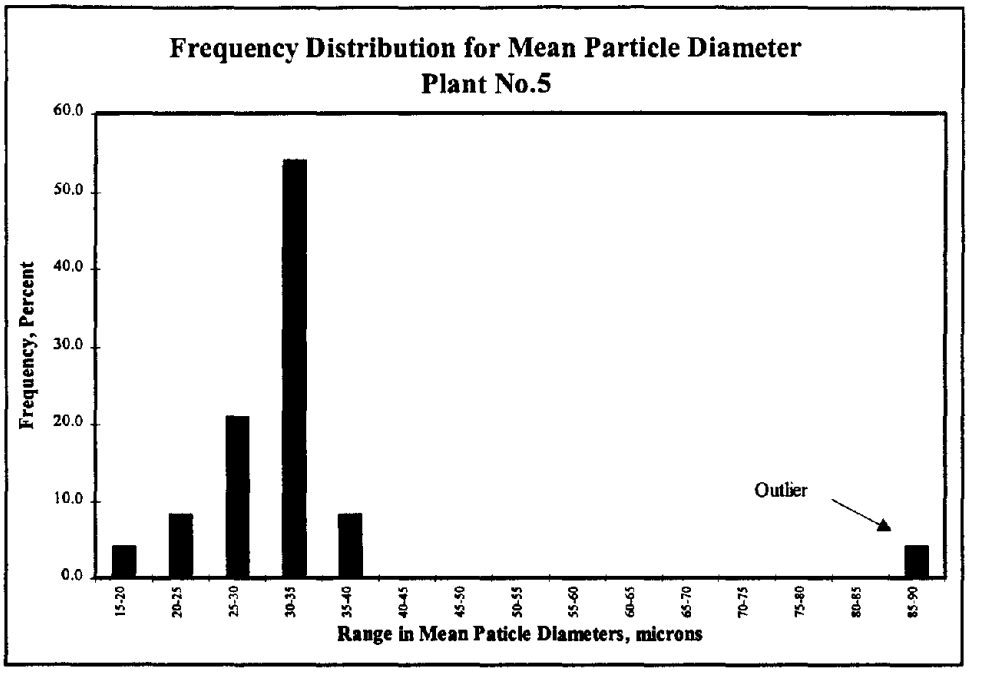

Figure 6.5: Frequency of MPD Data For Plant No. 5

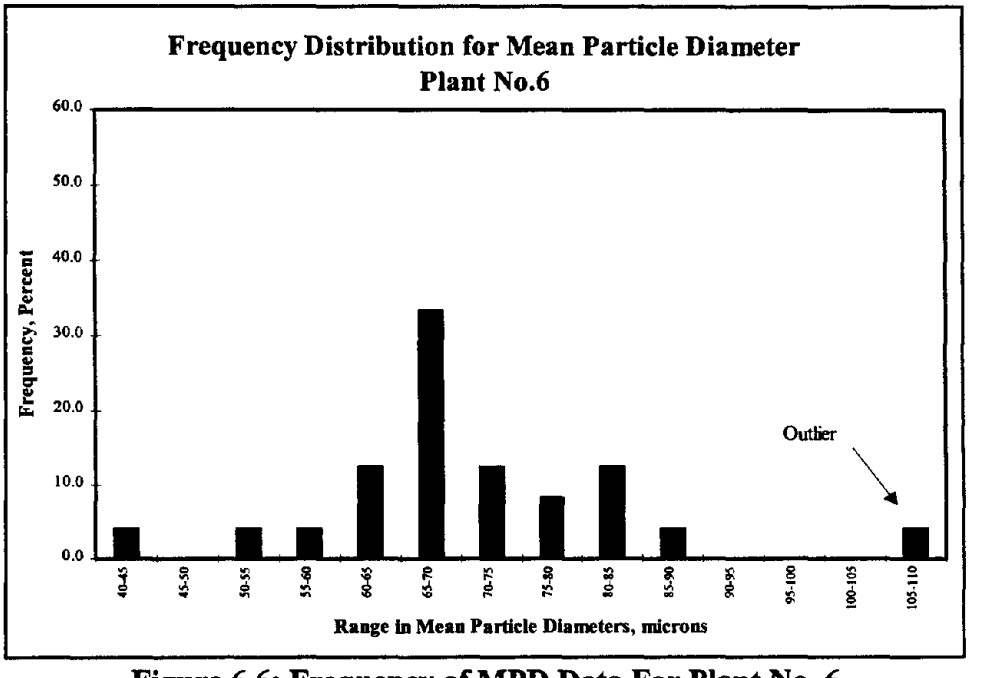

Figure 6.6: Frequency of MPD Data For Plant No. 6

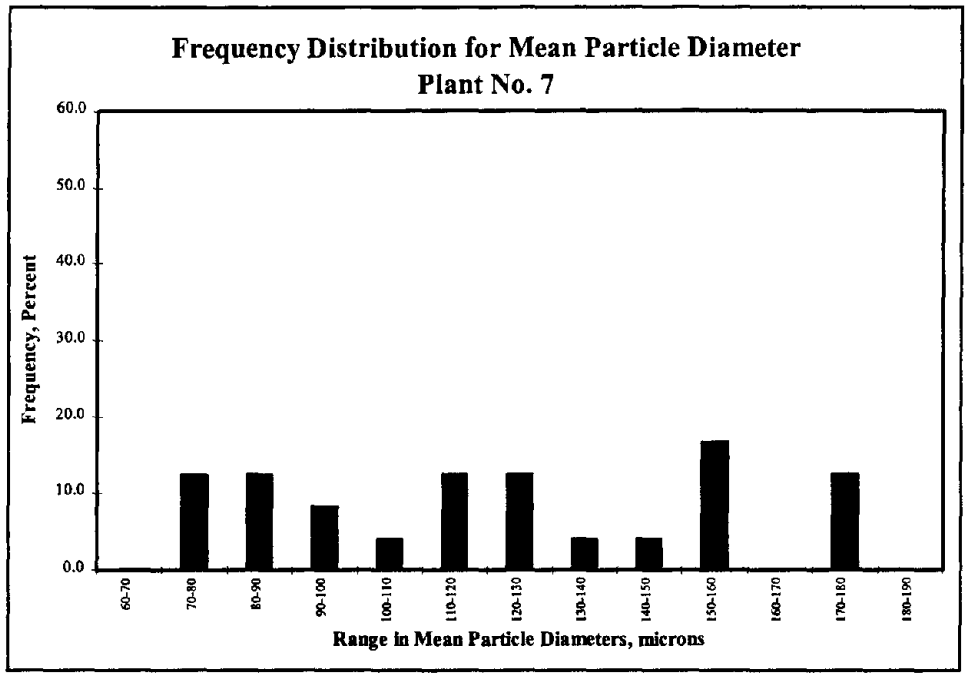

Figure 6.7: Frequency of MPD Data For Plant No. 7

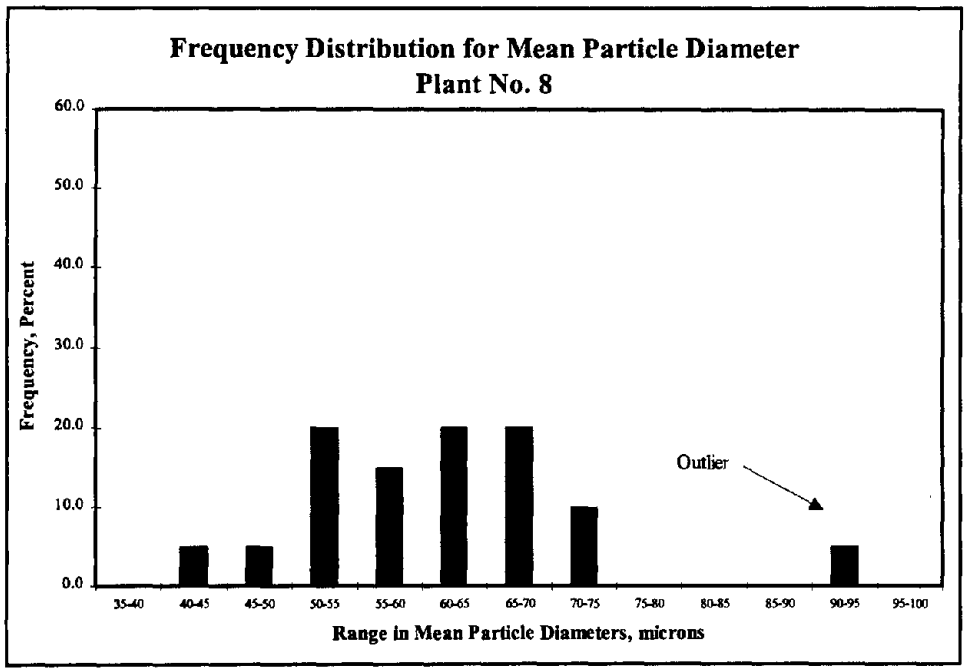

Figure 6.8: Frequency of MPD Data For Plant No. 8

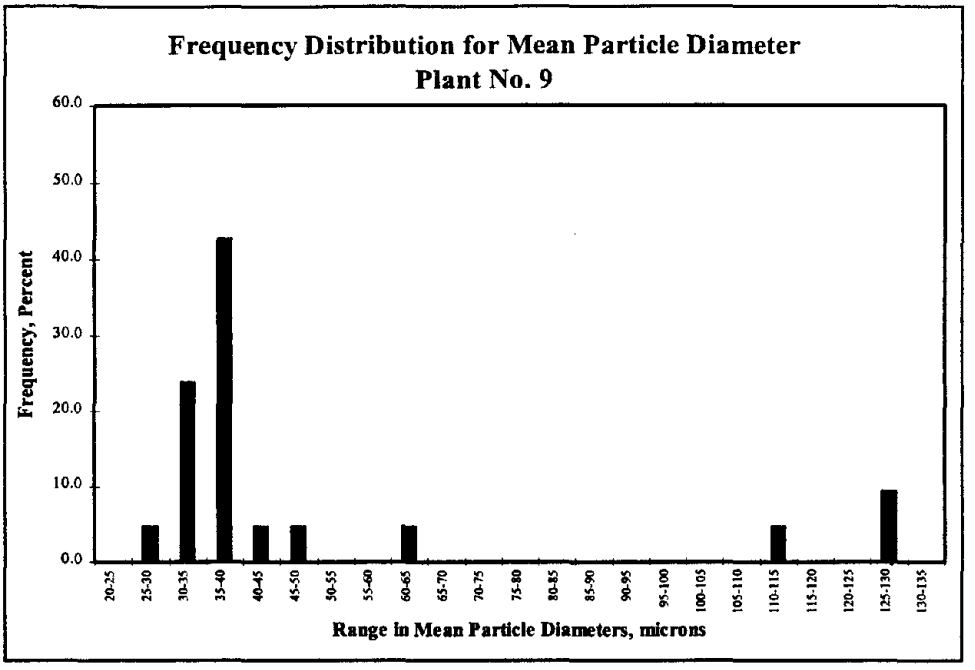

Figure 6.9: Frequency of MPD Data For Plant No. 9

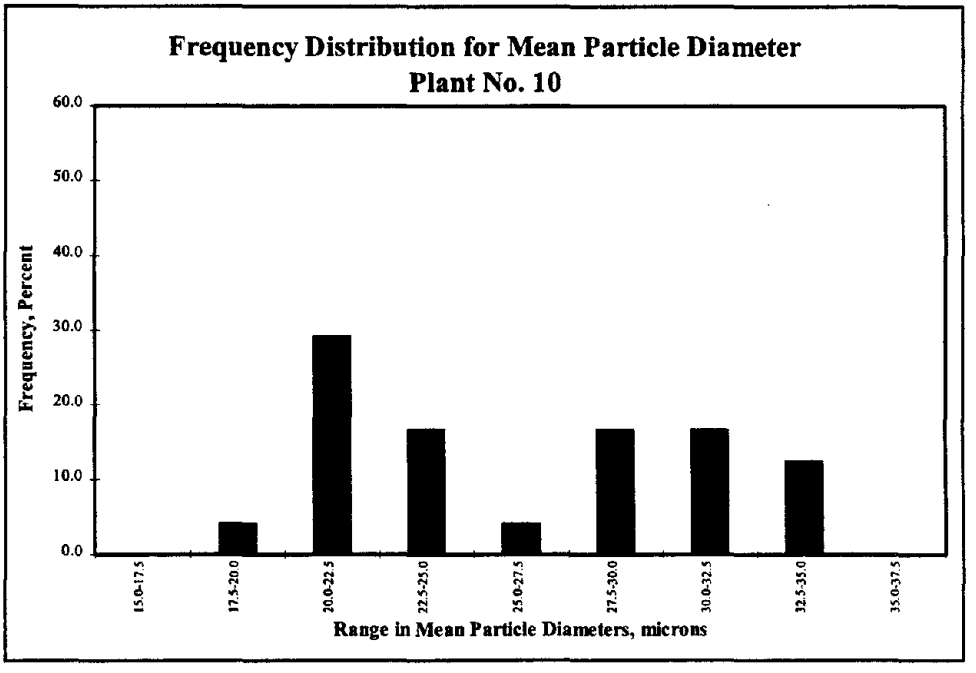

Figure 6.10: Frequency of MPD Data For Plant No. 10

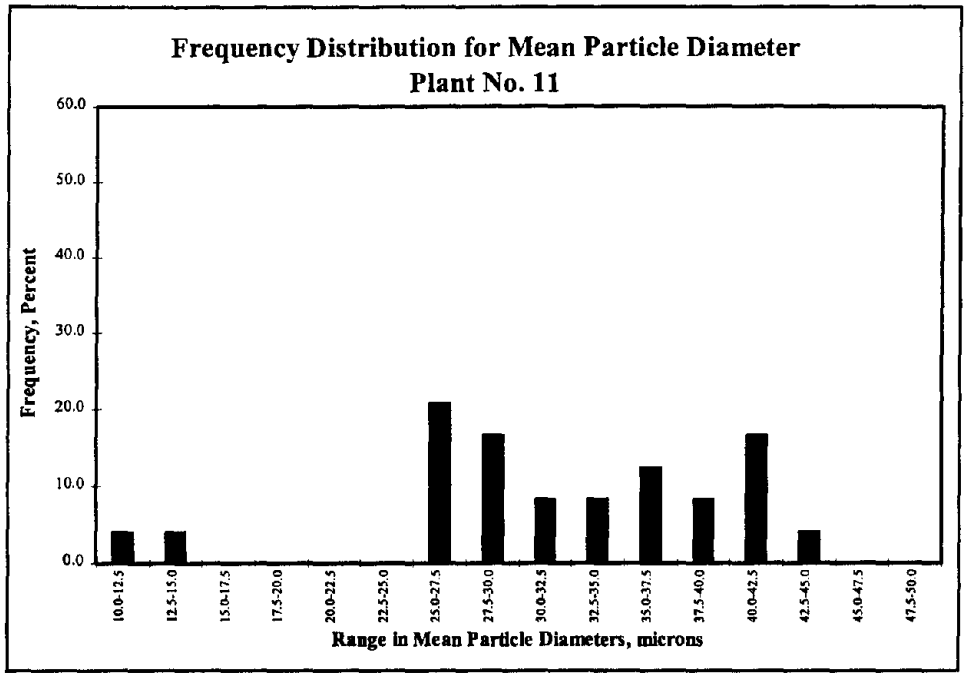

Figure 6.11: Frequency of MPD Data For Plant No. 11

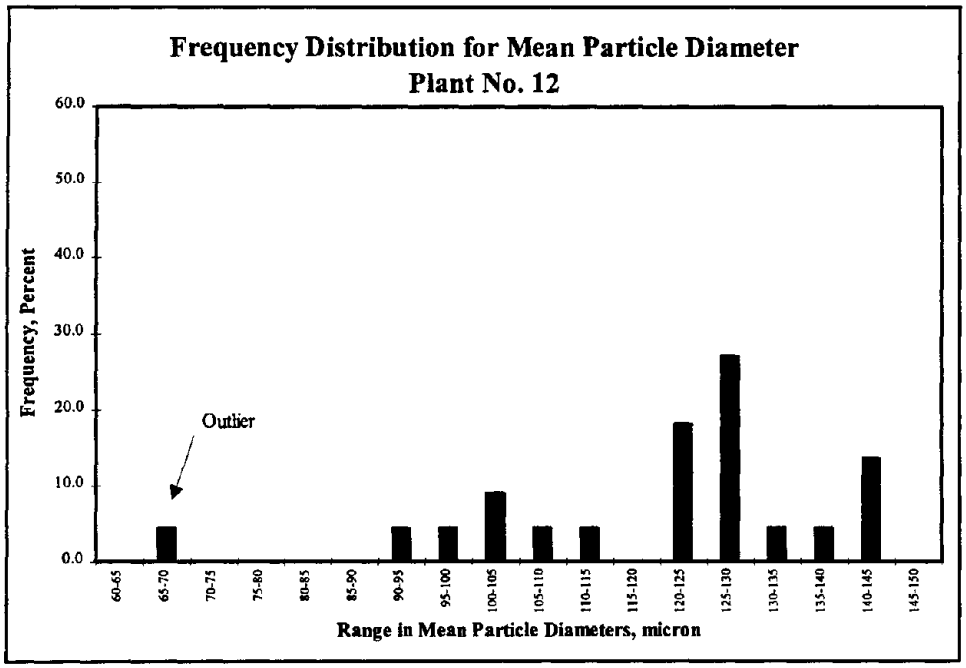

Figure 6.12: Frequency of MPD Data For Plant No. 12

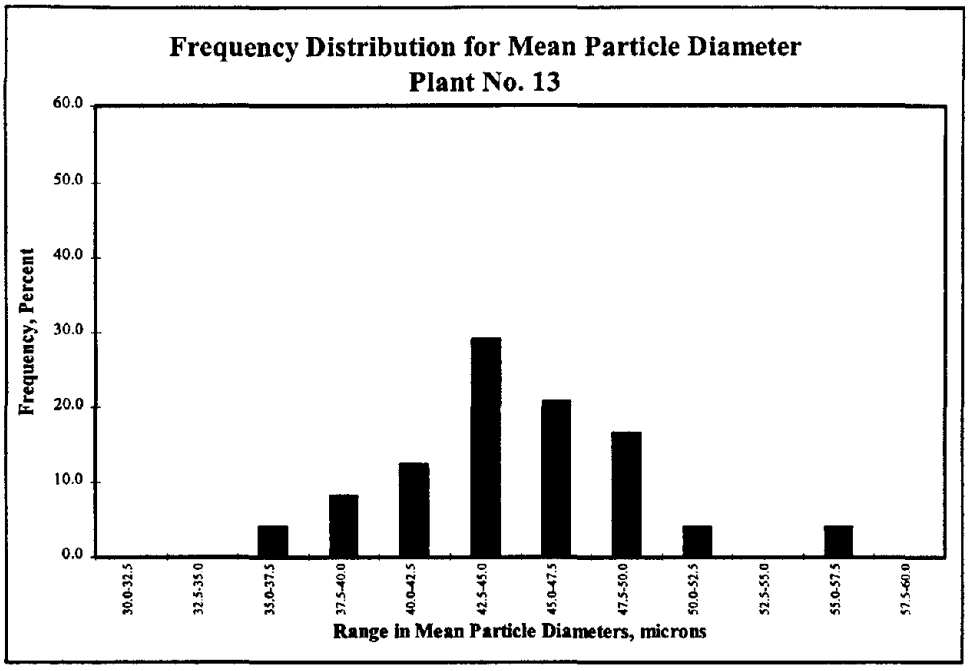

Figure 6.13: Frequency of MPD Data For Plant No. 13

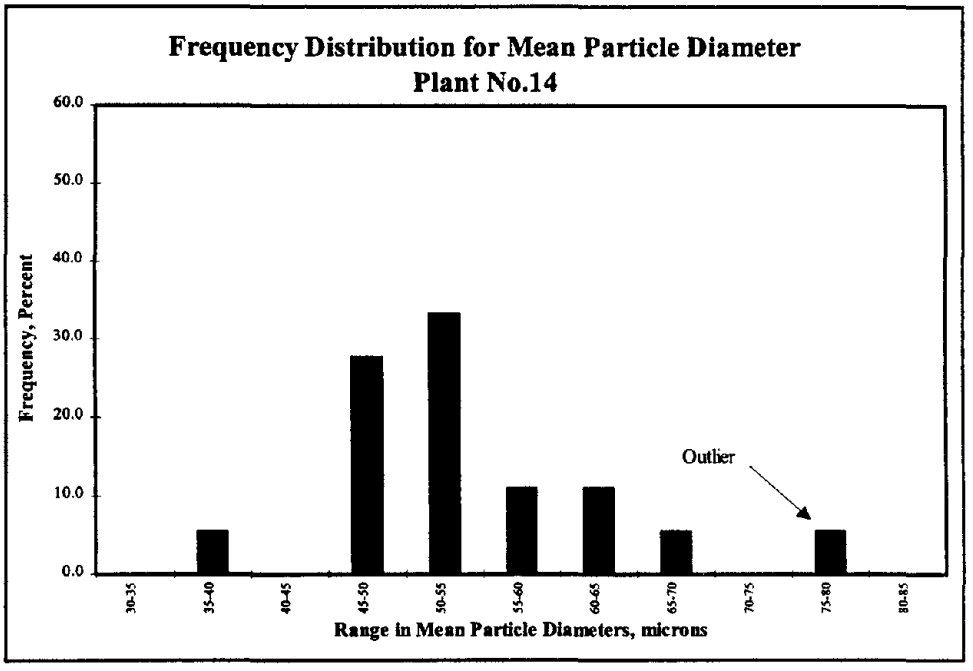

Figure 6.14: Frequency of MPD Data For Plant No. 14

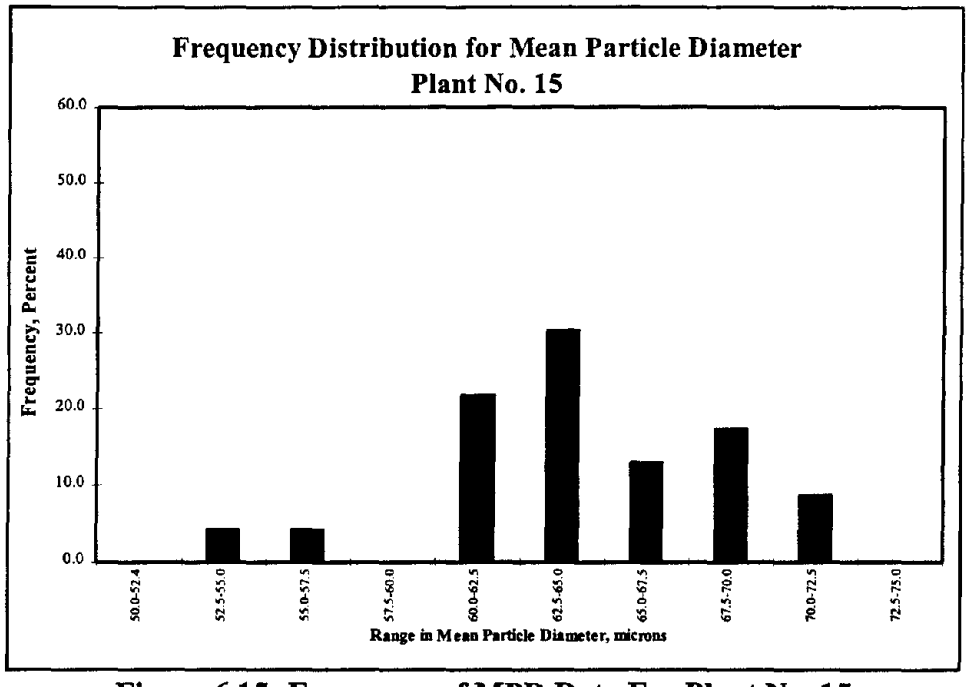

Figure 6.15: Frequency of MPD Data For Plant No. 15

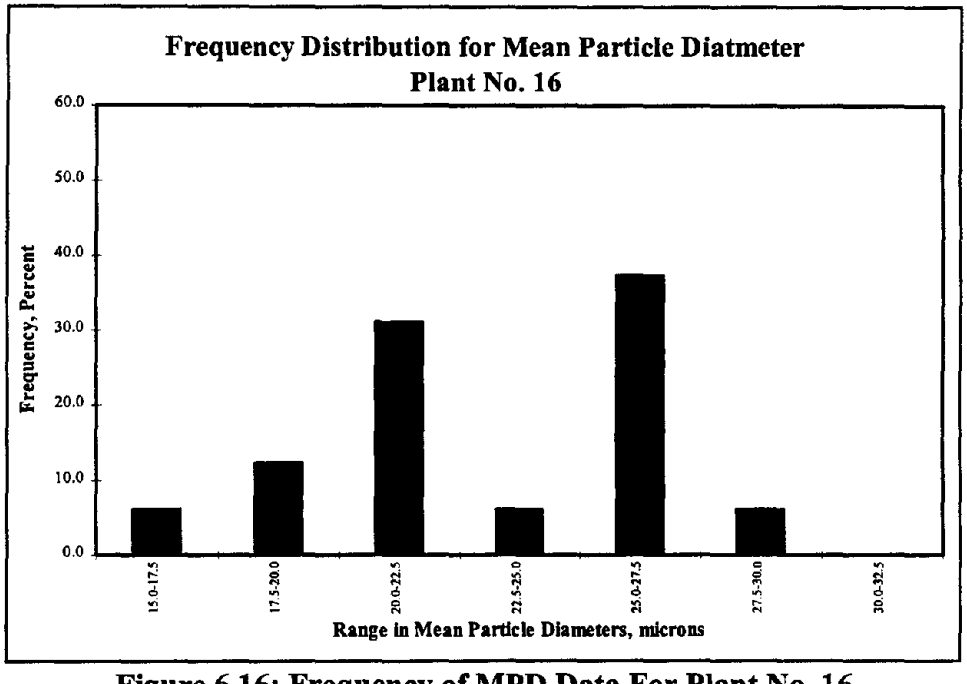

Figure 6.16: Frequency of MPD Data For Plant No. 16

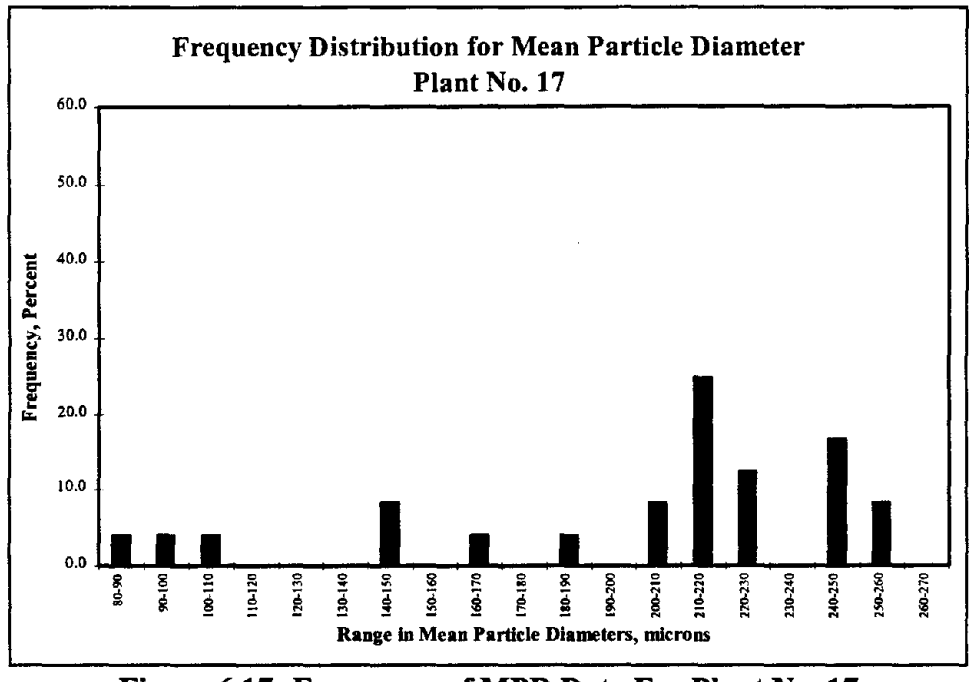

Figure 6.17: Frequency of MPD Data For Plant No. 17

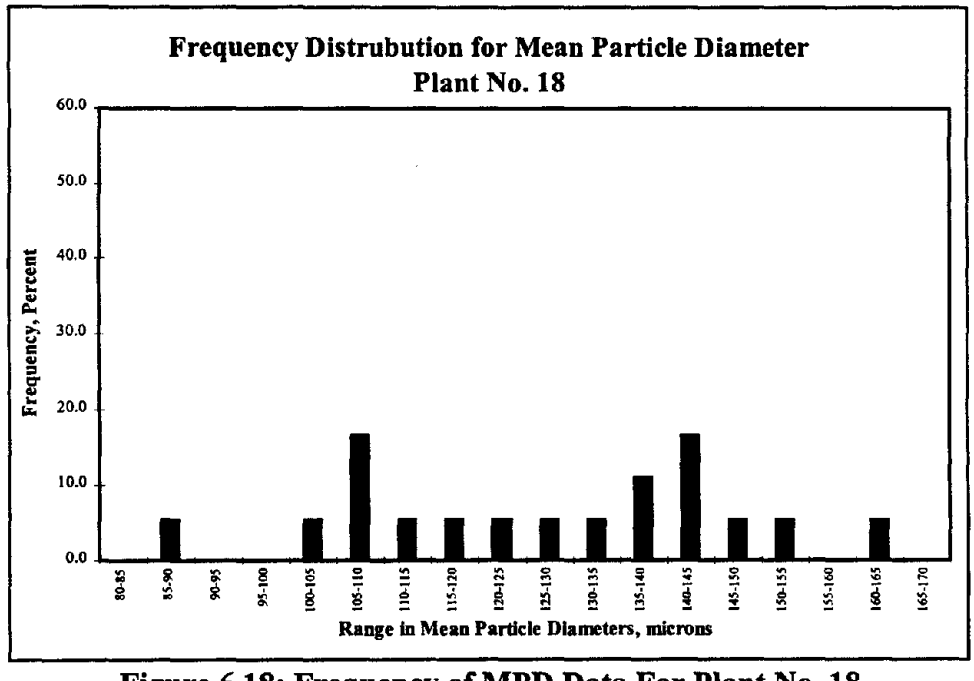

Figure 6.18: Frequency of MPD Data For Plant No. 18

1) the baghouse was cleaned out after the previous day of production;

2) the proper gradation was being sent through the plant (i.e., the gradation going through the plant is coarser or finer than the actual production gradation); and

3) asphalt was being injected into the drum. Plant No. 2 was a drum mix plant. If the asphalt binder was not being injected at the time the sample was taken, the dust created in the drum could not adhere to larger particles that were coated with asphalt and therefore all would be sent to the dust collection system.

The data point that is an outlier for Plant No. 5 represents a MPD of 85.5 μm. As with Plant No. 2, this sample was obtained during start up. Additionally, the field sampling log indicated that a heavy rain fell the night before the sample was obtained. The auger chute in which the sample was obtained had holes cut into the top to allow the contractor to clean the auger chute. Because of the rain, water had entered through these holes and had saturated the fines within the chute. This caused the fines to "stick" together and form dust cakes. These dust cakes fell from the auger chute into the sampling container. If these dust cakes were not completely broken up prior to the particle size analysis, the results could be nonrepresentative of the actual particle sizes within the baghouse fines. Either of these two reasons could explain why this sample was an outlier; however, the sample being obtained at start up is probably the best explanation.

The data point that is an outlier for Plant No. 6 represents a MPD of 108.2 μm. Evaluation of the field sampling logs did not indicate a possible reason as to why this sample is an outlier. However, several possibilities could have caused this sample and other samples to be outliers:

1) The contractor could have been making adjustments to the gradation, causing more coarse or fine aggregate in the gradation;
2) The sample could have been taken as the bags within the baghouse were being pulsed, causing a nonrepresentative sample; and
3) The plant could have just increased or decreased the rate of HMA production causing an increase or decrease in the drum gas velocity.

The data points that are outliers for Plants No. 8, 12, and 14 represent MPD's of 92.6, 69.7, and 75.1 μm, respectively. Again, evaluation of the field sampling logs for each plant did not indicate possible reasons as to why these samples are outliers. The possibilities presented for Plant No. 6 could have caused these outliers.

Based on these discussions on the different outliers, the outlying samples from Plant No. 2 and Plant No. 5 were discarded from further analyses. The two reasons given as to why each sample was an outlier illustrates that these samples are non-typical. However, the samples from Plants No. 6, 8, 12 and 14 were not discarded from further analyses. The reasons given as to why these samples were outliers are typical operating procedures and therefore do not indicate non-typical samples.

Next in the analyses of these data was to develop a chart that showed the variations in MPD for each plant and between plants. This was accomplished by determining the average ($\bar{x}$) and standard deviation (s) for the MPD data of each plant. These properties were then used to develop a chart that shows the average plus or minus two standard deviations ($\bar{x}\pm 2s$) for each plant (Figure 6.19). Plus or minus two standard deviations was selected because 95 percent of the data should fall within this range. This chart presents $\bar{x}$ as a horizontal black line. The vertical edges of the gray-shaded boxes represent $\bar{x}+2s$ and $\bar{x}-2s$. Also included on this figure is the configuration of the dust collection system. The "Cyc+BH" indicates that a cyclone was used as a primary collector and the baghouse was utilized as the secondary collector, the "KB+BH" indicates that a knockout box was used as the primary collector and the baghouse was the secondary collector, and a "BH" indicates that the baghouse was the only form of dust collection system.

Based on the figure, several observations can be made. First, the plants without primary collectors generally exhibited more variation in the MPD than did the plants with primary collectors. This statement is true for Plants No. 3, 7, and 17. This is indicated by the length of the gray-shaded boxes. Plants No. 4, 12, and 18 also show wide variations in the data but not to the extent of Plants 3, 7, and 17. However, Plants No. 10 and 11 do not show this wide variation. It is not known why these two plants did not show the large variations in MPD data. However, Plant No. 10 did experience

mechanical difficulties with the baghouse during sampling. The baghouse continued to become clogged. The rotary air lock malfunctioned on numerous occasions.

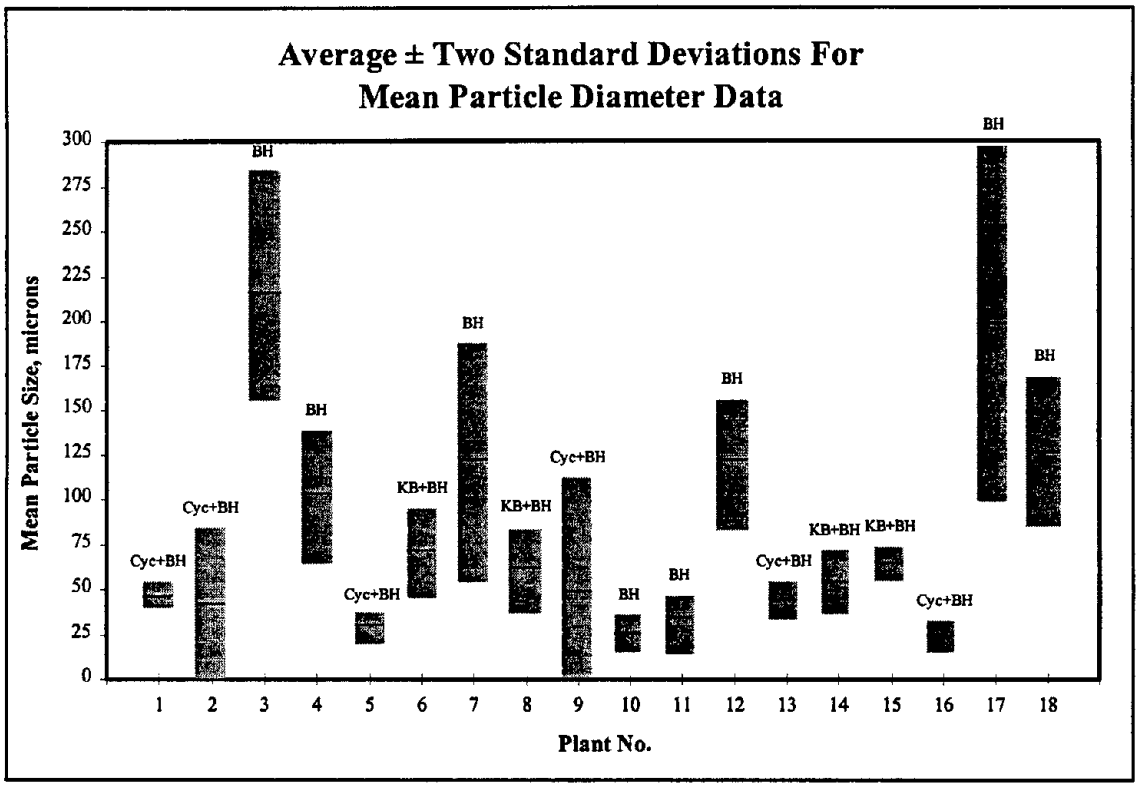

Figure 6.19: Average ± Two Standard Deviations Chart For Mean Particle Diameter Data For All Plants

The plants with a primary collector did not show as much variation in the data. This is probably due to most of the variation occuring in the coarser fraction of the fines. If this is the case, the primary collectors would capture these particles. Recall that at two plants the primary fines were sampled directly. These samples were also tested with the Coulter LS200 particle size analyzer. To determine if most of the

variation in baghouse fines does occur in the coarser fraction of the fines, the MPD data for the primary fines were evaluated in the same manner as the baghouse fines. An average and standard deviation was determined for the data of each plant. Figure 6.20 presents an $\bar{x}\pm 2s$ chart including both the baghouse fine and primary fine data for the two plants sampled.

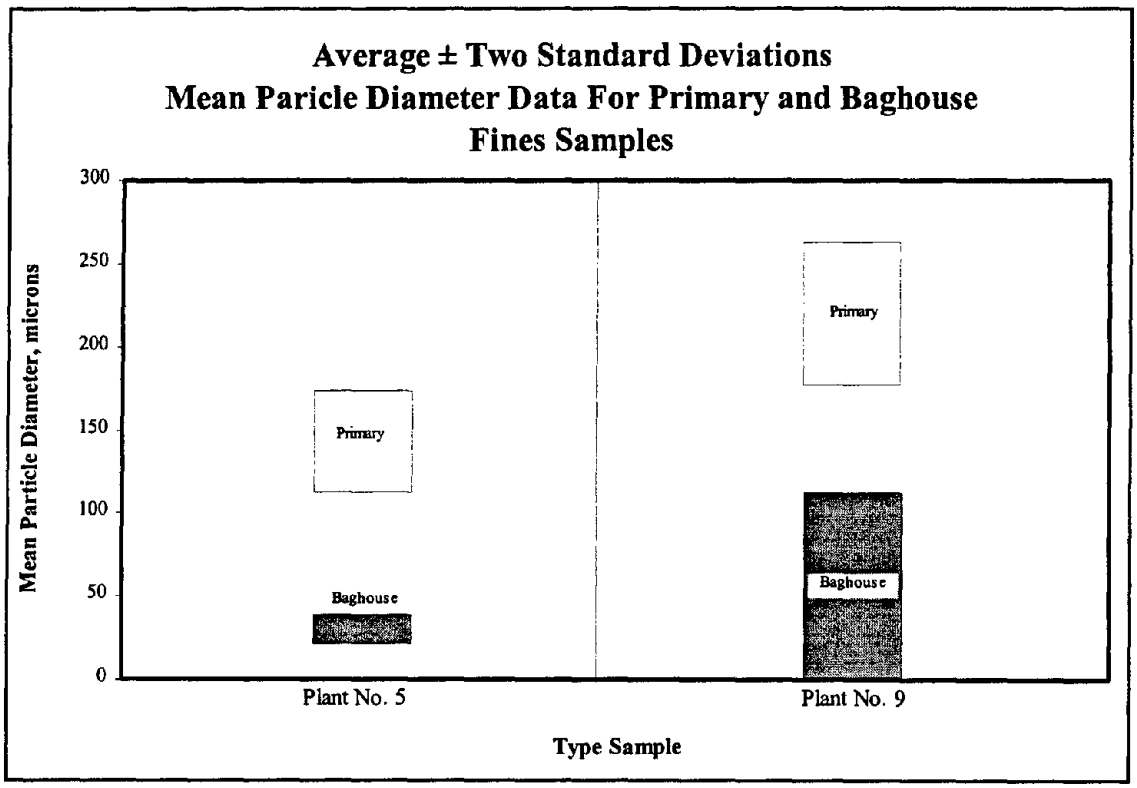

Figure 6.20: Average ±Two Standard Deviations of MPD Data For The Two Plants Where Both Primary and Baghouse Fines Were Obtained

For Plant No. 5, the largest amount of variation occurs in the primary fine data. However, the baghouse fine data for Plant No. 9 has the most variation. Referring back

to Figure 6.9 (frequency diagram for Plant No. 9), one data point is in the range of 110 to 115 μm and two data points are in the range of 125 to 130 μm. Even though these were not determined as outliers, it appears that these three points do not follow the overall pattern of the data. Evaluation of the field sampling logs indicates that two of these three samples were obtained at start-up. Therefore, if these two samples had been discarded, the variation in the baghouse fine data for Plant No. 9 would be less. Hence, the theory that most of the variation occurs in the coarser fines is probably correct.

6.2.1.1 Effect of Mixture Type

One of the factors that could cause the variations in mean particle diameter is the type of mixture being produced by the plant. If the exhaust gas stream picks up the majority of the material finer than 0.075 μm, the properties of the baghouse fines could change as the gradation of the aggregate becomes coarser or finer. To illustrate this theory, ten plants were selected to statistically analyze if significant differences occurred between the MPD data for different types of mixtures within a plant. These included Plants No. 2, 5, 6, 7, 8, 10, 11, 13, 14, and 18. The remaining eight plants were not analyzed because either only one type of mixture was produced during sampling or insufficient data existed for a plant. The minimum number of observations for a sample population for this analysis was set at three observations.

The statistical procedure utilized was an ANOVA (Table 6.1). For this analysis, H_o was that the average MPD data for the different mixtures were equal and the H_a was that they were not equal. Of the ten plants analyzed, three showed significant

differences occur in the MPD's for different types of mixtures the Duncan's Multiple Range Test (DMRT) was performed to rank the MPD data. Ranking was performed to distinguish which types of mixtures produced the coarsest baghouse fines.

Table 6.1: Results of ANOVA on Mean Particle Diameter Data For Different Mixtures

Plant No.	Different Mixtures Used	F-value	F_{crit}	Significant Differences?
2	Type 3, Type 4	2.67	4.32	No
5	Type 4, Type 1A	49.74	4.32	Yes
6	Type 4, Type 3, Type 1	4.06	3.49	Yes
7	Type 1, Binder	1.71	3.20	No
8	Type 3, Type 1, Binder, Black Base	0.57	3.06	No
10	Type 1A, Type 1 (private)	30.16	4.30	Yes
11	Binder, Type 1	0.40	4.30	No
13	Type 3, Binder, Type 1, Type 4	1.42	3.13	No
14	Type 1A, Black Base	0.22	4.75	No
18	Black Base, Type 3, Binder	2.29	3.74	No

Plant No. 5 was one of the three plants with significant differences in the MPD data due to mixture type. Two types of mixtures were produced during sampling of the baghouse fines, a Surface Type 4 and Surface Type 1A. Based on the DMRT rankings (Table 6.2), the average MPD data for the samples obtained for the Surface Type 1A mixture was significantly higher than for the Surface Type 4. The Surface Type 1A is a coarser mixture. It is a 19.0 nominal maximum aggregate size gradation compared to a 9.5 nominal maximum aggregate size gradation. The Surface Type 1A also had a lower percentage of material passing the 0.075 mm (No. 200) sieve (6.4 percent compared to

7.1 percent). This might explain why the average MPD of the baghouse fines is significantly higher for the Surface Type 1A than for the Surface Type 4.

Table 6.2: Average Mean Particle Diameter Results and Duncan's Ranking For Plant No. 5

Mixture	Average MPD	Duncan's Ranking*
Surface Type 1A	31.6	A
Surface Type 4	20.2	B
*Means with the same letter are not significantly different		

Plant No. 6 also showed significant differences in MPD for different mixtures. Four different mixtures were produced during sampling: a Surface Type 3, Surface Type 4, Surface Type 1, and a Binder. Only one sample was obtained while the binder course was being produced, therefore it was excluded from the statistical analysis. Based on the DMRT rankings (Table 6.3), the MPD data for the samples obtained for the Surface Type 4 and Surface Type 3 were significantly higher than for the Surface Type 1.

For Plant No. 6, the Surface Type 4 and Surface Type 3 mixtures used a 9.5 mm nominal maximum aggregate size gradation and the Surface Type 1 used a 12.5 mm nominal maximum aggregate size gradation. Both the Surface Type 3 and Surface Type 1 had percent passing the 0.075 mm sieve of approximately 5.0 percent, while the Surface Type 4 had almost six percent passing. Since the Surface Type 4 had the largest average MPD, this is opposite the observation made for Plant No. 5 where the coarser mixture had the highest average MPD.

Table 6.3: Average Mean Particle Diameter Results and Duncan's Ranking For Plant No. 6		
Mixture	Average MPD	Duncan's Ranking*
Surface Type 4	77.5	A
Surface Type 3	72.7	A
Surface Type 1	60.0	B
*Means with the same letter are not significantly different		

Plant No. 10 was the third plant that showed differences in MPD data for different types of mixtures produced: a Surface Type 1A and a Surface Type 1. The Surface Type 1 mixture was for private work. Based on the DMRT rankings (Table 6.4), the Surface Type 1A produced significantly higher MPDs than did the Surface Type 1. A copy of the job mix formula for the private Surface Type 1 mixture was not obtained, therefore no observation can be made about the differences between the mixtures.

Table 6.4: Average Mean Particle Diameter Results and Duncan's Ranking For Plant No. 10		
Mixture	Average MPD	Duncan's Ranking*
Surface Type 1A	30.0	A
Surface Type 1 (private)	22.6	B
*Means with the same letter are not significantly different		

Since only three of the ten plants analyzed for differences in MPD data due to the production of different types of mixtures showed significant differences, a conclusion can be drawn that variation in the MPD data caused by different types of

mixtures is plant specific and obviously depends on differences in mixtures. Some mixes may have minor differences and other mixes have major differences.

6.2.1.2 Effect of HMA Production

Another possible source of variation in the MPD data for a given plant is the rate of HMA production. Increases in the rate of HMA production requires an increase in the amount of aggregate entering the drum. As more aggregate enters the drum, more heat is required to dry the aggregate. Therefore, the flame within the drum must be increased. This is accomplished by increasing the amount of air driving the flame within the drum. Thus, there is an increase in drum gas velocity (29).

Recall that as the drum gas velocity increases, larger particles can be picked up into the exhaust gas stream. This concept has to do with the terminal velocity for a particular size of particle. In addition, a larger percentage of the finer particles can also enter the exhaust gas stream. Hence, the properties of the baghouse fines can change with an increase or decrease in the drum gas velocity.

To determine if the mean particle data for a given plant showed significant differences with changes in the rate of HMA production, the data for eleven plants was analyzed statistically. These plants included Plants No. 5, 6, 7, 8, 10, 11, 12, 14, 15, 16, and 17. The remaining seven plants were not analyzed because of insufficient data. For this analysis, a minimum sample population for a given rate of HMA production was set at three observations. For this analysis, H_o was that the average MPD data for the different rates of HMA production were equal and the H_a was that at least one differed.

Of the eleven plants, none showed significant differences in the MPD data for different rates of HMA production. Table 6.5 presents the results of the ANOVA for each of the eleven plants. Based on these results, an increase in drum gas velocity associated with an increase in the rate of HMA production does not significantly affect the MPD for baghouse fines within the ranges observed in South Carolina.

Other causes of variability in the drum gas velocity include: changes in the position of the damper, changes in the pressure drop through the baghouse, and leaks in the duct-work or primary collector (4). However, these properties could not be analyzed because they could not be determined and were therefore not measured.

Table 6.5: Results of ANOVA on Mean Particle Diameter Data For Different Rates of HMA Production

Plant No.	Different Production Rates Used (tons per hour)	F-value	F_{crit}	Significant Differences?
5	150, 175, 200	0.38	3.55	No
6	135, 140, 150, 200	0.97	3.71	No
7	130, 150, 160, 195	1.17	3.41	No
8	130, 140	0.00	4.67	No
10	240, 250	2.96	3.74	No
11	110, 115, 120	0.74	3.59	No
12	275, 300	1.78	4.84	No
14	140, 150, 160	2.46	4.46	No
15	175, 200	0.26	4.75	No
16	245, 250	1.15	5.12	No
17	200, 225	1.35	5.59	No

6.2.1.3 Effect of Different Equipment

During the two years of field sampling baghouses in South Carolina, two contractors bought new plants. For both contractors, baghouse fines were sampled from the original plants as well as the new plants. In each case the old plant was dismantled and replaced with a new plant. Since it has been shown that the type of HMA mixture does not consistently affect the MPD data for a given plant, a Student's t-Test was performed to determine if the change in plant equipment led to significant differences in the MPD data. For this analysis, the H_o was that the average MPD was equal between the two types of plants and the H_a was that they were significantly different. Based on the plant numbering system utilized, Plants No. 6 and 9 and Plants No. 11 and 12 were the same contractor at the same location and using the same aggregates, the only difference being plant equipment.

In the case of Plants No. 6 and 9, Plant No. 6 constitutes the old plant and Plant No. 9 was the new plant. The old plant was a batch plant with a dust collection system consisting of only a baghouse. Sampling at the old plant consisted of obtaining samples from an auger chute leading from the baghouse to the hot elevator. The new drum plant had both a primary collector (cyclone) and a baghouse as the dust collection system. The configuration for the new plant was such that the primary fines and baghouse fines were combined and then sent to the drum. Therefore, this analysis consisted of comparing the baghouse fines from the old plant to the combined sample of primary and baghouse fines from the new plant. This should constitute similar sample

populations. Results of this analysis showed that significant differences occurred in the MPD data between the two plants (t_{stat} = -19.44 and t_{crit} = 2.02). Figure 6.21 illustrates the differences in the average MPD data between Plant No. 6 and Plant No. 9.

In the case of Plants No. 11 and 12, Plant No. 11 constitutes the old plant and Plant No. 12 was the new plant. In each case, both plants were drum plants with a baghouse as the only form of dust collection. Results of this analysis again showed differences in the MPD data between the two plants (t_{stat} = -9.84 and t_{crit} = 2.02). Figure 6.22 illustrates these differences between Plant No. 11 and Plant No. 12.

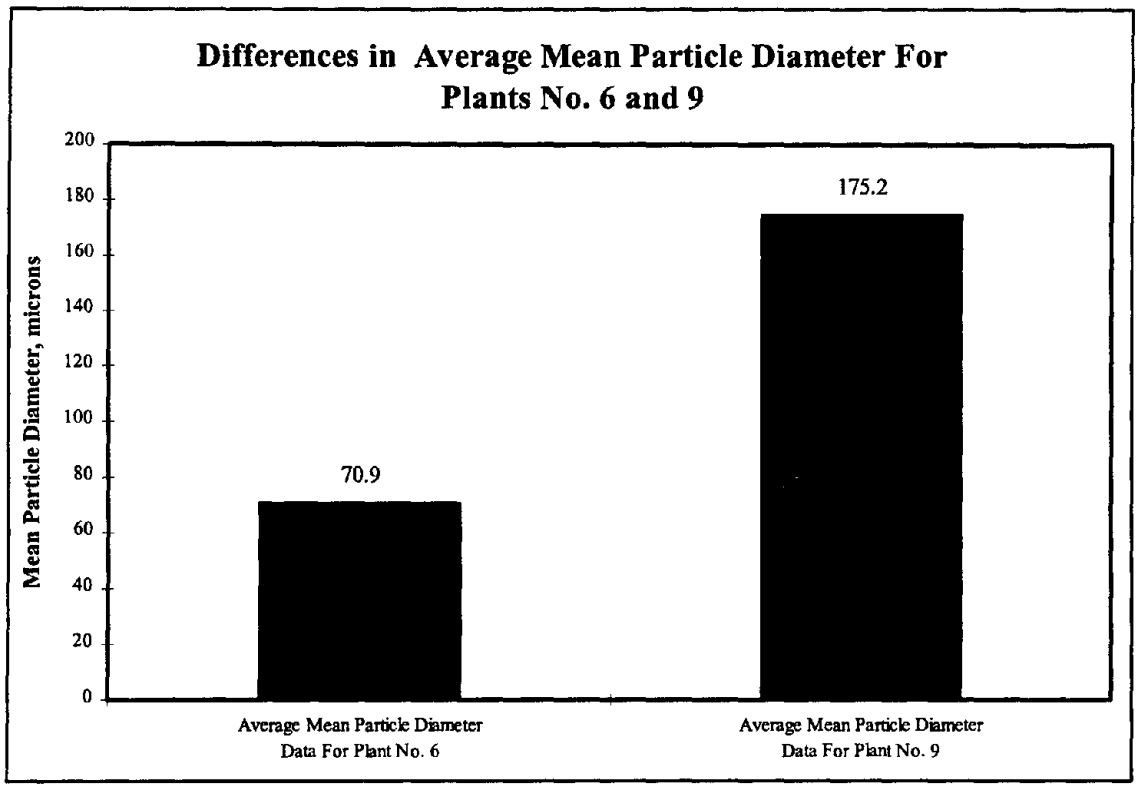

Figure 6.21: Differences in Mean Particle Diameter Data For Plants No. 6 and 9

Based on these two analysis, the MPD data were again plant specific. In each case, two different types of HMA producing facilities were located on the same plant site and using the same types of aggregate, but showed significant differences in MPD data. Interestingly though, in both cases the new MPD data for the new plant was higher. A probable explanation for this is that the newer plants would have more efficient air flows through the plant and would therefore pick up larger sized particles to be carried to the baghouse.

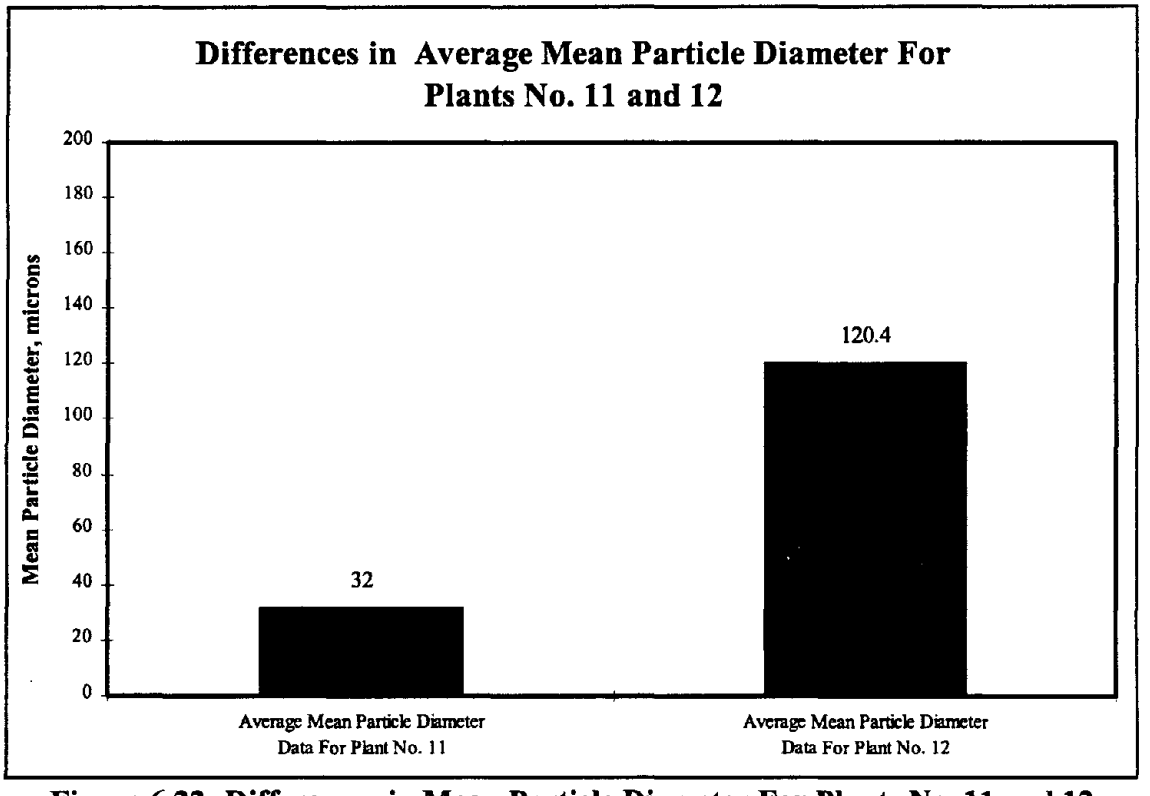

Figure 6.22: Differences in Mean Particle Diameter For Plants No. 11 and 12

6.2.2 Analysis of Modified Rigden Voids Test Data

Again, large amounts of data were accumulated as a result of the Modified Rigden's Voids (MRV) test performed on the samples obtained during field sampling. Results of this test include the percent voids within a dry compacted dust, percent bulk volume of the dry compacted dust, and the percent free asphalt in a dry compacted dust. Since, the percent bulk volume and percent free asphalt require a given dust-to-asphalt ratio for calculation, analysis was limited to the percent voids in a dry compacted dust.

As in the analysis of the mean particle diameter data, the first step in this analysis was to develop frequency distribution charts for each of the 18 plants sampled. Figures 6.23 through 6.40 present these charts for each of the 18 plants. Because of the relatively small range of MRV data (as compared to the MPD data), the x-axis for each of these charts is identical.

Next, Grubb's test for outlying observations was used to determine if outlying data existed for each plant. Plants No. 2, 7, and 17 exhibited outliers in their data. These outliers are illustrated on their respective frequency distribution charts. In each case, the evaluation of the field sampling logs did not indicate why these observations are outliers and therefore were not discarded.

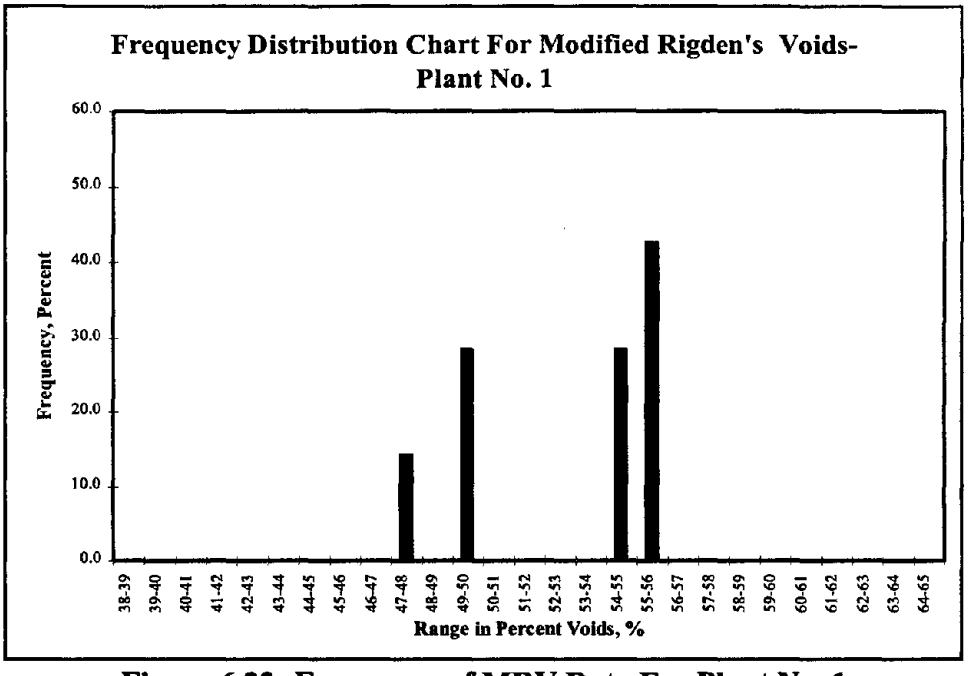

Figure 6.23: Frequency of MRV Data For Plant No. 1

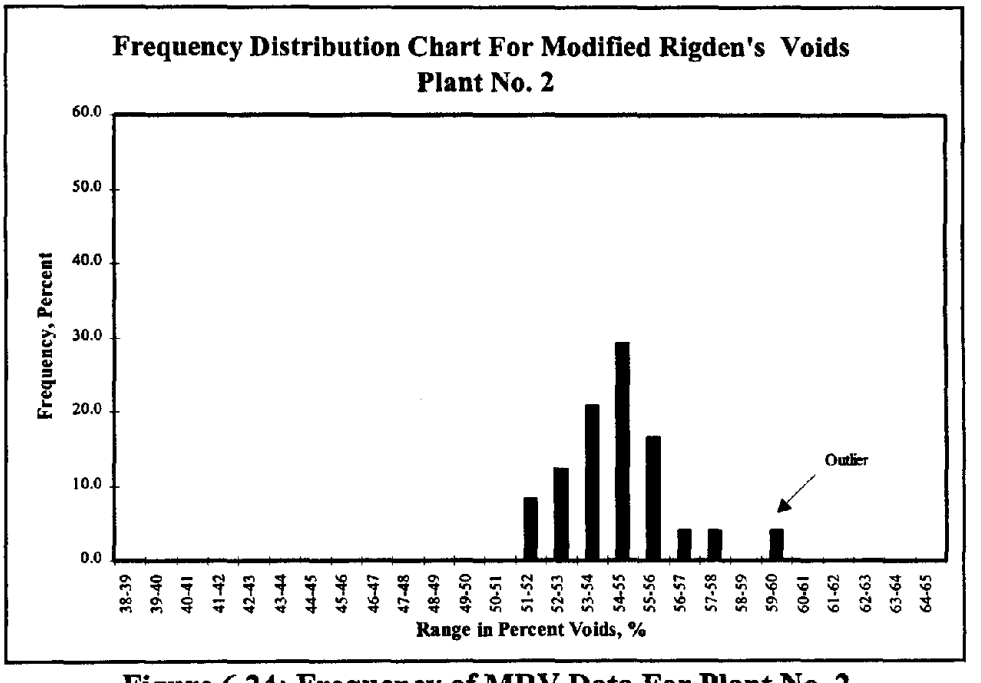

Figure 6.24: Frequency of MRV Data For Plant No. 2

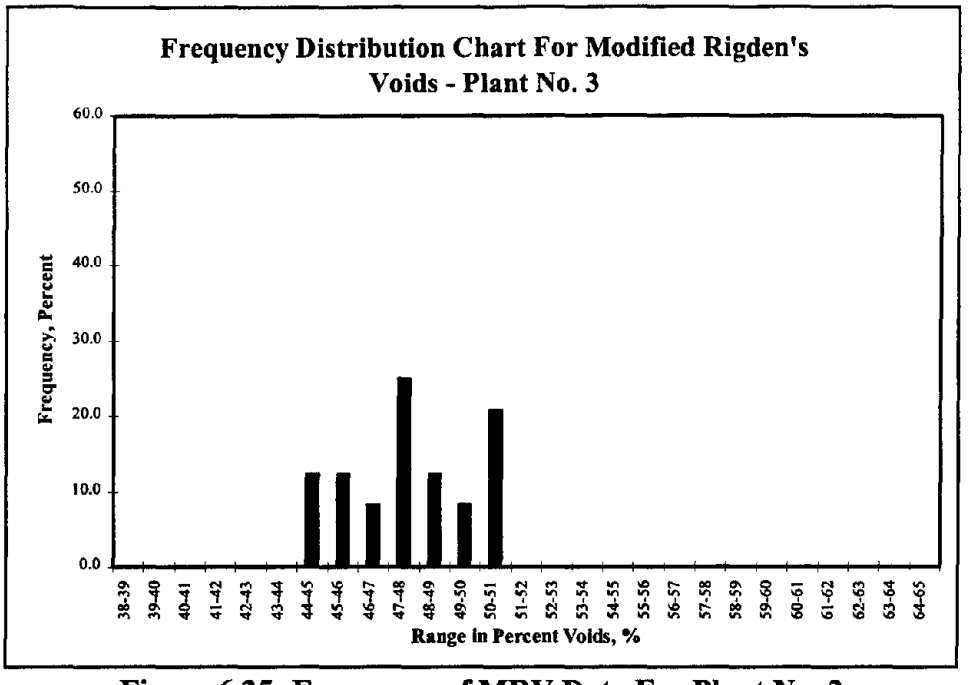

Figure 6.25: Frequency of MRV Data For Plant No. 3

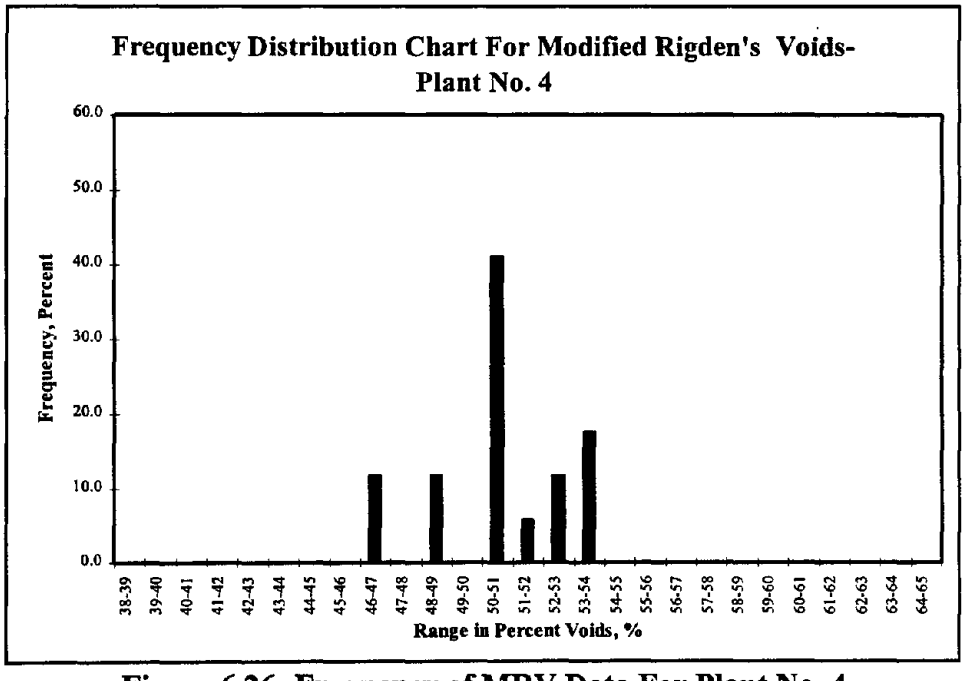

Figure 6.26: Frequency of MRV Data For Plant No. 4

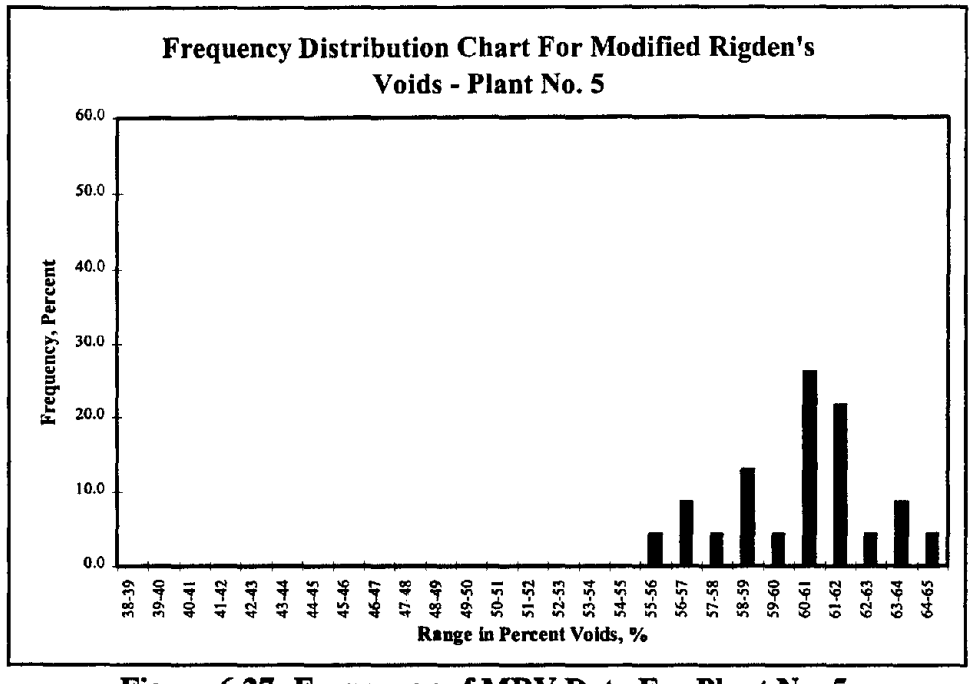

Figure 6.27: Frequency of MRV Data For Plant No. 5

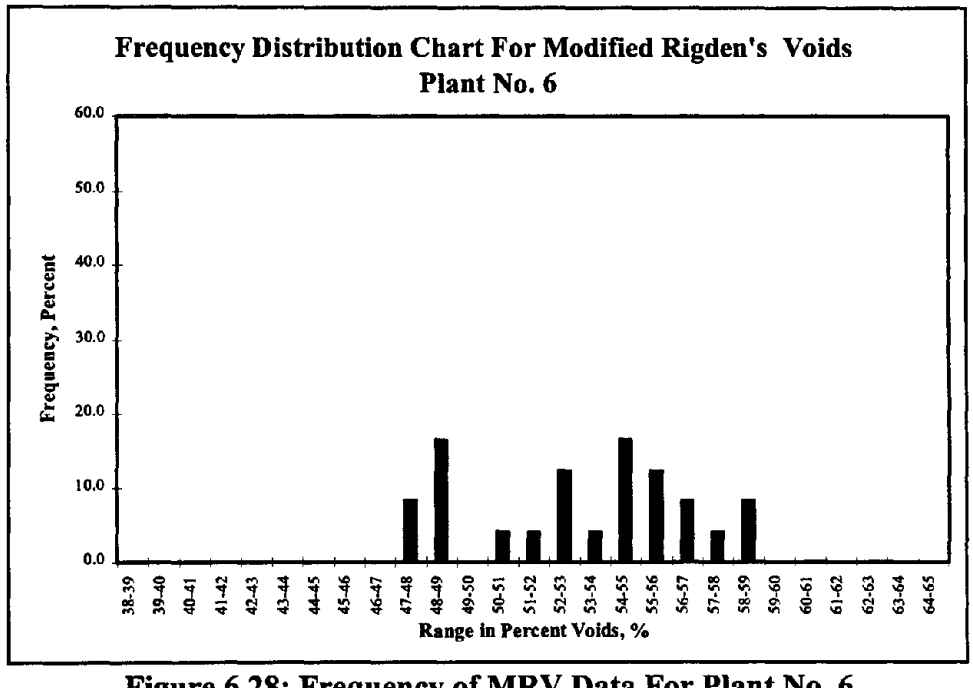

Figure 6.28: Frequency of MRV Data For Plant No. 6

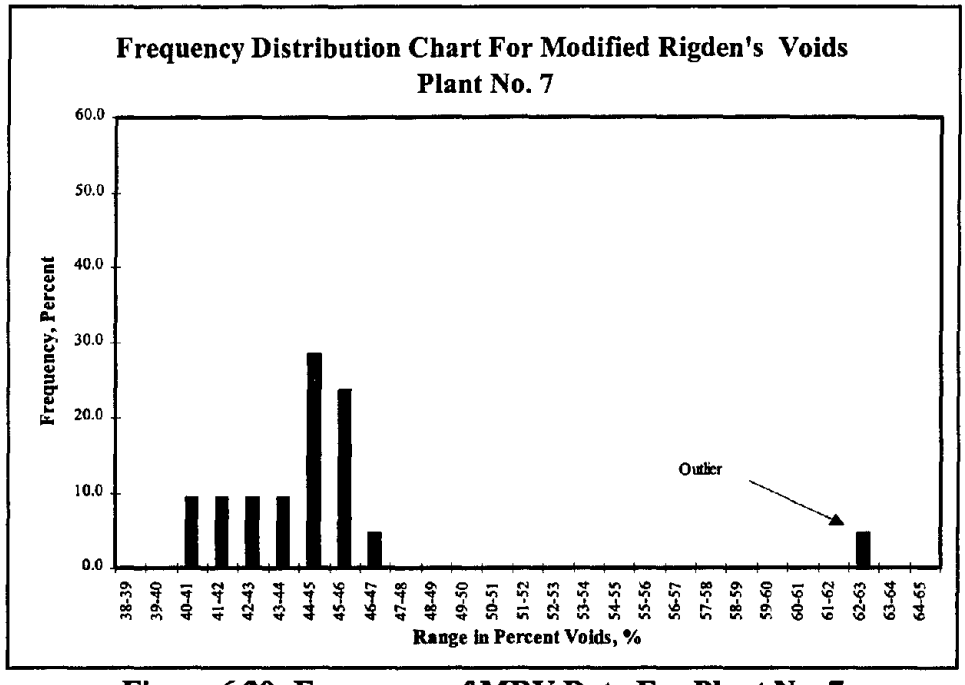

Figure 6.29: Frequency of MRV Data For Plant No. 7

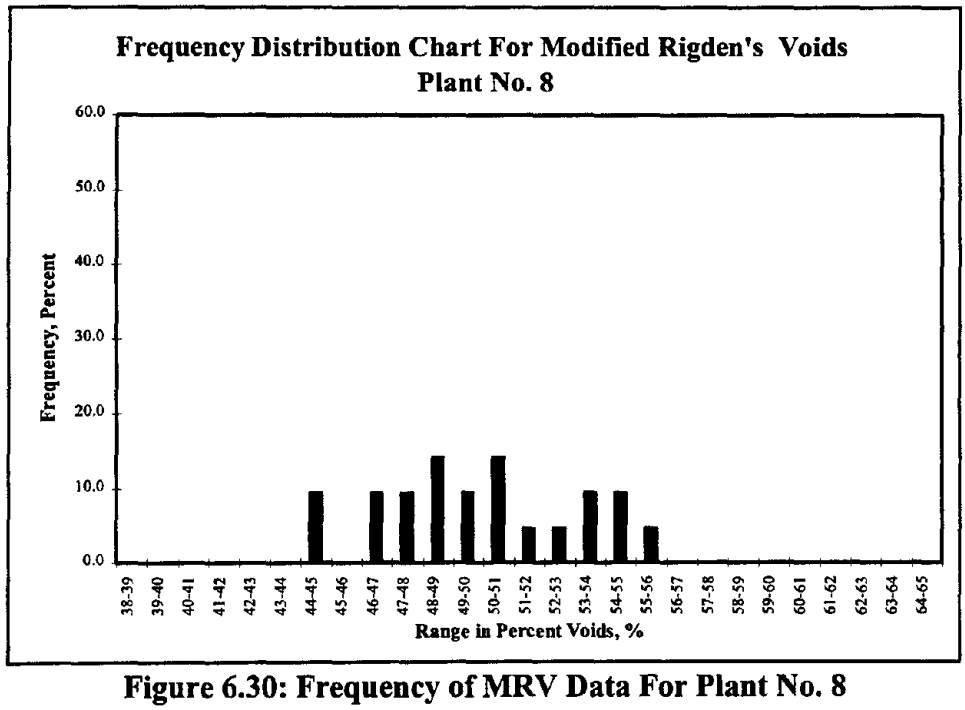

Figure 6.30: Frequency of MRV Data For Plant No. 8

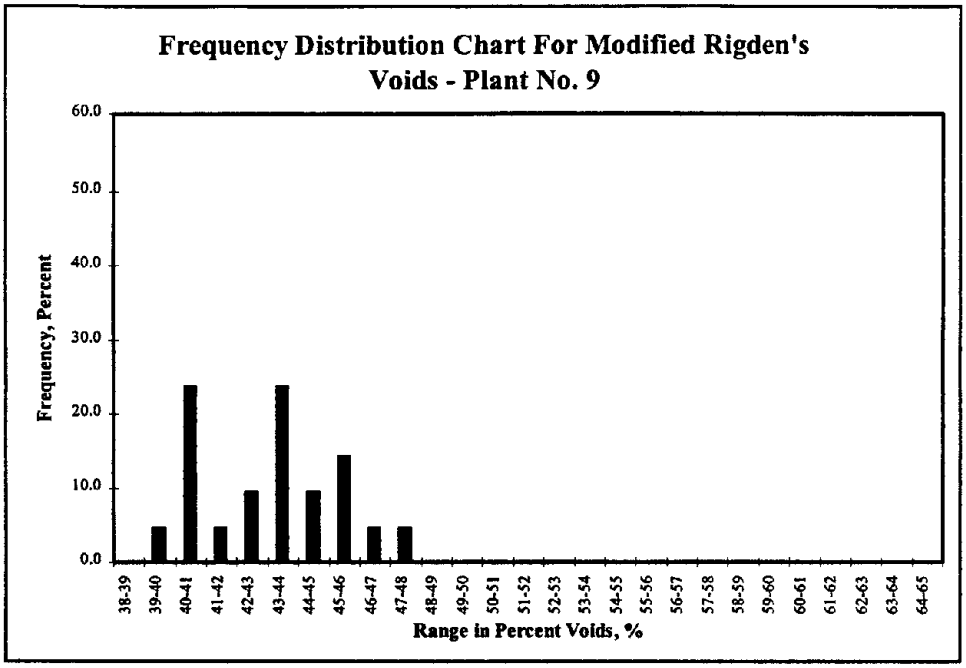

Figure 6.31: Frequency of MRV Data For Plant No. 9

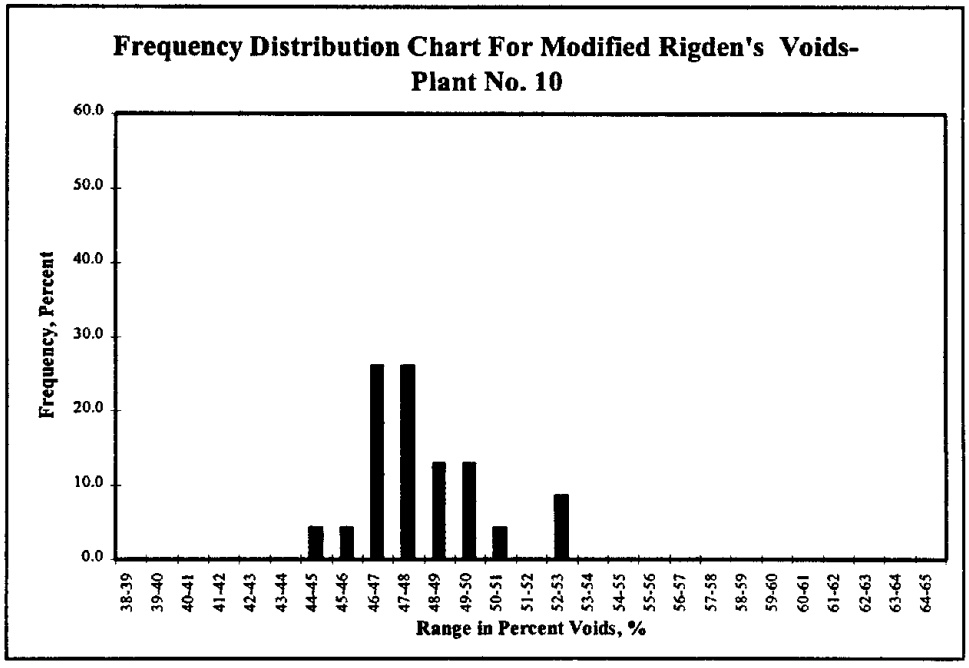

Figure 6.32: Frequency of MRV Data For Plant No. 10

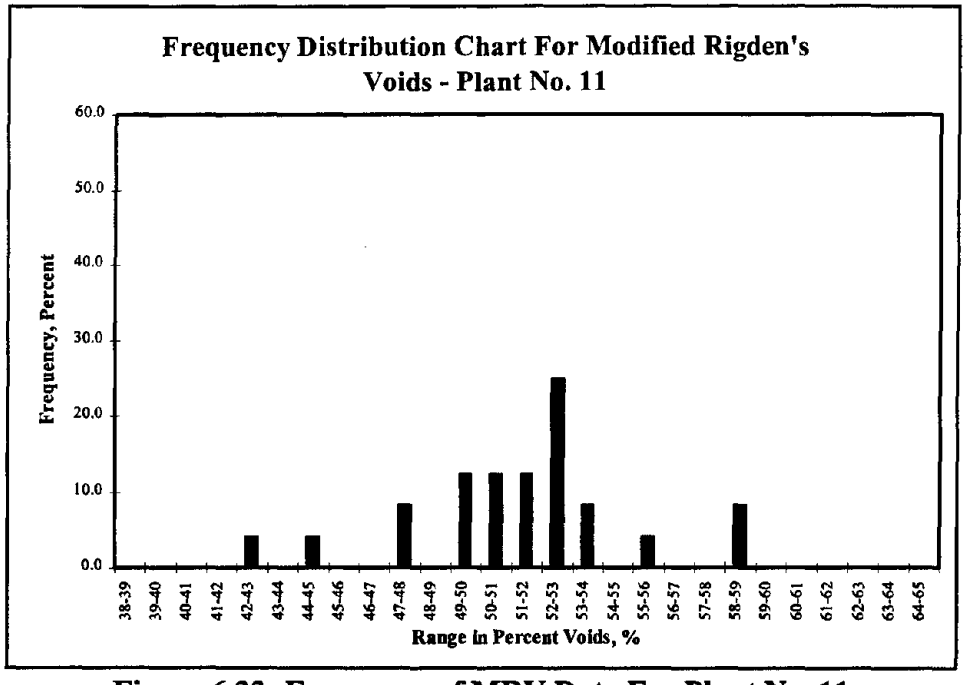

Figure 6.33: Frequency of MRV Data For Plant No. 11

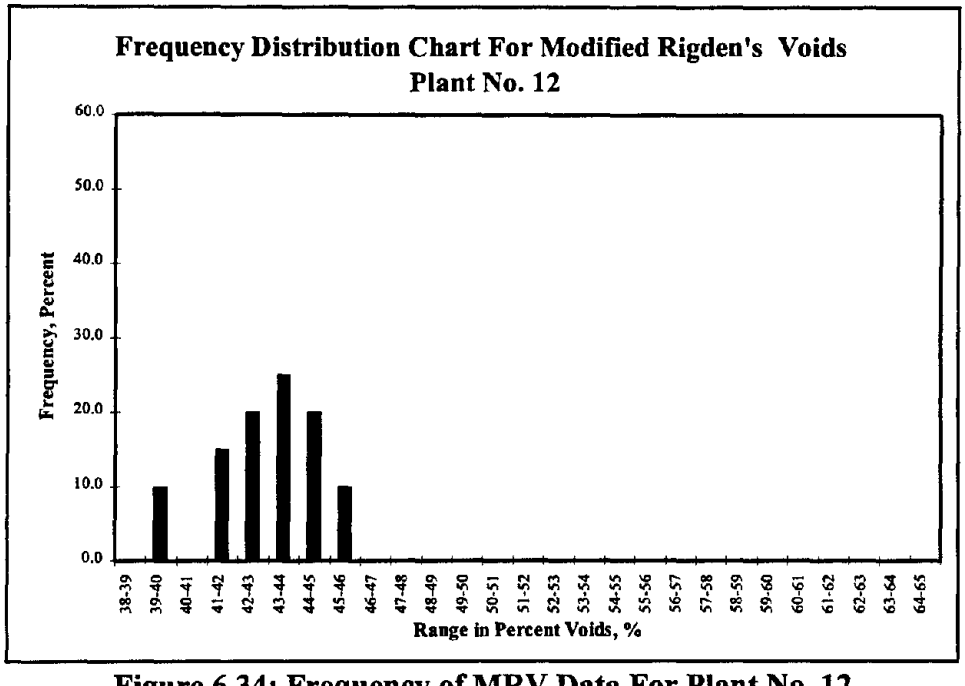

Figure 6.34: Frequency of MRV Data For Plant No. 12

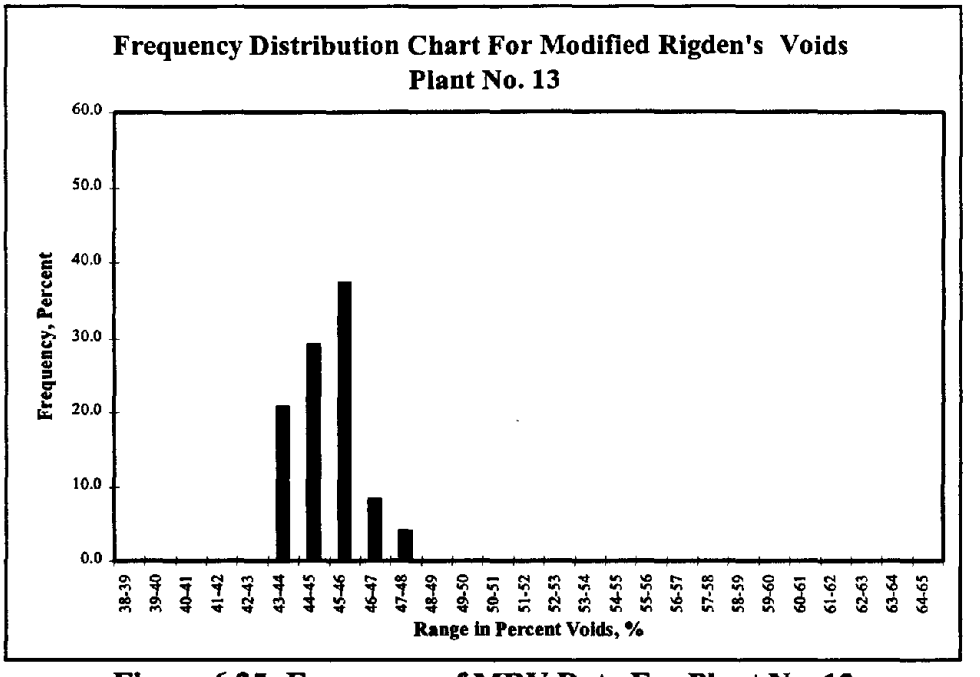

Figure 6.35: Frequency of MRV Data For Plant No. 13

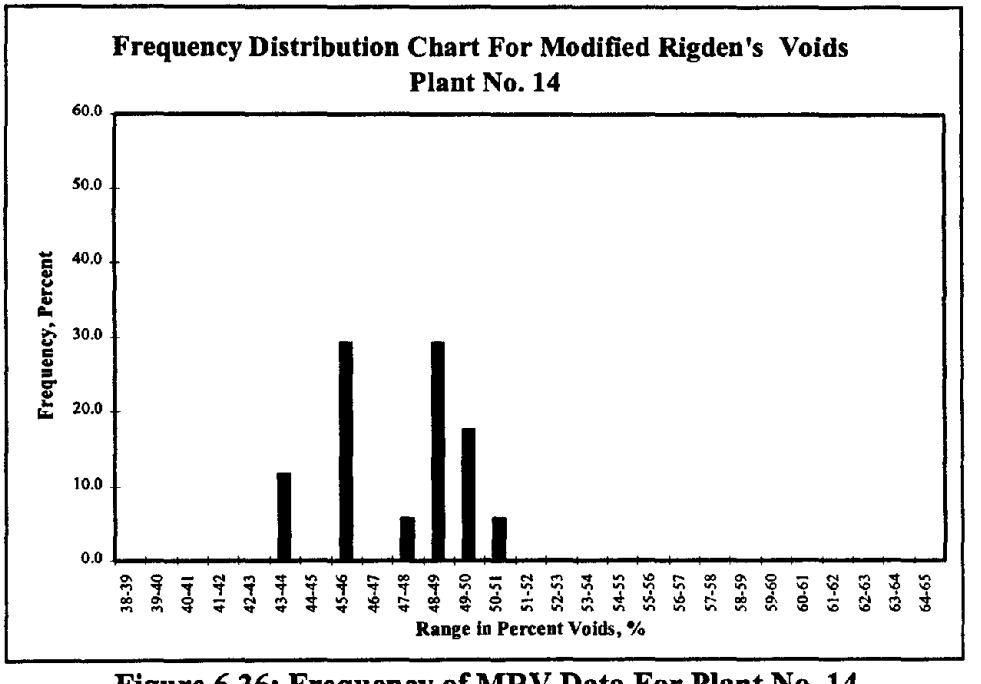

Figure 6.36: Frequency of MRV Data For Plant No. 14

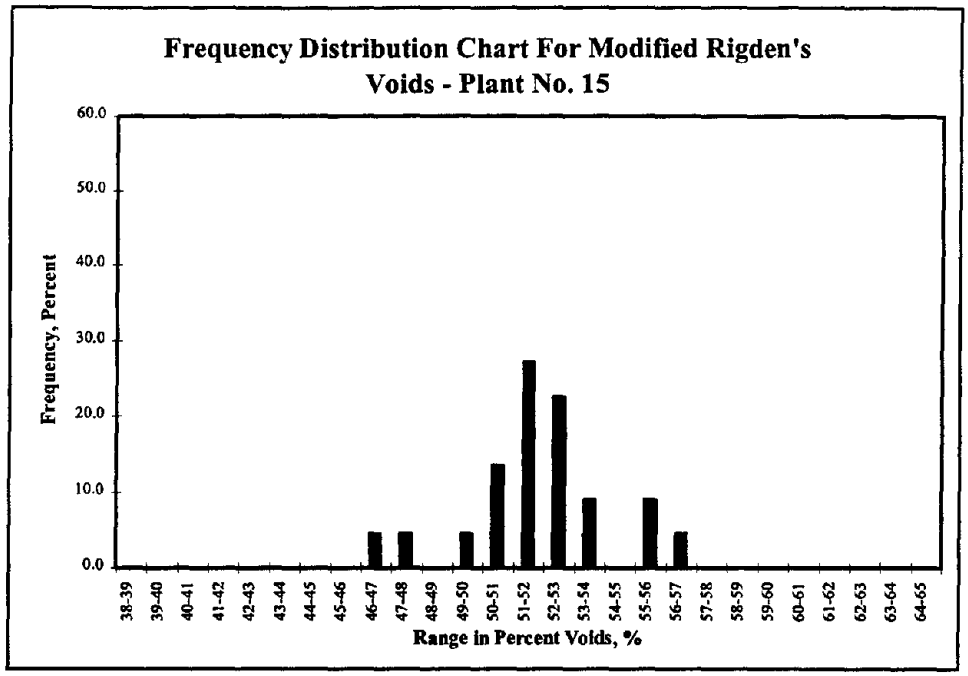

Figure 6.37: Frequency of MRV Data For Plant No. 15

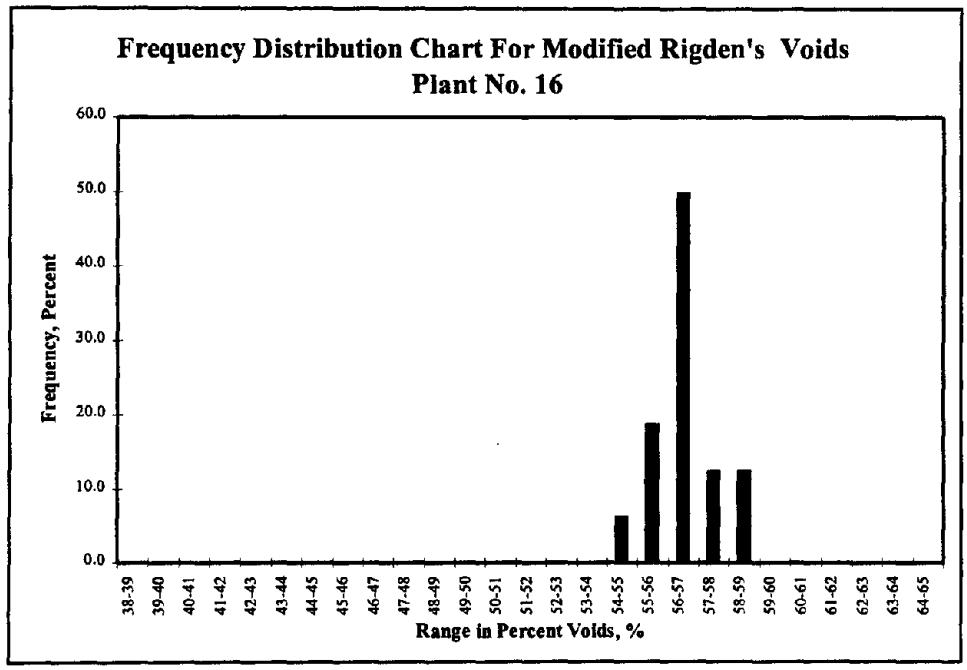

Figure 6.38: Frequency of MRV Data For Plant No. 16

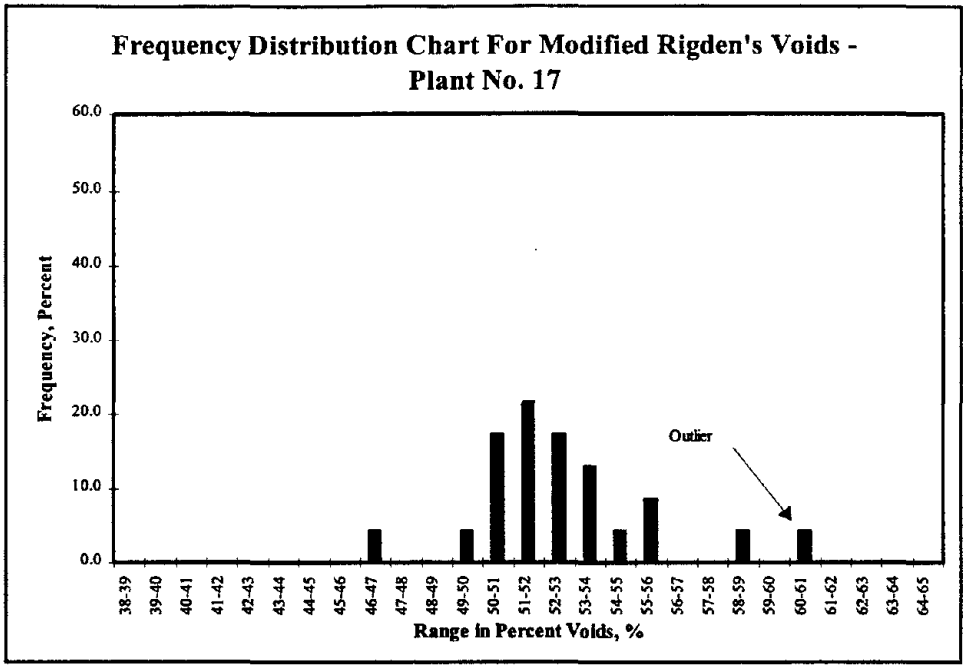

Figure 6.39: Frequency of MRV Data For Plant No. 17

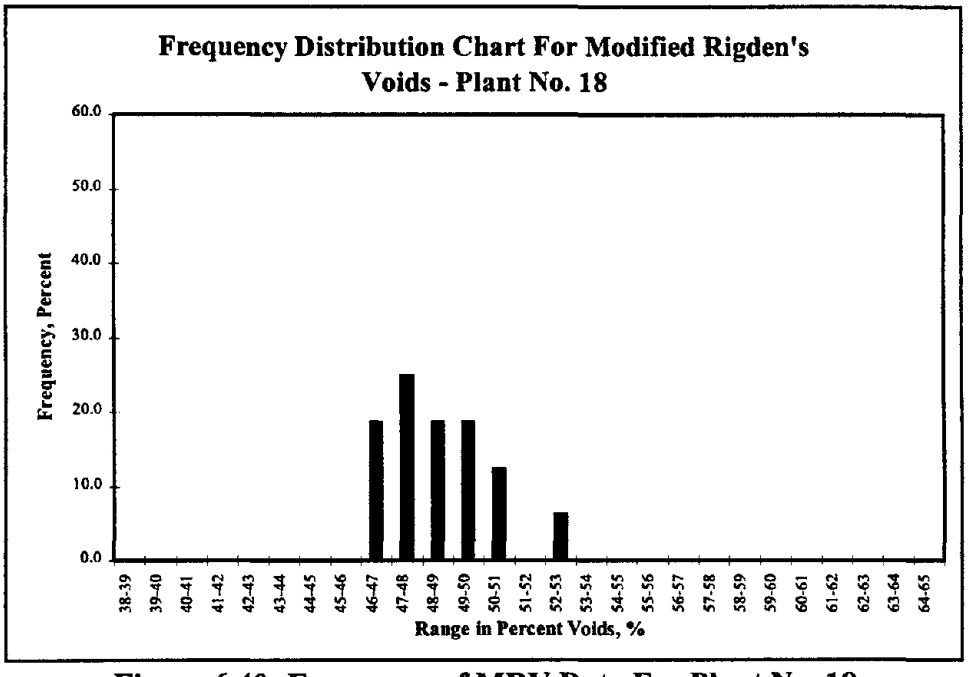

Figure 6.40: Frequency of MRV Data For Plant No. 18

After observing Figures 6.23 through 6.40, it is obvious that there is less variation in the MRV data than the MPD data. This may be because of the test procedure. Recall from Chapter 3 that to perform this test, the sample is first shaken over a 0.075 mm (No. 200) sieve.

The next step in the analysis of the MRV data was to develop a chart that showed variations in MRV data within a single plant and between plants. This was again accomplished by developing a chart that shows the $\bar{x}\pm 2s$ for each plant (Figure 6.41); $\bar{x}$ is shown as a horizontal black line.

After evaluating Figure 6.41, the question arose as to whether significant differences existed in the MRV data between plants. Therefore, an ANOVA test was performed. For this analysis, H_o was that the MRV data for each plant was equal and H_a was that they were significantly different. Results of the ANOVA showed significant differences existed in the MRV data between plants (F-value=69.87 and F_{crit}=1.67). Next, a DMRT ranking was performed to determine which plants produced the highest MRV data (Table 6.6).

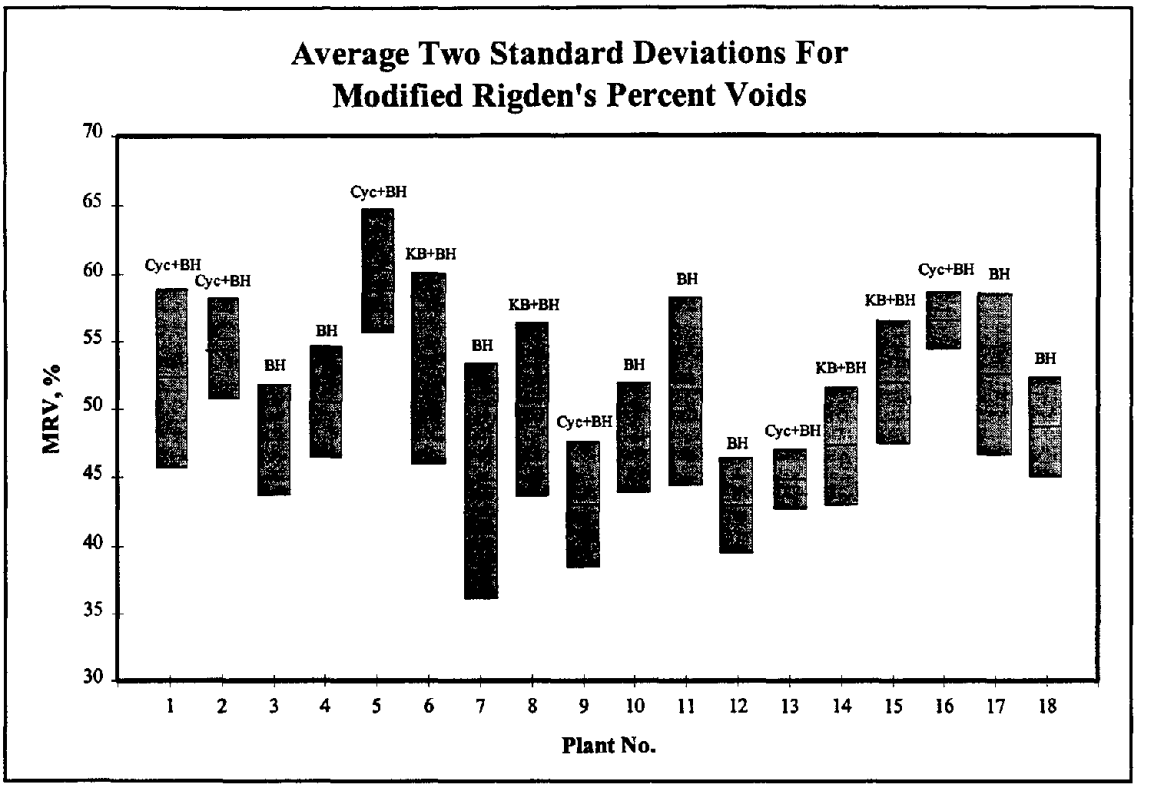

Figure 6.41: Average ± Two Standard Deviations Chart For MRV Data

Based on these rankings, it appears that the configuration of the dust collection system affected the MRV values for the baghouse fines. Therefore an additional ANOVA was used to evaluate this observation. For this analysis, H_o was that the MRV data was equal between dust collection systems and H_a was that they significantly differed. Results of the ANOVA showed significant differences in the MRV data occurred between dust collection systems (F-value=16.62 and F_{crit}=3.00). A DMRT ranking (Table 6.7) showed plants which utilized primary collectors yielded MRV data that was significantly higher than plants without a primary collector. However, the type of primary collector did not affect the MRV data.

Table 6.6: DMRT Rankings of Different Plants With MRV Data

Plant No.	Dust Collection System	Average MRV	Duncan's Ranking*
5	Cyclone+ Baghouse	60.1	A
16	Cyclone + Baghouse	56.5	B
2	Cyclone + Baghouse	54.4	C
6	Knockout Box + Baghouse	53.0	CD
17	Baghouse	52.5	D
1	Cyclone + Baghouse	52.3	D
15	Knockout Box + Baghouse	51.9	DE
11	Baghouse	51.4	DEF
4	Baghouse	50.5	EF
8	Knockout Box + Baghouse	50.0	FG
18	Baghouse	48.6	GH
10	Baghouse	47.9	H
3	Baghouse	47.7	H
14	Knockout Box + Baghouse	47.3	H
13	Cyclone + Baghouse	44.9	I
7	Baghouse	44.7	I
9	Cyclone + Baghouse	43.0	J
12	Baghouse	42.9	J

* Averages with the same letter are not significantly different

Table 6.7: Results of DMRT Ranking for Differing Dust Collection Systems With MRV Data		
Dust Collection System	Average MRV	Duncan's Ranking*
Cyc+BH	51.7	A
KB+BH	50.8	A
BH	48.3	B
* Averages with the same letter are not significantly different		

6.2.2.1 Effect of Mixture Type

A factor that could cause variation in the MRV data for a given plant is the type HMA mixture being produced. To determine if changes in the type HMA mixture affects the MRV data, ten plants (Plants No. 2, 5, 6, 7, 8, 10, 11, 13, 14, and 18) were selected to statistically analyze (ANOVA) if significant differences occurred between the MRV data for different types of HMA mixtures. The remaining eight plants were not analyzed because either only one type of mixture was produced during sampling or insufficient data existed for a plant. A minimum number of observations for a sample population was set at three.

For this analysis, H_0 was that the MRV data for different mixtures were equal and the H_a was that they were not equal. Of the ten plants analyzed, only two (Plants No. 6 and 8) showed significant differences in the MRV data for different mixtures (Table 6.8). Since only two of the ten plants showed significant differences, the affect of changing the type of HMA mixtures on the MRV data was plant specific. Recall that this was the same conclusion reached for different type HMA mixtures and the MPD data. If the same plants that had shown significant differences for the MPD data

had shown significant differences in the MRV data, a possible conclusion could be that the plant's equipment played a role in these differences. However, Plant No. 6 was the only plant that shows significant differences for both the MRV and MPD data. Therefore this conclusion can not be made.

Table 6.8: Results of ANOVA on MRV Data For Different Mixtures

Plant No.	Different Mixtures Used	F-value	F_{crit}	Significant Differences?
2	Type 3, Type 4	0.09	4.32	No
5	Type 4, Type 1A	0.10	4.32	No
6	Type 4, Type 3, Type 1	16.62	3.49	Yes
7	Type 1, Binder	3.71	3.74	No
8	Type 3, Type 1, Binder, Black Base	6.29	3.63	Yes
10	Type 1A, Type 1 (private)	2.20	4.32	No
11	Binder, Type 1	3.01	4.30	No
13	Type 3, Binder, Type 1, Type 4	1.09	3.55	No
14	Type 1A, Black Base	0.35	3.81	No
18	Black Base, Type 3, Binder	3.33	4.84	No

6.2.2.2 Effect of HMA Production

Another source of variation in the MRV data for a given plant is the rate of HMA production. To determine if the MRV data for a given plant showed significant differences with changes in the rate of HMA production, the data from twelve plants (Plants No. 5, 6, 7, 8, 9, 10, 11, 12, 14, 15, 16, and 17) was analyzed. The remaining seven plants were not analyzed because insufficient data existed. For this analysis, a

minimum sample population for a given rate of production was set at three observations. Also for this analysis, H_0 was that the MRV data for different rates of HMA production were equal and the H_a was that at least one differed.

Of the twelve plants analyzed, only one plant, Plant No. 6, showed significant differences in the MRV data for different rates of HMA production (Table 6.9). This leads to the conclusion that differences in MRV data as a result of different rates of HMA production is plant specific. It should be noted though that for some of the plants the rates of production are not significantly different.

Table 6.9: Results of ANOVA on MRV Data For Different Rates of HMA Production

Plant No.	Different Production Rates Used (tons per hour)	F-value	F_{crit}	Significant Differences?
5	150, 175, 200	0.71	3.55	No
6	135, 140, 150, 200	8.01	3.71	Yes
7	130, 150, 160, 195	2.12	3.41	No
8	130, 140	0.09	4.60	No
9	215, 320	0.43	7.71	No
10	240, 250	0.30	4.84	No
11	110, 115, 120	0.45	3.59	No
12	275, 300	3.29	4.96	No
14	140, 150, 160	0.81	4.26	No
15	175, 200	0.81	4.84	No
16	245, 250	1.63	5.12	No
17	200, 225	1.77	5.59	No

6.2.2.3 Effect of Different Equipment

Recall that two contractors bought new plants during the field sampling (Plants No. 6 and 9 and Plants No. 11 and 12). For these plants, the mean particle diameter data was plant specific for two different types of equipment using the same types of aggregates, therefore the same type analysis was performed to determine if the MRV data also showed these significant differences. Again, a Student's t-test was used to draw this conclusion.

Significant differences between Plants No. 6 and 9 when utilizing the MRV data (t_{stat} = 11.30 and t_{crit} =2.02) also occurred. Again, the combined samples obtained from Plant No. 9 were utilized to provide similar populations. Results of the analysis on Plants No. 11 and 12 also showed these differences (t_{stat} = 9.96 and t_{crit} =2.02). Based on these results and the previous analysis of the MPD data, the physical properties of baghouse fines (as determined by MPD and MRV) seem to be plant specific.

6.2.3 Mechanical Analysis of Baghouse Fines

Since the output from the Coulter LS200 PSA is not a standard particle size distribution (percentage by mass), samples were tested with the Coulter LS200 and by mechanical means to determine if both yielded similar results. Ten samples were randomly selected and the particle size distribution was determined (three replicates) by both methods. The analysis of this data consisted of determining if these two methods of particle size analyses are comparable.

First, an ANOVA was performed to see if significant differences occurred between the two methods using all data. No significant differences were found (F-value = 0.01 and F_{crit} =4.08). Next, another ANOVA (Table 6.10) was performed to determine if significant differences occurred between the two methods for individual samples. This was accomplished by comparing the results for the percent passing each of the four particle sizes (2000 μm, 420 μm, 75 μm, and 2 μm). The F-values in Table 6.10 show that were both methods yielded the same results.

Table 6.10: Results of Analyses Between Coulter LS200 and Mechanical Particle Size Distributions

Sample No.	F-value and Significant Difference? (Fcrit = 7.71)			
	2000 μm	420 μm	75 μm	2 μm
1	0.0, No	35.0, Yes	35.8, Yes	570.4, Yes
2	0.0, No	2.3, No	6.76, No	315.1, Yes
3	0.0, No	1.0, No	16.5, Yes	3.83, No
4	0.0, No	1.92, No	96.8, Yes	3.14, No
5	0.0, No	16.0, Yes	0.5, No	154.0, Yes
6	0.0, No	16.0, Yes	3.6, No	21.3, Yes
7	0.0, No	104.9, Yes	63.2,No	2645.0, Yes
8	0.0, No	0.0, No	0.0, No	58.47, Yes
9	0.0, No	85.0, Yes	0.0, No	189.4, Yes
10	0.0, No	2.9, No	0.2, No	1.38, No

As can be seen from Table 6.10, no significant differences occurred in the percent passing 2000 μm data; however, each of the other three particle sizes showed

significant differences. Figures 6.42, 6.43, and 6.44 illustrates the differences between the Coulter LS200 and mechanical particle size data for the percent passing 420 μm, 75 μm, and 2 μm, respectively.

Based on these figures, the Coulter LS200 and mechanical particle size analysis usually provide similar numbers. For some samples, the mechanical method yields lower values of percent passing and for other samples the mechanical method yields higher values of percent passing.

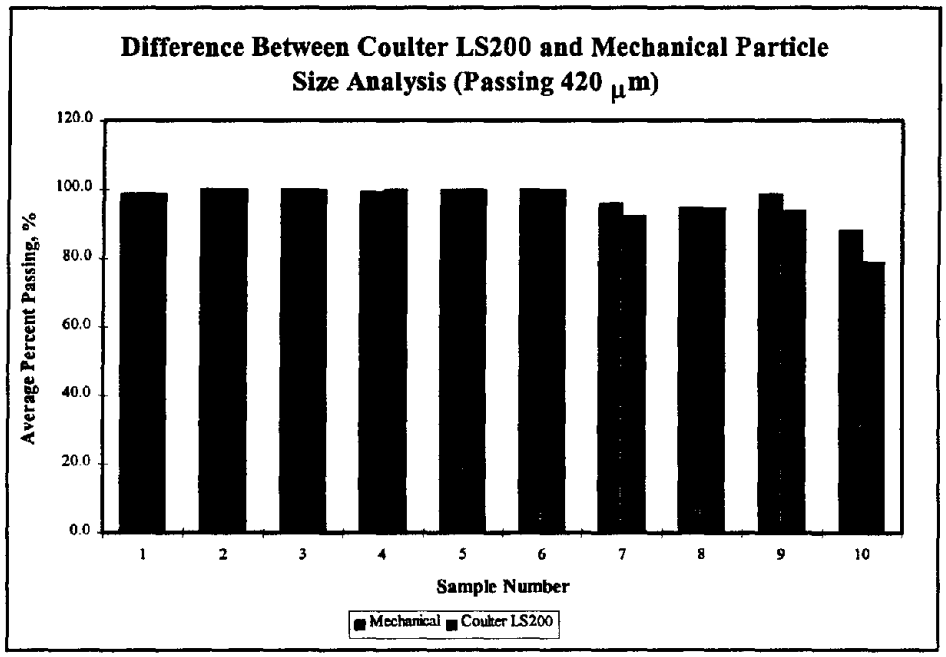

Figure 6.42: Differences Between Coulter LS200 and Mechanical Particle Size Analyses at 420 μm

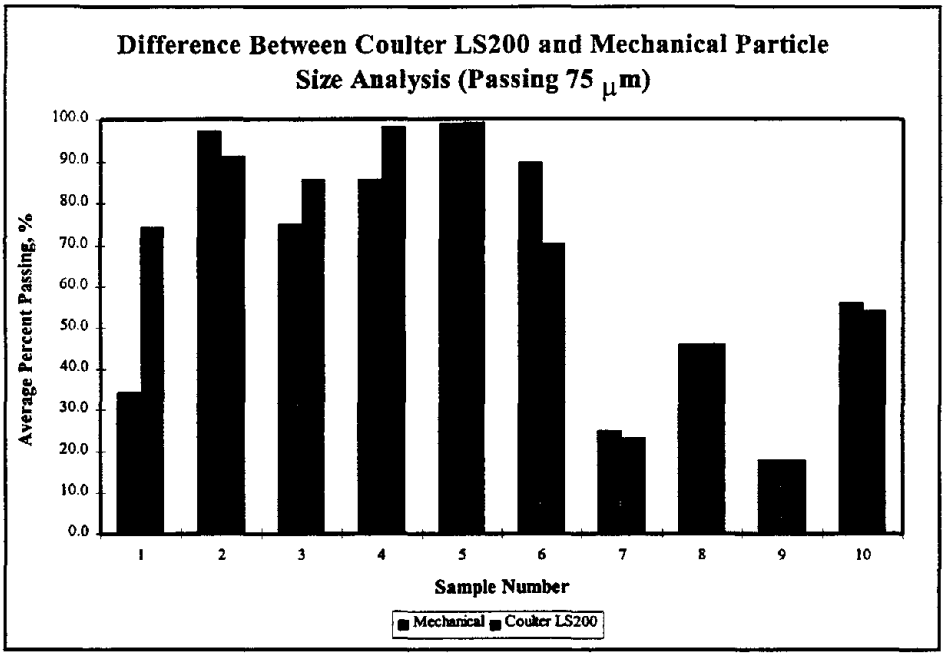

Figure 6.43: Differences Between Coulter LS200 and Mechanical Particle Size Analyses at 75 μm

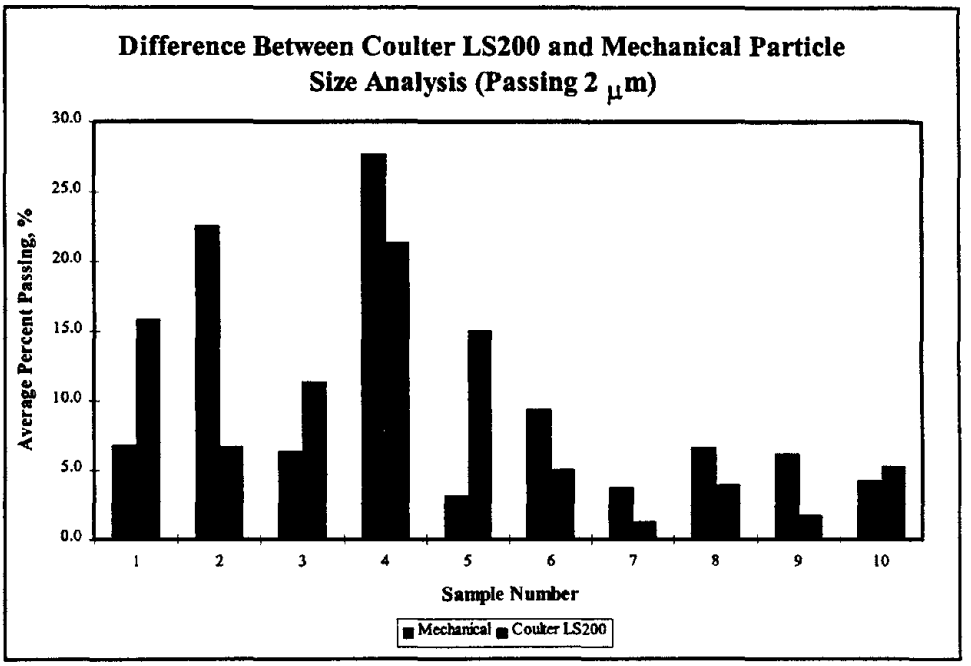

Figure 6.44: Differences Between Coulter LS200 and Mechanical Particle Size Analyses at 2 μm

6.3 Analysis of Mortar Testing

Statistical analysis of the data obtained during the mortar evaluation phase consisted of performing an ANOVA to determine if there were significant differences in the results for the laboratory tests. Three main effects were analyzed using the ANOVA: asphalt binders, baghouse fine combined samples (Fine), and fine-to-asphalt (F/A) ratios. The ANOVA procedure allows interactions between these main effects to be analyzed. The H_o was that all population means were equal, while H_a was that at least one population mean differed significantly from the remaining means.

Remember that mortar testing performed on the original mortars before aging was accomplished based on a completely randomized statistical design. Also, testing of the mortars in the TFOT and PAV aged conditions was accomplished based on a one-half fractional factorial statistical design. The procedure for determining significant differences between population means for the one-half fractional factorial design was also accomplished using the ANOVA procedure. However, as noted in Chapter 4, the one-half fractional factorial loses degrees of freedom because of the nature of the design.

6.3.1 Analysis of Softening Point Temperature Data

Table 6.11 presents the results of the ANOVA performed on the results of the softening point temperature test. This table shows significant differences between each of the three main effects (asphalt binder, Fine, and F/A ratio) and all interactions. Because of the significant differences between each of the main effects and all

interactions, further analysis using the results of this test was completed using all data points. Trends between the results of the softening point temperature testing and results from other tests were analyzed.

Table 6.11: Results of ANOVA for Softening Point Temperature Testing

Source of Variation	F-ratio	F_{crit}	Significant Difference?
Asphalt Binder	132.74	3.92	Yes
Fine	1074.87	1.90	Yes
F/A Ratio	3105.25	2.77	Yes
Asphalt Binder*Fine	44.04	1.90	Yes
Asphalt Binder*F/A Ratio	7.84	2.77	Yes
Fine*F/A Ratio	193.87	1.58	Yes
Asphalt Binder*Fine*F/A Ratio	8.74	1.58	Yes

One of the methods described in the literature review for determining the stiffening effect of the baghouse fines on asphalt binders was to evaluate the change in softening point temperature. This value is calculated by subtracting the softening point temperature for the neat asphalt binder from the softening point temperature of the mortar (ΔSP).

Two properties of the baghouse fines that showed good correlation with the ΔSP results were the percent bulk volume (Figure 6.45) and percent free asphalt (Figure 6.46) in a compacted fine (R^2 = 0.91 and 0.91, respectively). Based on the correlation values for these two properties, percent bulk volume or percent free asphalt can be used to characterize a fine's potential for stiffening an asphalt binder as measured by the

softening point test. These close correlation values are as expected. Recall from Chapter 4 that percent bulk volume and percent free asphalt are related in that they sum to 100 percent.

Results from the particle size analysis did not correlate well with the ΔSP data. Table 6.12 presents the correlation coefficients for the ΔSP data when compared to the different properties determined during the particle size analysis. Because the particle size data was obtained for the actual fines and can not be related to a given F/A ratio, the table shows the correlation coefficients for each F/A ratio. Both asphalt binders were included for these comparisons.

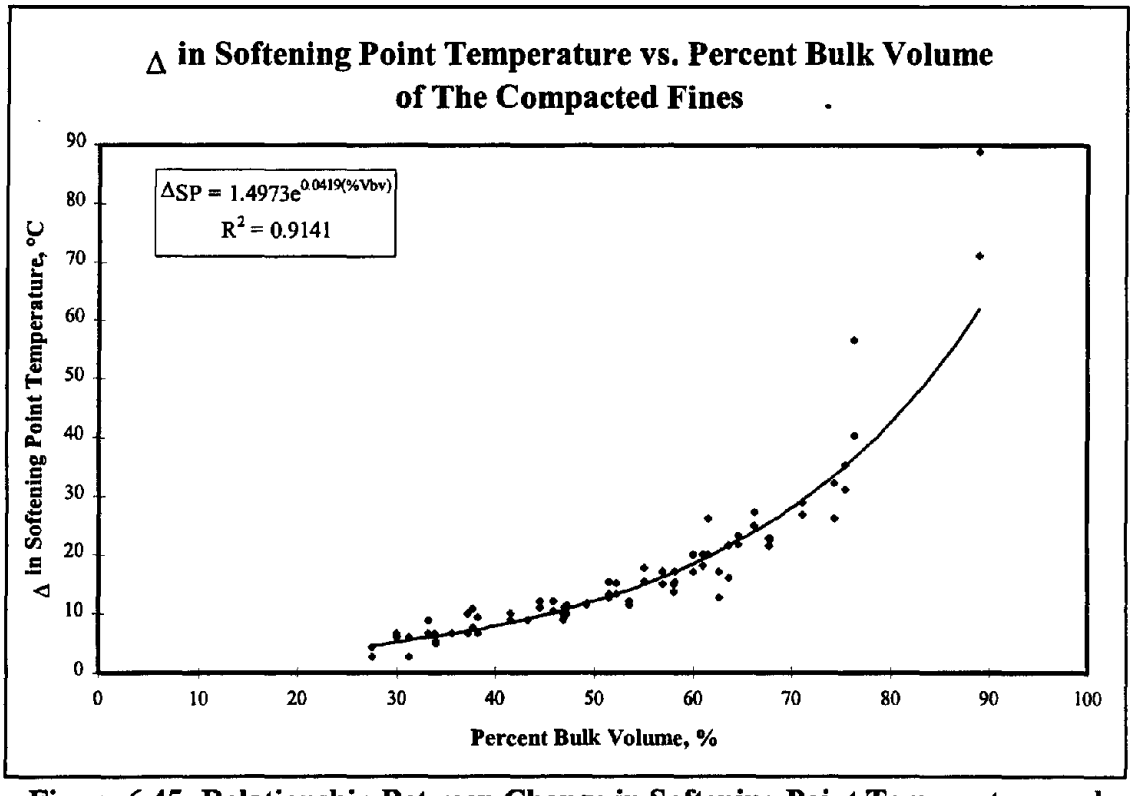

Figure 6.45: Relationship Between Change in Softening Point Temperature and Percent Bulk Volume of the Compacted Fines

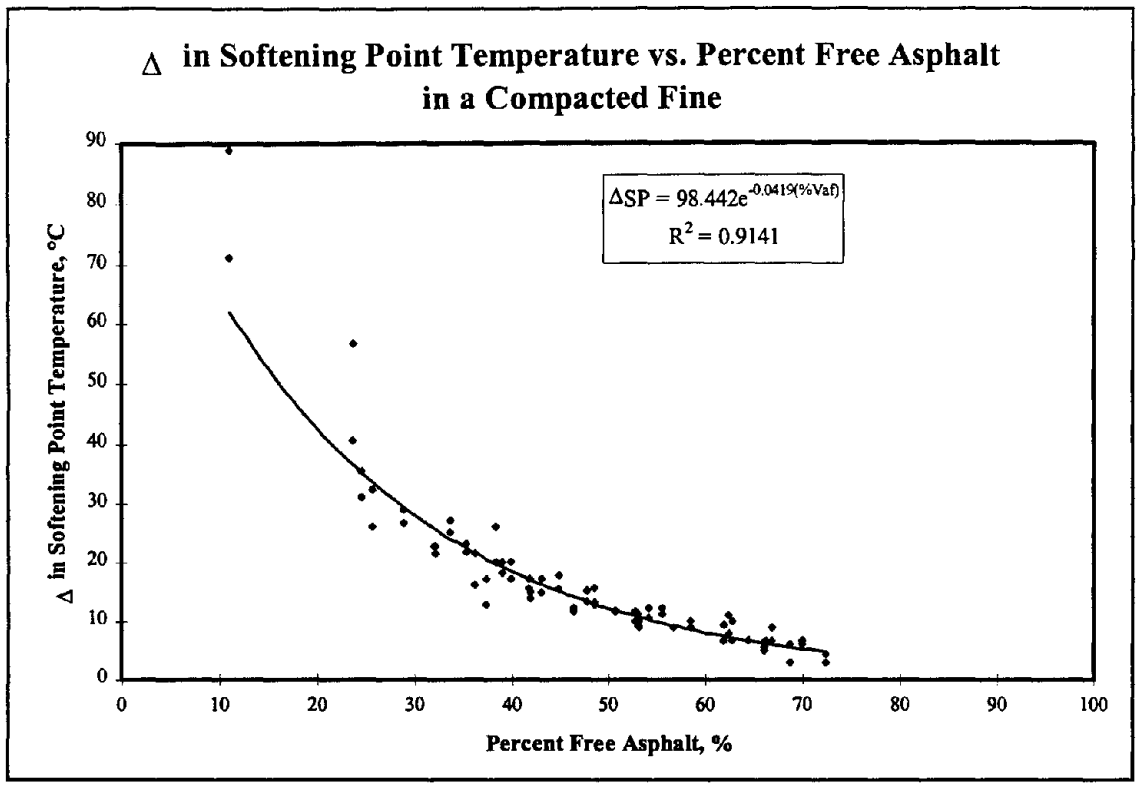

Figure 6.46: Relationship Between Change in Softening Point Temperature and Percent Free Asphalt of the Compacted Fines

Table 6.12: Correlation Coefficients for Relationships Between Particle Size Data and ΔSP

Particle Size Distribution Property	F/A Ratio	Correlation Coefficient (R^2)
Mean Particle Size, microns	0.2	0.08
	0.3	0.15
	0.4	0.15
	0.5	0.12
D_{10}, microns	0.2	0.06
	0.3	0.09
	0.4	0.07
	0.5	0.04

Table 6.12: Correlation Coefficients for Relationships Between Particle Size Data and ΔSP

Particle Size Distribution Property	F/A Ratio	Correlation Coefficient (R^2)
Coefficient of Uniformity	0.2	0.11
	0.3	0.09
	0.4	0.04
	0.5	0.03
Percent Clay-Size Particles	0.2	0.20
	0.3	0.21
	0.4	0.11
	0.5	0.11
Fineness Modulus	0.2	0.11
	0.3	0.18
	0.4	0.09
	0.5	0.12
Specific Surface Area, cm^2/ml	0.2	0.20
	0.3	0.22
	0.4	0.14
	0.5	0.14

6.3.2 Analysis of Brookfield Viscosity Testing at 135°C

Table 6.13 presents the results of the ANOVA performed on the results of the Brookfield viscosity measurements at 135°C. This table shows significant differences between each of the three main effects and all interactions.

As mentioned in the literature review another method of determining the stiffening effect of baghouse fines on asphalt binders was by calculating a stiffening

ratio. The stiffening ratio was defined as the viscosity of a mortar divided by the viscosity of the neat asphalt binder. If baghouse fines stiffen the asphalt binder, the viscosity of the mortar should be higher than the viscosity of the neat asphalt binder. Hence, the stiffening ratio (SR135) should increase if the baghouse fines stiffen the asphalt cement.

Table 6.13: Results of ANOVA for Brookfield Viscosity Measurements at 135°C

Source of Variation	F-ratio	F_{crit}	Significant Difference?
Asphalt Binder	160.33	3.92	Yes
Fine	571.66	1.90	Yes
F/A Ratio	1241.91	2.77	Yes
Asphalt Binder*Fine	70.49	1.90	Yes
Asphalt Binder*F/A Ratio	214.65	2.77	Yes
Fine*F/A Ratio	449.41	1.58	Yes
Asphalt Binder*Fine*F/A Ratio	14.04	1.58	Yes

As with the softening point temperature results, both percent bulk volume (Figure 6.47) and percent free asphalt (Figure 6.48) show good correlations with the SR135 data (R^2=0.91 and R^2=0.91, respectively). Based on the correlation values for these two properties, either the percent bulk volume or percent free asphalt can be used to characterize a baghouse fine's potential for stiffening an asphalt binder as measured by the Brookfield viscometer at 135 °C.

Figure 6.49 shows that there is also a good correlation between the ΔSP and SR135 data. This figure shows that as the SR135 for a mortar increases, so does the ΔSP. Therefore, both of these tests similarly indicate a mortar's stiffness.

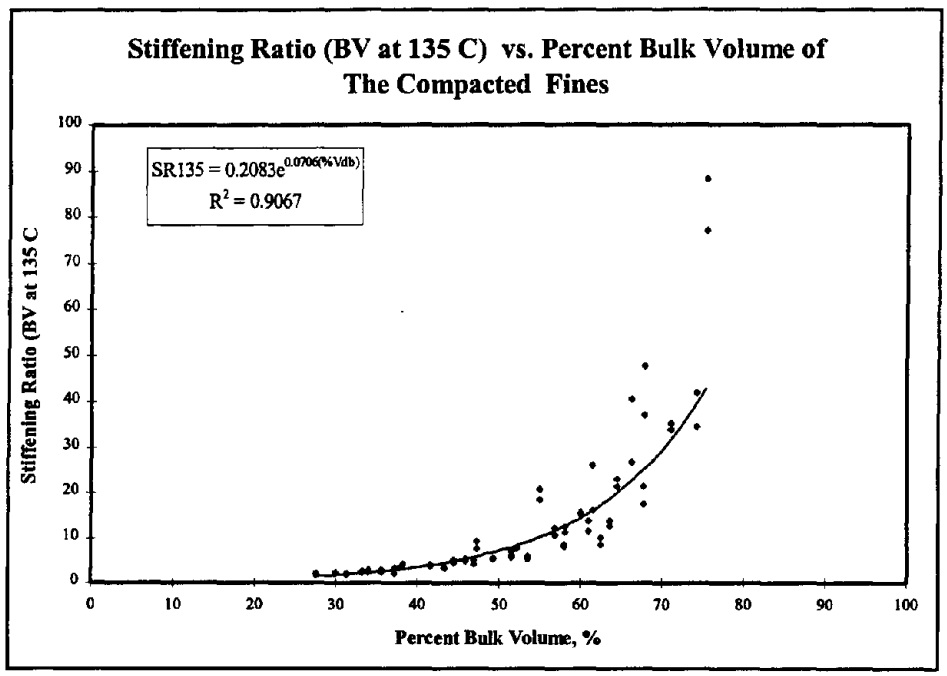

Figure 6.47: Relationship Between Stiffening Ratio and Percent Bulk Volume of the Compacted Fines

As with the ΔSP, there was little correlation between the SR135 data and the various properties determined during the particle size analyses (Table 6.14).

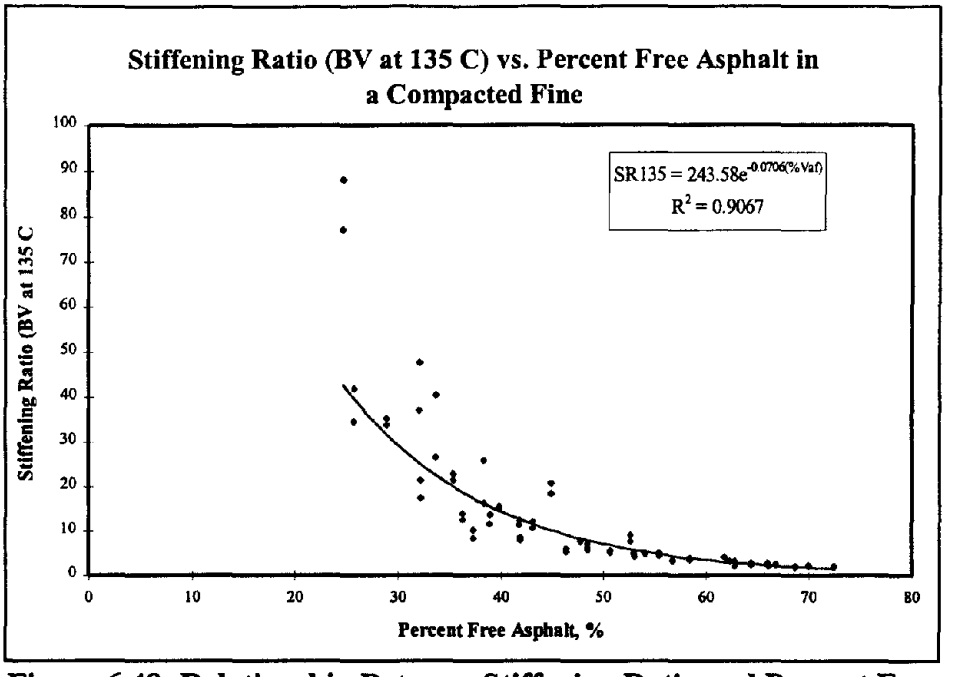

Figure 6.48: Relationship Between Stiffening Ratio and Percent Free Asphalt of the Compacted Fines

6.3.3 Analysis of Brookfield Viscosity Testing at 175°C

Table 6.15 presents the results of the ANOVA performed on the results of the Brookfield viscosity measurements at 175°C. This table shows significant differences between each of the three main effects and for all interactions.

Results from the Brookfield viscosity measurements at 175°C were also used to determine stiffening ratios (SR175). Similar to the SR135, the SR175 values showed a good correlation with percent bulk volume and percent free asphalt ($R^2 = 0.91$ and 0.91, respectively).

Table 6.14: Correlation Coefficients Relationships Between Particle Size Data and SR135 (BV at 135°C)

Particle Size Distribution Property	F/A Ratio	Correlation Coefficient (R^2)
Mean Particle Size, microns	0.2	0.25
	0.3	0.18
	0.4	0.18
	0.5	0.24
D_{10}, microns	0.2	0.12
	0.3	0.08
	0.4	0.08
	0.5	0.14
Coefficient of Uniformity	0.2	0.04
	0.3	0.03
	0.4	0.03
	0.5	0.04
Percent Clay-Size Particles	0.2	0.17
	0.3	0.11
	0.4	0.07
	0.5	0.14
Fineness Modulus	0.2	0.20
	0.3	0.14
	0.4	0.14
	0.5	0.21
Specific Surface Area, cm^2/ml	0.2	0.20
	0.3	0.14
	0.4	0.09
	0.5	0.10

Table 6.15: Results of ANOVA for Brookfield Viscosity Measurements At 175 C			
Source of Variation	F-ratio	F_{crit}	Significant Difference?
Asphalt Binder	160.33	3.92	Yes
Fine	571.66	1.90	Yes
F/A Ratio	124.91	2.77	Yes
Asphalt Binder*Fine	70.49	1.90	Yes
Asphalt Binder*F/A Ratio	214.65	2.77	Yes
Fine*F/A Ratio	449.41	1.58	Yes
Asphalt Binder*Fine*F/A Ratio	14.04	1.58	Yes

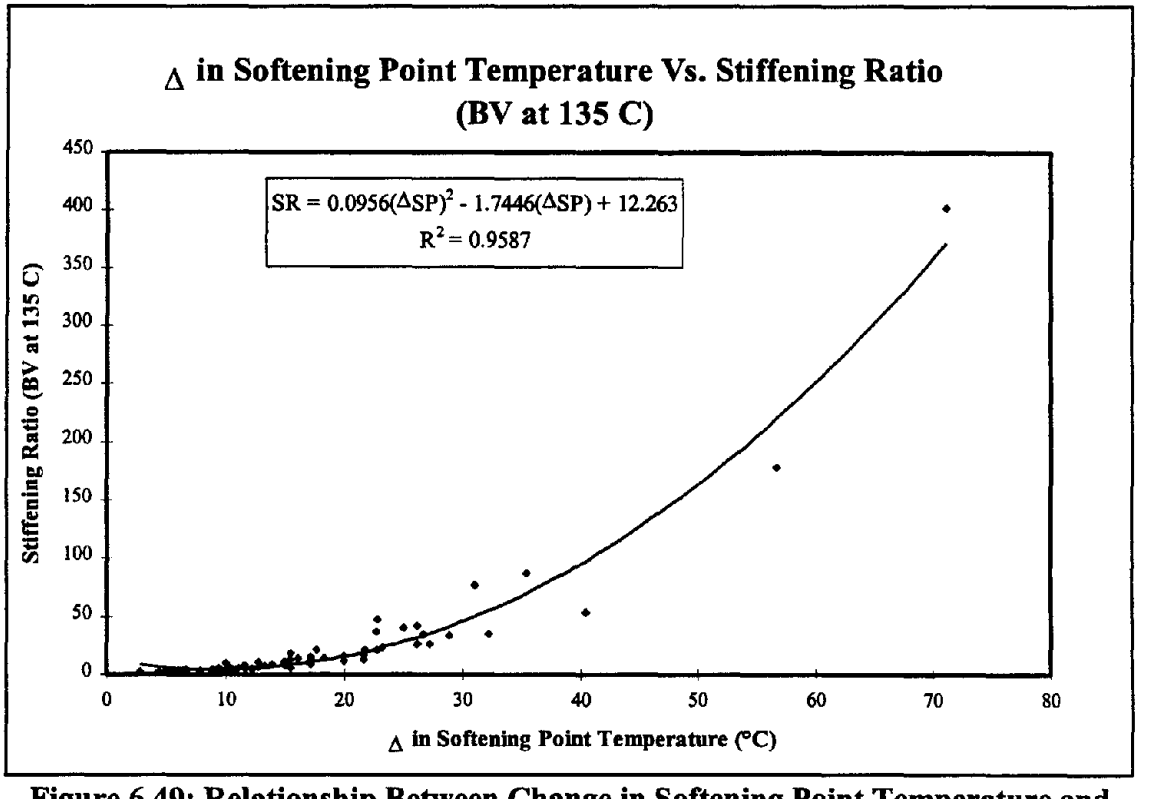

Figure 6.49: Relationship Between Change in Softening Point Temperature and Stiffening Ratio Based on BV at 135 C

However, the relationship between the SR135 values and the SR175 values were not linear (Figure 6.50), the data points tend to be above the Line of Equality. This would indicate that the stiffening ratios determined at 135°C are larger for a given asphalt binder, F/A ratio, and Fine combination. This can be explained in that when testing at the higher test temperature (175°C), the Fines may be settling in the less viscous mortar. Therefore, stiffening ratios determined at 135°C may give a better indication of the stiffness of the mortar.

Because of the strong relationship between the SR175 determined at 175°C and the SR135 determined at 135°C, an analysis between the SR175 and the different Fine's particle size data was not performed.

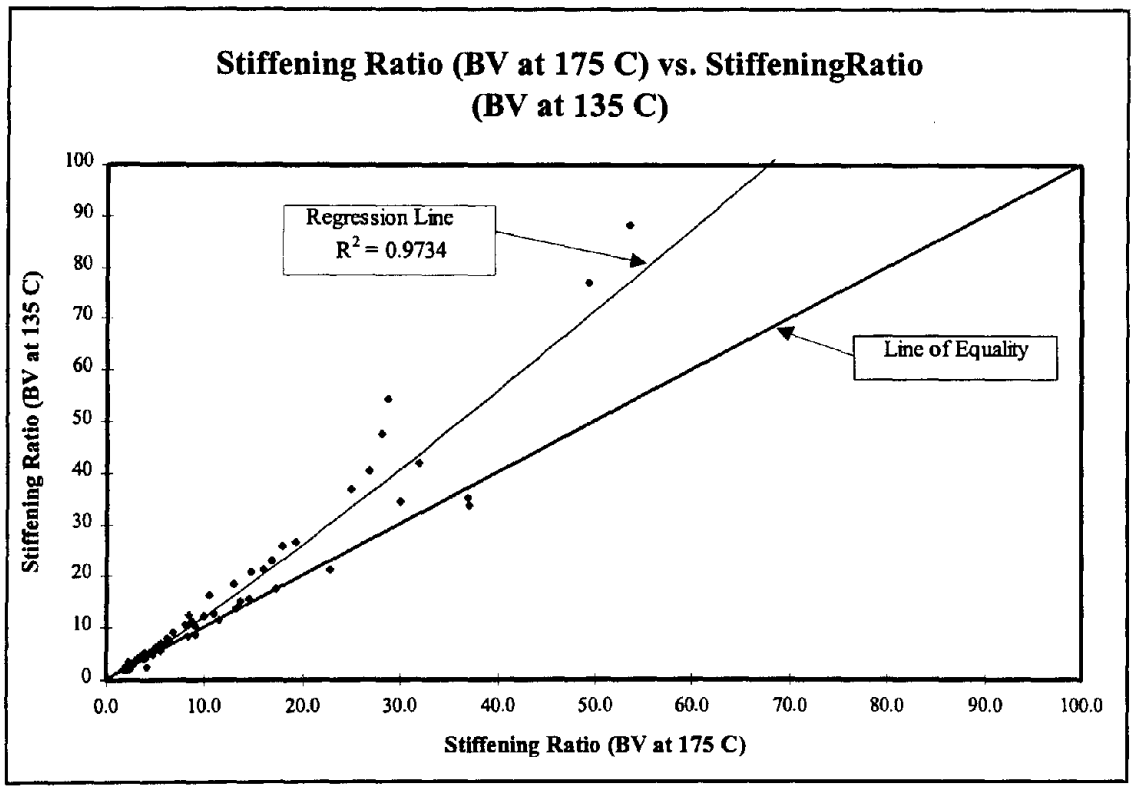

Figure 6.50: Relationship Between Stiffening Ratios Determined at 135°C and 175°C

6.3.4 Analysis of Dynamic Shear Rheometer Testing at 64°C on Original, Unaged Mortars

Tables 6.16 and 6.17 present the results of the ANOVA performed on the complex shear modulus (G*) and the phase angle (δ) data obtained during testing with the dynamic shear rheometer (DSR) at 64°C, respectively. Both G* and δ are distinct properties determined by the DSR, therefore separate analyses were performed on these data. Table 6.16 shows significant differences for each of the main effects and all interactions for G*. Table 6.17 shows that while each of the main effects are significantly different for δ, only the Asphalt Binder*Fine and Asphalt Binder*Fine*F/A ratio interactions are significantly different. The Fine*F/A ratio interaction is not significantly different.

Table 6.16: Results of ANOVA for G* as Determined By DSR Testing on the Original, Unaged Mortars

Source of Variation	F-ratio	F_{crit}	Significant Difference?
Asphalt Binder	72.19	3.92	Yes
Fine	88.23	1.90	Yes
F/A Ratio	936.29	2.77	Yes
Asphalt Binder*Fine	11.97	1.90	Yes
Asphalt Binder*F/A Ratio	11.26	2.77	Yes
Fine*F/A Ratio	9.60	1.58	Yes
Asphalt Binder*Fine*F/A Ratio	5.78	1.58	Yes

Table 6.17: Results of ANOVA for δ as Determined By DSR Testing on the Original, Unaged Mortars			
Source of Variation	F-ratio	F_{crit}	Significant Difference?
Asphalt Binder	615.89	3.92	Yes
Fine	17.23	1.90	Yes
F/A Ratio	18.39	2.77	Yes
Asphalt Binder*Fine	11.37	1.90	Yes
Asphalt Binder*F/A Ratio	0.37	2.77	No
Fine*F/A Ratio	8.82	1.58	Yes
Asphalt Binder*Fine*F/A Ratio	6.52	1.58	Yes

Because G* reflects a materials' stiffness, it is not surprising that it is a good indicator of a mortar's stiffness. Since previous results showed that ΔSP and SR135 were also good indicators of changes in mortar stiffness, there should be a good relationship between all three parameters. Figure 6.51 confirms this hypothesis by showing that as the ΔSP increases, so does G* ($R^2 = 0.76$).

As with the ΔSP and SR135, G* data is also well correlated with percent bulk volume and percent free asphalt (Figures 6.52 and 6.53, respectively).

Relationships with the particle size data were not explored because of the strong relationship G* had with ΔSP and SR135.

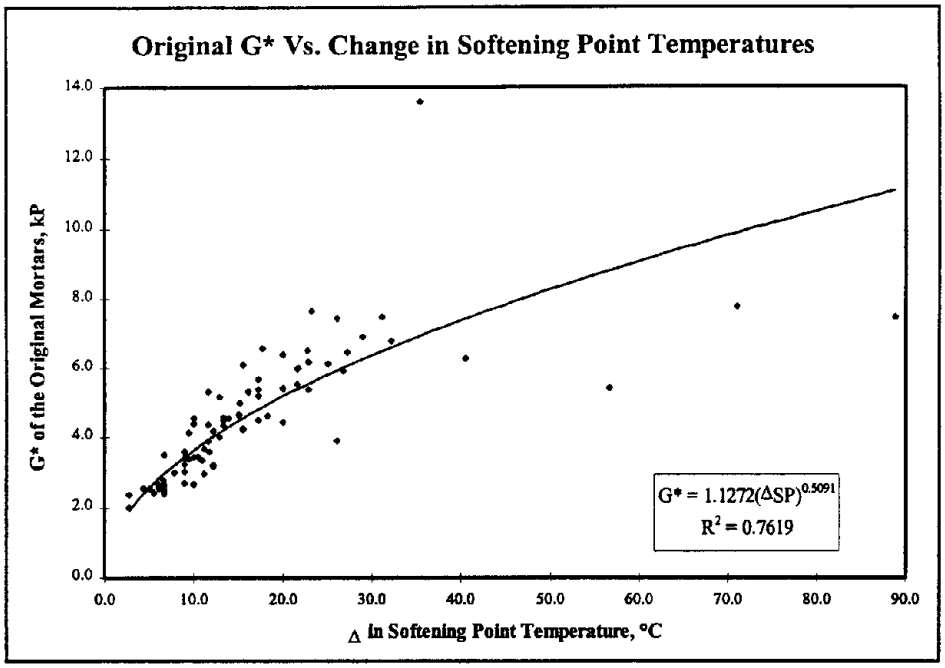

Figure 6.51: Relationship Between ΔSP and G*

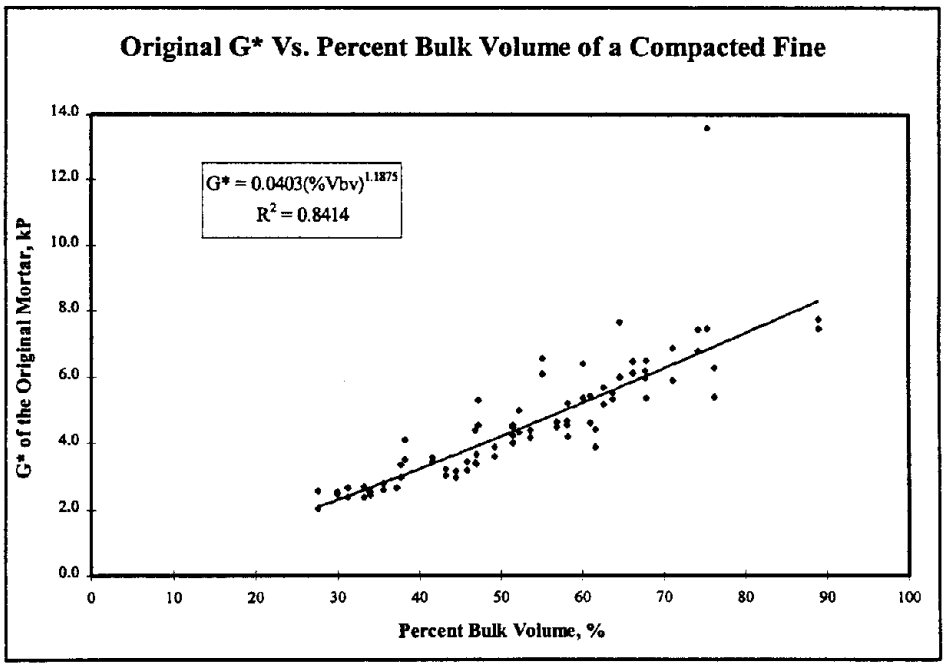

Figure 6.52: Relationship Between Percent Bulk Volume and G*

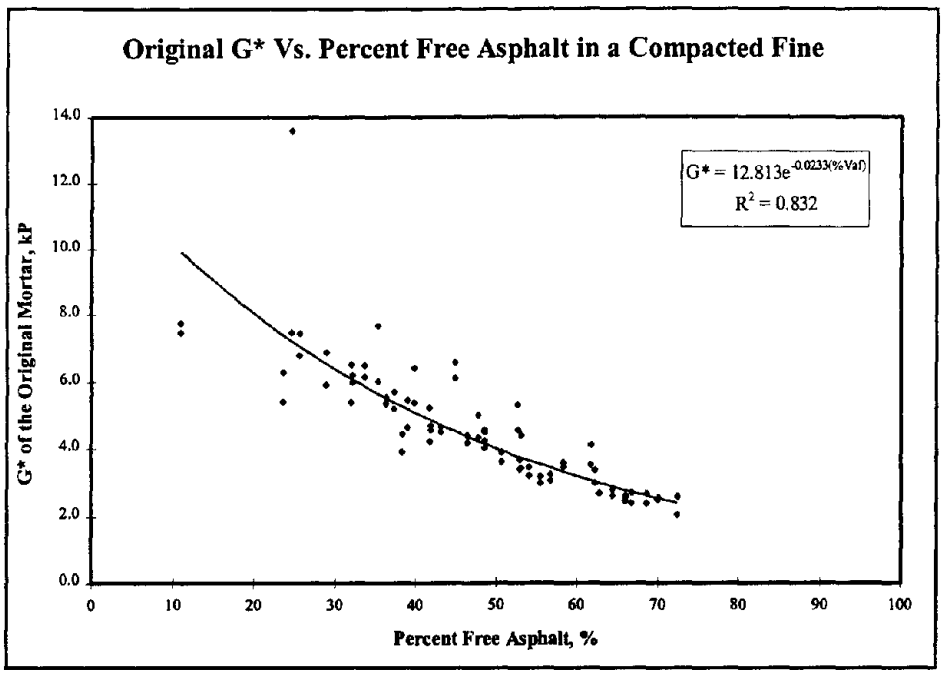

Figure 6.53: Relationship Between Percent Free Asphalt and G*

The DSR has been adopted by Superpave as an asphalt binder characterization test. Researchers for SHRP adopted a factor called "G-star over Sine Delta" (G*/Sin(δ)) as a performance related property. Previously it was shown that G* can be used as an indicator of a baghouse fine's stiffening effect on an asphalt binder. Even though δ is not an indicator of stiffening, it is a property determined during DSR testing. Therefore, the factor G*/Sin(δ) was compared to both ΔSP and SR135 to determine if it could be used as an indicator of a baghouse fine's potential for stiffening an asphalt binder. The correlation values were very similar for both ΔSP and SR135 (R^2 = 0.76 and 0.79, respectively). Therefore, G*/Sin(δ) can also be used as an indicator of stiffening. Because of the high correlation values, G*/Sin(δ) was also compared to percent bulk volume (R^2 = 0.84) and percent free asphalt (R^2=0.84). Based on these

relationships, percent bulk volume and percent free asphalt can be used to characterize a baghouse fine's potential for stiffening an asphalt binder as measured by G*/Sin(δ) on an original, unaged mortar.

6.3.5 Analysis of Dynamic Shear Rheometer Testing at 64°C on TFOT Aged Mortars

Tables 6.18 and 6.19 present the results of the ANOVA performed on the G* and δ data obtained during testing with the DSR at 64°C on TFOT aged mortars. Table 6.18 shows significant differences in G* for each of the main effects and all interactions. Table 6.19 shows significant differences in δ between each of the main effects but only the Asphalt Binder*Fine and Fine*F/A Ratio interactions. Further analysis of these data was accomplished to determine if the baghouse fines affect the aging characteristics of the asphalt binders and to determine if the baghouse fines affect the rutting susceptibility (as shown by G*/Sin(δ)) of the asphalt binder.

As mentioned in Chapter 4, asphalt binders age due to two mechanisms: volitization of light oils and oxidation. These aging mechanisms tend to stiffen an asphalt binder. When testing an asphalt binder in the original, unaged condition and then testing the same binder in the TFOT condition, the stiffening of the binder is evident. The two neat asphalt binders used for this project showed this stiffening. When comparing G* and δ as determined on the neat binders in the TFOT aged condition to the unaged condition, G* increased and δ decreased for both.

Table 6.18: Results of ANOVA for G* As Determined By DSR Testing on the TFOT Aged Mortars			
Source of Variation	F-ratio	F_{crit}	Significant Difference?
Asphalt Binder	126.71	4.00	Yes
Fine	23.66	2.10	Yes
F/A Ratio	795.87	3.15	Yes
Asphalt Binder*Fine	11.88	2.10	Yes
Asphalt Binder*F/A Ratio	21.82	2.76	Yes
Fine*F/A Ratio	12.68	2.10	Yes
Asphalt Binder*Fine*F/A Ratio	8.79	2.10	Yes

Table 6.19: Results of ANOVA for δ as Determined By DSR Testing on the TFOT Aged Mortars			
Source of Variation	F-ratio	F_{crit}	Significant Difference?
Asphalt Binder	130.35	4.00	Yes
Fine	6.73	2.10	Yes
F/A Ratio	6.51	3.15	Yes
Asphalt Binder*Fine	2.62	2.10	Yes
Asphalt Binder*F/A Ratio	0.83	2.76	No
Fine*F/A Ratio	3.99	2.10	Yes
Asphalt Binder*Fine*F/A Ratio	1.57	2.10	No

In order to determine if the different baghouse fines affect the aging characteristics of the asphalt binders, δ was examined. This material property was selected because it defines the ratio of the viscous and elastic properties of a mortar. In order to determine if the fines affected the asphalt binders, a δ-ratio was developed. This ratio was calculated as δ for a TFOT aged mortar divided by δ for the same mortar

in an unaged condition. The δ-ratio was calculated for both neat asphalt binders and the average for each of the ten mortars. The average δ-ratio value includes the four F/A ratios.

Figure 6.54 presents the δ-ratios for each of the mortars and for both neat asphalt binders. This figure has been divided into two sections to illustrate the effects of aging on δ for both asphalt binders. Both sections contain a solid horizontal line that represents the δ-ratios for both neat asphalt binders. If the different mortars do not affect the aging characteristics of the two asphalt binders, the different δ-ratios should fall along these solid lines. It can be seen from the figure that for both asphalt binders, the δ-ratios do fall along these two solid lines. Some variation does occur along these lines, but constitutes less than two degrees in δ and can be explained by experimental error and was deemed insignificant. Based on this figure, the different fines do not affect the aging characteristics of the two asphalt binders when aged by TFOT procedures.

Also included on this figure is a horizontal dashed line passing through both sections of the figure. This dashed line represents a δ-ratio of 1.00. If δ does not change due to TFOT aging, the δ-ratio would be 1.00. Since all δ-ratios are below 1.0, TFOT aging consistently decreases δ.

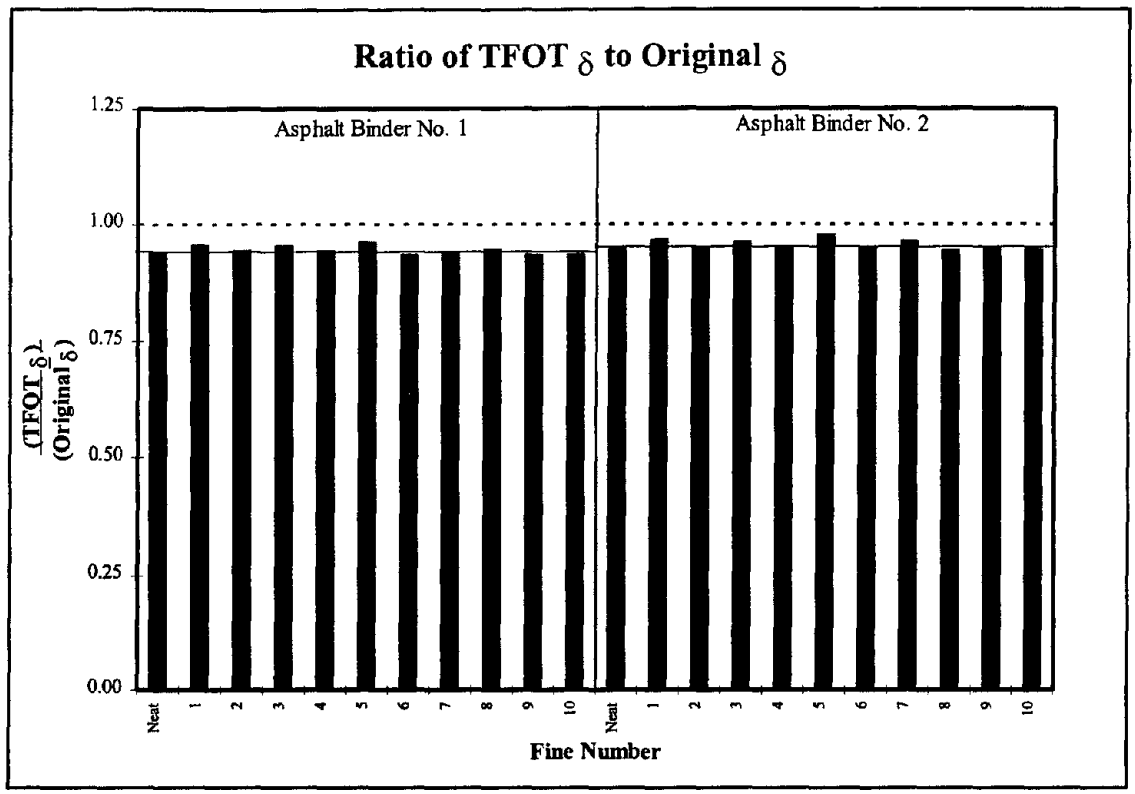

Figure 6.54: δ-Ratio for Each Asphalt Binder and Fine

As previously mentioned, the DSR has been adopted by Superpave as an asphalt binder characterization test. The factor G*/Sin(δ) for Rolling Thin Film Oven (RTFO) aged binders has been designated a rutting factor. Recall that the TFOT aging procedures were used for this study. The reason was that the mortars crawled out of the RTFO aging bottles during testing. However, the RTFO and TFOT procedures were designed to age an asphalt binder to approximately the same condition.

The total resistance of an asphalt concrete pavement to permanent deformation (rutting) is provided by both the aggregate and asphalt binder within the pavement. The importance of stone-on-stone contact of the aggregate is important, but a stiff, elastic

asphalt binder is also desirable. To ensure a desirable asphalt binder, Superpave has defined a minimum limit for G*/Sin(δ) of 2.20 kPa on the rutting factor. Therefore, as the rutting factor increases, the contribution of the mortar to the resistance of an asphalt concrete pavement to permanent deformation should also increase.

Figure 6.55 presents the rutting factors for the different mortars tested during this project. Data for the rutting factors are presented on this figure by small ovals. Each oval on the figure is labeled by the asphalt binder and Fine used to fabricate the mortar. For instance, AC1F1 indicates that Asphalt Binder No. 1 and Fine 1 were utilized in fabricating the mortar.

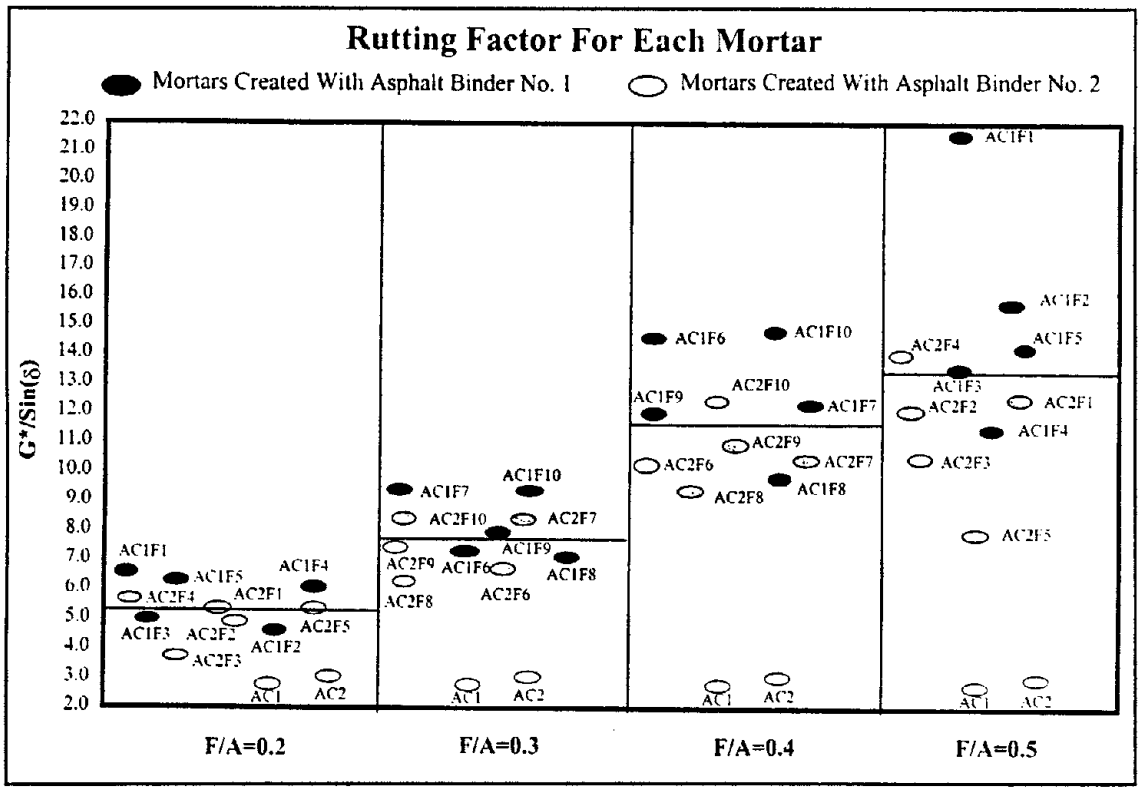

Figure 6.55: Rutting Factors For Each Mortar

This figure has been divided into four sections corresponding to the four F/A ratios utilized by volume. Based on this figure, the resistance to permanent deformation as provided by the mortar increases with increasing F/A ratios, as expected. A desirable mortar for permanent deformation resistance is stiff. Stiffness increases with the increasing F/A ratios as was illustrated by the ΔSP and SR135 data presented earlier in this chapter. Also from this figure, the rutting factor seems to be dependent on the asphalt binder utilized to fabricate the mortar. Rutting factor values for Asphalt Binder No. 1 are collectively higher than the rutting factors for Asphalt Binder No. 2.

Based on this analysis, the addition of baghouse fines may increase the resistance of an asphalt concrete pavement to permanent deformation. Also, as more baghouse fines are added (increasing F/A ratios), the resistance increases. However, this conclusion was based on mortar testing and the point must be made that an increase in fines within a HMA reduces the percentage of air voids which can result in more potential for rutting.

Relationships between the rutting factors and different physical properties of the Fines were examined. The best relationship occurred with percent bulk volume (R^2=0.79) (Figure 6.56). From this figure, the rutting factor increases with increasing values of percent bulk volume as expected. This agrees with previous results for the ΔSP and SR135 data. Based on this analysis, the percent bulk volume of a compacted fine can be used to indicate the ability of a mortar to help an asphalt concrete pavement resist permanent deformation.

6.3.6 Analysis of Dynamic Shear Rheometer Testing at 22°C of PAV Aged Mortars

Tables 6.20 and 6.21 present the results of the ANOVA performed on the G* and δ data obtained during testing with the DSR at 22°C on TFOT and PAV aged mortars. Table 6.20 shows significant differences in G* for each of the main effects but only the Fine*F/A Ratio interaction. Table 6.21 shows significant differences in δ between only the Asphalt Binder and Fine main effects but all interactions. Further analysis of these data was accomplished to determine if the baghouse fines affect the aging characteristics of the asphalt binders and to determine if the baghouse fines affect the fatigue cracking characteristics of the asphalt binders (as shown by G*Sin(δ)).

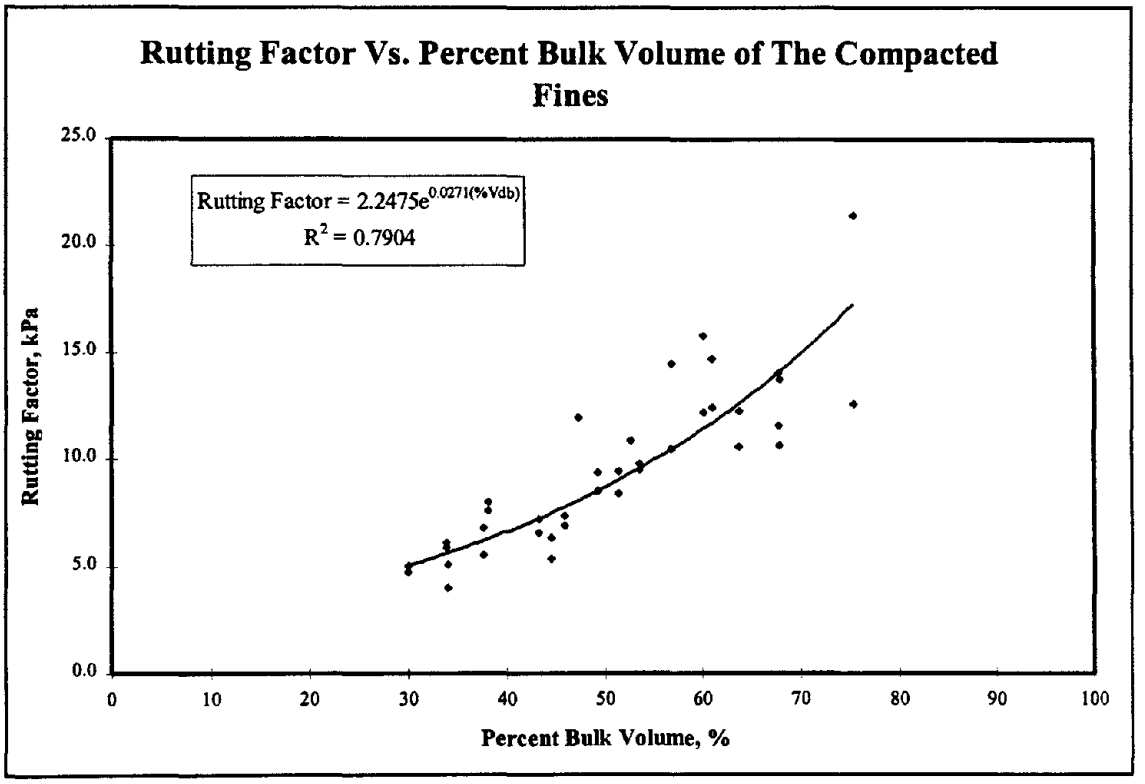

Figure 6.56: Relationship Between Rutting Factors and Percent Bulk Volume

Table 6.20: Results of ANOVA for G* As Determined By DSR Testing on the PAV Aged Mortars			
Source of Variation	F-ratio	F_{crit}	Significant Difference?
Asphalt Binder	28.74	4.00	Yes
Fine	5.36	2.10	Yes
F/A Ratio	92.47	3.15	Yes
Asphalt Binder*Fine	1.59	2.10	No
Asphalt Binder*F/A Ratio	0.22	2.76	No
Fine*F/A Ratio	4.92	2.10	Yes
Asphalt Binder*Fine*F/A Ratio	0.79	2.10	No

Table 6.21: Results of ANOVA for δ As Determined By DSR Testing on the PAV Aged Mortars			
Source of Variation	F-ratio	F_{crit}	Significant Difference?
Asphalt Binder	631.22	4.00	Yes
Fine	38.72	2.10	Yes
F/A Ratio	0.06	3.15	No
Asphalt Binder*Fine	5.58	2.10	Yes
Asphalt Binder*F/A Ratio	6.49	2.76	Yes
Fine*F/A Ratio	14.68	2.10	Yes
Asphalt Binder*Fine*F/A Ratio	4.48	2.10	Yes

Again, to determine if the different baghouse fines affect the aging characteristics of the asphalt binders, δ was examined. The δ-ratio was calculated for both neat asphalt binders and for each mortar tested.

Figure 6.57 presents the δ-ratios for each asphalt binder-Fine-F/A ratio combination tested by the one-half fractional factorial. Each column constitutes the

average value for three replicates and represents a different F/A ratio. The column labels along the horizontal axis correspond to two columns. This constitutes the two F/A ratios tested during the one-half fractional factorial. It can be seen from the figure that the different mortars did not age similar to the neat asphalt binders. Therefore, the baghouse fines did affect the aging characteristics of the neat asphalt binders when aged by both the TFOT and PAV aging procedures.

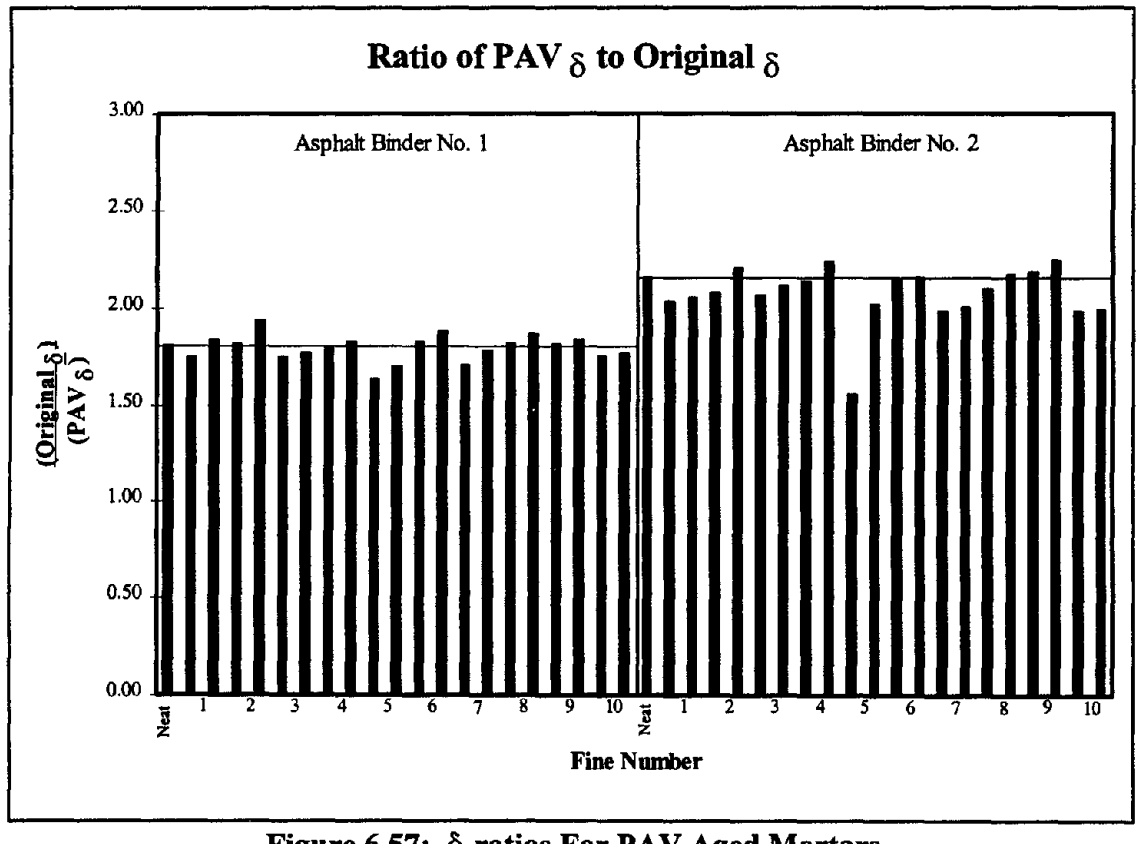

Figure 6.57: δ-ratios For PAV Aged Mortars

Similar to the rutting factor determined by G*/Sin(δ) on TFOT aged mortars, Superpave has adopted a fatigue cracking factor (FCF) called "G-star Sine Delta" (G*Sin(δ)) as a performance property related to fatigue cracking. The FCF is

determined by multiplying G* and the sine of delta. Recall that a stiff, elastic binder at high pavement temperatures is desirable to resist permanent deformation. Since fatigue cracking typically occurs at intermediate temperatures after a pavement has been in service for a period of time, the Superpave binder specification addresses fatigue cracking on a RTFO and PAV aged specimen tested at intermediate temperatures. This is the reason for testing at 22 °C. To resist fatigue cracking, it is desirable to have an asphalt binder that is soft and elastic. Therefore, low values of G* and δ are considered desirable, resulting in low values of G*Sin(δ). As G*Sin(δ) increases, the potential for fatigue cracking in an asphalt concrete pavement also increases. For a neat asphalt binder, Superpave has set a maximum value for G*Sin(δ) of 5000 kPa.

Figure 6.58 presents the fatigue cracking factors for the mortars and neat asphalt binders tested. Data for the FCFs are again presented on this figure by small ovals.

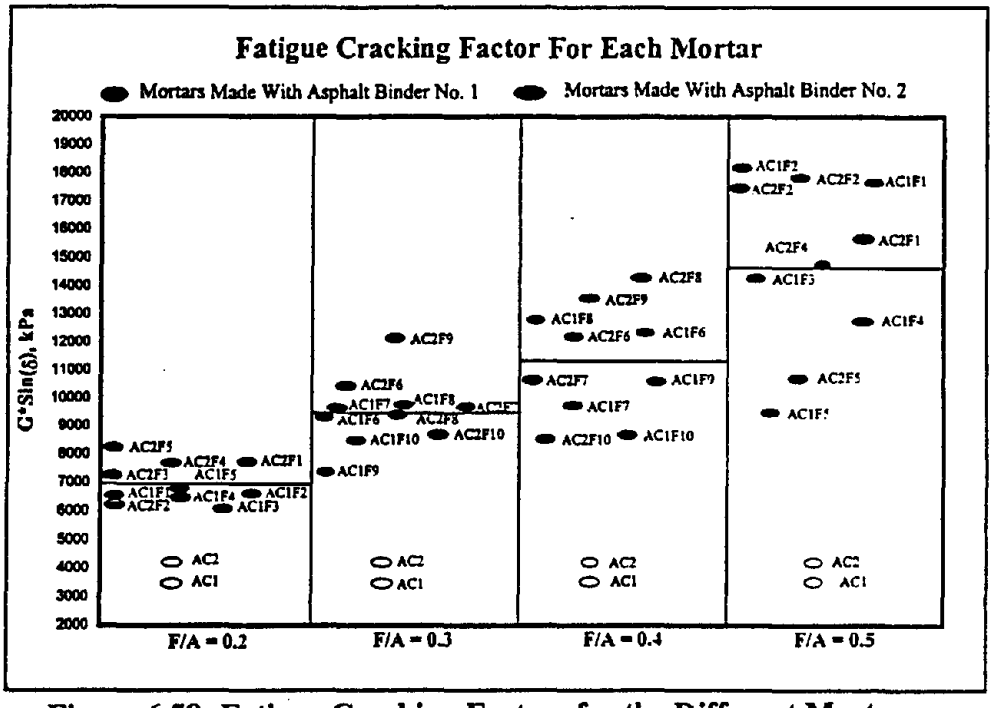

Figure 6.58: Fatigue Cracking Factors for the Different Mortars

Based on this figure, the potential for fatigue cracking increases as the F/A ratio increases. As more fines are introduced, the mortar becomes stiffer. This was also shown with both the ΔSP and the SR135 data. Also based on this figure, the FCF is dependent on the Fine within the mortar. For instance, AC2F5 has the highest FCF value for Asphalt Binder No. 2 at a F/A ratio of 0.2 and has the lowest FCF value for Asphalt Binder No. 2 at a F/A ratio of 0.5. However, AC2F2 has the lowest FCF for Asphalt Binder No. 2 at a F/A ratio of 0.2 and has the highest FCF for Asphalt Binder No. 2 at a F/A ratio of 0.5. This would indicate that for Asphalt Binder No. 2, increases in the amount of Fine 5 does not affect the fatigue cracking properties as much as increases in Fine 2.

Also based on this figure, an interaction between certain fines and the asphalt binders appears to be occurring. For instance, at a F/A ratio of 0.3 the FCF for AC2F9 is much higher than the FCF for AC1F9. This also occurs at a F/A ratio of 0.4 for the two asphalt binders and Fine 9. However, this does not occur for all fines. At a F/A ratio of 0.4, the FCF for AC1F6 and AC2F6 are very similar.

Relationships between the FCF and different Fines were examined. The best relationship again occurred with the percent bulk volume (R^2=0.64). This relationship is presented in Figure 6.59. From this figure, the FCF increases with an increasing percent bulk volume.

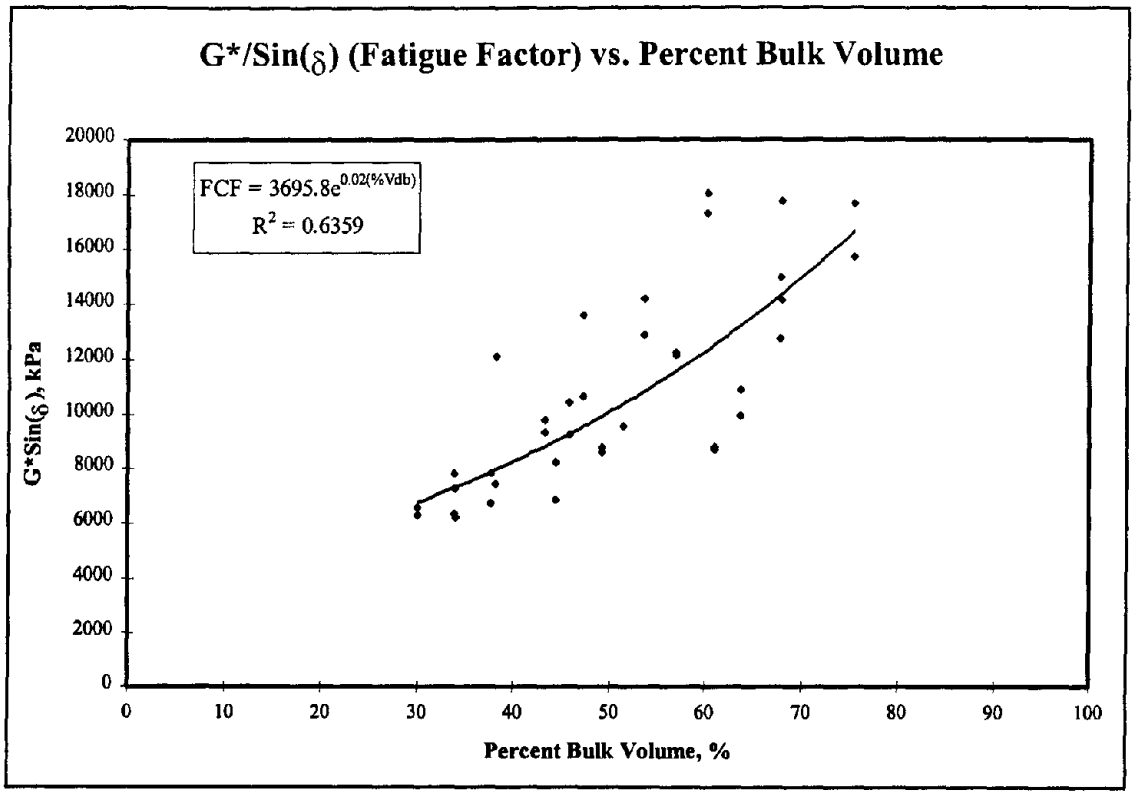

Figure 6.59: Relationship Between Fatigue Cracking Factor and Percent Bulk Volume

Based on this analysis, as the percentage of fines are increased in a mortar, the resistance (as provided by the mortar) of an asphalt concrete pavement to fatigue cracking decreases. Also, the percent bulk volume can be used as an indicator of the fatigue cracking resistance provided by a mortar. As the percent bulk volume increases, the resistance to fatigue cracking decreases.

6.3.7 Analysis of Bending Beam Rheometer Testing at -18°C on PAV Aged Mortars

When an asphalt concrete pavement's temperature decreases, the asphalt binder within the pavement shrinks. As the binder shrinks, tensile stresses build up within the pavement. When these tensile stresses exceed the tensile strength of the asphalt concrete

matrix, a low temperature crack occurs. The majority of this tensile stress resistance comes from the asphalt binder. Superpave developed the BBR test procedure to determine a binder's resistance to these tensile stresses. By knowing an asphalt binder beam's geometry and the magnitude of an applied creep load, the creep stiffness and m-value can be determined. If S is too high, an asphalt binder is too brittle and therefore is susceptible to low temperature cracking. If the m-value is too low, the asphalt binder does not have the ability to relieve the tensile stresses upon contraction at low temperatures.

Tables 6.22 and 6.23 present the results of the ANOVA performed on the Creep Stiffness (S) and the slope of the creep stiffness versus loading time (m-value) data obtained during testing with the BBR at -18°C on TFOT and PAV aged mortars. Table 6.22 shows significant differences in S between each of the three main effects and all interactions. Table 6.23 shows significant differences in m-values between each of the three main effects and all interactions except the Fine*F/A Ratio. Further analysis of these data was accomplished to determine if the different Fines affect the cold temperature properties of the asphalt binders.

Figure 6.60 presents the creep stiffness data obtained during BBR testing. This figure has been divided into four sections corresponding to the four F/A ratios. The S data are presented as small ovals.

Table 6.22: Results of ANOVA for S As Determined By BBR Testing on the PAV Aged Mortars			
Source of Variation	F-ratio	F_{crit}	Significant Difference?
Asphalt Binder	368.57	4.00	Yes
Fine	21.32	2.10	Yes
F/A Ratio	1153.13	3.15	Yes
Asphalt Binder*Fine	9.41	2.10	Yes
Asphalt Binder*F/A Ratio	14.42	2.76	Yes
Fine*F/A Ratio	8.69	2.10	Yes
Asphalt Binder*Fine*F/A Ratio	3.96	2.10	Yes

Table 6.23: Results of ANOVA for the m-value As Determined By BBR Testing on the PAV Aged Mortars			
Source of Variation	F-ratio	F_{crit}	Significant Difference?
Asphalt Binder	577.99	4.00	Yes
Fine	4.13	2.10	Yes
F/A Ratio	83.57	3.15	Yes
Asphalt Binder*Fine	3.39	2.10	Yes
Asphalt Binder*F/A Ratio	12.78	2.76	Yes
Fine*F/A Ratio	1.13	2.10	No
Asphalt Binder*Fine*F/A Ratio	5.03	2.10	Yes

Based on this figure, the potential for an asphalt concrete pavement to develop low temperature cracking should increase as more fines are introduced into an asphalt binder. This is illustrated by the increase in S with increasing F/A ratios. Also from this figure, the neat asphalt binder used to create the mortars influences the low temperature cracking potential. Collectively, the S values for Asphalt Binder No. 2 are higher. This

indicates that mortars created with Asphalt Binder No. 2 are more critical with regard to low temperature cracking.

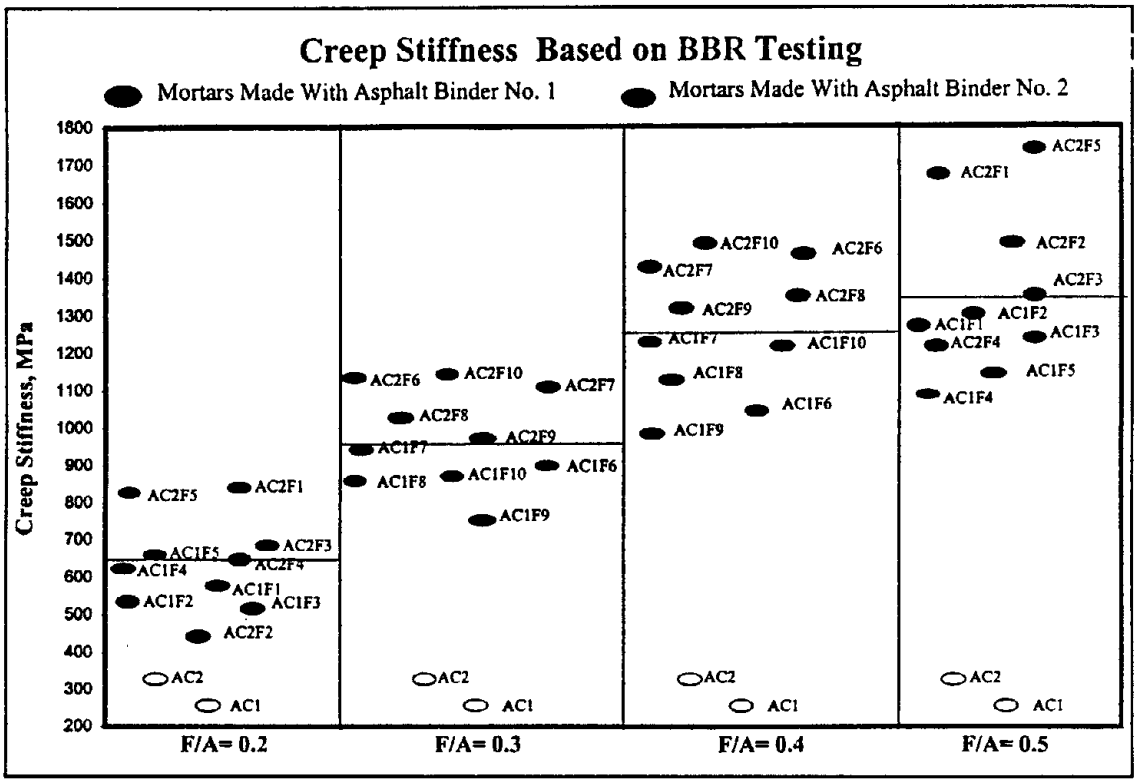

Figure 6.60: Creep Stiffness Data on BBR Tested Mortars

In order to determine if the creep stiffness could be correlated with a physical property of the different Fines, relationships between S and the different physical properties of the Fines were examined. The best relationship again occurred with the percent bulk volume (R^2=0.72). Figure 6.61 illustrates this relationship between S and

percent bulk volume. As the percent bulk volume of the Fines increases, so should the potential for low temperature cracking in an asphalt concrete pavement.

Based on this analysis, as the F/A ratio increases, the potential for low temperature cracking in an asphalt concrete pavement should also increase. Also, both the percent bulk volume and percent free asphalt are good indicators for a mortar's resistance to low temperature cracking. As the percent bulk volume increases, the potential also increases. As the percent free asphalt increases, the potential decreases.

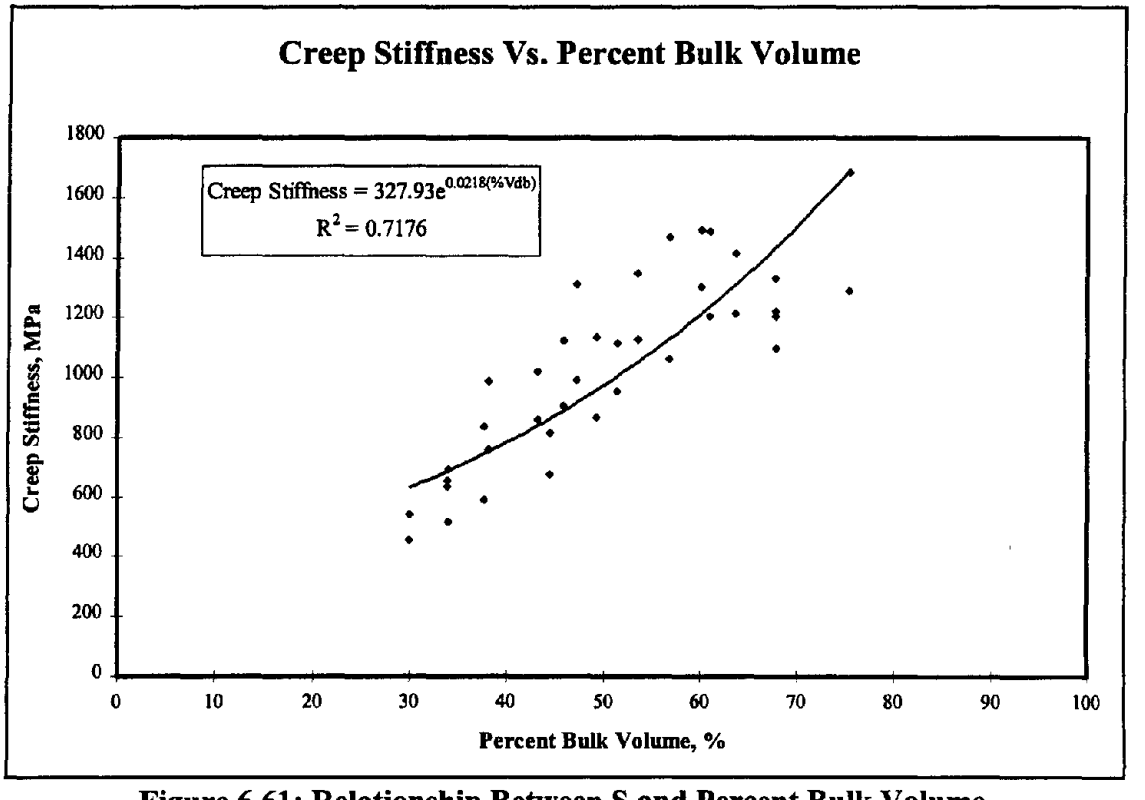

Figure 6.61: Relationship Between S and Percent Bulk Volume of a Compacted Fine

Figure 6.62 presents the m-value data obtained during BBR testing. This figure has been divided into four sections corresponding to the four F/A ratios.

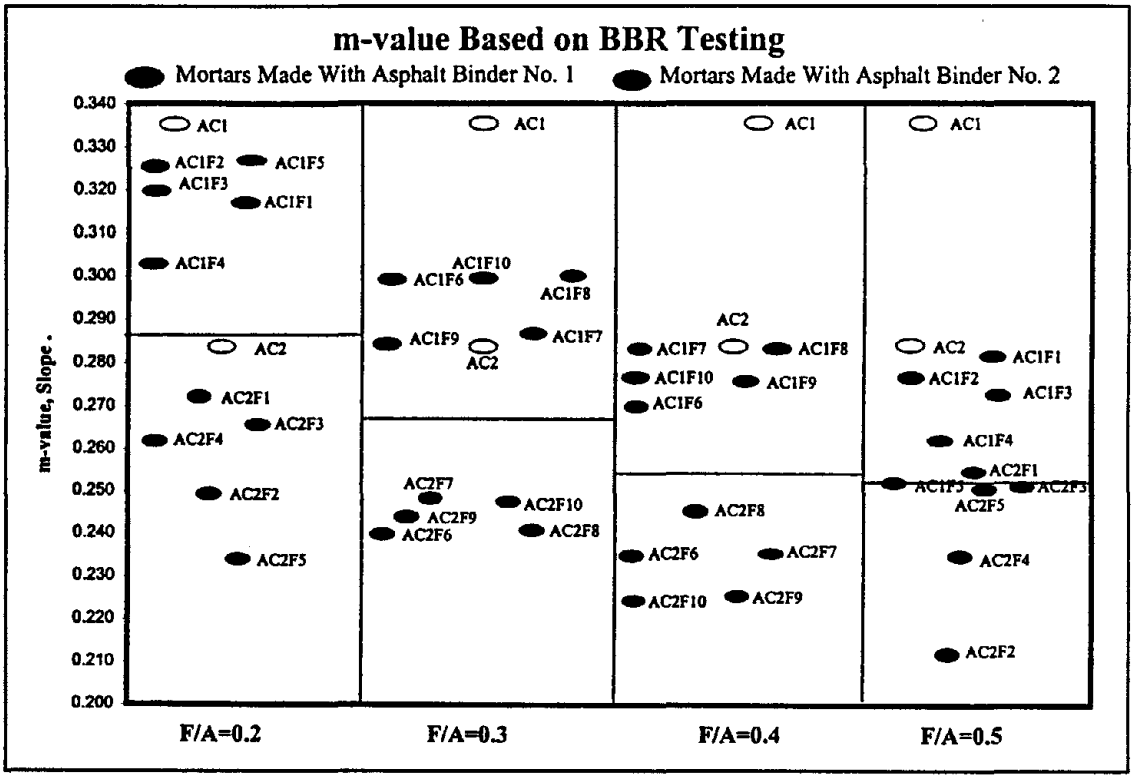

Figure 6.62: m-value Data For Each Mortar

Based on this figure, the m-value decreases as more fines are introduced into an asphalt binder. This is illustrated by decreasing m-values with increasing F/A ratios. This indicates that as the F/A ratio increases, the ability of mortars to relax over time decreases. Also from the figure, the m-values are very asphalt binder specific. Collectively the m-values for Asphalt Binder No. 1 are larger. Recall from the ANOVA

table for the m-values that the asphalt binder main effect had the largest variation. This is readily seen from this figure.

In order to determine if the creep stiffness could be correlated with a physical property of the different Fines, relationships between the m-values and different physical properties of the Fines were examined. The best relationship occurred with percent bulk volume (R^2=0.15). This is a low correlation coefficient, as expected. The m-values are more dependent on the type asphalt binder than the Fines within the mortars. This was also shown by the results of the ANOVA. The F-ratio for the different Fines was much smaller than for the asphalt binders.

However, based on this analysis the ability for a mortar to relieve tensile stresses decreases as the F/A ratio increases. Also, no physical properties of the different Fines correlated well with the ability to relieve the tensile stresses. As expected, the type asphalt binder played a more prominent role.

6.3.8 Observations About Mortar Analysis

Binder testing performed for this project included three tests that are related to the performance of HMA pavements: DSR testing on TFOT aged binders, DSR testing on TFOT and PAV aged binders, and BBR testing on TFOT and PAV aged binders. Figures 6.56, 6.59, and 6.61, respectively, compared the results of these tests to the percent bulk volume of the compacted fines. Evaluation of these three figures showed that an inflection point occurred at a percent bulk volume of approximately 55 percent.

Figures 6.63 through 6.65 again present Figures 6.56, 6.59, and 6.61, respectively, but showing the inflection points.

Referring to Figure 6.63, the rutting factor increases as the percent bulk volume increases. According to Superpave guidelines, this is desirable because it provides a stiff binder to help resist permanent deformation. However, at high rutting factors, the mortars may be too stiff. Based on the regression equation for this figure, the rutting factor at a percent bulk volume of 55 percent would be 10 kPa.

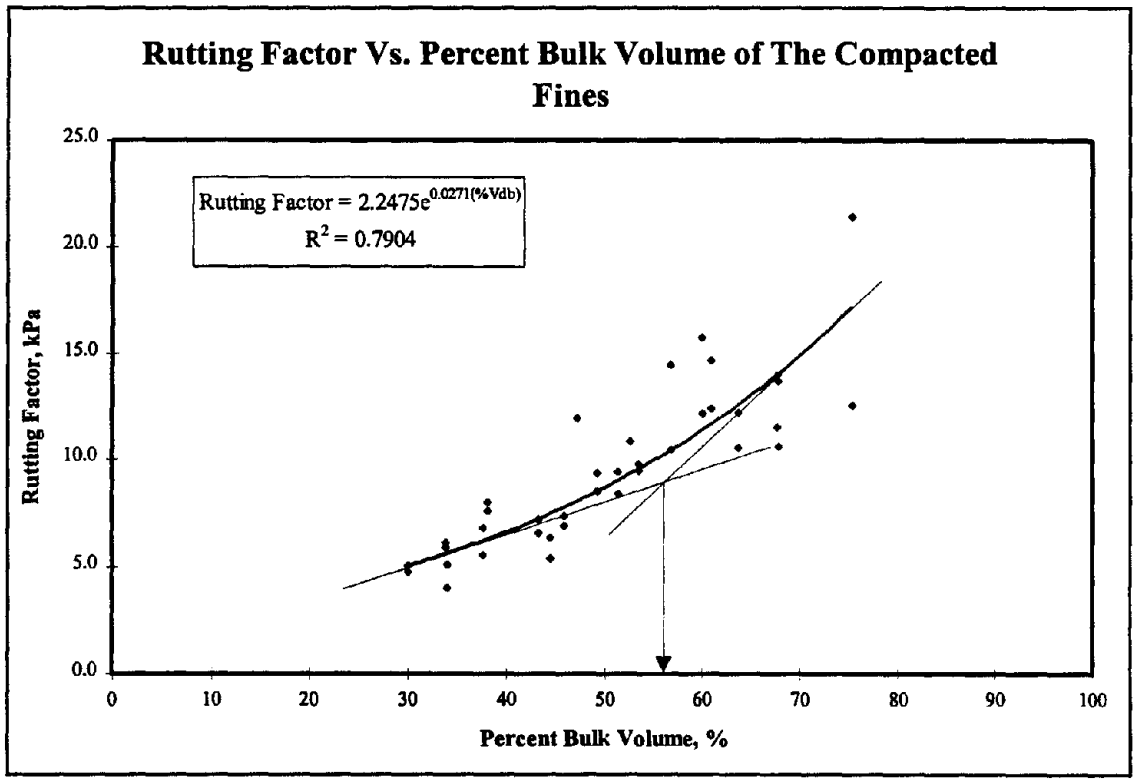

Figure 6.63: Inflection Point for Rutting Factor vs. Percent Bulk Volume

Referring to Figure 6.64, the fatigue cracking factor increases as the percent bulk volume increases. According to Superpave, this is not desirable. For fatigue cracking, a soft elastic binder is desirable. Based on the regression equation for this figure, the fatigue cracking factor at a percent bulk volume of 55 percent would be 11,100 kPa.

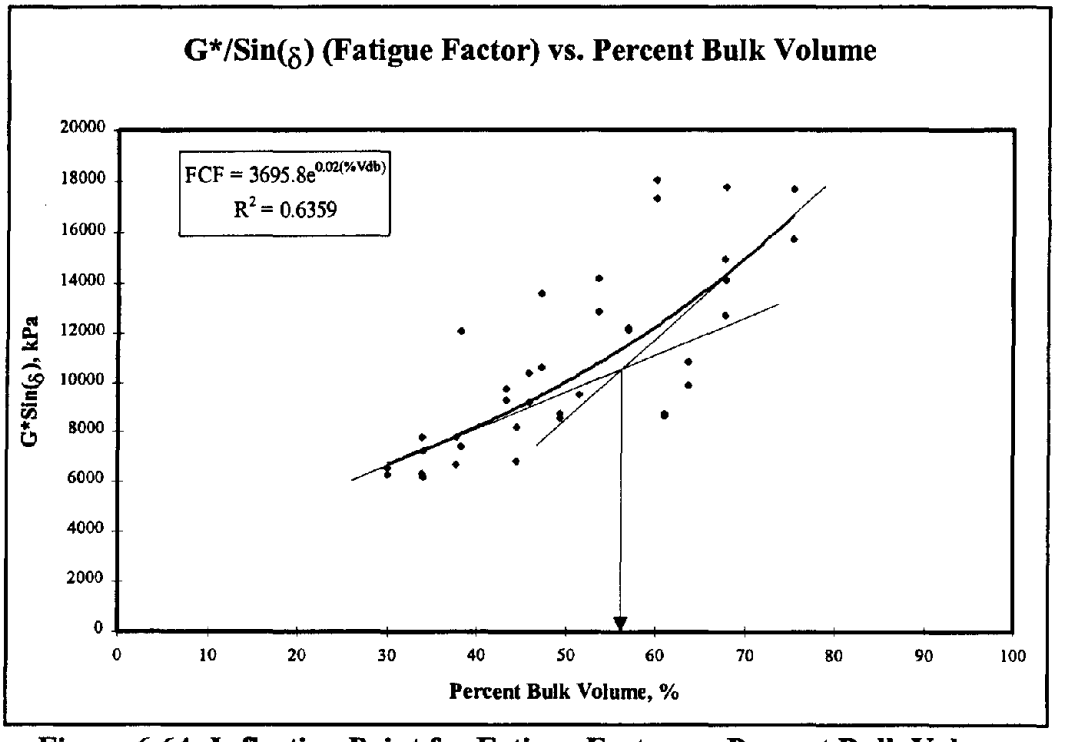

Figure 6.64: Inflection Point for Fatigue Factor vs. Percent Bulk Volume

Referring to Figure 6.65, as the percent bulk volume increases, so does the creep stiffness. High values of creep stiffness are considered undesirable because they indicate a binder that is brittle and therefore susceptible to low temperature cracking. Based on the regression equation for this figure, the creep stiffness at a percent bulk volume of 55 percent is 1090 Mpa. This critical percent bulk volume value of 55 percent agrees with

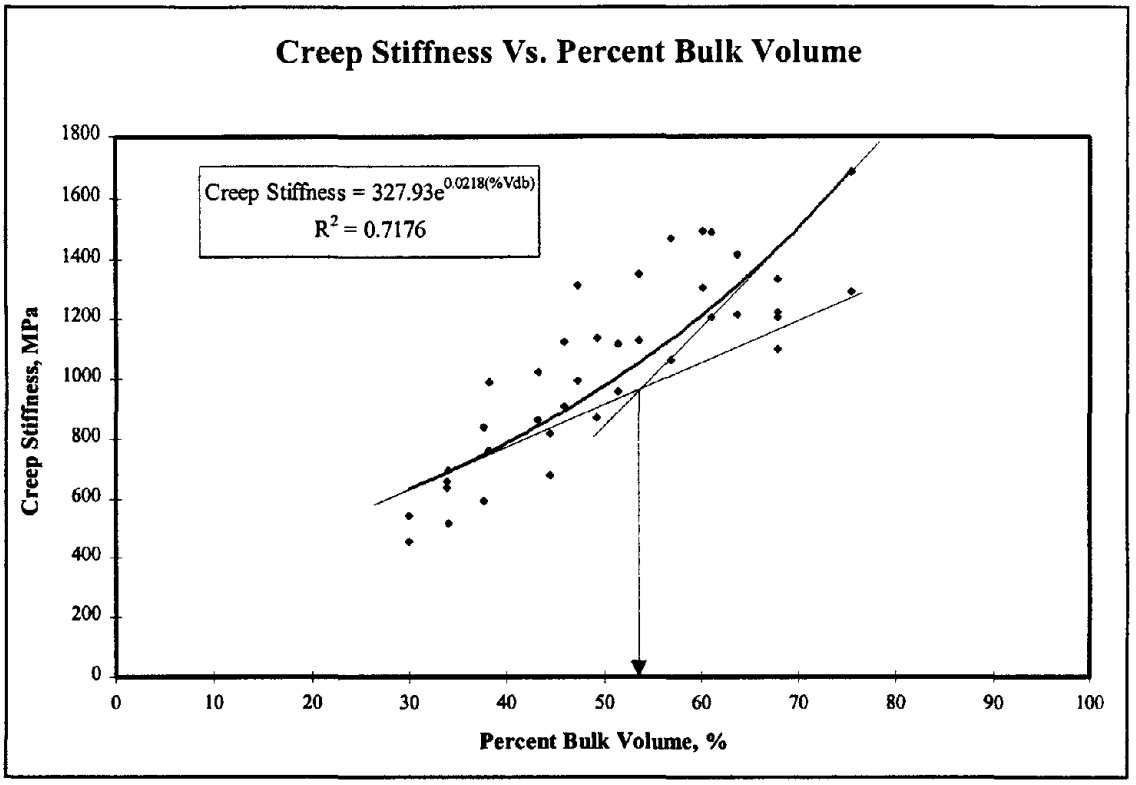

Figure 6.65: Inflection Point for Creep Stiffness vs. Percent Bulk Volume

previous research. As discussed in the Literature Review, Kandhal selected 50 percent as a critical value (17), Hucheck and Angst (18) concluded 60 percent should be the maximum, and Anderson (16) suggested 45 percent. Referring back to Table 5.3, at F/A ratios less than 0.4 most of the baghouse fine combined samples have a percent bulk volume values of less than 55 percent. However, most of the samples had percent bulk volume values more than 55 percent at a F/A ratio of 0.4. Therefore, a F/A ratio of 0.4 seems to be critical.

Because of the strong relationships that percent bulk volume had with the change in softening point temperature (R^2=0.91), the stiffening ratio as determined by the

Brookfield viscometer at 135°C (R^2=0.91), and the complex shear modulus as determined at 64°C on unaged mortars (R^2=0.84), critical values for these tests can be determined. Table 6.24 presents the values for the ΔSP, SR135, and G* that correspond to a percent bulk volume of 55 percent.

Table 6.24: Critical Values Based on a Percent Bulk Volume of 55 percent

Property	Critical Value as Determined by Regression Equations
ΔSP	15°C
SR135	10
G*	4.70 kPa

The values for ΔSP and SR135 in Table 6.24 also agree with previous research. Kandhal (17) suggested that the critical ΔSP was 11°C. Anderson (16) said that stiffening ratios of greater than 10 to 15 were critical.

6.4 Analysis of HMA Mixture Testing

Analysis of this data consisted of performing an ANOVA to determine if significant differences occurred in the results for the laboratory tests. Three main effects were analyzed using the ANOVA: asphalt binders, Fines, and F/A ratios. The H_o for these analyses was that all population means were equal, while H_a was that at least one population mean differed from the remaining means.

6.4.1 Analysis of Volumetric Data

Included within the volumetric data were the percent air voids in total mix (VTM), percent voids in mineral aggregate (VMA), and percent voids filled with asphalt (VFA). The VTM was calculated utilizing Equation 6.5, VMA was calculated by Equation 6.6, and VFA was determined by Equation 6.7.

$$VTM,\ \% = 100 \times \left[\ 1 - \frac{G_{mb}}{G_{mm}}\ \right] \qquad \textbf{Eq.: 6.5}$$

$$VMA,\ \% = 100 - \left[\ \frac{G_{mb}\ P_s}{G_{sb}}\ \right] \quad (Ref.\ 30) \qquad \textbf{Eq.:6.6}$$

$$VFA,\ \% = 100 \times \left[\frac{VMA - VTM}{VMA}\ \right] \quad (Ref.\ 30) \qquad \textbf{Eq.: 6.7}$$

where:

G_{mb} = bulk specific gravity of the mixture

G_{mm} = theoretical maximum specific gravity of the mixture

P_s = percent aggregate by total weight of mixture

G_{sb} = bulk specific gravity of the aggregate.

Results of the ANOVA for VTM, VMA, and VFA are presented in Tables 6.25, 6.26, and 6.27, respectively. For each of these volumetric properties, significant differences occurred between each main effect and all interactions.

Table 6.25: Results of ANOVA for VTM

Source of Variation	F-ratio	F_{crit}	Significant Difference?
Asphalt Binder	340.30	4.00	Yes
Fine	318.14	2.53	Yes
F/A Ratio	138.40	3.15	Yes
Asphalt Binder*Fine	15.22	2.53	Yes
Asphalt Binder*F/A Ratio	8.50	3.15	Yes
Fine*F/A Ratio	23.00	2.04	Yes
Asphalt Binder*Fine*F/A Ratio	4.58	2.04	Yes

Table 6.26: Results of ANOVA for VMA

Source of Variation	F-ratio	F_{crit}	Significant Difference?
Asphalt Binder	485.66	4.00	Yes
Fine	335.05	2.53	Yes
F/A Ratio	210.63	3.15	Yes
Asphalt Binder*Fine	24.65	2.53	Yes
Asphalt Binder*F/A Ratio	5.81	3.15	Yes
Fine*F/A Ratio	22.70	2.04	Yes
Asphalt Binder*Fine*F/A Ratio	4.80	2.04	Yes

Figures 6.66, 6.67, and 6.68 present the data for each combination of asphalt binder, Fine, and F/A ratio for VTM, VMA, and VFA, respectively. Figure 6.66 illustrates that as the F/A ratio increases, the general trend of the data shows a decrease

in VTM. This would be expected. For a constant volume of asphalt binder and constant compactive effort, the increase in amount of filler (Fines) should decrease the amount of air voids within the mixture.

Table 6.27: Results of ANOVA for VFA

Source of Variation	F-ratio	F_{crit}	Significant Difference?
Asphalt Binder	305.75	4.00	Yes
Fine	334.40	2.53	Yes
F/A Ratio	112.95	3.15	Yes
Asphalt Binder*Fine	19.04	2.53	Yes
Asphalt Binder*F/A Ratio	8.70	3.15	Yes
Fine*F/A Ratio	22.97	2.04	Yes
Asphalt Binder*Fine*F/A Ratio	4.36	2.04	Yes

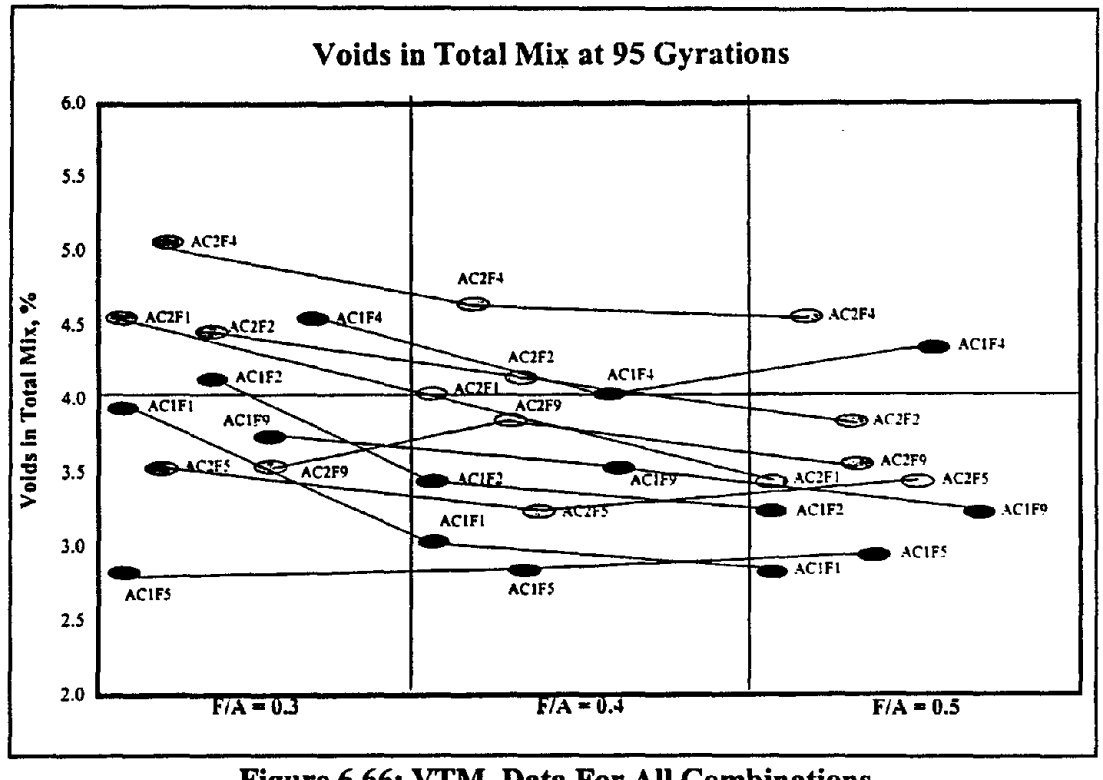

Figure 6.66: VTM Data For All Combinations

Recall that optimum asphalt content was defined as the asphalt content that produces 4.0 percent VTM at N_{des} (95 gyrations). Located on Figure 6.66 is a horizontal line corresponding to 4.0 percent VTM. Also, the F/A ratio utilized during the mixture design was 0.43 for both asphalt binders. Based on this figure the different Fines affected the optimum asphalt content of the mixture. At a F/A ratio of 0.4, only two of the Fines had VTM values of 4.0 percent (AC1F4 and AC2F1). However, two other fines were close enough to suggest that they also correspond to optimum asphalt content (AC2F2 and AC2F9).

Interestingly though, mixtures containing Asphalt Binder No. 1 and Fine 4 showed an increase in VTM from a F/A ratio of 0.4 to 0.5. Fine 4 was the coarsest of the four fines utilized based on the particle size analyses with the Coulter LS200. Also, mixtures made with Asphalt Binder No. 1 and Fine 5 did not show any differences in VTM for the three F/A ratios. Fine 5 was the second finest of the four fines utilized.

Figure 6.67 illustrates that as the F/A ratio increases, the general trend of the data shows a decrease in VMA. This also would be expected. For a Type 1B 19.0 mm nominal maximum aggregate size gradation (as was used for this study), the SCDOT specifies that the minimum VMA should be 14.0 percent. From Figure 6.67 it can be seen that at a F/A ratio of 0.3, only three of the ten combinations meet this minimum criteria (AC2F1, AC2F2, and AC2F4). At a F/A ratio of 0.4, only one of the ten meet (AC2F4). At a F/A ratio of 0.5, none of the combinations meet. Based on this

discussion, the amount of Fines influences the VMA in a resulting mixture. Also, as the amount of Fines increases, the VMA decreases.

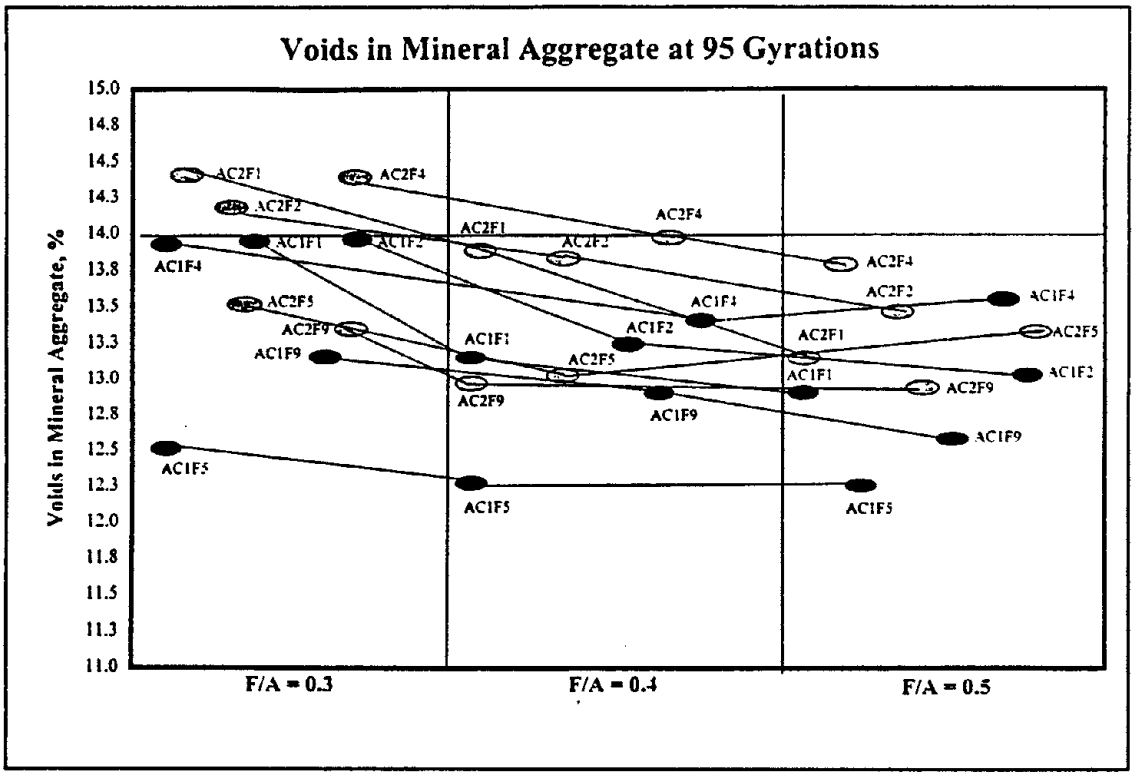

Figure 6.67: VMA Data For All Combinations

Figure 6.68 illustrates that as the F/A ratio increases, the general trend of the data shows an increase in VFA. This indicates that the decrease in VMA associated with the introduction of the fines influences the mixture more so than the decrease in VTM. If the VMA and VTM were influenced similarly, the resulting VFA would have stayed approximately the same.

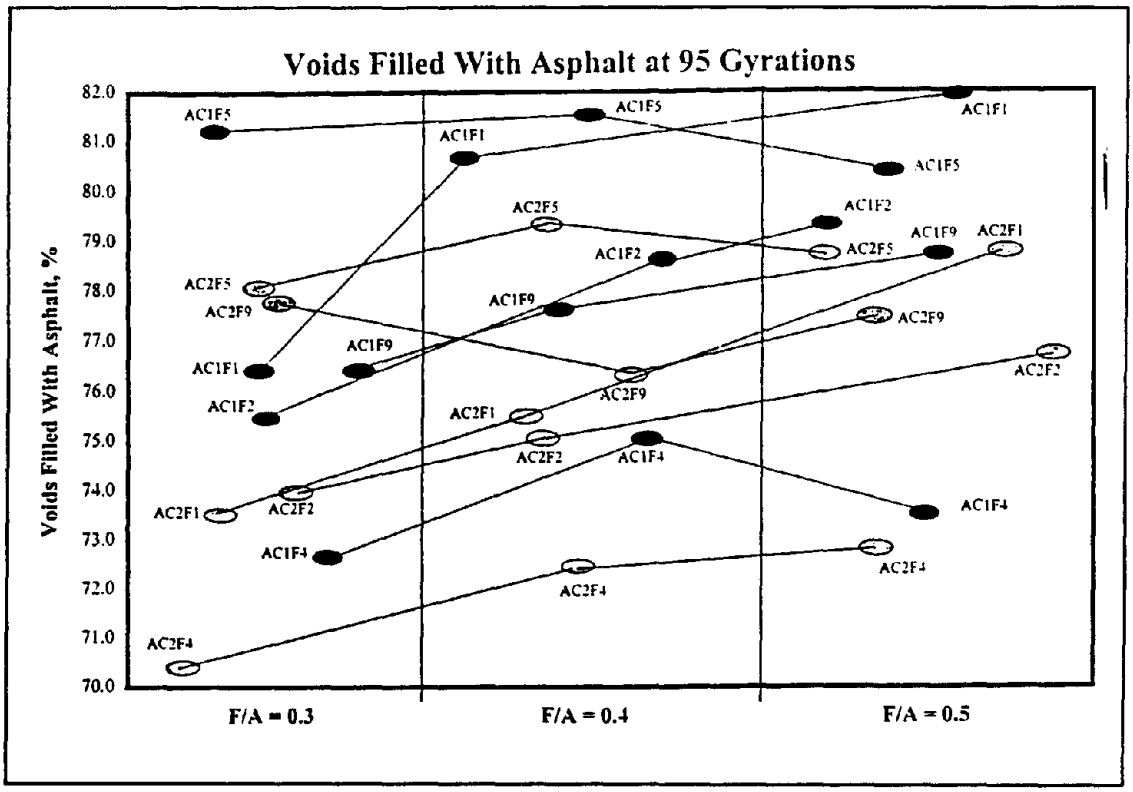

Figure 6.68: VFA Data For All Combinations

6.4.2 Analysis of Compactibility Data

Compactibility was defined as the slope of the densification curve produced during the compaction of each specimen. Results from the ANOVA showed no significant differences between the main effects or any interactions. This is probably due to the strong aggregate skeleton used for this project. The Surface Type 1B gradation was developed as a high volume surface mixture. These results are presented in Table 6.28. Because of the lack of significant differences, no further analysis was performed.

Table 6.28: Results of ANOVA for Compactibility			
Source of Variation	F-ratio	F_{crit}	Significant Difference?
Asphalt Binder	0.59	4.00	No
Fine	0.35	2.53	No
F/A Ratio	1.22	3.15	No
Asphalt Binder*Fine	0.78	2.53	No
Asphalt Binder*F/A Ratio	0.82	3.15	No
Fine*F/A Ratio	1.05	2.04	No
Asphalt Binder*Fine*F/A Ratio	0.95	2.04	No

6.4.3 Analysis of Indirect Tensile Testing

Recall that two tensile properties were determined using the IDT: tensile strength at failure (S_t) and tensile strain at failure (ϵ_t). Results of the ANOVA for S_t and ϵ_t are presented in Tables 6.29 and 6.30, respectively. Table 6.29 shows that significant differences occurred between each of the main effects and all interactions except the asphalt binder*Fine*F/A ratio interaction. Therefore, further analysis of the S_t data will be accomplished utilizing all of the data. Table 6.30 shows that for ϵ_t significant differences only occurred between the Fines main effect. Further analysis of this data will be to show the differences between the Fines.

Table 6.29: Results of ANOVA for S_t			
Source of Variation	F-ratio	F_{crit}	Significant Difference?
Asphalt Binder	12.51	4.00	Yes
Fine	67.30	2.53	Yes
F/A Ratio	19.28	3.15	Yes
Asphalt Binder*Fine	3.32	2.53	Yes
Asphalt Binder*F/A Ratio	5.64	3.15	Yes
Fine*F/A Ratio	3.61	2.04	Yes
Asphalt Binder*Fine*F/A Ratio	1.94	2.04	No

Table 6.30: Results of ANOVA for ϵ_t			
Source of Variation	F-ratio	F_{crit}	Significant Difference?
Asphalt Binder	0.90	4.00	No
Fine	6.30	2.53	Yes
F/A Ratio	0.87	3.15	No
Asphalt Binder*Fine	1.05	2.53	No
Asphalt Binder*F/A Ratio	0.36	3.15	No
Fine*F/A Ratio	0.84	2.04	No
Asphalt Binder*Fine*F/A Ratio	0.46	2.04	No

Figure 6.69 presents the S_t data for each combination of asphalt binder, Fine, and F/A ratio. This figure has been divided into three sections to correspond to the three F/A ratios. Based on the figure, increases in the F/A ratio result in increasing tensile strength. However, an exception does occur. This exception is the combination AC1F4. At a F/A ratio of 0.5, the tensile strength of this combination is lower than for the other F/A ratios. Referring back to Table 5.2, this particular Fine (Fine 4) was the coarsest of

the five utilized for the HMA mixture evaluation. However, after visual inspection of Fine 4, this Fine had a large percentage of micaceous material. Mica is a very soft material and its presence would better explain why the tensile strength would decrease with increasing amounts of this fine. No test procedure utilized in this study determined the amount of mica within the different Fines.

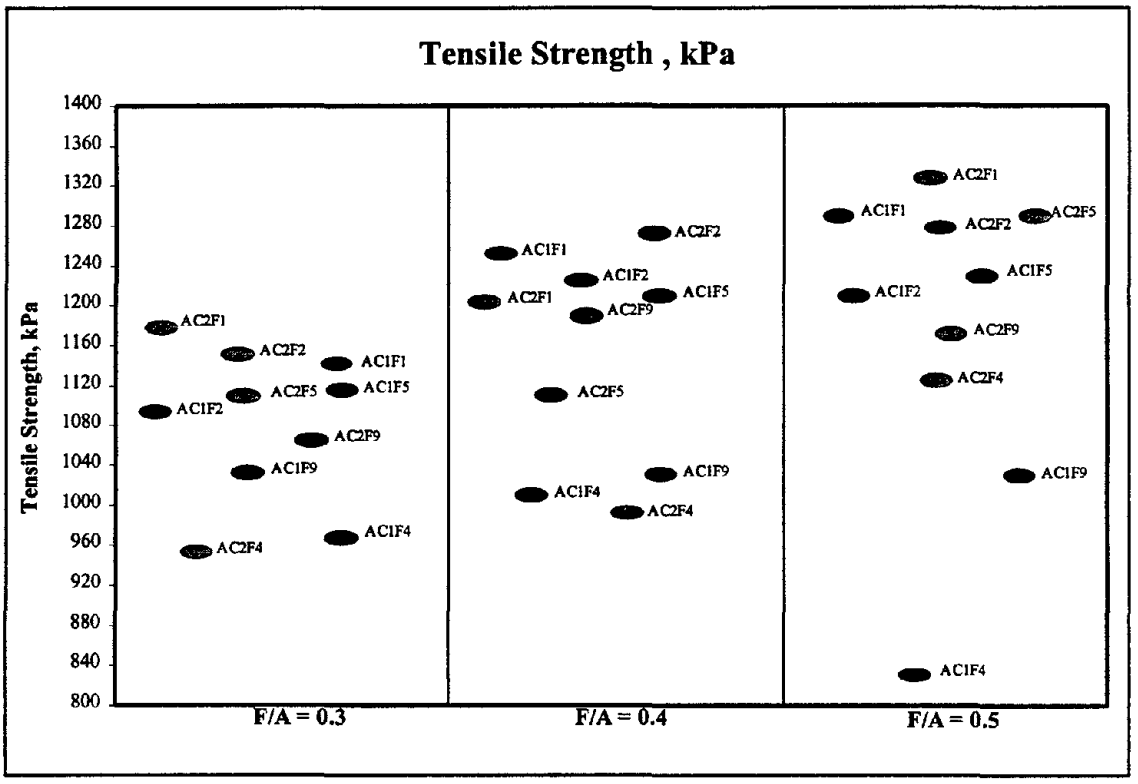

Figure 6.69: Indirect Tensile Strengths For Each Combination

Because the ϵ_t data only showed significant differences between the different Fines, a DMRT was performed to rank the different Fines. Table 6.31 presents this ranking.

Table 6.31: Average ϵ_t Results For Each Fine and Duncan's Rankings		
Fine	Average ϵ_t	Duncan's Ranking*
4	0.00669	A
5	0.00637	B
2	0.00627	BC
9	0.00621	BC
1	0.00596	C
* Averages with the same letter are not significantly different		

Tensile strain at failure is useful in predicting the cracking potential of mixtures (21). Mixtures with higher ϵ_t values can tolerate higher strains and are therefore more resistant to cracking. Based on the DMRT rankings, Fine 4 would be the most resistant to cracking and Fines 2, 9, and 1 would be the least resistant. Again, the presence of the soft, elastic mica within Fine 4 may explain why Fine 4 has the highest ϵ_t values.

6.4.4 Analysis of Root-Tunnicliff Moisture Susceptibility Testing

A statistical analysis could not be performed on this data because only one replicate was tested per asphalt binder-Fine-F/A ratio. Therefore, analysis consisted of looking for trends in the data.

One trend found that as the F/A ratio increased, the TSR also increased (Figure 6.70). This would seem logical because the SCDOT requires lime to be added to HMA mixtures as an anti-stripping agent. Lime is typically finer than about a 0.300 mm (No. 50) sieve. Reason would suggest that the lime would be picked up into the exhaust gas stream and carried to the baghouse. Therefore, as more baghouse fines are added to a HMA mixture, the moisture sensitivity of the mixture should decrease.

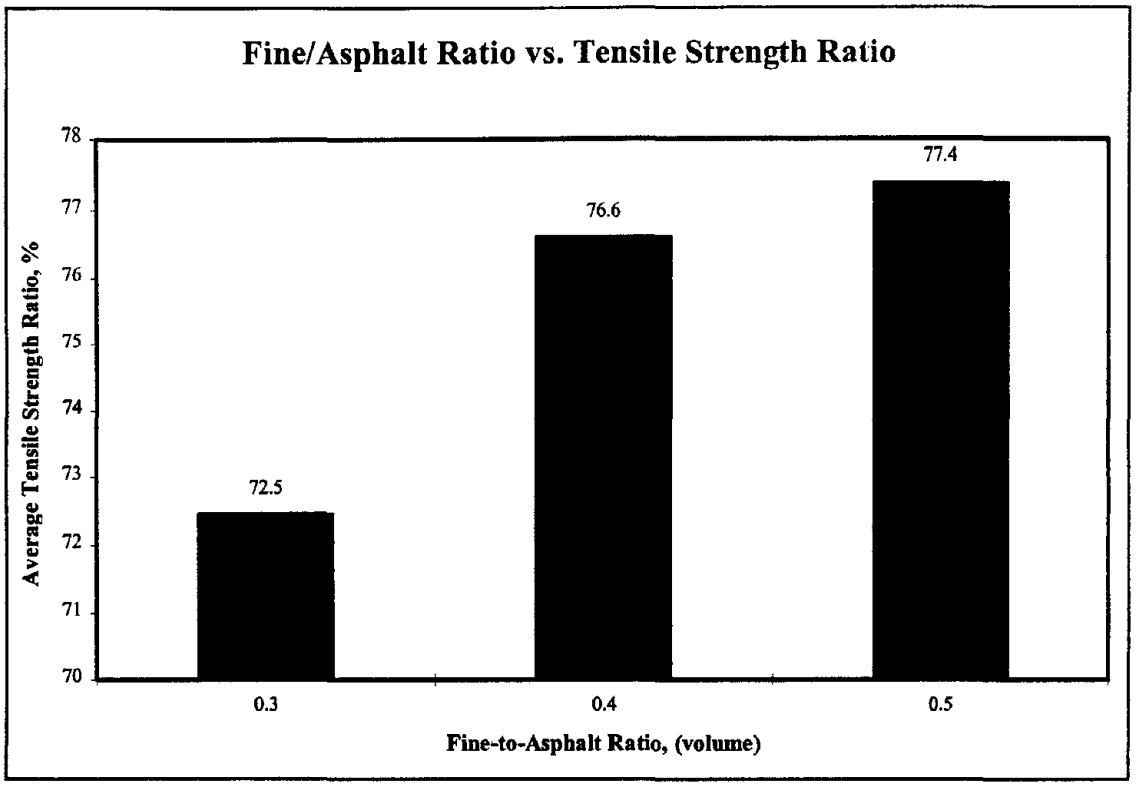

Figure 6.70: Average Tensile Strength Ratios for Each F/A Ratio

Also, recall that the Methylene Blue test was performed on each of the combined baghouse fine samples. This test was performed because it has been shown to be a good indicator of moisture susceptible fines (22). Figure 6.71 shows that, generally, as the Methylene Blue Value increases for a Fine, the moisture susceptibility of the resulting mixture also increases. This would indicate that the Methylene Blue test would be a good quality control test for indicating the moisture sensitivity of baghouse fines.

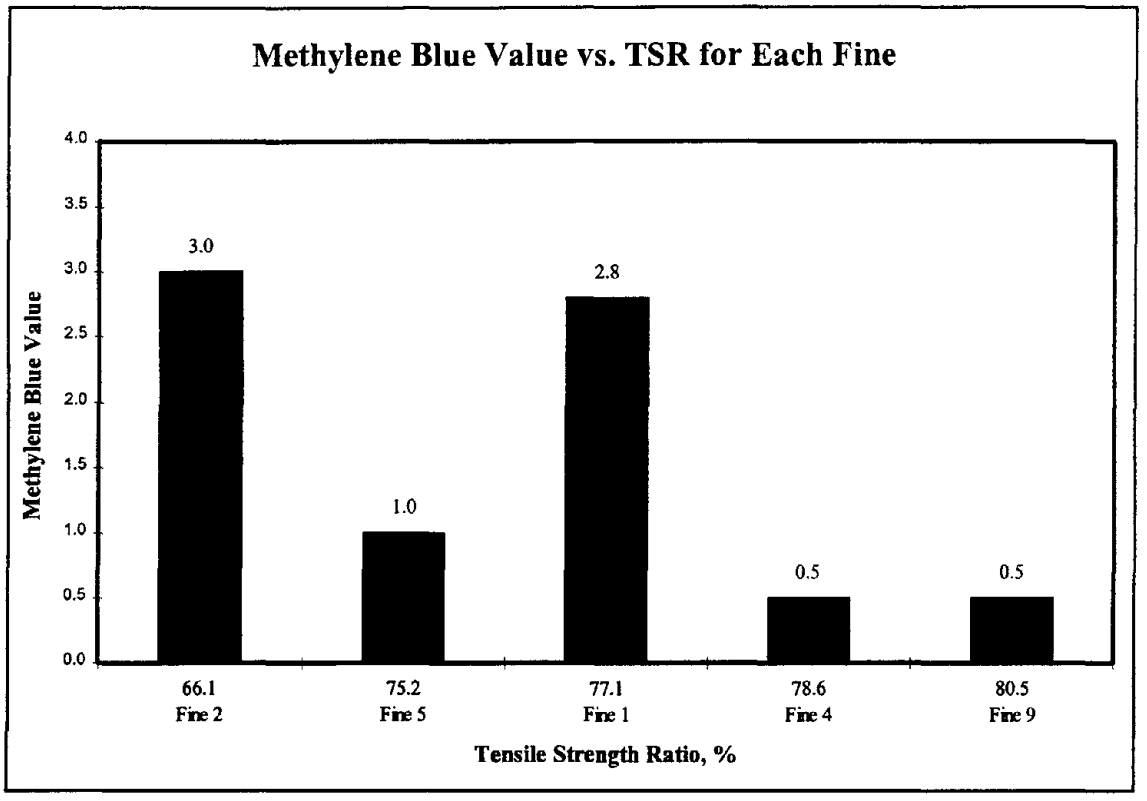

Figure 6.71: Average Methylene Blue Value and Tensile Strength Ratio For Each Fine

6.4.5 Analysis of Long Term Aging Testing

Similar to the Root-Tunnicliff data, only one replicate per combination of asphalt binder-Fine-F/A ratio was tested. Therefore, no statistical analysis could be performed.

Table 6.32 presents the LTR data for each combination. This table also shows the average LTR for each combination, F/A ratio, and asphalt binder. Based on this table, it appears that the only differences in the data are between the different Fines used to make the mortars. Based on this analysis, the different fines do affect the durability of

a HMA mixture. It was attempted to find a property of the fines that would predict the affect on durability; however, no relationships could be found.

Table 6.32: LTR Data and Averages

Asphalt Binder-Fine Combinations	LTR Data			Combination Average	Asphalt Binder Average
	F/A = 0.3	F/A = 0.4	F/A = 0.5		
AC1F1	0.79	0.77	0.85	0.80	0.95
AC1F2	0.91	0.75	0.78	0.81	
AC1F4	1.30	0.92	1.11	1.11	
AC1F5	1.02	1.02	1.08	1.04	
AC1F9	0.94	0.99	1.03	0.99	
AC2F1	0.75	0.90	0.56	0.74	0.95
AC2F2	0.78	0.71	1.08	0.86	
AC2F4	10.92	0.92	1.15	1.00	
AC2F5	1.13	1.28	0.97	1.13	
AC2F9	1.00	1.04	1.13	1.06	
F/A Averages	0.95	0.93	0.97		

6.4.2 Analysis of Confined Repeated Load Deformation Test Data

Analysis of the confined repeated load deformation test data consisted of performing an ANOVA to determine if significant differences occurred between the main effects. The H_o for this analysis was that no significant differences occurred between the main effects, and the H_a was that significant differences did occur. Results

from the ANOVA showed no significant differences between the main effects. These results are presented in Table 6.33.

Table 6.33: Results of ANOVA for Confined Repeated Load Deformation Test

Source of Variation	F-ratio	F_{crit}	Significant Difference?
Asphalt Binder	0.91	4.00	No
Fine	1.01	2.53	No
F/A Ratio	0.66	3.15	No

Gabrielson (31) developed the following equation to predict rut depths in HMA pavements using results of the confined repeated load deformation test.

$$Rut\ Depth = 1.334\ (Strain)^{0.5} + 0.05 \qquad \textbf{Eq.: 6.8}$$

This equation was developed by correlating actual field pavement rut depths with the results of the confined repeated load deformation test on core specimens obtained from the pavements. Traffic levels for these pavements ranged from 0.9 to 11.3 million equivalent single axle loads (ESALS). Table 6.34 presents the predicted rut depths for the laboratory made specimens using the above equation.

The predicted rut depths range from 5.49 to 9.73 mm (¼ to ⅜ in.). These rut depths are not considered to be significant. One reason for these low rut depths could be the strong aggregate skeleton (Type 1B Gradation) used to fabricate each of the specimens. One reason for the lack of differences could be because this particular test

method is not capable of determining the differences in Fines used to create the HMA specimens.

Table 6.34: Predicted Rut Depths Based on Gabrielson's Formula

Asphalt Binder-Fine Combinations	Rut Depths, mm			Combination Average	Asphalt Binder Average
	F/A = 0.3	F/A = 0.4	F/A = 0.5		
AC1F1	6.10	5.36	5.49	5.65	6.75
AC1F2	8.05	8.69	6.45	7.73	
AC1F4	6.31	7.58	***	6.94	
AC1F5	6.30	5.16	5.08	5.51	
AC1F9	5.54	8.76	9.40	7.90	
AC2F1	5.97	6.17	7.14	6.43	6.79
AC2F2	6.40	6.58	5.89	6.29	
AC2F4	***	6.63	8.07	7.35	
AC2F5	5.97	9.73	6.58	7.43	
AC2F9	6.55	6.58	6.27	6.47	
F/A Averages	6.35	7.12	6.71		

CHAPTER 7: CONCLUSIONS AND RECOMMENDATIONS

The objectives for this study as stated in the original problem statement were "to identify the range of baghouse particle sizes produced at typical asphalt plants in South Carolina, determine the effects of baghouse fines in asphalt mixes, and establish valid criteria for their inclusion in hot mix asphalts." To accomplish these objectives a comprehensive field sampling and laboratory testing program was accomplished. Based on the analysis of the test results from that program the following conclusions and recommendations are provided.

7.1 Conclusions

1. The quantity and type of baghouse fines being returned to the asphalt mix has a significant effect on the performance of HMA mixtures.
2. Variation in particle sizes caused by different mixture types is plant specific and small variations in the rate of HMA production does not significantly affect the particle sizes of the baghouse fines. The particle sizes captured in a baghouse can range from 2 mm (No. 10 sieve) to less than 1 μm and the mean particle diameter for baghouse fines can range from 12 to 280 μm.

3. The percent bulk volume, derived from the modified Rigden's voids test, can be used to characterize a fines' potential for stiffening an asphalt binder as measured by the softening point test, Brookfield viscometer at 135°C, and the DSR on unaged mortars.

   A. The modified Rigden's percent voids in a dry compacted dust can range from 39 to 65 percent.

   B. Plants that utilize primary collectors yielded baghouse fines that had higher modified Rigden's percent voids in a dry compacted dust than did plants without primary collectors. However, the type of primary collector (cyclone or knockout box) did not significantly affect the modified Rigden's voids for baghouse fines.

   C. The effect of changing the type of HMA mixture or differing rates of HMA production on the modified Rigden's voids was plant specific.

4. The complex shear modulus as determined by the DSR at 64°C on aged mortars can be used to characterize a fine's potential for stiffening an asphalt binder.

   A. Baghouse fines do not affect the aging characteristics of asphalt binders when aged by the TFOT.

   B. The addition of baghouse fines will increase the stiffness (measured by the DSR at 64°C on TFOT aged mortars) of the mortar thereby resulting in a possible increase in the resistance of a HMA pavement to

permanent deformation (for a given air void content). Each of the baghouse fine samples tested showed this increase in stiffness.

C The percent bulk volume of the filler can be used as an indicator of a mortar's contribution to a HMA pavement's resistance to permanent deformation as measured by the DSR on TFOT aged mortars

D. As the percentage of baghouse fines is increased in a mortar, the resistance (as provided by the mortar) of a HMA pavement to fatigue cracking decreases.

E. The percent bulk volume of the filler can be used as an indicator of the fatigue cracking resistance (as provided by the mortar) as measured by the DSR on TFOT and PAV aged mortars.

F. As the percentage of baghouse fines is increased in a mortar, the resistance (as provided by the mortar) of a HMA pavement to low temperature cracking decreases.

G. The percent bulk volume can be used as an indicator of the low temperature cracking resistance provided by a mortar as measured by the BBR on TFOT and PAV aged mortars.

5. As the percentage of baghouse fines increases, the percent voids in total mix and percent voids in mineral aggregate decrease and the voids filled with asphalt increases (for a constant volume of asphalt binder and constant compactive effort).

6. Baghouse fines did not affect the laboratory compactibility of HMA mixtures as measured with the Superpave gyratory compactor. This was shown by the lack of significant differences in the slope of compaction curve data of mixtures compacted with different baghouse fines.

7. As the percentage of baghouse fines increases, the tensile strength of a HMA also increases. This was probably due to the decrease in voids in total mix and voids in mineral aggregate and/or increase in mortar stiffness.

8. The effect of baghouse fines on a HMA's potential for cracking as determined by the tensile strain at failure is baghouse fine specific. However, based on tensile strain, no physical properties (particle size or modified Rigden's void test data) could be found to indicate which fillers had more potential for cracking in HMA.

9. As the percentage of baghouse fines increase, a HMA's resistance to moisture susceptibility also increases. This is probably due to the fact that in South Carolina most of the fines contain lime which is picked up into the exhaust gas stream and taken to the baghouse.

10. The Methylene Blue test can be used to indicate a baghouse fine's potential for moisture susceptibility.

11. The effect of baghouse fines on the durability, as determined by the long term aging ratio, of a HMA pavement seems to be baghouse fine specific. However, based on this study, no physical properties (particle size or modified Rigden's

void test data) could be found to indicate which fillers influenced durability more.

7.2 Recommendations

Based on the information included in this report the following are presented for consideration by the South Carolina Department of Transportation:

1. The use of the Superpave guidelines for fine to asphalt (F/A) ratios of 0.6 to 1.2 by weight are reasonable. However, the use of the Superpave binder tests should be included in the mix design process to evaluate the mortars. Typical values encountered for this study using the Superpave binder tests included: $G^*/\sin(\delta)$ on TFOT aged mortars of 10 kPa, $G^*\sin(\delta)$ on TFOT and PAV aged mortars of 11,100 kPa, and S on TFOT and PAV aged mortars of 1090 kPa. In the future, the Department should perform these tests on mortars fabricated from materials used on construction projects. Based on the experience of the Department and the data accumulated over this time period, the Department can determine limiting values for these properties.
2. The percentage of baghouse fines greatly influences the volumetric properties of a HMA mixture; therefore, care should be taken to insure that the laboratory mix designs include any additional fines that may be generated during production of HMA. The mix must be monitored during construction and adjusted to meet the required volumetric requirements.

3. The percentage of baghouse fines greatly influences the volumetric properties of a HMA mixture; therefore, the HMA contractor should be required to introduce the baghouse fines back into the mixing process in a consistent manner. Close control of the volumetrics and F/A ratio at the plant site should ensure that the baghouse fines are introduced in a consistent manner. Several types of equipment can be used to introduce the baghouse fines in a consistent manner. A vane feeder or rotary air-lock at the mouth of the baghouse that varies the amount of dust discharge with changes in the rate of HMA production will assist in the return of baghouse fines in a uniform manner. However, these two pieces of equipment could lead to dust surges within the baghouse. Two options available to ensure that adjustments can be made to the amount of baghouse fines returning to the mixture include a separate silo or washed aggregate. A separate silo would allow a contractor to return less baghouse fines than are generated. Again a vane feeder or rotary air-lock can be used to assist in the return of baghouse fines in a uniform manner. In addition, a weigh hopper could be used at a batch plant to ensure the proper amount of baghouse fines being returned to the HMA production process. A separate silo would also assist in wasting baghouse fines if need be. Secondly, the use of washed aggregates could reduce the amount of collected baghouse fines and thus a separate silo may not be required.

4. If the baghouse fines must be wasted, they should be wasted in an environmentally appropriate manner. Based on limited conversations with the South Carolina Department of Health and Environmental Control, an environmental problem may exist with disposing the baghouse fines off-site because of their exposure to the fuel used to produce the flame during mixing. This factor should be considered when deciding upon an appropriate manner of disposal.

REFERENCES

1. "Primary and Secondary Collection Systems for Environmental Control," Proceedings from NAPA's 15th Annual Midyear Meeting, July 30-August 1, 1971 and the 17th Annual Convention, January 4-14, 1972, Information Series (IS) 38.

2. "The Fundamentals of the Operation and Maintenance of the Exhaust Gas System in a Hot Mix Asphalt Facility," The National Asphalt Pavement Association, Information Series (IS) 52 (2nd Edition), 1987.

3. "The Maintenance and Operation of Exhaust Systems in the Hot Mix Plant," The National Asphalt Pavement Association, Information Series (IS) 52 (2nd Edition) and 52A (Combined Volumes), 1975.

4. Anderson, David A. and Joseph P. Tarris., "Adding Dust Collector Fines to Asphalt Paving Mixtures," National Cooperative Highway Research Program Report (NCHRP) 252, Washington D. C, December 1982.

5. Scrimsher, T., "Baghouse Dust and Its Effect on Asphaltic Mixtures," Research Report CA-DOT-TL-3140-1-76-50., California Department of Transportation, Sacramento, CA, 1976.

6. Brock, J. Donald, "Control of Baghouse Fines," National Asphalt Pavement Association, Quality Improvement Publication 120, June 1993.

7. Champion, Richard J., "Baghouse fines: Their Effect on Quality HMA Mixes," Focus, Published by National Asphalt Pavement Association, pp. 10-15, Summer 1991.

8. Brock, J. Donald, "Baghouse Fines," Technical Paper T-121, Astec Industries.

9. Eick, J.H. and J. F. Shook, "The Effects of Baghouse Fines on Asphalt Mixtures," Research Report 78-3 (RR-78-3), The Asphalt Institute, College Park, MD, November 1978.

10. American Society of Testing and Materials, 1994 Annual Book of ASTM Standards, Section 4, Volume 04.03, Philadelphia, PA, 1990.

11. Warden, W.B., S. B. Hudson, and H. C. Howell, "Evaluation of Mineral Fillers in Terms of Practical Pavement Performance," *Proceedings of the Association of Asphalt Paving Technologists*, Vol. 28, pp. 316-354, 1959.

12. Tunnicliff, David G., "A Review of Mineral Filler," *Proceedings of the Association of Asphalt Paving Technologists*, Vol. 31, pp. 118-150, 1962.

13. Tunnicliff, David G., "Binding Effects of Mineral Filler," *Proceedings of the Association of Asphalt Paving Technologists*, Vol. 36, pp.114-156, 1967.

14. Traxler, R.N., "The Evaluation of Mineral Powders as Fillers for Asphalt," *Proceedings of the Association of Asphalt Paving Technologists*, Vol. 8, pp 60-67, 1937.

15. Puzinauskas, V. P., "Filler in Asphalt Mixtures," Research Report No. 69-2 (RR-69-2), Asphalt Institute, College Park, MD, Revised April 1983.

16. Anderson, David A., "Guidelines on the Use of Baghouse Fines," Information Series (IS) 101-11/87, National Asphalt Pavement Association, 1987.

17. Kandhal, Prithvi S., "Evaluation of Baghouse Fines in Bituminous Paving Mixtures," *Proceedings of the Association of Asphalt Paving Technologists*, Vol. 50, pp. 150-210, 1981.

18. Huscheck, S. and Angst, Ch., "Mechanical Properties of Filler-Bitumen Mixes at High and Low Service Temperatures," *Proceedings of the Association of Asphalt Paving Technologists*, Vol. 49, pp. 440-475, 1980.

19. Rigden, P.J., "The Use of Fillers in Bituminous Road Surfacings. A Study of Filler-Binder Systems in Relation to Filler Characteristics," J. Soc. Che. Ind. 66 , pp. 299, 1947.

20. Anderson, David .A., Joseph P. Tarris, and J. Donald Brock, "Dust Collector Fines and Their Influence on Mixture Design." *Proceedings of the Association of Asphalt Paving Technologists*, Vol. 51, pp. 363-397,1982.

21. Roberts, F. L., Prithvi S. Kandhal, Elton R. Brown, Dah-Yin Lee, and Thomas W. Kennedy, Hot Mix Asphalt Materials, Mixture Design, and Construction, NAPA Education Foundation, Lanham, MD, 1991.

22. Aschenbrener, Timothy, "Comparison of Colorado Component Hot Mix Asphalt Materials with Some European Specifications," Colorado Department of Transportation, Report Number CDOT-DTD-R-92-14, Denver Colorado, December 1992.

23. "Test Method for Determination of Methylene Blue Adsorption Value (MBV) of Mineral Aggregate fillers and Fines," International Slurry Surfacing Association, Technical Bulletin No. 145, Proposed February 1989.

24. "Performance Graded Asphalt Binder Specification and Testing, Superpave Series No. 1 (SP-1)," Asphalt Institute, (no date given).

25. Yoder, E. J. and M.W. Witczak, Principles of Pavement Design, Second Edition, New York, John Wiley & Sons, Inc., 1975.

26. Maxwell, E. A., Introduction to Statistical Thinking, 1st Edition, Englewood Cliffs, New Jersey, Prentice-Hall, Inc., 1983.

27. Kleinbaum, D. G. and Kupper, L. L., Applied Regression Analysis and Other Multivariate Methods, 1st Edition, Belmont, California, Wadsworth Publishing Company, Inc., 1978.

28. Taylor, John K., Quality Assurance of Chemical Measurements, 6th Printing, Chelsea, Michigan, Lewis Publishers, Inc., 1987.

29. Ketchum, Joe, Astec Industries, Personal Conversation Via Telephone, March 19, 1997

30. McGennis, R. B., Anderson, R. M., Kennedy, T. W., and Solaimanian, M., Background of Superpave Asphalt Mixture Design and Analysis, FHWA-SA-95-003, November 1994.

31. Gabrielson, Jay R., "Evaluation of Hot Mix Asphalt (HMA) Static creep and Repeated Load Tests," Doctor of Philosophy, Dissertation, Auburn University, Alabama, December 1992.

Appendix A: Results of Questionnaire

Table A.1: Results For Survey of State Departments of Transportation

Question #1: Does your state have a dust-to-asphalt specification?	
Response	States
Yes	Arkansas, Arizona, California, Connecticut, Delaware, Florida, Illinois, Massachusetts, Michigan, Minnesota, Mississippi, Missouri, Montana, Nebraska, Ohio, Oklahoma, Tennessee, Vermont, West Virginia, Virginia
No	Alaska, Colorado, Georgia, Hawaii, Idaho, Kentucky, Indiana, Louisiana, Maine, Nevada, New Jersey, New Hampshire, New Mexico, New York, North Dakota, Oregon, Texas, Utah, Washington, D.C. Department of Public Works, Wyoming
Question #2: Do you consider baghouse fines to be detrimental to the life of Hot Mix Asphalt?	
Response	States
Yes	Alaska, Colorado, Delaware, Florida, Georgia, Hawaii, Kentucky, Maine, Michigan, Montana, New York, North Dakota, Ohio, Tennessee, Texas, Utah, Vermont, Virginia
No	Arkansas, Arizona, California, Colorado, Connecticut, Idaho, Illinois, Indiana, Louisiana, Massachusetts, Minnesota, Mississippi, Missouri, Nebraska, Nevada, New Jersey, New Hampshire, New Mexico, North Dakota, Ohio, Oklahoma, Oregon, Washington, D. C. Department of Public Works, West Virginia, Wyoming
Question #3: Do you currently require the contractor to waste the baghouse fines?	
Response	States
Yes	Arizona, Montana, Nevada, North Dakota, Wyoming
No	Alaska, Arkansas, Arizona, California, Colorado, Connecticut, Delaware, Florida, Georgia, Hawaii, Idaho, Illinois, Kentucky, Indiana, Louisiana, Maine, Massachusetts, Michigan, Minnesota, Mississippi, Missouri, Nebraska, New Jersey, New Hampshire, New Mexico, New York, Ohio, Oklahoma, Oregon, Tennessee, Texas, Utah, Vermont, Washington, D. C. Department of Public Works, West Virginia, Virginia

Appendix B: Modified Rigden's Void Test

TEST METHOD FOR DETERMINING THE PERCENTAGE OF FREE ASPHALT IN A DUST/ ASPHALT MIXTURE—DRY COMPACTION METHOD

1. Scope

This test procedure describes a method for determining the void volume in a dry-compacted dust and the percentage of free asphalt in a dust asphalt mixture. The test method is based upon the assumption that the densest packing (maximum bulk density) of a fine mineral dust can be obtained by compacting the dry dust in a mold.

2. Applicable Documents

C 188	Specific Gravity of Hydraulic Cement
D 422	Particle Size Analysis of Soils
D 854	Specific Gravity of Soils
E 11	Specification for Wire-Cloth Sieves for Testing Purposes

3. Summary of Method

In this test method, the volume of the voids in a dry-compacted bed of mineral dust is determined by compacting the dust in a small mold. The volume of asphalt required to fill these voids is called fixed asphalt. Any asphalt that is added to a dust/asphalt mixture that is in excess of the fixed asphalt is called free asphalt.

4. Definitions

4.1 *Maximum packing* occurs when the particles are packed together in their minimum volume with a minimum void volume. Maximum packing results in a maximum bulk density.

4.2 The *bulk density* of the compacted dust is defined as the dry weight of the dust divided by the bulk volume of the compacted dust. The bulk volume includes the sum of the solid volume of the dust particles and the volume of the voids between the particles.

4.3 The *density* of the dust solids is defined as the dry weight of the dust divided by the solid volume of the dust particles. This density can be obtained from ASTM Test Method C 188 or D 854, or another appropriate test method.

4.4 The *fixed asphalt volume*, V_{afx}, is defined as the volume of asphalt required to fill the voids in a dust that has been densified to its maximum dry density.

4.5 *Free asphalt volume*, V_{afr}, is defined as the volume of asphalt added to a dust/asphalt mixture, that is in excess of the fixed asphalt volume.

4.6 *Stiffening* is defined as the increase in consistency that occurs when mineral dust is added to asphalt cement. Stiffening is measured by comparing the penetration, viscosity, or softening point of the dust/asphalt mixture with the penetration, viscosity, or softening point of the plain asphalt cement.

5. Significance

The void volume in a dry-compacted dust is sensitive to changes in gradation and other properties of the dust, and, therefore, the dry compaction test has been proposed as a test for monitoring the uniformity of the dust collected in HMA facilities.

The percentage of free asphalt in the dust/asphalt fraction in HMA has also been correlated with the stress-strain response of HMA. Therefore, the percentage of free asphalt has been proposed as a simple indicator which can be used to monitor and control the uniformity of dust added to HMA.

6. Apparatus

6.1 *Compaction Hammer.* A compaction hammer, as shown in Figure B-1, is required to compact the dust into the test mold. The dust is compacted in one layer, using 25 blows of the hammer.

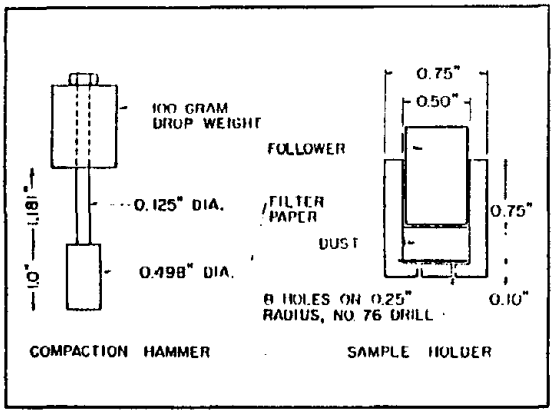

Figure B-1

6.2 *Compaction Pedestal.* A steel block, 1 inch thick x 4 inch x 4 inch is used as a base for the mold (Figure B-2).

Figure B-2

6.3 *Thickness Measuring System.* A dial gauge with 0.001-inch gradations mounted as shown in Figure B-3 is required for measuring the thickness of the compacted bed of dust.

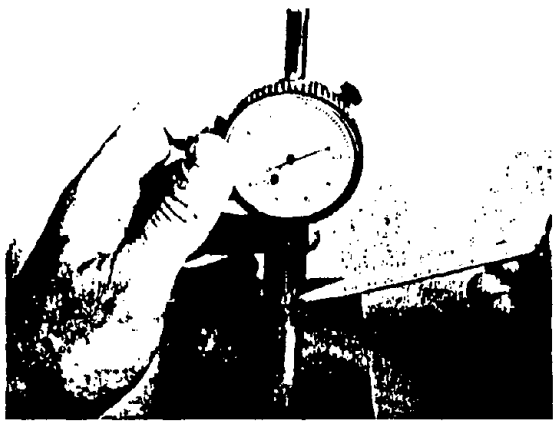

Figure B-3

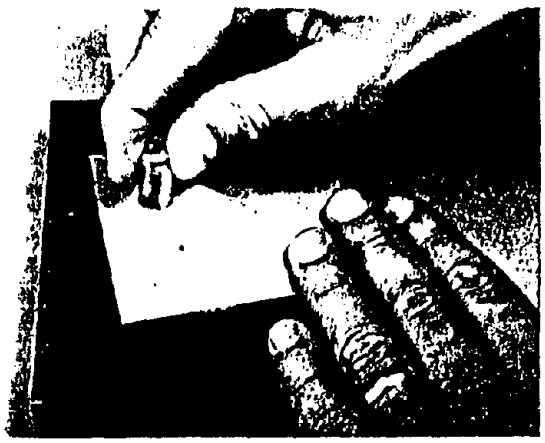

Figure B-4

6.4 *Test Mold.* A test mold, as shown in Figure B-2, is required for measuring the volume of the compacted bed of dust.

6.5 *Filter Membrane.* Small, ½-inch-diameter disks must be cut from the Millipore No. SCWP0190R filter membrane. The cutting tool shown in Figure B-4 is recommended for this purpose.

6.6 *Tweezers.* Tweezers are needed for handling the filter disks.

6.7 *No. 200 Sieve.* A No. 200 sieve meeting the requirements of ASTM E 11 is needed to remove the particles larger than 75 μm.

6.8 *Balance or Scale.* A balance or scale rated to 200 grams and sensitive to 0.01 gram is required.

7. Sample Preparation

The dust may be obtained from a primary or secondary dust collector, the coarse or fine aggregate, or the aggregate extracted from a mixture. Particles larger than 75 μm should be removed by sieving. Dry sieving is usually adequate if several sieves coarser than the No. 200 sieve are placed above the No. 200 sieve during the sieving operation to avoid overloading the No. 200 sieve. Wet sieving should be avoided because the fine particles tend to stick together after they are dried.

8. Procedure

8.1 Use the cutting tool (Figure B-4) to cut a number of ½-inch diameter filter disks. Place two of these disks in the bottom of the sample cup, place the follower over the top of the disks, and seat the follower on the filter disks using firm finger pressure (Figure B-5). Insert the entire assembly under the dial gauge. Record the dial gauge reading as t_1.

8.2 Weigh the empty mold, two filter disks, and the follower, and record the weight as W_1. Remove the follower and the two filter disks.

8.3 Place a filter disk in the bottom of the sample cup (Figure B-6), making certain that it is centered and firmly in place at the bottom of the mold. Select a representative sample of minus No. 200 dust that weights approximately 1.0 - 1.3 grams. Carefully place the dust in the sample cup over the top of the filter disk. Place a second filter disk over the top of the dust, and use the follower and firm hand pressure to seat the disk on top of the dust. This procedure will result in some initial compaction of the dust and is to be expected.

8.4 Remove the follower, place the sample cup on the steel base plate, and apply 25 blows with the compaction hammer (Figure B-7). Use caution during the compac-

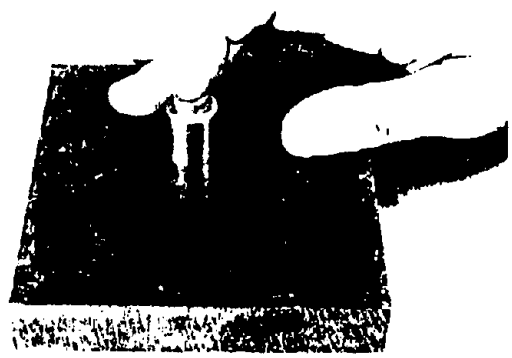

Figure B-5

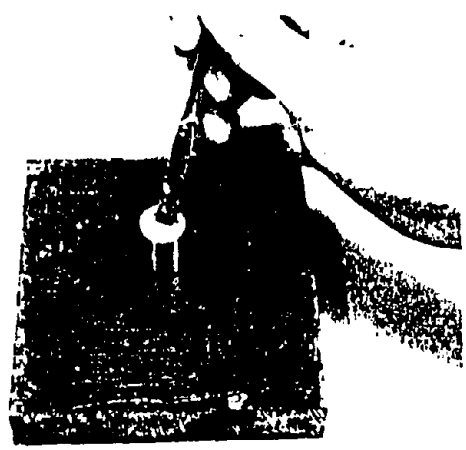

Figure B-6

Figure B-7

tion process to be certain that the mold is seated firmly on the compaction pedestal, the drop weight falls its full height, and the drop weight falls freely.

8.5 Remove the compaction hammer and insert the follower on top of the compacted dust and filter disk. Insert the entire assembly under the dial gauge and record the dial gauge reading, t_2. Weigh the entire mold assembly, and record as the weight W_2.

8.6 The specific gravity of the dust solids is required to complete the calculations. If the specific gravity of the dust solids is not known, it will be necessary to measure it using ASTM procedure C 188 or D 854. Caution: The specific gravity of the dust solids may not be the same as for the other aggregate fractions. Although kerosene has been used as a liquid for determining specific gravity, water can also be used without adversely affecting the accuracy of the results.

9. Calculations

9.1 *Notation*

- D/A_v = Dust/asphalt ratio, volumetric basis
- D/A_w = Dust/asphalt ratio, weight basis
- d = Diameter of test mold (in.)
- G_A = Specific gravity of asphalt cement
- G_{DS} = Specific gravity of the dust solids
- t = Thickness of compacted sample (in.)
- t_1 = Initial dial gauge reading (in.)
- t_2 = Final dial gauge reading (in.)
- V_{AFR} = Volume of free asphalt in dust/asphalt mixture (cm^3)
- $\%V_{AFR}$ = Volume of free asphalt in dust/asphalt mixture expressed as a percentage of total mixture volume
- V_{DB} = Bulk volume of compacted dust sample (cm^3)
- V_{DS} = Volume of dust solids, cm^3
- V_{DV} = Volume of voids in compacted dust (cm^3)
- $\%V_{DV}$ = Volume of voids in compacted dust expressed as percentage of bulk volume
- W_D = Weight of dry dust solids (g)
- γ_{DB} = Bulk density (unit weight) of compacted dust (g/cm^3)
- γ_w = Density (unit weight) of water (1.00 g/cm^3)

9.2 *Compacted Dust*

9.2.1 Calculate the bulk volume of the compacted dust, V_{DB}, as follows:

$$V_{DB} = \frac{15.70\, d^2\, t}{4}\ cm^3$$

where:

d = diameter of mold (in.)

$t = t_2 - t_1$, sample thickness (in.)

9.2.2 Calculate the volume of the dust solids, V_{DS}, as follows:

$$V_{DS} = \frac{W_D}{\gamma_w G_{DS}}\ cm^3$$

where:

W_D = $W_2 - W_1$, weight of compacted dust (grams)

γ_w = unit weight of water (1.000 g/cm^3)

G_{DS} = specific gravity of dust solids as determined from ASTM C 188 or D 854, or another suitable test method

9.2.3 Calculate the volume of the voids in the compacted dust, V_{DV}, as follows:

$$V_{DV} = V_{DB} - V_{DS}$$

9.2.4 Calculate the percentage of voids in the compacted dust as follows:

$$\%V_{DV} = \frac{V_{DB} - V_{DS}}{V_{DB}}\ 100\%$$

9.2.5 Calculate the bulk density of the compacted dust as follows:

$$\gamma_{DB} = \frac{W_D}{V_{DB}}\ g/cm^3$$

9.3 *Dust/Asphalt Mixtures*

When dust and asphalt are mixed together, the amount of added asphalt must first be sufficient to fill the voids between the dust particles. This asphalt is called fixed asphalt. Additional asphalt is needed to keep the particles separated and lubricate the dust/asphalt mixture; otherwise the mixture will be excessively stiff. This additional asphalt is called free asphalt. The calculations below can be used to calculate the percentage of free asphalt in a dust/asphalt mixture.

9.3.1 Calculate the percentage of free asphalt, $\%V_{AFR}$, in the dust/asphalt mixture as follows:

$$\%V_{AFR} = \frac{V_A + V_{DS} - V_{DB}}{V_A + V_{DS}}\ 100\%$$

where:

$$V_A = W_A/G_A\gamma_w$$

9.3.2 When the dust/asphalt ratio is given on a volumetric basis, the percentage of free asphalt in a dust/asphalt mixture is calculated as follows:

$$\frac{1 + D/A_v\left(1 - \frac{G_{DS}\,\gamma_w}{\gamma_{DB}}\right)}{1 + D/A_v} \times 100\%$$

Appendix C: Methylene Blue Test Procedure

INTERNATIONAL SLURRY SURFACING ASSOCIATION

TECHNICAL BULLETIN

1101 CONNECTICUT AVE., N.W., WASHINGTON D.C. 20036

No. 145
Proposed
February
1989

Test Method for Determination of Methylene Blue Adsorption Value (MBV) of Mineral Aggregate Fillers and Fines

1. SCOPE

This test method is used to quantify the amount of harmful clays of the smectite group, organic matter and iron hydroxides present in an aggregate, thus giving an overall indication of the surface activity of a given aggregate.

2. APPARATUS AND REAGENTS

(a) 50 ml or suitable burette mounted on a titration stand.
(b) 250 ml or suitable glass beaker.
(c) Magnetic mixer with stir bar or variable speed mixer capable of 700 RPM.
(d) 2000 gram capacity scale or balance sensitive to within 0.01 gram.
(e) Glass rod 8 mm diameter x 250 mm.
(f) Laboratory timer or stop watch.
(g) 8" standard US Sieves #200 (75 mm) and #325 (44 mm) (or others as designated) and pan.
(h) 1000 ml volumetric flask.
(i) Methylene Blue - reagent grade.
(j) Distilled or deionized water.
(k) Whatman No. 40 filter paper.

3. PROCEDURE

A representative sample of the fine aggregate to be tested is dried to constant weight and screened through either the #200 Sieve or the #325 Sieve. The portion of the aggregate passing the desired sieve is retained for testing while the balance is discarded. One gram weighed to the nearest .05 gram, of the 0/#200 or 0/#325 aggregate is combined with 30 grams of distilled water in a suitable beaker and stirred until thoroughly wet and dispersed. A magnetic stirrer has been found to be satisfactory.

One gram of Methylene Blue is dissolved in distilled water, made up to 1000 ml so that 1 ml of solution contains 1 mg of methylene blue. This MB solution is titrated stepwise in .5 ml aliquotes from the burette into the continually stirred fine aggregate suspension. After each addition of MB, stirring is continued for 1 minute. After this time, a small drop of the aggregate suspension is removed and placed on the filter paper with the glass rod. Successive additions of MB are repeated until the end point is reached.

Initially, a well defined circle of Methylene Blue-stained dust is formed and is surrounded with an outer ring or corona of clear water. The end point is reached when a permanent light blue coloration or "halo" is observed in this ring of clear water. When the initial end point is reached, stirring is continued for five minutes and the test repeated to ascertain the permanent endpoint. Small additions of Methylene Blue are continued until the 5 minute permanent end point is reached.

4. REPORT

The Methylene Blue Value of a specific fine aggregate fraction is reported as milligrams of Methylene Blue per gram of specific fine aggregate fraction; e.g.,

MBV = 5.5 mg/g, 0/#200, or
MBV = 4.0 mg/g, 0/#325, or
MBV = 2.3 mg/g, 0/#8, etc.

NOTES

1. The literature at our disposal reports many variations of the method. MB solution concentrations are reported as 1 mg/ml, 4.5 mg/ml, 10 mg/ml and 1 mol to .08 mol solutions. Sample sizes reported are 1 gram, 20 grams, 30 grams, 200 grams and 1000 grams. Specimen gradations are 0/#325, 0/#200, 0/#10, 0/#8, 0/#4 and clean 3/8" one-size chips. For simplification and standardization, we suggest reporting the MBV as mg of MB/g of specific aggregate fraction.
2. The preparation of the aggregate for testing also varies. When whole aggregate gradations as received are used, it is possible to detect and quantify adherent fines. Some procedures use laboratory crushers to reduce large size clean aggregates to specific fines fractions for testing.
3. Though no standard MBV is proposed in this Technical Bulletin, Standards have been set in Northern Ireland for Chip Seal (Surface Dressing) aggregate fines produced by crushing as follows:

   "The aggregate should be rejected if the Blue Value exceeds the values given below ...:

	%MB by weight	(mg/g)
Basalt Rock	1.0	(10.0)
Gritstone	.7	(7.0)

REFERENCES

1. Afnor Tentative Standard P18-592, July, 1980. "Aggregates-Methylene Blue Test" Afnor Tour Europe, Cedex 7, 92080 Paris La Defense (copyrighted).
2. Alan Woodside, personal communication to Benedict, University of Ulstor, at Jordanstown, Northern Ireland, 5/85.
3. Michael Breunan, personal communication to Coyne 1/89, School Engineering, University College, Galway, Ireland.
4. M. Doyle "Methylene Blue Test on Fine Aggregates" Sahuaro Pet. In-house test method, Phoenix, Arizona.
5. T. Szymoniak and T. S. Vinson "Determining Clay Minerals in Basalt Aggregates," TRB 1989, Session 123 (#880019).

From J. Chemical Tech. & Biotechnology, 1985.
Digest 35A (a compendium):

6. E. T. Stewart & L. M. McCullough, "The Use of the Methylene Blue Test to Indicate the Soundness of Road Aggregates" (Belfast).
7. J. F. Hills & G. S. Pettifer, "The Clay Mineral Content of Various Rock Types Compared with the Methylene Blue Value" (Wimpey Labs, Middlesex).
8. J. Bemstead "Application of the Methylene Blue Test to Cement Raw Materials" (Blue Circle Ind., Greenhithe, Kent).
9. J. R. Hosking & D. C. Pike, "The Methylene Blue Dye Adsorption Test in Relation to Aggregate Drying Shrinkage" (Trrl, Crowthorne, Berkshire).
10. R. K. Taylor "Cation Exchange of Clays and Mudrocks by Methylene Blue," Univ. /Durham/UK.

Appendix D: Mixing Sequence Side-Study

MIXING SEQUENCE SIDE-STUDY

D.1 Introduction and Problem Statement

For the purposes of this side-study, the three main constituents of HMA are defined as "aggregate", "filler", and asphalt binder. "Aggregate" is the inert material retained on the No. 200 sieve and "filler" is the inert material passing the No. 200 sieve. Based on these definitions, baghouse fines can typically be placed in the category of filler. This is not intended to imply that all particles contained within baghouse fines pass the No. 200 sieve. Baghouse fines can have a wide range in particle sizes. However, these variations are beyond the scope of this side-study. Stipulating that a large portion of baghouse fines are filler is sufficient.

As alluded to in the Literature Review, baghouse fines are captured on the outside of filter fabric bags within the baghouse. Cleaning cycles are used to remove the baghouse fines from these bags. During cleaning, the baghouse fines fall from the bags into the bottom of the baghouse. At the bottom of the baghouse is an auger chute that pushes the fines toward the exiting point at the end of the baghouse. This process is very similar for most baghouses. However, differences do occur in how baghouse fines are reintroduced into the HMA production process. These differences are unique to the type of HMA facility: batch or drum.

Baghouse fines captured at batch plants are typically reintroduced into the HMA production process at the hot elevator. Within the hot elevator, the baghouse fines are

added to the hot aggregate coming from the drying unit. From the hot elevator, both the baghouse fines and hot aggregate are taken to the screen deck where they are separated into specific sizes and fall into the hot bins. From each hot bin, certain weights of aggregate are dropped into the pugmill. Within the pugmill the aggregates are premixed for a short duration, called "dry" mixing. Next, the asphalt binder is added to the pugmill for further mixing, "wet" mixing. This defines one mixing sequence. The filler and aggregate are premixed, then the asphalt binder is added.

Drum plants can introduce the baghouse fines in several manners. They can be augered back to the aggregate conveyor belt or into the drum. They can also be blown back into the drum. If the fines are blown back into the drum, the point at which they are introduced is of importance. If the fines are blown into the drum at a point at which they are not mixed with the asphalt binder, then typically all of the constituents (aggregate, filler, and asphalt binder) are mixed simultaneously within the drum. If the fines are blown back at a point in which they are premixed with the asphalt binder, then the fines and asphalt binder are premixed before being added to the aggregate for final mixing. This is illustrated in Figure D.1. Another method of blowing the fines back into the drum is by using a device called an impinging cone. An impinging cone is a device by which the asphalt binder and baghouse fines are premixed before being added back to the drum (Figure D.2). A benefit of using an impinging cone is that the baghouse fines will not be re-entrained into the exhaust gas stream. Based on this discussion of drum plants, two more mixing sequences have been defined. One is in

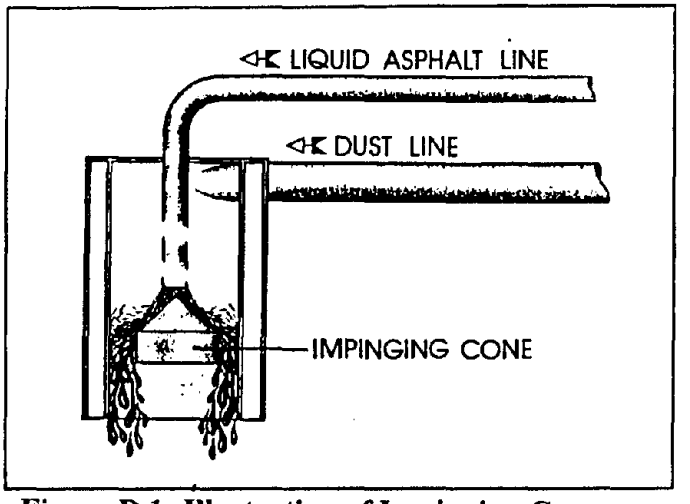

Figure D.1: Illustration of Impinging Cone (UN-13, 1991)

which all of the constituents are mixed simultaneously and the other is where the filler and the asphalt binder are premixed before being added to the aggregate. As can be seen by this illustration, a study that determines if these three different mixing sequences affect the final properties of the HMA is needed.

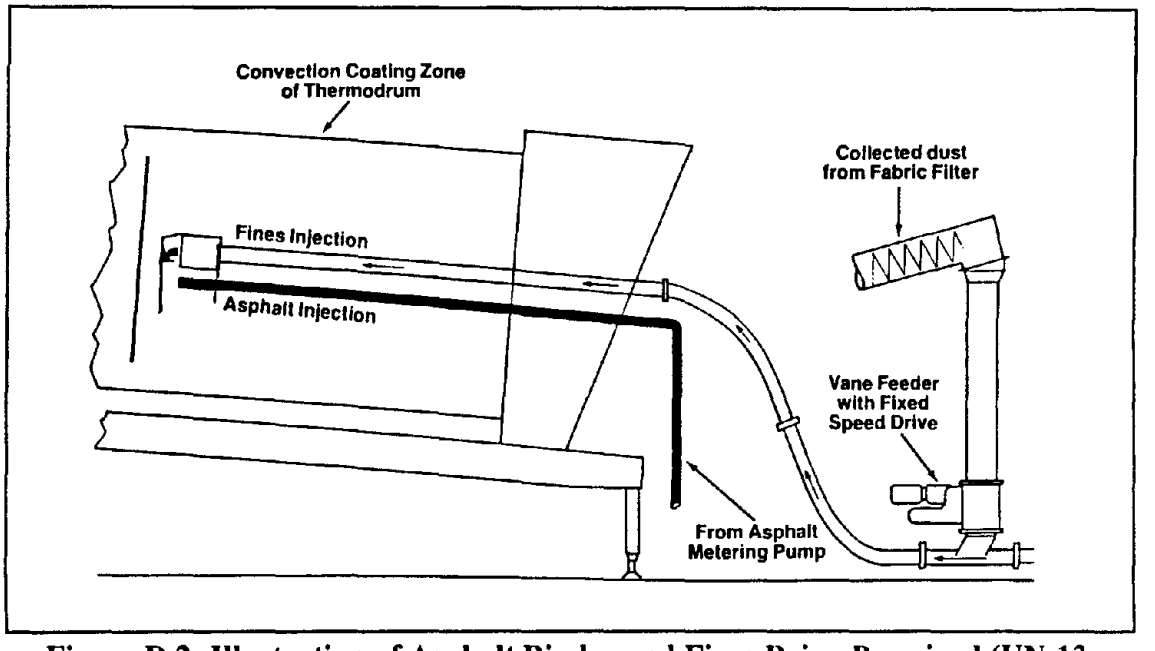

Figure D.2: Illustration of Asphalt Binder and Fines Being Premixed (UN-13, 1991)

D.2 Objective

The objective of this side-study is to determine if the mixing sequence of HMA constituents affects the properties of the finished HMA. If differences do occur in the properties, a mixing sequence must be selected for the SCDOT baghouse fines study.

D.3 Scope

To accomplish the above stated objective, a series of HMA mixtures were prepared using different mixing sequences. A total of eighteen briquettes were fabricated. This includes one type of aggregate, one type of filler, two asphalt binders, three mixing sequences, and three replicates. Laboratory testing of the briquettes consisted of compacting the specimens with a Superpave Gyratory Compactor (to evaluate compactibility), determining the bulk specific gravity (to determine volumetric properties), and indirect tensile tests at 25°C (to evaluate tensile properties).

D.4 Test Plan

The test plan consisted of fabricating and testing eighteen briquettes. This included one source of aggregate, one filler, two asphalt binders, three mixing sequences, and three replicates. The mixing sequences were as follows:

A. [(asphalt + filler) + aggregate]
B. [asphalt + (filler + aggregate)]
C. [asphalt + filler + aggregate]

Where: ( ) designates premixed, and
[ ] designates final mixture.

The aggregate and filler used for this side-study were a 100 percent crushed granite-gneiss obtained from a quarry near Spartanburg, South Carolina. The two asphalt binders were a Shell AC-20 and a Citgo AC-20, both of which are used in South Carolina.

Laboratory work consisted of batching the aggregate, filler, and asphalt binder to the proper weights, premixing the proper constituents , fabricating the briquette specimens, determining the bulk specific gravity of each specimen, and performing indirect tensile tests. This is illustrated in Figure D.3.

An SCDOT Type 1B gradation was used for this study. The aggregate and filler were batched to the proper proportions for 100 mm diameter specimens. The asphalt binder content used was the optimum asphalt content determined during the baghouse fines main study (4.3 percent).

Once all of the constituents were batched to the proper proportions, premixing was accomplished. For mixing sequence A (MSA),premixing of the asphalt binder and filler was accomplished by the same method described in Section 3.3.1 "Mortar Preparation." For mixing sequence B (MSB), premixing of the aggregate and filler consisted of placing both into a plastic zip-lock bag and shaking vigorously. For mixing sequence C (MSC), all constituents were placed in the mixing bowl simultaneously.

Final mixing of the constituents consisted of placing the premixed portions and the other constituent in a mixing bowl and mixing for 90 seconds with an automated mixer.

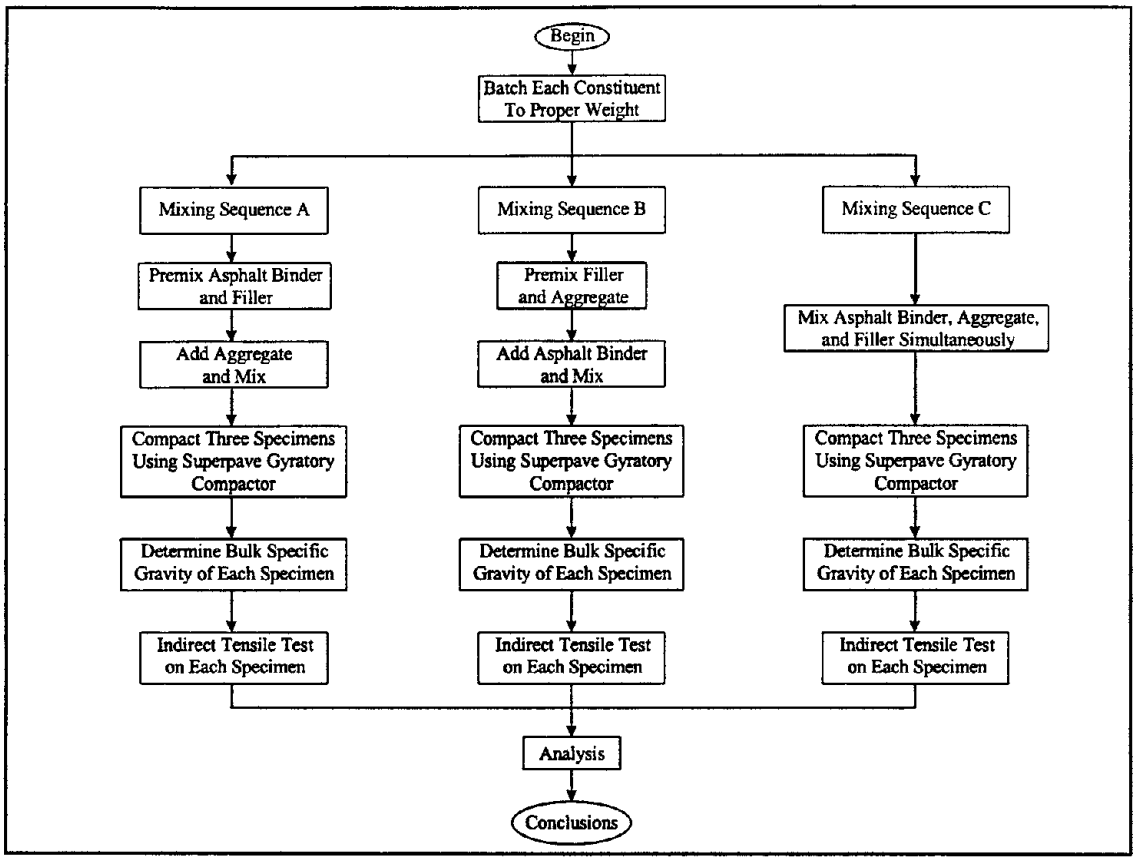

Figure D.3: Test Plan for Mixing Sequence Side-Study

Compaction of each specimen was attained with a Superpave Gyratory Compactor. This method of compaction was selected so that the relative compactibility of each mixing sequence could be determined. The design number of gyrations (N_{des}) was set at 95 revolutions. This corresponds to a maximum number of gyrations (N_{max}) of 150 and an initial number of gyrations (N_{ini}) of 8. Compaction was performed at 150°C for each specimen.

Relative compactibility of each specimen was calculated from the results of gyratory compaction. Output from the gyratory compactor consists of the specimen's height for each gyration. Based on a specimen's height, the percent of TMD can be calculated for that height. Compaction curves are presented as the percentage of TMD versus the number of gyrations. When the number of gyrations are plotted on a logarithmic scale, these curves are essentially a straight line. In-field compactibility can be represented by the slope of this line between N_{max} and N_{ini}. Mixtures that have a steep slope (higher compactibility value) tend to be more resistant to rutting than mixtures with a flatter slope.

Once each of the eighteen specimens were fabricated, they were allowed to cool to room temperature 25°C (77°F). After room temperature was attained , the bulk specific gravity of each specimen was determined. This was done so that the volumetrics of each briquette could be determined.

Finally, each specimen was subjected to indirect tensile tests (IDT) at 25°C. This test was performed to determine if the different mixing sequences had any effect on the tensile properties of the final mixture. The IDT was selected because of the ease and relative swiftness that the test can be performed.

D.5 Test Results

Results of all testing are presented in Table D.1 through D.3. Results for mixing sequence A are presented in Table D.1, while results for mixing sequences B and C are presented in Tables D.2 and D.3, respectively.

Table D.1: Test Results for Mixing Sequence A

Asphalt Binder	Rep.	Bulk Specific Gravity	TMD	VTM %	VMA %	VFA %	S_t, kPa	ϵ_t, mm/mm	Slope of Compaction Curve
1	1	2.407	2.492	3.4	15.6	78.2	1090.1	0.0061	6.71
1	2	2.401	2.492	3.7	15.9	76.9	1132.8	0.0068	7.24
1	3	2.410	2.492	3.3	15.5	78.9	1212.1	0.0068	6.82
Rep. Average		2.406	2.492	3.5	15.7	78.0	1145.0	0.0065	6.92
2	1	2.395	2.478	3.4	16.1	79.0	1149.4	0.0063	7.08
2	2	2.403	2.478	3.0	15.8	80.8	1332.1	0.0072	7.14
2	3	2.400	2.478	3.2	15.9	80.2	1183.9	0.0068	7.31
Rep. Average		2.399	2.478	3.2	15.9	80.0	1221.8	0.0068	7.18
Overall Avg.		2.403	2.485	3.3	15.8	79.0	1183.4	0.0067	7.05

Table D.2: Test Results for Mixing Sequence B

Asphalt Binder	Rep.	Bulk Specific Gravity	TMD	VTM %	VMA %	VFA %	S_t, kPa	ϵ_t, mm/mm	Slope of Compaction Curve
1	1	2.421	2.492	2.9	15.2	81.1	1206.6	***	6.46
1	2	2.412	2.492	3.2	15.4	79.3	1123.9	0.0063	6.53
1	3	2.427	2.492	2.6	14.9	82.5	1199.0	0.0068	6.47
Rep. Average		2.420	2.492	2.9	15.2	81.0	1176.5	0.0065	6.49
2	1	2.412	2.478	2.7	15.5	82.7	1214.2	0.0059	6.81
2	2	2.409	2.478	2.8	15.6	82.0	1269.4	0.0061	6.80
2	3	2.409	2.478	2.8	15.5	82.2	1406.6	0.0061	6.52
Rep. Average		2.410	2.478	2.8	15.5	82.3	1296.7	0.0060	6.71
Overall Avg.		2.415	2.478	2.8	15.4	81.6	1236.6	0.0063	6.60

Table D.3: Test Results for Mixing Sequence C

Asphalt Binder	Rep.	Bulk Specific Gravity	TMD	VTM %	VMA %	VFA %	S_t, kPa	ϵ_t, mm/mm	Slope of Compaction Curve
1	1	2.416	2.492	3.0	15.3	80.1	1191.5	0.0068	6.67
1	2	2.416	2.492	3.0	15.3	80.2	1241.1	0.0061	6.45
1	3	2.415	2.492	3.1	15.3	80.0	1141.1	0.0061	6.70
Rep. Average		2.416	2.492	3.0	15.3	80.1	1191.2	0.0063	6.61
2	1	2.393	2.478	3.4	16.1	78.8	1201.1	0.0063	7.08
2	2	2.404	2.478	3.0	15.7	80.9	1159.0	0.0075	6.52
2	3	2.402	2.478	3.1	15.8	80.6	1262.5	0.0063	7.00
Rep. Average		2.400	2.478	3.2	15.9	80.1	1207.5	0.0067	6.87
Overall Avg.		2.408	2.485	3.1	15.6	80.1	1199.4	0.0065	6.74

D.5 Analysis

The objective of this study was to determine the effects of mixing sequence on HMA properties. To accomplish this, each of the obtained properties were analyzed statistically. This was accomplished by using an ANOVA. The ANOVA was performed at a level of significance of 0.05.

Table D.4 presents the results of the analyses for each of the obtained properties. This table presents the F-value and F_{crit} for each property. Based on the analyses, each of the volumetric properties (VTM, VMA, and VFA) as well as the compactibility (slope of compaction curve) showed significant differences between mixing sequences. However, neither property determined during indirect tensile testing showed significant differences.

Table D.4: Results of ANOVA for Mixing Sequence			
Property	F-value	Fcrit	Significant Difference?
VTM	9.70	3.68	Yes
VMA	3.99	3.68	Yes
VFA	7.33	3.68	Yes
Tensile Strength at Failure	0.73	3.68	No
Tensile Strain at Failure	1.28	3.74	No
Compactibility	6.56	3.68	Yes

For the four obtained properties that did show significant differences, a DMRT was performed to rank each mixing sequence. Tables D.5 through D.8 present these rankings.

Table D.5: DMRT Rankings for VTM		
Mixing Sequence	Average VTM	DMRT Ranking*
A	3.3	A
C	3.1	A
B	2.8	B
* Averages with the same letter are not significantly different		

Table D.6: DMRT Rankings for VMA

Mixing Sequence	Average VMA	DMRT Ranking*
A	15.8	A
C	15.6	AB
B	15.4	B

* Averages with the same letter are not significantly different

Table D.7: DMRT Rankings for VFA

Mixing Sequence	Average VTM	DMRT Ranking*
B	81.7	A
C	80.0	B
A	79.0	B

* Averages with the same letter are not significantly different

Table D.8: DMRT Rankings for Compactibility

Mixing Sequence	Average VTM	DMRT Ranking*
A	7.05	A
C	6.74	B
B	6.60	B

* Averages with the same letter are not significantly different

D.6 Conclusions

Based on this investigation, it was determined that the mixing sequence in which the constituents of a HMA mixture are blended can affect the final properties of the mixture. Properties that were significantly affected include VTM, VMA, VFA, and compactibility. However, it was also determined that the tensile properties, based on the indirect tensile test, were not significantly affected.

The significance of these findings, as they relate to the NCAT South Carolina baghouse fines study, is that a particular mixing sequence must be selected. If no differences were determined, then any of the mixing sequences could be utilized.

When fabricating briquettes in the laboratory, it is typical to batch both the filler and aggregate together and then add the asphalt binder. Therefore, the filler and aggregate are premixed. For batch plants, this is sufficient. However, this would not simulate what is happening at drum plants. Recall that at drum plants, baghouse fines and the asphalt binder are typically added in a manner in which the baghouse fines and asphalt binder are premixed. Since approximately half of HMA producing facilities are now drum plants and most of the new facilities being manufactured are drum plants, mixing sequence A was selected as the method of mixing the constituents for the baghouse fines study.

Reference

UN-13 (CEMP-ET), Hot-Mix Asphalt Paving Handbook, 31 July 1991, US Army Corps of Engineers.

Appendix E: Plant Equipment and Operations

PLANT EQUIPMENT AND OPERATIONS

Contractor, Plant, and Assigned Plant Number

CONTRACTOR	PLANT	PLANT NO
APAC	Conway	01
APAC	Florence	02
APAC	Georgetown	03
Ashmore	Greer	04
Banks	Charleston	05
J.F. Cleckley	Orangeburg	06
J.F. Cleckley	Ridgeland	07
REA Construction	Greelyville	08
REA Construction	Ridgeland	09
REA Construction	Rockhill	10
Sanders Brothers I	Summerville	11
Sanders Brothers II	Summerville	12
Sloan Construction	Columbia	13
Sloan Construction	Sandy Flat I	14
Sloan Construction	Sandy Flat II	15
Vulcan Materials	Anderson	16
Vulcan Materials	Lyman	17
Vulcan Materials	Pacolet	18

Plant No. 1

Type Plant: Double-barrel Drum

Manufacturer of baghouse: Astec

Type Primary Collector: Horizontal Cyclone

Type Secondary Collector: Baghouse

Normal Temperature in Baghouse: 210° F

Type Aggregate: Granite

Age of Filter Bags: 1 yr

Type Fuel: Natural Gas

% Baghouse Dust Returned To Mix: 100

% Primary Dust Returned To Mix: 100

Fabric Used For Bags:

Rated Production: 400 tph

Sampling Times

Time of Day	DATE							
	7/19/94	7/22/94	10/25/95	11/13/95	11/15/95			
Start-up				7:45	8:00			
A.M.	10:40	7:55	7:30	9:30	9:00			
A.M.		9:30	9:00	11:00	10:30			
A.M.		11:40			11:30			
P.M.	15:15	15:30	13:15	12:30	12:30			
P.M.		16:55	14:30	15:30	13:30			
P.M.					14:30			

NOTE:

Primary Dust Handling: The primary fines were collected at the bottom of the horizontal cyclone and then added to the baghouse fines in an auger chute located at the bottom of the cyclone.

Secondary Dust Handling: The baghouse fines were collected in the bottom of the baghouse in an auger chute, where they were added back to the primary fines underneath the cyclone. The combined baghouse and primary fines were then added to the outside barrel of the drum before blending with the mixture.

Location of Sample(s): The primary fines could not be directly sampled, therefore a combined sample of primary and baghouse fines was obtained from the auger chute leading from the bottom of the cyclone to the outside drum of the plant. The baghouse fines were obtained from the bottom of the baghouse.

E.4

Plant No. 2

Type Plant: Drum

Manufacturer of baghouse: Cedar Rapids

Type Primary Collector: Vertical Cyclone

Type Secondary Collector: Baghouse

Normal Temperature in Baghouse: 280°

Type Aggregate: Granite

Age of Filter Bags: 8 mo

Type Fuel: Recycled Oil

% Baghouse Dust Returned To Mix: 100

% Primary Dust Returned To Mix: 100

Fabric Used For Bags: Nomex

Rated Production: 400 tph

Sampling Times

Time of Day	DATE							
	7/7/94	7/8/94	7/11/94	7/12/94	7/13/94			
Start-up	9:05				7:50			
A.M.	10:25	8:45	7:25	7:50	10:05			
A.M.	11:45	10:05	9:25	9:15	11:30			
A.M.			11:20	10:30				
P.M.	13:45		13:00	12:10	13:00			
P.M.	15:15		14:10	15:35	14:15			
P.M.				16:45	16:45			

NOTE: At the time of sampling, there were holes in the duct-work leading from the drum to the cyclone and the cyclone. Material was being lost from both of these openings. The duct-work leading from the drum to the cyclone was unusually long, approximately 75 to 100 feet.

Primary Dust Handling: The primary fines were collected at the bottom of the vertical cyclone, which is approximately 10 feet in the air. The fines then fell by gravity into a auger chute that contained the baghouse fines.

Secondary Dust Handling: The baghouse fines were collected in the bottom of the baghouse where they were removed by an auger chute. The primary fines were added to the baghouse fines in the auger chute and both were sent to the drum via this auger chute. The fines were added back to the drum at a point behind the flame.

Location of Sample(s): The primary fines were obtained from a hole that was cut into the bottom of the auger chute at a point past where the baghouse fines were introduced. The baghouse fines were obtained in a similar manner at a point before the introduction of the primary fines.

Plant No. 3

Type Plant: Double-barrel Drum

Manufacturer of Baghouse: Astec

Type Primary Collector: N/A

Type Secondary Collector: Baghouse

Normal Temperature in Baghouse: 280°F

Type Aggregate: Granite

Age of Filter Bags: 5 yrs

Type Fuel: #2 Diesel

% Baghouse Dust Returned To Mix: 100

% Primary Dust Returned To Mix: N/A

Fabric Used For Bags: 18 oz Aramid

Rated Production: 334

Sampling Times

Time of Day	DATE							
	10/17/95	10/18/95	10/19/95	10/24/95				
Start-up								
A.M.	8:00	8:30	9:00	9:30				
A.M.	9:30	10:00	10:30	11:00				
A.M.	11:00	11:30	12:30 pm	13:00 pm				
P.M.	12:30	13:00	14:00	14:00				
P.M.	14:00	14:30	15:30	15:00				
P.M.	15:30	15:45	16:15	16:00				

NOTE:

Primary Dust Handling: N/A

Secondary Dust Handling: The fines were collected at the bottom of the baghouse and augered to the outside drum..

Location of Sample(s): The sample was taken from the bottom of the baghouse.

Plant No. 4

Type Plant: Drum

Type Secondary Collector: Baghouse

Type Primary Collector: N/A

Normal Temperature in Baghouse: 315°F

Type Aggregate: Granite

Age of Filter Bags: 2 yrs

Type Fuel: Natural Gas

% Baghouse Dust Returned To Mix: 100

% Primary Dust Returned To Mix: N/A

Rated Production: 400 tph

Sampling Times

Time of Day	DATE							
	6/3/96	6/4/96	6/5/96	6/6/96				
Start-up								
A.M.	9:30	9:00	8:55	8:00				
A.M.	10:30	10:45	9:55	10:30				
A.M.		11:55	11:00					
P.M.		13:30	11:55 am	15:30				
P.M.		14:30	1:30					
P.M.			2:30					

NOTE:

Primary Dust Handling: N/A

Secondary Dust Handling: The baghouse fines were collected in the bottom of the baghouse before being blown pneumatically into the drum.

Location of Sample(s): The contractor placed a "T" connection on the pneumatic line running from the baghouse to the drum. On this connection a valve was placed to divert the baghouse fines into a container. The baghouse fine samples were sampled from this container.

Plant No. 5

Type Plant: Double-barrel Drum

Manufacturer of Baghouse: Aztec

Type Primary Collector: Vertical Cyclone

Type Secondary Collector: Baghouse

Normal Temperature in Baghouse: 250°F

Type Aggregate: Granite

Age of Filter Bags: 5 ½ yrs

Type Fuel: Natural Gas

% Baghouse Dust Returned To Mix: 100

% Primary Dust Returned To Mix: 100

Fabric Used For Bags: Nomex

Rated Production: 400 tph

Sampling Times

Time of Day	DATE							
	7/25/94	7/26/94	7/28/94	8/4/94	8/8/94	8/9/94	8/10/94	8/11/94
Start-up		7:20						8:05
A.M.	10:15	9:05	7:25			9:10	10:10	
A.M.	11:45	10:50	9:00			10:35		
A.M.								
P.M.	15:40	12:30		14:15	16:00	12:10	14:10	12:35
P.M.		13:50				13:35	15:30	
P.M.		15:05				16:05	16:40	

NOTE: The auger chute leading from the baghouse to the outside drum had holes cut into the top of the chute. A big rain fell the night of 8/9/94. When sampling the next morning, the chute was full of water. The baghouse fines within the chute were sticking together. This occurred for the 8:05 sample of the 11th. However, this problem did not show up for the 12:35 sample.

Primary Dust Handling: The primary fines were collected in the bottom of the vertical cyclone and gravity fed to a chute which combines the primary and baghouse fines at the outer drum

Secondary Dust Handling: The baghouse fines were collected in the baghouse and augered to the outside drum. The baghouse fines were added to the primary fines at a portal located on the outside barrel.

Location of Sample(s): The primary fines were obtained from a cleaning portal located at the bottom of the cyclone. The baghouse fines were obtained from the auger chute leading from the baghouse to the drum.

Plant No. 6

Type Plant: Drum

Manufacturer of Baghouse: Gencor-Bituma

Type Primary Collector: Knockout Box

Type Secondary Collector: Baghouse

Normal Temperature in Baghouse: 310

Type Aggregate: Granite

Age of Filter Bags: 1 wk to 8 yrs

Type Fuel: #5 Waste Oil

% Baghouse Dust Returned To Mix: 100

% Primary Dust Returned To Mix: 100

Fabric Used For Bags: Nomex

Rated Production: 300 tph

Sampling Times

Time of Day	DATE							
	6/28/94	6/29/94	6/30/94	7/1/94	9/1/94	9/2/94	9/6/94	
Start-up		7:55	7:45		7:30	6:35		
A.M.	8:20		8:55	8:00	8:50	7:55	7:35	
A.M.	9:55		10:10		10:10	9:25	9:00	
A.M.			11:25			11:25	10:35	
P.M.	13:15	13:50			12:45		12:15	
P.M.	14:30							
P.M.	16:25							

NOTE:

Primary Dust Handling: The primary fines fall onto the mix at the end of the drum.

Secondary Dust Handling: The baghouse fines were collected in the bottom of the baghouse and sent through a rotary air-lock to the drum. The fines were introduced on the end of the drum opposite the flame.

Location of Sample(s): The primary fines could not be sampled. The baghouse fines were sampled from the bottom of the baghouse.

Plant No. 7

Type Plant: Batch

Manufacturer of Baghouse: Estee

Type Primary Collector: N/A

Type Secondary Collector: Baghouse

Normal Temperature in Baghouse: 300°F

Type Aggregate: Granite

Age of Filter Bags: 2 yrs

Type Fuel: #5 Waste Oil

% Baghouse Dust Returned To Mix: 100

% Primary Dust Returned To Mix: N/A

Fabric Used For Bags: Nomex

Rated Production: 300 tph

Sampling Times

Time of Day	DATE							
	6/20/94	6/21/94	6/22/94	6/23/94	7/14/94	7/15/94		
Start-up		7:25	7:15					
A.M.	9:25	9:45	8:40	10:30		8:35		
A.M.	10:45	11:30	10:00			10:05		
A.M.						11:15		
P.M.	13:00		12:45	14:00	12:45			
P.M.	15:00		14:30		14:15			
P.M.	16:45		16:00					

NOTE:

Primary Dust Handling: N/A

Secondary Dust Handling: The baghouse fines were collected in the bottom of the baghouse and augered to the hot elevator by an auger chute.

Location of Sample(s): The baghouse fines were sampled from the auger leading from the baghouse to the hot elevator.

Plant No. 8

Type Plant: Drum

Manufacturer of Baghouse: Astec

Type Primary Collector: Knockout Box

Type Secondary Collector: Baghouse

Normal Temperature in Baghouse: 330°F

Type Aggregate: Granite

Age of Filter Bags: 1 yr

Type Fuel: #2 Diesel

% Baghouse Dust Returned To Mix: 100

% Primary Dust Returned To Mix: 100

Fabric Used For Bags: Nomex

Rated Production: 300 tph

Sampling Times

Time of Day	DATE							
	4/15/96	4/16/96	4/17/96	4/18/96	5/1/96	5/7/96	5/8/96	5/9/96
Start-up				7:50				
A.M.	10:45	7:55	8:00	10:00	10:30		9:55	
A.M.			11:20				10:55	
A.M.							11:35	
P.M.	13:55	12:00	12:55	13:40	13:46	12:45	12:15	11:15
P.M.						15:45	13:15	12:15
P.M.						17:00	14:15	15:15

NOTE:

Primary Dust Handling: The knockout box was located above the baghouse. The primary fines fall into an auger that contained the baghouse fines.

Secondary Dust Handling: The baghouse fines were collected at the bottom of the baghouse. From there an auger took the baghouse fines to the drum.

Location of Sample(s): The knockout box could not be sampled. Samples of the baghouse fines were obtained from the bottom of the baghouse.

Plant No. 9

Type Plant: Double-Barrel Drum

Manufacturer of Baghouse: Astec

Type Primary Collector: Horizontal Cyclone

Type Secondary Collector: Baghouse

Normal Temperature in Baghouse: 230/270°F

Type Aggregate: Granite

Age of Filter Bags: 8 months

Type Fuel: # 5 Waste Oil

% Baghouse Dust Returned To Mix: 100

% Primary Dust Returned To Mix: 100

Fabric Used For Bags:

Rated Production: 300 tph

Sampling Times

Time of Day	DATE							
	8/13/96	8/14/96	8/15/96	8/16/96				
Start-up		7:45	7:30	8:30				
A.M.	10:45	8:45	8:30	10:00				
A.M.	11:50	9:45	11:25					
A.M.		10:45						
P.M.	14:45	12:30	13:45	15:30				
P.M.	15:45	13:30	15:00	16:30				
P.M.	16:45	14:30						

NOTE:

Primary Dust Handling: The primary fines were collected at the bottom of the cyclone. The fines were then augered to another auger chute where they were combined with the baghouse fines.

Secondary Dust Handling: The secondary fines were collected at the bottom of the baghouse and sent to an auger chute where they were combined with the primary fines before being sent to the outside drum.

Location of Sample(s): The primary fines were sampled in the auger chute underneath the cyclone. The baghouse fines were sampled prior to being added to the primary fines. An additional combined primary and baghouse fines sample was obtained after the two were combined and before being added to the drum.

Plant No. 10

Type Plant: Batch

Manufacturer of Baghouse:

Type Primary Collector: N/A

Type Secondary Collector: Baghouse

Normal Temperature in Baghouse: 290°F

Type Aggregate: Granite

Age of Filter Bags: ½ to 3 yrs

Type Fuel: Natural Gas

% Baghouse Dust Returned To Mix: 100

% Primary Dust Returned To Mix: N/A

Fabric Used For Bags:

Rated Production: 250 tph

Sampling Times

Time of Day	DATE							
	7/17/96	7/18/96	7/23/96	7/24/96	7/25/96			
Start-up		8:30	8:00	9:00	7:30			
A.M.	7:30	9:30	9:00	10:00	8:30			
A.M.	8:30	10:30	10:00	11:00	9:30			
A.M.	9:30	11:30	11:00					
P.M.	11:00 am	12:30	12:00					
P.M.		13:30	13:00					
P.M.		14:30	15:30					

Primary Dust Handling: N/A

Secondary Dust Handling: The baghouse fines were collected in the bottom of the baghouse before being augered back to the hot elevator.

Location of Sample(s): The baghouse fines were sampled from the chute leading from the baghouse to the hot elevator.

Plant No. 11

Type Plant: Drum

Manufacturer of Baghouse: CMI

Type Primary Collector: N/A

Type Secondary Collector: Baghouse

Normal Temperature in Baghouse: 220°F

Type Aggregate: Granite

Age of Filter Bags: 1½ yrs

Type Fuel: Propane

% Baghouse Dust Returned To Mix: 100

% Primary Dust Returned To Mix: N/A

Fabric Used For Bags: Nomex

Rated Production: 300 tph

Sampling Times

Time of Day	DATE							
	8/2/94	8/3/94	8/4/94	8/5/94	8/8/94	8/10/94	8/11/94	
Start-up			6:30			7:15		
A.M.	6:50	7:15	7:45	9:10	8:35	8:35	9:30	
A.M.	8:25	9:50	9:00		10:15		11:05	
A.M.	10:50	11:45	10:30		11:30			
P.M.	12:40		12:00		14:10	12:00		
P.M.					15:20	13:30		
P.M.								

NOTE: This plant had mechanical problems with the baghouse while on-site. The rotary air-lock malfunctioned numerous times.

Primary Dust Handling: N/A

Secondary Dust Handling: The baghouse fines were collected in the bottom of the baghouse and sent to the drum through a rotary air-lock. The fines were blown into the drum at the opposite end of the drum from the flame.

Location of Sample(s): The baghouse fines were sampled from the bottom of the baghouse.

Plant No. 12

Type Plant: Drum

Manufacturer of Baghouse: CMI

Type Primary Collector: N/A

Type Secondary Collector: Baghouse

Normal Temperature in Baghouse: 220/230°F

Type Aggregate: Granite

Age of Filter Bags: 3 mo

Type Fuel: Propane

% Baghouse Dust Returned To Mix: 100

% Primary Dust Returned To Mix: N/A

Fabric Used For Bags: Cloth

Rated Production: 400 tph

Sampling Times

Time of Day	DATE					
	5/19/96	5/20/96	5/21/96	5/22/96	5/23/96	
Start-up						
A.M.		12:50	1:30	1:50	2:20	
A.M.		3:00	2:30	2:55	3:20	
A.M.		18:30 pm	20:25 pm	19:45	4:00	
P.M.	11:20	17:05	21:30	21:00	4:20 am	
P.M.		22:00	22:30	22:00	5:00 am	
P.M.		23:15	23:30	23:00		

NOTE: This plant utilized a storage pod between the baghouse and the reintroduction point at the drum. This pod allowed the fines to be introduced in a uniform manner. Excess baghouse fines could be wasted over the top of the pod.

Primary Dust Handling: N/A

Secondary Dust Handling: The baghouse fines were collected in the bottom of the baghouse in an auger chute. From the baghouse, the fines were augered to a storage pod. From the pod, the fines were augered to the drum.

Location of Sample(s): The baghouse fine samples were obtained from the wasting point above the storage pod.

Plant No. 13

Type Plant: Batch

Manufacturer of Baghouse: Astec

Type Primary Collector: Horizontal Cyclone

Type Secondary Collector: Baghouse

Normal Temperature in Baghouse: 240°F

Type Aggregate: Granite

Age of Filter Bags: 1 mo

Type Fuel: # 5 Waste Oil

% Baghouse Dust Returned To Mix: 100

% Primary Dust Returned To Mix: 100

Fabric Used For Bags: Nomex

Rated Production: 200 tph

Sampling Times

Time of Day	DATE							
	8/22/94	8/23/94	8/24/93	8/25/94	8/26/94	8/29/94		
Start-up			6:50		7:15			
A.M.	8:15	7:20	9:15	7:00	8:50	9:00		
A.M.		9:35		9:00	10:15	10:30		
A.M.		10:45		11:05	11:45			
P.M.		12:20		12:40		12:00		
P.M.		13:50		15:40		13:30		
P.M.		15:30		17:20		16:30		

Primary Dust Handling: The primary fines were collected at the bottom of the horizontal cyclone and gravity fed to an auger chute which contained the baghouse fines.

Secondary Dust Handling: The baghouse fines were collected in the bottom of the baghouse and augered through a chute which combined the primary fines and baghouse fines. Both fines were then augered to the hot elevator.

Location of Sample(s): The primary fines could not be sampled. The baghouse fines were sampled from the bottom of the baghouse. Because the primary fines could not be sampled, a combined sample of primary and baghouse fines was obtained from the auger chute leading to the hot elevator.

Plant No. 14

Type Plant: Batch

Manufacturer of Baghouse: Barber-Greene

Type Primary Collector: Knockout Box

Type Secondary Collector: Baghouse

Normal Temperature in Baghouse: 245°F

Type Aggregate: Granite

Age of Filter Bags: 1 yr

Type Fuel: #4 Waste Oil

% Baghouse Dust Returned To Mix: 100

% Primary Dust Returned To Mix: 100

Fabric Used For Bags:

Rated Production: 325 tph

Sampling Times

Time of Day	DATE							
	9/7/94	9/8/94	9/9/94	8/29/95	8/30/95	8/31/95	9/1/95	
Start-up		7:45						
A.M.	11:40	9:25	8:55		8:45	8:00	7:45	
A.M.		11:05			10:05	10:00	10:45	
A.M.				13:20 pm	11:30			
P.M.		13:55		14:40	13:05	12:40		
P.M.		15:30		16:00	14:30	14:45		
P.M.				17:30	15:00	17:00		

NOTE: This plant was originally a 3-ton batch plant but was modified with a rotary mixer to act as a drum.

Primary Dust Handling: The primary fines were collected just above the hot elevator. They were captured in the knockout box and fell through a chute into the hot elevator.

Secondary Dust Handling: The baghouse fines were collected in the bottom of the baghouse and subsequently augered to the hot elevator.

Location of Sample(s): The primary fines could not be sampled. The baghouse fines were sampled at a cleaning portal on the auger chute leading from the baghouse to the hot elevator.

Plant No. 15

Type Plant: Batch

Manufacturer of Baghouse: Barber-Greene

Type Primary Collector: Knockout Box

Type Secondary Collector: Baghouse

Normal Temperature in Baghouse: 245°F

Type Aggregate: Granite

Age of Filter Bags: 2 yrs

Type Fuel: #4 Waste Oil

% Baghouse Dust Returned To Mix: 100

% Primary Dust Returned To Mix: 100

Fabric Used For Bags: Nomex

Rated Production: 325 tph

Sampling Times

Time of Day	DATE							
	6/2/96	6/3/96	6/4/96	6/5/96	6/6/96			
Start-up	8:15	8:00	8:00					
A.M.	9:30	9:00	9:40	9:00	8:00			
A.M.	10:30	10:00	10:40	10:00	10:00			
A.M.	11:30	11:00	11:40					
P.M.	12:40	12:20	12:40					
P.M.	13:40	13:20	13:40					
P.M.	15:00	14:40						

NOTE: This plant was originally a 3-ton batch plant but was modified with a rotary mixer to act as a drum.

Primary Dust Handling: The primary fines were collected just above the hot elevator. They were captured in the knockout box and fell through a chute into the hot elevator.

Secondary Dust Handling: The baghouse fines were collected in the bottom of the baghouse and subsequently augered to the hot elevator.

Location of Sample(s): The primary fines could not be sampled. The baghouse fines were sampled at a cleaning portal on the auger chute leading from the baghouse to the hot elevator.

Plant No. 16

Type Plant: Drum

Manufacturer of Baghouse: Estee

Type Primary Collector: Cyclone

Type Secondary Collector: Baghouse

Normal Temperature in Baghouse: 250°F

Type Aggregate: Granite

Age of Filter Bags:

Type Fuel: Diesel

% Baghouse Dust Returned To Mix: 100

% Primary Dust Returned To Mix: 100

Fabric Used For Bags: Nomex

Rated Production: 400 tph

Sampling Times

Time of Day	DATE							
	8/14/95	8/15/95	8/16/95	8/17/95	8/18/95			
Start-up			7:00	7:00	7:00			
A.M.		8:40	7:05	7:06	7:10			
A.M.		9:30	7:53	8:10	9:10			
A.M.			11:50	9:30				
P.M.	15:45	13:20	13:15	10:15 am				
P.M.		14:03						
P.M.								

Primary Dust Handling: The primary fines were collected at the bottom of the cyclone and fed to an auger chute that contained the baghouse fines.

Secondary Dust Handling: The baghouse fines were collected at the bottom of the baghouse. The fines were then augered to a point where they were combined with the primary fines and subsequently augered to the drum.

Location of Sample(s): The primary fines could not be sampled. The baghouse fines were sampled at the end of the baghouse right before entering the auger chute.

Plant No. 17

Type Plant: Drum

Manufacturer of Baghouse: Astec

Type Primary Collector: N/A

Type Secondary Collector: Baghouse

Normal Temperature in Baghouse: 230°F

Type Aggregate: Granite

Age of Filter Bags: 1 mo

Type Fuel: #2 Diesel

% Baghouse Dust Returned To Mix: 100

% Primary Dust Returned To Mix: N/A

Fabric Used For Bags:

Rated Production: 400 tph

Sampling Times

Time of Day	DATE						
	11/7/94	11/8/94	11/9/94	11/11/94	11/14/94	11/15/94	
Start-up			9:00	8:20			
A.M.	8:30	7:00	9:45	8:50	11:30	7:30	
A.M.	9:45	8:00	10:45	9:30		8:30	
A.M.	11:15	10:00	11:40	9:35			
P.M.		11:00 am	13:15	9:40 am			
P.M.		12:15	14:00	9:45 am			
P.M.		13:20	14:50	9:50 am			

Primary Dust Handling: N/A

Secondary Dust Handling: The baghouse fines were collected in the bottom of the baghouse and subsequently augered to the drum.

Location of Sample(s): The baghouse fine sample was obtained from the auger chute leading from the baghouse to the drum.

Plant No. 18

Type Plant: Drum

Manufacturer of Baghouse: Gencor

Type Primary Collector: N/A

Type Secondary Collector: Baghouse

Normal Temperature in Baghouse: 280°F

Type Aggregate: Granite

Age of Filter Bags: 2 yrs

Type Fuel: #2 Diesel

% Baghouse Dust Returned To Mix: 100

% Primary Dust Returned To Mix: N/A

Fabric Used For Bags:

Rated Production: 400 tph

Sampling Times

Time of Day	DATE							
	4/25/95	4/26/95	4/27/95	6/27/95	6/28/95			
Start-up	7:00		6:30		7:00			
A.M.	8:50	8:30	7:00	10:40	8:30			
A.M.	10:05		8:20	11:40	10:40			
A.M.	11:15		10:35					
P.M.	13:15	12:15	11:50 am	13:40				
P.M.	14:40	15:19						
P.M.	16:20							

Primary Dust Handling: N/A

Secondary Dust Handling: The baghouse fines were collected in the bottom of the baghouse and subsequently augered to the drum.

Location of Sample(s): The baghouse fine samples were obtained from the auger chute leading from the baghouse to the drum.

Appendix F: Results of Particle Size Analyses for All Plants

Table F.1: Results of Particle Size Analyses for Plant No. 1

Sample Description		Results of Particle Size Analyses							
Sample No.	Type Sample	Mean Particle Size, μm	D_{10}, μm	D_{30}, μm	D_{60}, μm	C_u	% Clay	FM	Specific Surface Area, cm^2/ml
1	Baghouse	42.1	3.9	15.6	37.3	9.63	5.10	5.12	6574
1	Combined	94.8	7.3	30.5	86.4	11.92	3.28	6.23	4254
2	Baghouse	41.6	3.7	15.0	36.3	9.76	5.25	5.07	6745
2	Combined	111.7	8.0	32.8	89.8	11.26	3.24	6.30	4120
3	Baghouse	48.3	3.7	16.8	42.1	11.36	5.52	5.27	6669
3	Combined	139.2	10.4	43.0	116.8	11.19	2.85	6.60	3558
4	Baghouse	47.0	3.7	16.2	40.7	11.10	5.51	5.22	6728
4	Combined	151.6	9.1	40.2	117.5	12.92	3.12	6.52	3808
5	Baghouse	47.9	3.8	17.1	41.8	10.90	5.39	5.27	6564
5	Combined	160.5	12.0	50.2	131.0	10.88	2.68	6.74	6294
6	Baghouse	48.0	4.0	17.2	42.0	10.43	5.10	5.29	6364
6	Combined	130.2	10.8	43.4	118.2	10.96	2.80	6.61	3502
7	Baghouse	48.6	4.1	17.6	42.4	10.48	5.12	5.31	6346
7	Combined	137.6	9.0	39.0	111.2	12.41	3.22	6.49	3904
8	Baghouse								
8	Combined								
9	Baghouse	174.8	9.3	42.6	130.0	14.0		6.58	3786
9	Combined								
10	Baghouse								
10	Combined								
11	Baghouse	159.2	5.3	30.5	101.8	19.03		6.22	5041
11	Combined								
12	Baghouse	205.1	11.0	53.1	160.1	14.57		6.77	333.8
12	Combined								

Table F.1: Results of Particle Size Analyses for Plant No. 1

Sample Description		Results of Particle Size Analyses							
Sample No.	Type Sample	Mean Particle Size, μm	D_{10}, μm	D_{30}, μm	D_{60}, μm	C_u	% Clay	FM	Specific Surface Area, cm^2/ml
13	Baghouse	233.0	12.6	54.1	167.0	13.75		6.81	3095
13	Combined								
14	Baghouse	202.2	11.7	52.7	154.4	13.8		6.77	3347
14	Combined								
15	Baghouse	177.2	7.1	33.6	118.1	16.54		6.36	4291
15	Combined								
16	Baghouse	110.0	13.0	53.8	149.4	11.47		6.82	2942
16	Combined								
17	Baghouse	218.8	11.6	62.1	184.7	15.94		6.87	3185
17	Combined								
18	Baghouse	169.9	12.2	52.4	144.6	11.81		6.78	3210
18	Combined								
19	Baghouse	137.4	5.5	32.1	106.5	19.19		6.28	4897
19	Combined								
20	Baghouse	136.2	8.5	34.8	101.5	11.99		6.39	3885
20	Combined								
21	Baghouse	185.3	13.8	59.6	156.4	11.35		6.89	2959
21	Combined								
22	Baghouse	156.6	12.4	49.9	130.7	10.56		6.74	3300
22	Combined								
23	Baghouse	155.5	14.4	56.3	135.2	9.36		6.86	3057
23	Combined								

Table F.2: Results of Particle Size Analyses for Plant No. 2

Sample Description		Results of Particle Size Analyses							
Sample No.	Type Sample	Mean Particle Size, µm	D_{10}, µm	D_{30}, µm	D_{60}, µm	C_u	% Clay	FM	Specific Surface Area, cm^2/ml
1	Baghouse	39.6	2.4	10.2	30.3	12.58	8.10	4.69	9132
1	Combined	302.5	21.4	73.7	205.5	9.62	2.06	7.11	2470
2	Baghouse	37.0	2.4	10.0	29.3	12.04	7.99	4.65	9120
2	Combined	254.3	13.3	60.6	169.1	12.74	2.49	6.89	3021
3	Baghouse	33.0	2.2	8.7	25.8	11.74	8.96	4.66	9994
3	Combined	265.0	7.3	42.8	159.0	21.75	3.48	6.55	4046
4	Baghouse	28.6	1.8	6.6	21.6	11.82	11.15	4.15	11784
4	Combined	221.4	5.7	33.8	122.1	21.27	4.10	6.34	4684
5	Baghouse	34.7	2.2	9.2	27.5	12.41	8.89	4.54	9835
5	Combined	186.8	5.0	30.9	112.2	22.31	4.53	6.24	5073
6	Baghouse	30.2	2.1	8.1	23.8	11.43	9.55	4.32	10533
6	Combined	131.6	4.4	23.9	94.7	21.69	4.81	6.03	5526
7	Baghouse	41.2	2.5	11.1	33.2	13.18	7.78	4.83	8758
7	Combined	206.1	7.2	39.6	132.6	18.53	3.65	6.48	4220
8	Baghouse	39.5	2.5	10.6	32.4	13.23	7.98	4.77	8965
8	Combined	230.0	8.7	45.6	142.2	16.36	3.20	6.61	3784
9	Baghouse	38.3	2.5	10.4	30.8	12.54	7.93	4.72	9002
9	Combined	260.4	8.3	46.3	157.3	18.91	3.24	6.62	3804
10	Baghouse	120.8	2.5	11.2	35.6	14.09	7.74	4.95	8618
10	Combined	219.7	7.0	36.7	129.8	18.58	3.50	6.43	4189
11	Baghouse	37.8	2.6	10.6	31.1	12.14	7.56	4.74	8755
11	Combined								
12	Baghouse	30.7	2.1	8.1	24.1	11.43	9.42	4.35	10431
12	Combined	106.8	4.5	24.4	89.0	19.65	4.66	6.02	5425

Table F.2: Results of Particle Size Analyses for Plant No. 2

Sample Description		Results of Particle Size Analyses							
Sample No.	Type Sample	Mean Particle Size, μm	D_{10}, μm	D_{30}, μm	D_{60}, μm	C_u	% Clay	FM	Specific Surface Area, cm^2/ml
13	Baghouse	35.3	2.2	9.0	27.0	12.13	8.85	4.52	9844
13	Combined	129.6	5.2	28.5	98.2	18.84	4.25	6.17	4982
14	Baghouse	35.8	2.4	10.0	29.4	12.10	8.03	4.65	9155
14	Combined	248.1	10.7	48.9	175.5	16.48	2.38	6.73	3130
15	Baghouse	36.7	2.4	10.0	29.6	12.13	7.97	4.67	9106
15	Combined	145.7	5.1	27.5	101.1	19.86	4.27	6.15	5021
16	Baghouse	33.4	2.4	9.5	27.2	11.51	8.27	4.54	9441
16	Combined	127.2	5.2	28.6	97.1	18.81	4.30	6.17	5017
17	Baghouse	35.7	2.4	9.7	29.1	12.35	8.33	4.63	9374
17	Combined	275.0	10.2	58.9	189.0	18.48	2.86	6.81	3369
18	Baghouse	35.6	2.5	9.9	28.2	11.45	7.88	4.61	9111
18	Combined	145.3	5.7	29.6	101.1	17.72	3.92	6.22	4713
19	Baghouse	276.8	5.6	35.7	233.2	41.50	4.10	6.45	4582
19	Combined	174.8	10.4	51.8	140.8	13.46	3.10	6.73	3583
20	Baghouse	92.4	2.3	9.4	30.2	13.37	8.72	4.72	9542
20	Combined	141.8	5.3	30.1	99.1	18.82	4.34	6.21	4986
21	Baghouse	34.5	2.4	9.6	27.1	11.18	8.01	4.55	9269
21	Combined	239.6	7.0	38.7	135.5	19.32	3.55	6.46	4179
22	Baghouse	29.6	2.2	8.2	23.3	10.67	9.01	4.32	10209
22	Combined	119.6	5.7	29.9	97.7	17.03	3.94	6.22	4728
23	Baghouse	33.5	2.5	9.7	26.7	10.78	7.80	4.54	9142
23	Combined	145.3	6.4	30.0	100.6	15.82	3.48	6.25	4401
24	Baghouse	37.1	2.8	11.3	31.7	11.45	6.94	4.79	8284
24	Combined	210.6	8.2	39.1	139.4	17.05	2.93	6.52	3737

Table F.3: Results of Particle Size Analyses for Plant No. 3

Sample Description		Results of Particle Size Analyses							
Sample No.	Type Sample	Mean Particle Size, μm	D_{10}, μm	D_{30}, μm	D_{60}, μm	C_u	% Clay	FM	Specific Surface Area, cm^2/ml
1	Baghouse	245.6	9.5	46.1	189.2	19.89	2.74	6.67	3430
2	Baghouse	276.4	12.3	63.1	223.9	18.23	2.66	6.89	3125
3	Baghouse	264.3	13.1	70.6	233.2	17.75	2.52	6.95	2972
4	Baghouse	240.9	10.5	54.9	195.9	18.60	2.86	6.78	3385
5	Baghouse	253.0	14.7	72.1	217.5	14.82	2.37	6.99	2833
6	Baghouse	218.6	10.6	55.3	182.2	17.14	2.79	6.79	3343
7	Baghouse	175.1	9.1	44.2	153.3	16.89	2.90	6.62	3600
8	Baghouse	196.9	9.4	47.4	157.4	16.77	3.10	6.67	3660
9	Baghouse	194.7	9.2	41.0	149.1	16.26	2.77	6.57	3552
10	Baghouse	230.8	12.8	59.0	189.8	14.84	2.24	6.87	2885
11	Baghouse	202.8	11.3	56.7	175.5	15.59	2.83	6.81	3331
12	Baghouse	213.0	11.2	58.2	182.6	16.36	2.87	6.82	3345
13	Baghouse	216.0	10.4	56.1	185.8	17.80	2.73	6.79	3310
14	Baghouse	189.4	9.8	45.6	148.1	15.06	2.78	6.65	3475
15	Baghouse	203.6	9.8	47.6	166.5	17.04	2.84	6.68	3482
16	Baghouse	152.6	6.3	30.2	111.7	17.79	3.66	6.27	4479
17	Baghouse	166.3	6.4	29.5	116.3	18.20	3.54	6.26	4403
18	Baghouse	244.1	10.5	46.1	172.7	16.43	2.49	6.68	3237
19	Baghouse	176.6	8.5	41.3	134.1	15.70	3.26	6.55	3890
20	Baghouse	240.7	11.0	54.3	166.8	15.23	2.86	6.78	3379
21	Baghouse	238.3	11.6	60.8	197.8	17.02	2.66	6.86	3179
22	Baghouse	238.9	10.7	52.0	183.6	17.24	2.84	6.75	3386
23	Baghouse	237.3	11.8	57.8	187.8	15.97	2.71	6.83	3225
24	Baghouse	228.0	12.2	61.1	198.6	16.28	2.67	6.87	3157

Table F.4: Results of Particle Size Analyses for Plant No. 4

Sample Description		Results of Particle Size Analyses							
Sample No.	Type Sample	Mean Particle Size, μm	D_{10}, μm	D_{30}, μm	D_{60}, μm	C_u	% Clay	FM	Specific Surface Area, cm^2/ml
1	Baghouse	100.2	5.0	26.5	73.9	14.78	4.51	6.00	5268
2	Baghouse	113.2	4.5	24.8	70.1	15.74	4.99	5.91	5666
3	Baghouse	68.4	3.3	18.7	57.6	17.35	6.20	5.58	6836
4	Baghouse	122.1	5.3	29.1	85.2	16.16	4.35	6.13	5040
5	Baghouse	100.9	4.9	27.3	80.2	16.23	4.57	6.06	5269
6	Baghouse	97.2	4.6	25.9	75.8	16.55	4.83	5.99	5508
7	Baghouse	76.5	4.1	22.5	66.7	16.35	5.20	5.82	5963
8	Baghouse	100.4	4.8	26.5	77.5	16.09	4.72	6.02	5397
9	Baghouse	114.9	4.4	23.9	114.9	16.22	4.96	5.9	5686
10	Baghouse	103.7	4.9	27.3	77.0	15.75	4.65	6.04	5328
11	Baghouse	84.7	5.0	27.6	75.5	15.26	4.65	6.03	5324
12	Baghouse	125.1	4.8	24.9	70.5	14.84	4.71	5.93	5464
13	Baghouse	76.7	4.7	24.2	67.0	14.40	4.73	5.88	5543
14	Baghouse	85.6	5.0	26.8	73.6	14.69	4.59	6.00	5313
15	Baghouse	119.6	5.0	26.9	74.3	14.84	4.58	6.01	5291
16	Baghouse	125.7	5.6	30.4	84.0	14.98	4.22	6.16	4909
17	Baghouse	121.3	5.6	28.3	121.3	13.56	4.28	6.07	5026

Table F.5: Results of Particle Size Analyses for Plant No. 5

Sample Description		Results of Particle Size Analyses							
Sample No.	Type Sample	Mean Particle Size, μm	D_{10}, μm	D_{30}, μm	D_{60}, μm	C_u	% Clay	FM	Specific Surface Area, cm^2/ml
1	Baghouse	21.8	1.7	5.4	16.6	9.67	12.18	3.80	12989
1	Cyclone	138.9	27.4	73.2	153.6	5.61	1.30	7.21	1867
2	Baghouse	16.2	1.4	3.9	11.7	8.14	15.6	3.32	15912
2	Cyclone	143.4	26.3	76.4	159.7	6.07	1.32	7.21	1894
3	Baghouse	36.2	2.4	9.9	33.8	14.37	2.86	4.75	9257
3	Cyclone	135.9	27.2	66.4	137.6	5.07	0.48	7.16	1872
4	Baghouse	28.5	2.2	8.4	24.1	10.99	8.99	4.34	10151
4	Cyclone	154.9	33.8	83.1	159.2	4.71	0.79	7.36	1397
5	Baghouse	29.3	2.3	8.6	24.5	10.78	8.61	4.37	9875
5	Cyclone	145.9	27.5	65.2	135.0	4.91	0.42	7.16	1758
6	Baghouse	29.1	2.1	8.1	24.0	11.43	9.48	4.32	10482
6	Cyclone								
7	Baghouse	32.7	2.6	10.6	28.8	11.15	7.52	4.62	8804
7	Cyclone	151.9	29.4	68.2	139.0	4.73	0.99	7.21	1653
8	Baghouse	31.5	2.6	10.0	26.9	10.44	7.46	4.54	8916
8	Cyclone	126.7	25.1	60.9	127.8	5.08	1.26	7.07	1962
9	Baghouse	32.0	2.5	10.3	28.1	11.20	7.75	4.58	9008
9	Cyclone	147.3	26.4	64.1	133.1	5.05	1.21	7.13	1878
10	Baghouse	26.4	2.2	8.2	22.2	9.89	8.72	4.24	10127
10	Cyclone	121.1	22.8	54.8	118.7	5.21	1.06	6.98	1910
11	Baghouse	36.4	2.6	11.3	36.1	13.73	7.39	4.86	8495
11	Cyclone	134.6	30.8	72.2	140.5	4.56	0.82	7.27	1497
12	Baghouse	32.9	2.8	10.5	28.3	10.99	7.55	4.60	8857
12	Cyclone	160.0	29.0	70.6	145.8	5.02	1.02	7.22	1617

Table F.5: Results of Particle Size Analyses for Plant No. 5

Sample Description		Results of Particle Size Analyses							
Sample No.	Type Sample	Mean Particle Size, μm	D_{10}, μm	D_{30}, μm	D_{60}, μm	C_u	% Clay	FM	Specific Surface Area, cm^2/ml
13	Baghouse	22.6	1.7	5.4	17.0	10.00	12.29	3.85	12999
13	Cyclone	150.7	31.2	82.1	164.3	5.27	0.96	7.32	1554
14	Baghouse	29.3	2.2	8.5	24.3	11.13	9.02	4.36	10147
14	Cyclone	150.5	32.9	83.7	159.0	4.84	0.88	7.35	1476
15	Baghouse	33.1	2.7	11.0	29.1	10.84	7.23	4.65	8572
15	Cyclone	125.7	27.6	63.7	127.9	4.63	0.93	7.15	1679
16	Baghouse	31.3	2.5	10.0	26.6	10.51	7.61	4.52	9018
16	Cyclone	149.1	32.8	82.5	163.5	4.99	1.03	7.34	1541
17	Baghouse	33.7	2.9	11.7	30.0	10.47	6.72	4.71	8151
17	Cyclone	132.3	27.9	65.9	135.5	4.86	0.95	7.17	1677
18	Baghouse	33.9	2.8	11.5	30.2	10.79	6.90	4.71	8279
18	Cyclone	131.3	27.7	66.5	135.1	4.89	1.10	7.17	1783
19	Baghouse	32.3	2.6	10.7	28.3	10.86	7.44	4.61	8768
19	Cyclone	148.8	26.0	63.6	133.7	5.13	1.12	7.12	1829
20	Baghouse	32.2	2.7	11.0	28.4	10.39	7.08	4.62	8508
20	Cyclone	145.2	23.7	60.0	129.3	5.45	1.17	7.05	1933
21	Baghouse	30.6	2.3	9.3	26.0	11.13	8.38	4.47	9584
21	Cyclone	136.8	23.0	59.4	128.0	5.58	1.31	7.03	2046
22	Baghouse	30.3	2.3	8.7	24.4	10.79	8.69	4.38	9911
22	Cyclone	145.2	27.1	64.5	132.5	4.89	1.00	7.15	1724
23	Baghouse	85.5	3.1	11.6	31.0	9.98	5.97	4.87	7603
23	Cyclone	191.8	31.8	89.1	184.3	5.80	0.78	7.36	1382
24	Baghouse	30.1	2.3	9.4	26.1	11.17	8.40	4.46	9582
24	Cyclone	125.4	24.5	59.0	125.0	5.11	1.15	7.05	1914

Table F.6: Results of Particle Size Analyses for Plant No. 6

Sample Description		Results of Particle Size Analyses							
Sample No.	Type Sample	Mean Particle Size, μm	D_{10}, μm	D_{30}, μm	D_{60}, μm	C_u	% Clay	FM	Specific Surface Area, cm^2/ml
1	Baghouse	108.2	2.6	16.6	77.1	29.42	7.60	5.67	7749
2	Baghouse	66.3	2.5	13.0	59.9	24.22	7.94	5.40	8300
3	Baghouse	71.6	2.7	17.0	68.4	25.20	7.32	5.63	7604
4	Baghouse	71.3	2.7	16.6	68.5	25.03	7.23	5.62	7569
5	Baghouse	72.2	2.8	17.5	71.6	25.69	7.15	5.68	7466
6	Baghouse	67.1	2.7	15.8	64.8	24.11	7.37	5.56	7726
7	Baghouse	69.3	3.0	21.0	70.8	23.65	6.75	5.78	7056
8	Baghouse	69.8	2.6	17.0	67.3	25.81	7.64	5.63	7810
9	Baghouse	66.3	2.4	13.7	62.4	22.36	8.37	5.43	8502
10	Baghouse	68.6	2.5	14.9	65.8	26.55	8.02	5.53	8180
11	Baghouse	68.8	2.5	14.2	63.4	25.70	8.03	5.48	8246
12	Baghouse	69.8	2.1	10.8	63.2	30.43	9.59	5.32	9478
13	Baghouse	60.9	2.8	15.9	55.7	20.09	7.20	5.45	7677
14	Baghouse	62.5	2.8	16.1	57.6	20.88	7.29	5.48	7700
15	Baghouse	62.3	2.9	16.3	57.5	19.72	6.91	5.50	7430
16	Baghouse	54.1	2.5	13.7	48.8	19.58	8.00	5.26	8398
17	Baghouse	42.7	2.0	9.5	38.2	18.81	9.85	4.86	10075
18	Baghouse	84.1	2.2	15.1	87.4	39.45	9.01	5.67	8690
19	Baghouse	87.5	2.1	14.7	96.5	46.40	9.62	5.68	9081
20	Baghouse	76.9	1.9	10.9	81.8	42.25	10.37	5.46	9826
21	Baghouse	77.7	2.2	13.8	84.3	38.19	9.01	5.65	8762
22	Baghouse	83.9	2.1	14.8	91.0	43.48	9.56	5.69	9027
23	Baghouse	80.5	2.0	12.2	85.9	43.91	10.25	5.55	9634
24	Baghouse	59.8	1.7	8.0	52.6	30.97	12.02	5.04	11318

Table F.7: Results of Particle Size Analyses for Plant No. 7

Sample Description		Results of Particle Size Analyses							
Sample No.	Type Sample	Mean Particle Size, μm	D_{10}, μm	D_{30}, μm	D_{60}, μm	C_u	% Clay	FM	Specific Surface Area, cm^2/ml
1	Baghouse	150.1	8.8	65.6	154.9	17.69	3.49	6.82	3876
2	Baghouse	176.9	10.9	82.0	176.5	16.18	3.17	6.97	3458
3	Baghouse	72.7	3.0	16.9	65.8	21.88	6.65	5.62	7206
4	Baghouse	174.6	4.6	36.5	148.2	32.54	4.84	6.38	5195
5	Baghouse	159.7	10.5	67.7	144.7	13.73	3.14	6.90	3521
6	Baghouse	173.2	9.4	74.9	175.4	18.72	3.33	6.90	3646
7	Baghouse	112.4	9.3	49.3	123.7	13.30	3.55	6.67	3968
8	Baghouse	124.9	5.8	37.2	119.9	20.65	4.51	6.41	4875
9	Baghouse	82.7	4.7	30.5	78.2	16.63	4.90	6.12	5445
10	Baghouse	125.3	8.3	42.7	110.8	13.40	3.56	6.53	4118
11	Baghouse	156.2	14.0	62.3	145.8	10.41	2.83	6.91	3234
12	Baghouse	156.9	48.6	102.3	165.5	3.41	1.12	7.53	1497
13	Baghouse	144.9	17.6	69.0	140.5	8.00	2.58	7.03	2969
14	Baghouse	95.2	7.2	33.8	86.3	12.05	3.94	6.29	4576
15	Baghouse	106.8	4.3	27.9	113.5	26.41	5.11	6.17	5576
16	Baghouse	128.0	33.0	73.6	132.4	4.01	1.78	7.24	2223
17	Baghouse	116.1	8.7	43.8	106.1	12.20	3.59	6.55	4092
18	Baghouse	130.4	5.0	32.2	119.2	23.97	4.83	6.30	5224
19	Baghouse	80.2	6.0	29.5	77.3	12.81	4.42	6.12	5049
20	Baghouse	98.9	9.9	44.4	94.0	9.46	3.35	6.56	3923
21	Baghouse	116.9	7.0	39.3	107.3	15.36	3.90	6.45	4430
22	Baghouse	84.4	4.5	26.2	84.1	18.91	4.99		5601
23	Baghouse	79.4	4.1	24.4	81.0	19.94	5.27		5880
24	Baghouse	79.1	4.2	24.8	80.3	19.14	5.09		5750

Table F.8: Results of Particle Size Analyses for Plant No. 8

Sample Description		Results of Particle Size Analyses							
Sample No.	Type Sample	Mean Particle Size, μm	D_{10}, μm	D_{30}, μm	D_{60}, μm	C_u	% Clay	FM	Specific Surface Area, cm^2/ml
1	Baghouse	73.0	2.7	14.0	61.9	22.74	7.19	5.47	7753
2	Baghouse	66.1	2.4	11.6	53.8	22.93	8.43	5.26	8787
3	Baghouse								
4	Baghouse								
5	Baghouse								
6	Baghouse	57.0	2.3	10.8	45.5	20.01	8.68	5.11	9115
7	Baghouse	60.1	2.5	11.7	50.4	20.16	7.78	5.24	8414
8	Baghouse	68.5	2.4	12.4	55.7	23.28	8.28	5.32	8612
9	Baghouse	51.4	2.1	10.0	41.5	19.50	9.32	4.99	9652
10	Baghouse	92.6	3.2	19.8	95.3	30.27	6.34	5.89	6746
11	Baghouse	61.4	2.3	10.7	45.9	19.84	8.52	5.12	9004
12	Baghouse	41.6	2.0	8.2	30.6	15.20	9.93	4.64	10449
13	Baghouse	50.7	2.9	15.0	46.3	15.78	6.76	5.27	7562
14	Baghouse	46.8	2.9	14.0	42.7	14.93	6.90	5.16	7771
15	Baghouse	62.6	3.3	18.1	57.5	17.22	6.03	5.57	6782
16	Baghouse	54.9	3.0	16.0	49.7	16.39	6.59	5.37	7339
17	Baghouse	69.8	3.0	16.4	64.7	21.79	6.67	5.59	7252
18	Baghouse	71.9	3.2	17.7	66.9	21.23	6.30	5.66	6925
19	Baghouse	53.8	3.1	15.0	46.1	15.02	6.45	5.29	7356
20	Baghouse								
21	Baghouse	63.1	3.1	16.8	56.7	18.23	6.44	5.51	7122
22	Baghouse	55.5	2.8	14.1	48.1	17.04	6.97	5.29	7731
23	Baghouse	59.5	3.4	17.0	53.9	15.89	5.82	5.49	6743
24	Baghouse	69.7	4.1	20.3	64.7	15.87	4.91	5.75	5888

Table F.9: Results of Particle Size Analyses for Plant No. 9

Sample Description		Results of Particle Size Analyses							
Sample No.	Type Sample	Mean Particle Size, μm	D_{10}, μm	D_{30}, μm	D_{60}, μm	C_u	% Clay	FM	Specific Surface Area, cm^2/ml
1	Baghouse	30.6	1.9	7.4	24.1	12.74	10.69	4.30	11285
1	Cyclone	197.5	3.4	22.2	118.8	34.99	6.08	6.00	6391
1	Combined	221.3	17.3	87.7	200.2	11.55	3.02	7.13	3136
2	Baghouse	32.1	2.0	7.9	24.9	12.57	10.10	4.36	10821
2	Cyclone	213.8	19.3	88.5	200.3	10.41	2.81	7.16	2973
2	Combined	190.2	4.0	29.1	145.9	36.65	5.34	6.23	5669
3	Baghouse	34.6	2.1	8.7	27.7	13.51	9.75	4.51	10401
3	Cyclone	243.2	41.2	112.1	220.9	5.36	2.19	7.41	2309
3	Combined	201.6	14.0	88.6	193.0	13.77	3.02	7.09	3212
4	Baghouse	36.4	2.3	10.4	30.7	13.53	8.72	4.69	9494
4	Cyclone	196.0	19.1	82.6	173.6	9.09	3.08	7.13	3181
4	Combined	158.6	6.5	50.6	145.6	22.58	4.24	6.63	4498
5	Baghouse	36.5	2.3	10.3	30.5	13.30	8.64	4.67	9461
5	Cyclone	173.6	10.4	62.3	153.5	14.79	3.62	6.86	3790
5	Combined	177.5	7.6	52.4	157.0	20.80	3.74	6.68	4102
6	Baghouse	126.6	3.0	16.4	62.5	20.55	6.63	5.56	7194
6	Cyclone	238.0	45.9	117.0	219.4	4.78	2.01	7.46	2156
6	Combined	206.7	12.0	85.1	197.3	16.50	3.07	7.02	3317
7	Baghouse	39.65	2.2	10.3	32.7	14.80	8.97	4.75	9596
7	Cyclone	231.7	50.0	109.4	205.7	4.11	1.70	7.51	1888
7	Combined	162.5	5.7	41.4	138.8	24.31	4.36	6.49	4724
8	Baghouse	34.3	2.2	9.4	28.8	13.33	9.21	4.57	9963
8	Cyclone	197.8	25.9	85.6	174.3	6.72	2.67	7.21	2831
8	Combined	171.4	6.6	49.8	149.1	22.52	4.05	6.62	4379

Table F.9: Results of Particle Size Analyses for Plant No. 9

Sample Description		Results of Particle Size Analyses							
Sample No.	Type Sample	Mean Particle Size, μm	D_{10}, μm	D_{30}, μm	D_{60}, μm	C_u	% Clay	FM	Specific Surface Area, cm^2/ml
9	Baghouse	36.0	2.3	10.6	30.8	13.37	8.60	4.68	9406
9	Cyclone	224.4	34.7	95.9	195.1	5.63	2.46	7.32	2568
9	Combined	203.3	7.5	54.8	156.5	20.90	3.98	6.70	4231
10	Baghouse	38.9	2.3	10.9	32.7	14.28	8.67	4.76	9348
10	Cyclone	224.5	42.0	98.8	195.6	4.66	2.02	7.41	2189
10	Combined	172.6	8.3	51.7	146.6	17.73	3.64	6.68	4023
11	Baghouse	41.69	2.5	12.3	36.0	14.33	7.94	4.92	8686
11	Cyclone	233.0	38.8	97.6	195.0	5.03	2.14	7.37	2301
11	Combined	172.3	5.9	43.2	140.4	23.96	4.37	6.52	4691
12	Baghouse	36.4	2.2	9.6	30.2	13.92	9.14	4.64	9847
12	Cyclone	224.1	47.6	103.5	196.5	4.13	1.66	7.48	1882
12	Combined	127.5	4.3	27.8	107.5	24.86	5.08	6.16	5559
13	Baghouse	32.4	2.0	8.6	26.7	13.08	9.81	4.45	1052
13	Cyclone	223.3	44.4	95.3	186.6	4.21	1.73	7.44	1959
13	Combined	172.6	8.1	53.6	142.7	17.55	3.59	6.69	3994
14	Baghouse	38.6	2.3	10.4	32.4	14.14	8.65	4.74	9401
14	Cyclone	232.8	44.9	96.6	187.2	4.17	1.65	7.45	1900
14	Combined	186.1	12.0	66.8	157.2	13.06	2.97	6.92	3349
15	Baghouse	60.1	2.4	11.3	39.1	16.08	8.11	5.02	8795
15	Cyclone	228.5	47.2	111.0	208.3	4.41	1.92	7.47	2073
15	Combined	180.6	6.5	57.9	170.7	26.38	3.98	6.69	4295
16	Baghouse	38.1	2.3	10.3	31.3	13.66	8.63	4.70	9425
16	Cyclone	196.5	32.8	89.6	175.9	5.36	2.53	7.28	2666
16	Combined	144.7	5.9	43.4	135.0	22.80	4.28	6.52	4643

Table F.9: Results of Particle Size Analyses for Plant No. 9

Sample Description		Results of Particle Size Analyses							
Sample No.	Type Sample	Mean Particle Size, μm	D_{10}, μm	D_{30}, μm	D_{60}, μm	C_u	% Clay	FM	Specific Surface Area, cm^2/ml
17	Baghouse	126.1	2.6	13.0	49.6	19.37	7.75	5.28	8261
17	Cyclone	215.8	44.9	102.8	198.6	4.43	1.93	7.44	2106
17	Combined	192.2	11.2	75.4	178.2	15.85	3.19	6.96	3461
18	Baghouse	38.6	2.1	8.9	30.1	14.68	9.71	4.61	10265
18	Cyclone	270.3	60.1	126.9	234.7	3.90	1.40	7.60	1589
18	Combined	160.4	15.9	91.4	200.6	12.64	2.71	7.13	2961
19	Baghouse	47.9	2.3	10.4	34.7	15.20	8.68	4.85	9334
19	Cyclone	213.5	43.0	99.7	190.2	4.43	1.94	7.42	2140
19	Combined	167.8	9.6	64.7	156.8	16.40	3.40	6.85	3722
20	Baghouse	112.7	3.4	20.6	93.3	27.86	6.15	5.88	6564
20	Cyclone	216.3	28.7	89.7	191.0	6.66	2.69	7.24	2809
20	Combined	159.7	5.0	40.2	145.5	28.98	4.69	6.45	4992
21	Baghouse	29.6	2.0	7.7	23.7	12.0	10.15	4.29	10942
21	Cyclone	226.1	16.9	77.5	189.0	11.20	2.90	6.26	3102
21	Combined	149.1	4.7	30.3	125.1	26.67	4.75	7.07	5236

Table F.10: Results of Particle Size Analyses for Plant No. 10

Sample Description		Results of Particle Size Analyses							
Sample No.	Type Sample	Mean Particle Size, μm	D_{10}, μm	D_{30}, μm	D_{60}, μm	C_u	% Clay	FM	Specific Surface Area, cm^2/ml
1	Baghouse	31.2	1.9	7.6	23.9	12.80	10.82	4.26	11353
2	Baghouse	32.3	1.9	7.8	24.8	13.28	10.69	4.31	11200
3	Baghouse	28.2	1.8	7.5	23.6	12.80	10.98	4.21	11498
4	Baghouse	33.0	1.9	7.9	25.1	13.25	10.67	4.33	11160
5	Baghouse	28.1	1.9	7.5	23.5	12.71	10.96	4.20	11488
6	Baghouse	33.8	1.9	8.0	25.4	13.36	10.62	4.35	11102
7	Baghouse	20.4	1.7	5.6	16.9	20.4	12.07	3.75	12911
8	Baghouse	32.3	2.0	8.8	32.3	12.67	9.82	4.38	10526
9	Baghouse	29.0	2.0	8.4	24.6	12.49	10.19	4.29	10860
10	Baghouse	33.6	2.0	8.6	25.5	12.75	9.99	4.37	10654
11	Baghouse	32.0	2.0	8.5	25.3	12.76	10.13	4.35	10769
12	Baghouse	26.6	1.9	7.9	23.2	12.09	10.47	4.19	11172
13	Baghouse	22.3	1.8	6.3	18.6	10.27	11.32	3.89	12210
14	Baghouse	22.6	1.7	5.8	17.7	10.23	11.96	3.83	12724
15	Baghouse	21.2	1.7	5.4	16.5	9.91	12.59	3.73	13292
16	Baghouse	21.4	1.8	5.9	17.4	9.90	11.71	3.80	12603
17	Baghouse	20.4	1.7	5.6	16.9	9.80	12.07	3.75	12911
18	Baghouse	19.8	1.7	5.7	16.8	9.69	11.94	3.73	12849
19	Baghouse	24.2	1.7	5.6	17.9	10.59	12.34	3.84	12947
20	Baghouse	21.5	1.7	5.4	17.2	10.42	12.70	3.77	13267
21	Baghouse	20.6	1.7	5.4	17.2	10.41	12.68	3.76	13265
22	Baghouse	23.2	1.7	5.4	17.1	10.28	12.59	3.79	13202
23	Baghouse	29.6	1.7	5.9	19.6	11.37	12.04	3.92	12333
24	Baghouse	24.6	1.7	5.6	17.7	10.46	12.32	3.83	12956

Table F.11: Results of Particle Size Analyses for Plant No. 11

Sample Description		Results of Particle Size Analyses							
Sample No.	Type Sample	Mean Particle Size, μm	D_{10}, μm	D_{30}, μm	D_{60}, μm	C_u	% Clay	FM	Specific Surface Area, cm^2/ml
1	Baghouse	38.6	1.5	4.7	24.7	16.02	13.98	4.29	13595
2	Baghouse	13.6	1.2	2.9	9.6	8.35	21.35	3.08	19670
3	Baghouse	35.9	1.3	3.7	17.9	13.91	17.55	4.00	16175
4	Baghouse	29.5	1.2	3.4	14.8	12.02	18.75	3.77	17203
5	Baghouse	31.8	1.3	3.4	14.6	11.61	18.52	3.80	17040
6	Baghouse	28.8	1.2	3.2	13.0	10.75	19.46	3.67	17788
7	Baghouse	35.5	1.3	3.5	17.1	13.73	18.36	3.96	16728
8	Baghouse	30.4	1.2	3.4	15.2	12.23	18.60	3.79	17063
9	Baghouse	27.2	1.2	2.9	11.1	9.60	21.03	3.53	18970
10	Baghouse	33.7	1.2	3.4	15.5	12.74	19.04	3.88	17268
11	Baghouse	39.9	1.3	4.0	20.7	15.54	16.76	4.15	15511
12	Baghouse	41.2	1.3	4.0	22.4	16.98	16.89	4.20	15523
13	Baghouse	44.8	1.7	6.4	32.4	19.16	12.23	4.59	12022
14	Baghouse	33.1	1.3	3.5	13.6	10.31	17.65	3.79	16564
15	Baghouse	29.4	1.4	3.5	12.4	9.15	17.10	3.68	16424
16	Baghouse	26.5	1.2	2.9	9.7	8.23	20.79	3.42	19080
17	Baghouse	25.8	1.2	2.9	9.9	8.28	20.49	3.43	18859
18	Baghouse	25.2	1.2	2.8	9.1	7.92	21.64	3.35	19684
19	Baghouse	25.4	1.2	3.1	11.1	9.12	19.80	3.51	18273
20	Baghouse	11.8	1.1	2.6	8.1	7.25	22.87	2.90	20855
21	Baghouse	40.8	1.6	5.8	31.7	19.77	13.07	4.51	12626
22	Baghouse	40.1	1.5	4.6	29.6	20.34	14.96	4.37	14025
23	Baghouse	42.0	1.5	5.1	30.0	19.67	13.99	4.44	13335
24	Baghouse	37.4	1.4	4.1	21.9	15.61	15.88	4.16	14927

Table F.12: Results of Particle Size Analyses for Plant No. 12

Sample Description		Results of Particle Size Analyses							
Sample No.	Type Sample	Mean Particle Size, μm	D_{10}, μm	D_{30}, μm	D_{60}, μm	C_u	% Clay	FM	Specific Surface Area, cm^2/ml
1	Baghouse								
2	Baghouse								
3	Baghouse	104.0	3.7	20.6	82.6	22.61	5.67	5.86	6273
4	Baghouse	129.4	3.7	22.2	84.5	22.93	5.68	5.92	6199
5	Baghouse	125.9	4.3	27.6	102.2	23.88	5.15	6.14	5618
6	Baghouse	142.9	4.6	31.5	112.8	24.41	4.90	6.26	5327
7	Baghouse	139.2	5.0	35.5	121.3	24.11	4.68	6.36	5073
8	Baghouse	126.8	4.8	30.4	108.5	22.42	5.01	6.22	5440
9	Baghouse								
10	Baghouse								
11	Baghouse								
12	Baghouse								
13	Baghouse	123.1	3.6	20.5	79.6	22.43	5.86	5.84	6403
14	Baghouse	120.9	4.1	27.8	100.0	24.45	5.34	6.14	5751
15	Baghouse	124.3	4.3	28.2	99.7	23.25	5.17	6.15	5617
16	Baghouse								
17	Baghouse	126.3	4.9	33.7	111.7	22.66	4.76	6.31	5188
18	Baghouse								
19	Baghouse	114.8	4.5	30.2	102.8	23.10	5.11	6.20	5513
20	Baghouse	134.9	4.9	33.6	114.2	23.26	4.77	6.31	5178
21	Baghouse	129.9	4.9	33.9	113.9	23.29	4.82	6.31	5206

Table F.13: Results of Particle Size Analyses for Plant No. 13

Sample Description		Results of Particle Size Analyses							
Sample No.	Type Sample	Mean Particle Size, μm	D_{10}, μm	D_{30}, μm	D_{60}, μm	C_u	% Clay	FM	Specific Surface Area, cm^2/ml
1	Baghouse	43.5	2.8	13.1	37.4	13.25	6.97	4.97	7983
1	Combined	156.5	11.2	54.7	135.9	12.19	2.85	6.79	3403
2	Baghouse	43.8	3.0	13.9	39.3	13.32	6.71	5.03	7719
2	Combined	117.3	6.4	37.5	111.3	17.39	3.89	6.40	4492
3	Baghouse	45.2	2.9	14.5	40.3	13.89	6.92	5.21	7786
3	Combined	129.8	12.0	54.6	124.2	10.37	3.02	6.81	3494
4	Baghouse	48.5	3.1	16.5	46.0	14.85	6.63	5.24	7377
4	Combined	109.8	6.9	38.2	104.1	15.16	4.09	6.34	4571
5	Baghouse	47.7	3.0	15.9	44.5	14.78	6.77	5.25	7527
5	Combined	114.6	8.4	44.9	113.0	13.49	3.69	6.56	4151
6	Baghouse	38.8	2.6	11.8	33.6	13.11	7.69	4.69	8644
6	Combined	123.2	13.8	56.9	124.7	9.03	2.82	6.84	3294
7	Baghouse	46.7	2.9	15.1	43.6	14.89	6.88	5.25	7675
7	Combined	133.3	15.7	64.0	137.1	8.76	2.64	6.97	3076
8	Baghouse	56.2	3.0	15.1	42.7	14.41	6.80	5.20	7614
8	Combined	148.4	7.8	41.3	122.2	15.64	3.64	6.52	4172
9	Baghouse	39.4	2.6	11.9	34.5	13.41	7.67	4.89	8591
9	Combined	84.8	3.8	21.6	74.9	19.49	5.54	5.85	6163
10	Baghouse	45.8	2.9	14.1	40.6	13.91	6.84	5.13	7759
10	Combined	102.3	6.5	34.8	96.8	14.89	3.96	6.31	4592
11	Baghouse	36.5	2.6	11.7	32.5	12.49	7.57	4.83	8597
11	Combined	195.1	17.3	64.1	145.2	8.41	2.31	6.97	2812
12	Baghouse	42.2	2.8	13.3	36.8	13.14	7.08	5.05	8047
12	Combined	164.7	9.4	46.2	117.4	12.44	3.22	6.65	3790

Table F.13: Results of Particle Size Analyses for Plant No. 13

Sample Description		Results of Particle Size Analyses							
Sample No.	Type Sample	Mean Particle Size, μm	D_{10}, μm	D_{30}, μm	D_{60}, μm	C_u	% Clay	FM	Specific Surface Area, cm^2/ml
13	Baghouse	45.5	2.9	13.9	38.9	13.26	6.77	5.08	7759
13	Combined	102.1	6.5	34.5	97.7	14.94	3.83	6.34	4517
14	Baghouse	41.6	3.2	15.1	42.2	13.41	6.38	5.22	7383
14	Combined	108.5	6.7	34.5	100.2	15.07	3.91	6.35	4543
15	Baghouse	42.5	2.9	13.6	37.2	12.72	6.78	5.03	7821
15	Combined	116.2	8.0	42.0	117.2	14.57	3.70	6.50	4232
16	Baghouse	43.1	2.8	12.8	35.7	12.90	7.14	4.98	8142
16	Combined	164.7	6.3	35.5	115.3	18.17	3.88	6.37	4507
17	Baghouse	43.8	3.0	14.1	39.4	13.36	6.77	5.13	7739
17	Combined	154.8	8.1	42.4	123.0	15.21	3.55	6.53	4089
18	Baghouse	48.5	3.0	15.2	42.9	14.23	6.71	5.21	7558
18	Combined	113.5	5.5	31.2	93.9	17.05	4.43	6.22	5006
19	Baghouse	44.7	3.1	15.5	40.9	13.29	6.61	5.15	7500
19	Combined	232.7	18.9	70.7	160.9	8.54	2.36	7.05	2764
20	Baghouse	44.8	3.2	16.2	42.3	13.00	6.31	5.21	7238
20	Combined	132.1	9.2	42.6	114.0	12.46	3.37	6.57	3937
21	Baghouse	49.9	3.5	17.6	46.3	13.14	5.87	5.35	6807
21	Combined	114.7	9.6	44.7	113.9	11.85	3.27	6.60	3841
22	Baghouse	50.1	3.6	17.4	45.8	12.65	5.72	5.35	6723
22	Combined	116.6	9.5	43.7	112.9	11.94	3.28	6.58	3868
23	Baghouse	47.4	2.8	14.1	38.5	13.58	7.07	5.05	7931
23	Combined	107.3	7.5	39.2	106.2	14.12	3.72	6.26	4298
24	Baghouse	42.9	2.8	14.0	39.6	13.92	7.03	5.06	7917
24	Combined	128.1	11.4	54.9	132.6	11.59	2.98	6.78	3480

Table F.14: Results of Particle Size Analyses for Plant No. 14

Sample Description		Results of Particle Size Analyses							
Sample No.	Type Sample	Mean Particle Size, μm	D_{10}, μm	D_{30}, μm	D_{60}, μm	C_u	% Clay	FM	Specific Surface Area, cm^2/ml
1	Baghouse	60.2	3.6	16.3	47.1	13.15	5.56	5.38	6666
2	Baghouse								
3	Baghouse								
4	Baghouse	51.7	3.4	15.4	32.1	9.54	5.91	5.26	7010
5	Baghouse	49.3	3.2	14.6	41.2	12.73	6.07	5.18	7209
6	Baghouse	49.4	3.3	15.0	41.7	12.69	6.01	5.20	7135
7	Baghouse	48.8	3.3	14.9	40.8	12.26	5.92	5.18	7099
8	Baghouse								
9	Baghouse	75.1	4.7	27.4	69.6	14.96	5.13	5.97	5658
10	Baghouse	60.8	4.0	22.5	57.7	14.57	5.64	5.70	6263
11	Baghouse	68.5	4.2	24.3	63.0	15.8	5.47	5.82	6035
12	Baghouse	47.1	3.2	15.1	40.9	12.73	6.19	5.17	7255
13	Baghouse								
14	Baghouse	38.4	2.9	12.9	34.9	11.96	6.71	4.92	7892
15	Baghouse	50.2	3.4	15.6	42.1	12.40	5.89	5.24	6997
16	Baghouse	45.4	3.0	13.5	37.5	12.55	6.58	5.04	7693
17	Baghouse								
18	Baghouse	51.6	3.4	15.2	42.6	12.60	5.84	5.24	6996
19	Baghouse								
20	Baghouse								
21	Baghouse	56.9	3.7	16.6	46.3	12.38	5.33	5.38	6498
22	Baghouse								
23	Baghouse	56.0	3.9	16.9	33.9	8.70	5.11	5.38	6341
24	Baghouse	53.5	3.7	16.2	44.0	12.00	5.41	5.31	6617

Table F.15: Results of Particle Size Analyses for Plant No. 15

Sample Description		Results of Particle Size Analyses							
Sample No.	Type Sample	Mean Particle Size, µm	D_{10}, µm	D_{30}, µm	D_{60}, µm	C_u	% Clay	FM	Specific Surface Area, cm^2/ml
1	Baghouse	64.3	2.3	14.9	52.2	22.48	8.63	5.34	8656
2	Baghouse	70.5	2.5	18.1	59.6	23.47	8.01	5.54	8022
3	Baghouse	64.48	2.2	15.5	54.1	24.25	9.01	5.37	8847
4	Baghouse	68.8	2.3	15.9	57.7	25.43	8.83	5.44	8676
5	Baghouse	71.2	2.5	17.2	59.5	24.01	8.15	5.51	8157
6	Baghouse	69.3	2.5	17.1	58.1	23.19	8.06	5.49	8119
7	Baghouse	64.4	2.5	15.8	53.2	21.63	8.17	5.39	8303
8	Baghouse	66.2	3.1	17.1	52.6	17.26	6.67	5.46	7266
9	Baghouse	61.6	2.9	16.5	50.1	17.15	6.94	5.39	7503
10	Baghouse	62.5	3.0	17.4	51.8	17.43	6.88	5.44	7397
11	Baghouse	60.6	2.6	15.9	50.5	19.20	7.64	5.36	7989
12	Baghouse	60.4	2.5	14.7	49.7	19.72	7.91	5.31	8238
13	Baghouse	65.7	2.6	16.1	54.4	20.84	7.69	5.43	7971
14	Baghouse	69.7	3.1	20.3	60.5	19.58	6.72	5.64	7072
15	Baghouse	65.7	2.6	15.9	54.3	21.03	7.78	5.42	8041
16	Baghouse	69.1	2.7	17.2	57.6	21.49	7.53	5.50	7783
17	Baghouse	60.3	2.3	14.5	50.3	21.50	8.58	5.30	8669
18	Baghouse	63.4	2.5	16.4	53.0	21.21	8.09	5.40	8220
19	Baghouse								
20	Baghouse	57.2	2.5	15.0	48.2	19.42	8.12	5.28	8376
21	Baghouse	53.8	3.6	16.2	44.2	12.21	5.50	5.31	6671
22	Baghouse	62.6	2.9	17.7	52.6	18.08	7.01	5.46	7453
23	Baghouse	62.3	3.0	17.7	52.4	17.59	6.85	5.46	7352
24	Baghouse	62.8	2.7	17.5	52.9	19.37	7.45	5.45	7745

Table F.16: Results of Particle Size Analyses for Plant No. 16

Sample Description		Results of Particle Size Analyses							
Sample No.	Type Sample	Mean Particle Size, μm	D_{10}, μm	D_{30}, μm	D_{60}, μm	C_u	% Clay	FM	Specific Surface Area, cm^2/ml
1	Baghouse	26.7	2.9	10.8	25.0	8.55	6.46	4.44	8304
2	Baghouse	23.8	2.7	9.3	22.5	8.31	6.84	4.43	8850
3	Baghouse	17.2	2.0	6.4	17.7	9.04	10.30	3.77	11700
4	Baghouse	19.9	1.9	7.0	19.6	10.08	10.35	3.93	11484
5	Baghouse	19.7	1.9	6.7	19.5	10.29	10.69	3.90	11721
6	Baghouse								
7	Baghouse	21.9	2.2	8.2	21.9	10.06	9.08	4.11	10404
8	Baghouse	26.0	2.4	8.2	22.4	9.49	8.12	4.24	9750
9	Baghouse	20.6	2.0	7.4	20.8	10.37	9.98	4.00	11122
10	Baghouse	22.1	2.0	8.4	22.9	11.24	9.79	4.12	10758
11	Baghouse	26.2	2.2	8.8	23.7	11.03	9.25	4.27	10318
12	Baghouse	22.3	2.2	8.9	23.1	10.39	8.89	4.17	10137
13	Baghouse	25.5	2.1	8.6	23.8	11.20	9.34	4.28	10367
14	Baghouse	20.1	2.1	7.7	20.5	9.84	9.55	3.98	10856
15	Baghouse	25.4	2.2	8.6	23.0	10.54	9.05	4.23	10249
16	Baghouse								
17	Baghouse	27.4	2.6	9.2	23.8	9.33	7.44	4.35	9140
18	Baghouse	30.5	2.8	10.6	26.4	9.55	6.89	4.52	8510

No.	Sample	Particle Size, µm	µm	µm	µm		Clay		Surface Area, cm^2/ml
1	Baghouse	224.6	71.5	131.1	219.5	3.07	0.54	7.74	910
2	Baghouse	211.7	71.1	126.5	208.6	2.94	0.55	7.75	905
3	Baghouse	217.6	68.3	126.1	212.5	3.11	0.65	7.71	1009
4	Baghouse	250.5	75.5	145.2	248.8	3.30	0.49	7.76	823
5	Baghouse	247.0	81.8	143.2	239.0	2.93	0.31	7.81	662
6	Baghouse	241.5	88.8	147.7	236.1	2.66	0.20	7.85	563
7	Baghouse	229.9	77.9	138.1	226.0	2.90	0.56	7.75	898
8	Baghouse	141.3	4.5	35.8	122.9	27.08	4.03	6.32	4833
9	Baghouse	256.0	65.5	142.9	251.7	3.85	0.99	7.65	1281
10	Baghouse	168.7	16.4	73.6	167.1	10.20	1.66	7.07	2365
11	Baghouse	216.8	37.6	110.9	211.2	5.61	1.34	7.43	1754
12	Baghouse	189.4	18.3	91.4	187.7	10.25	1.97	7.19	2451
13	Baghouse	201.6	26.4	102.4	198.1	7.50	1.75	7.31	2169
14	Baghouse	213.1	43.9	113.6	206.1	4.70	1.35	7.48	1706
15	Baghouse	201.1	35.4	102.7	196.0	5.53	1.49	7.39	1894
16	Baghouse	211.2	52.4	110.7	201.9	3.85	0.69	7.60	1120
17	Baghouse	215.4	67.3	124.4	208.6	3.10	0.37	7.73	790
18	Baghouse	143.1	9.9	51.5	136.9	13.87	0.98	6.73	2169
19	Baghouse	224.8	59.2	133.1	225.6	3.81	1.03	7.78	1382
20	Baghouse	85.7	4.4	25.5	76.9	17.65	4.73	7.81	5506
21	Baghouse	97.4	5.5	30.7	89.2	16.26	3.90	7.43	4740
22	Baghouse	105.2	5.3	33.6	103.7	19.49	3.83	7.52	4644
23	Baghouse	247.5	78.6	142.6	243.3	3.10	0.37	7.71	720
24	Baghouse	240.3	83.1	144.3	237.1	2.85	0.35	7.65	689

No.	Sample	Particle Size, µm	µm	µm	µm		Clay		Surface Area, cm^2/ml
1	Baghouse	161.4	8.4	58.6	155.5	18.47	3.43	6.76	3835
2	Baghouse	143.3	7.8	48.1	133.2	17.12	3.50	6.63	4003
3	Baghouse	149.5	8.2	51.0	135.9	16.49	3.48	6.68	3942
4	Baghouse								
5	Baghouse	155.0	9.8	56.9	145.8	14.82	3.08	6.78	3575
6	Baghouse	141.8	8.8	50.0	132.4	15.08	3.25	6.68	3784
7	Baghouse								
8	Baghouse	139.6	6.5	42.2	129.2	19.91	3.86	6.51	4370
9	Baghouse	142.4	7.9	43.6	120.0	52.21	3.42	6.56	4009
10	Baghouse	129.6	6.7	40.4	115.7	17.32	3.56	6.47	4230
11	Baghouse	133.3	5.2	34.0	106.9	20.40	4.24	6.31	4853
12	Baghouse								
13	Baghouse	124.2	5.1	34.1	108.9	21.40	4.49	6.31	5003
14	Baghouse								
15	Baghouse	105.7	3.2	22.4	97.2	30.46	6.47	5.95	6701
16	Baghouse	136.5	5.1	37.0	121.8	23.93	4.65	6.38	5021
17	Baghouse	110.2	3.7	26.5	96.8	26.02	5.71	6.07	6052
18	Baghouse	85.7	4.0	21.4	71.2	17.93	5.20	5.82	5975
19	Baghouse	119.5	3.4	24.1	86.1	25.24	6.16	5.95	6456
20	Baghouse	105.8	3.9	27.3	95.8	24.44	5.51	6.09	5896
21	Baghouse	103.3	3.3	23.0	83.4	24.96	6.21	5.91	6545
22	Baghouse	105.8	3.9	27.3	95.8	24.43	5.51	6.09	5896

Appendix G: Results of Modified Rigden's Void Test for All Plants

Table G.1: Results of Modified Rigden's Voids and Specific Gravity Testing for Plant No. 1

Sample Description		Results of Testing	
Sample No.	Type Sample	% Voids in Compacted Dust	Specific Gravity
1	Baghouse	47.4	2.825
1	Combined	44.3	2.803
2	Baghouse	49.7	2.850
2	Combined	44.0	2.839
3	Baghouse	49.7	
3	Combined	56.0	2.827
4	Baghouse	54.5	2.902
4	Combined	48.8	2.870
5	Baghouse	54.1	2.750
5	Combined	50.5	2.868
6	Baghouse	55.5	2.789
6	Combined	49.5	2.858
7	Baghouse	55.4	2.830
7	Combined	49.7	2.862
8	Baghouse		
8	Combined		
9	Baghouse	50.4	
9	Combined		
10	Baghouse		
10	Combined		
11	Baghouse	55.6	
11	Combined		
12	Baghouse		
12	Combined		
13	Baghouse	51.1	

Table G.1: Results of Modified Rigden's Voids and Specific Gravity Testing for Plant No. 1			
Sample Description		Results of Testing	
Sample No.	Type Sample	% Voids in Compacted Dust	Specific Gravity
13	Combined		
14	Baghouse		
14	Combined		
15	Baghouse	51.5	
15	Combined		
16	Baghouse	47.5	
16	Combined		
17	Baghouse	50.1	
17	Combined		
18	Baghouse	47.6	
18	Combined		
19	Baghouse	49.8	
19	Combined		
20	Baghouse	47.8	
20	Combined		
21	Baghouse	49.9	
21	Combined		
22	Baghouse	50.0	
22	Combined		
23	Baghouse	51.0	
23	Combined		

Table G.2: Results of Modified Rigden's Voids and Specific Gravity Testing for Plant No. 2

Sample Description		Results of Testing	
Sample No.	Type Sample	% Voids in Compacted Dust	Specific Gravity
1	Baghouse	52.6	
1	Combined	42.4	
2	Baghouse	54.2	
2	Combined	44.7	
3	Baghouse	53.9	
3	Combined	46.4	
4	Baghouse	53.8	
4	Combined	47.6	
5	Baghouse	54.3	
5	Combined	45.8	
6	Baghouse	52.8	2.717
6	Combined	47.1	
7	Baghouse	54.7	
7	Combined	48.0	
8	Baghouse	55.3	
8	Combined	46.9	
9	Baghouse	55.6	
9	Combined	48.3	
10	Baghouse	53.5	2.719
10	Combined	46.8	
11	Baghouse	54.8	
11	Combined	45.9	
12	Baghouse	52.0	2.669
12	Combined	45.8	
13	Baghouse	53.4	

Table G.2: Results of Modified Rigden's Voids and Specific Gravity Testing for Plant No. 2

Sample Description		Results of Testing	
Sample No.	Type Sample	% Voids in Compacted Dust	Specific Gravity
13	Combined	47.4	
14	Baghouse	55.6	
14	Combined		2.770
15	Baghouse	55.9	
15	Combined	51.6	2.840
16	Baghouse	57.7	
16	Combined	47.5	
17	Baghouse	54.0	
17	Combined	46.9	
18	Baghouse	54.0	
18	Combined	50.0	
19	Baghouse	53.3	
19	Combined	43.5	
20	Baghouse	56.9	
20	Combined	47.1	
21	Baghouse	54.9	
21	Combined	47.2	
22	Baghouse	59.0	
22	Combined	52.1	
23	Baghouse	51.1	
23	Combined	42.8	
24	Baghouse	51.9	
24	Combined	45.1	

Table G.3: Results of Modified Rigden's Voids and Specific Gravity Testing for Plant No. 3			
Sample Description		Results of Testing	
Sample No.	Type Sample	% Voids in Compacted Dust	Specific Gravity
1	Baghouse	50.6	
2	Baghouse	48.0	
3	Baghouse	47.8	
4	Baghouse	50.6	
5	Baghouse	47.8	2.628
6	Baghouse	47.8	
7	Baghouse	46.8	
8	Baghouse	46.9	
9	Baghouse	50.4	
10	Baghouse	44.7	
11	Baghouse	45.7	2.79
12	Baghouse	47.1	2.83
13	Baghouse	47.5	
14	Baghouse	44.9	
15	Baghouse	48.0	
16	Baghouse	45.2	2.756
17	Baghouse	44.5	
18	Baghouse	45.4	2.80
19	Baghouse	48.9	
20	Baghouse	49.6	
21	Baghouse	47.4	
22	Baghouse	50.6	
23	Baghouse	49.3	
24	Baghouse	50.0	

Table G.4: Results of Modified Rigden's Voids and Specific Gravity Testing for Plant No. 4			
Sample Description		Results of Testing	
Sample No.	Type Sample	% Voids in Compacted Dust	Specific Gravity
1	Baghouse	52.5	2.756
2	Baghouse	48.0	
3	Baghouse	46.9	
4	Baghouse	50.5	
5	Baghouse	50.9	
6	Baghouse	50.3	
7	Baghouse	50.1	
8	Baghouse	50.2	
9	Baghouse	53.1	
10	Baghouse	53.2	2.787
11	Baghouse	53.12	
12	Baghouse	51.1	2.755
13	Baghouse	52.1	
14	Baghouse	50.9	
15	Baghouse	50.5	2.753
16	Baghouse	48.7	
17	Baghouse	46.6	2.791

Table G.5: Results of Modified Rigden's Voids and Specific Gravity Testing for Plant No. 5

Sample Description		Results of Testing	
Sample No.	Type Sample	% Voids in Compacted Dust	Specific Gravity
1	Baghouse	58.9	
1	Cyclone	50.3	
2	Baghouse	60.2	2.502
2	Cyclone	51.4	2.763
3	Baghouse	60.6	2.806
3	Cyclone	46.5	
4	Baghouse	61.0	2.767
4	Cyclone	45.3	
5	Baghouse	58.8	
5	Cyclone	49.5	
6	Baghouse	61.9	
6	Cyclone		
7	Baghouse	61.1	2.874
7	Cyclone	48.0	
8	Baghouse	60.3	
8	Cyclone	47.6	
9	Baghouse	63.9	
9	Cyclone	47.3	2.908
10	Baghouse	58.6	
10	Cyclone	47.7	
11	Baghouse	61.1	2.654
11	Cyclone	47.9	
12	Baghouse	63.3	
12	Cyclone	51.2	2.886
13	Baghouse	60.2	2.300

Table G.5: Results of Modified Rigden's Voids and Specific Gravity Testing for Plant No. 5			
Sample Description		Results of Testing	
Sample No.	Type Sample	% Voids in Compacted Dust	Specific Gravity
13	Cyclone	62.3	
14	Baghouse	60.4	2.731
14	Cyclone	45.7	
15	Baghouse	59.2	
15	Cyclone	49.6	
16	Baghouse	56.8	
16	Cyclone	43.5	
17	Baghouse	57.0	2.715
17	Cyclone	46.8	2.906
18	Baghouse	56.2	
18	Cyclone	46.4	
19	Baghouse	60.2	
19	Cyclone	49.1	
20	Baghouse	61.4	
20	Cyclone	48.1	
21	Baghouse	55.9	2.741
21	Cyclone	49.3	
22	Baghouse		
22	Cyclone	48.7	2.835
23	Baghouse	64.1	
23	Cyclone	46.3	
24	Baghouse	62.7	
24	Cyclone	46.9	

Table G.6: Results of Modified Rigden's Voids and Specific Gravity Testing for Plant No. 6

Sample Description		Results of Testing	
Sample No.	Type Sample	% Voids in Compacted Dust	Specific Gravity
1	Baghouse	53.8	
2	Baghouse	58.3	
3	Baghouse	54.7	
4	Baghouse	54.3	
5	Baghouse	54.8	
6	Baghouse	55.1	
7	Baghouse	56.5	
8	Baghouse	55.7	
9	Baghouse	58.6	
10	Baghouse	57.2	
11	Baghouse	55.3	
12	Baghouse	56.1	
13	Baghouse	52.2	
14	Baghouse	51.9	
15	Baghouse	52.6	
16	Baghouse	52.6	2.800
17	Baghouse	50.2	
18	Baghouse	48.9	
19	Baghouse	54.0	2.658
20	Baghouse	48.3	
21	Baghouse	48.6	
22	Baghouse	47.4	
23	Baghouse	47.7	
24	Baghouse	48.2	

Table G.7: Results of Modified Rigden's Voids and Specific Gravity Testing for Plant No. 7			
Sample Description		Results of Testing	
Sample No.	Type Sample	% Voids in Compacted Dust	Specific Gravity
1	Baghouse	41.6	
2	Baghouse	40.4	
3	Baghouse	44.5	
4	Baghouse	44.8	
5	Baghouse	41.8	
6	Baghouse	42.1	
7	Baghouse	44.6	
8	Baghouse	45.6	
9	Baghouse	45.2	
10	Baghouse	43.8	
11	Baghouse	44.2	
12	Baghouse	43.7	
13	Baghouse	45.8	2.726
14	Baghouse	46.2	
15	Baghouse	40.7	
16	Baghouse	44.1	
17	Baghouse	45.9	
18	Baghouse	42.9	2.658
19	Baghouse	62.0	
20	Baghouse	44.0	
21	Baghouse	45.5	2.714
22	Baghouse		
23	Baghouse		
24	Baghouse		

Table G.8: Results of Modified Rigden's Voids and Specific Gravity Testing for Plant No. 8

Sample Description		Results of Testing	
Sample No.	Type Sample	% Voids in Compacted Dust	Specific Gravity
1	Baghouse		
2	Baghouse	47.9	
3	Baghouse		2.590
4	Baghouse	49.8	2.688
5	Baghouse	48.8	
6	Baghouse	52.1	
7	Baghouse	49.7	2.720
8	Baghouse	50.3	
9	Baghouse		
10	Baghouse	54.3	
11	Baghouse	53.6	
12	Baghouse	55.6	
13	Baghouse	48.0	
14	Baghouse	47.8	
15	Baghouse	51.2	
16	Baghouse	48.5	
17	Baghouse	46.5	
18	Baghouse	50.6	2.652
19	Baghouse	54.9	
20	Baghouse	53.4	
21	Baghouse	50.8	2.772
22	Baghouse	44.4	
23	Baghouse	44.9	
24	Baghouse	46.8	

Table G.9: Results of Modified Rigden's Voids and Specific Gravity Testing for Plant No. 9			
Sample Description		Results of Testing	
Sample No.	Type Sample	% Voids in Compacted Dust	Specific Gravity
1	Baghouse	47.4	
1	Cyclone	44.2	
1	Combined	43.8	
2	Baghouse	43.7	
2	Cyclone	43.0	
2	Combined	44.3	2.634
3	Baghouse	42.1	
3	Cyclone	44.3	
3	Combined	38.2	
4	Baghouse	45.8	
4	Cyclone	44.1	
4	Combined	42.5	
5	Baghouse	43.1	
5	Cyclone	43.7	2.655
5	Combined	39.2	
6	Baghouse	44.3	
6	Cyclone	45.0	
6	Combined	41.3	
7	Baghouse	43.3	
7	Cyclone	43.6	
7	Combined	41.1	
8	Baghouse	44.1	
8	Cyclone	44.9	
8	Combined	38.4	
9	Baghouse	45.6	

Table G.9: Results of Modified Rigden's Voids and Specific Gravity Testing for Plant No. 9

Sample Description		Results of Testing	
Sample No.	Type Sample	% Voids in Compacted Dust	Specific Gravity
9	Cyclone	44.5	
9	Combined	41.2	
10	Baghouse	40.5	
10	Cyclone	45.1	
10	Combined	40.5	2.663
11	Baghouse	43.8	
11	Cyclone	42.8	
11	Combined	42.0	
12	Baghouse	39.2	
12	Cyclone	44.9	
12	Combined	43.1	
13	Baghouse	41.8	
13	Cyclone	44.9	
13	Combined	41.9	
14	Baghouse	40.5	2.665
14	Cyclone	42.9	
14	Combined	38.8	
15	Baghouse	46.1	
15	Cyclone	41.9	
15	Combined	41.3	
16	Baghouse	43.5	
16	Cyclone	43.9	
16	Combined	40.0	2.659
17	Baghouse	40.0	
17	Cyclone	43.8	2.686

Table G.9: Results of Modified Rigden's Voids and Specific Gravity Testing for Plant No. 9

Sample Description		Results of Testing	
Sample No.	Type Sample	% Voids in Compacted Dust	Specific Gravity
17	Combined	39.7	
18	Baghouse	42.1	
18	Cyclone	42.6	
18	Combined	38.8	
19	Baghouse	40.5	
19	Cyclone	45.0	
19	Combined	38.7	
20	Baghouse	40.7	
20	Cyclone	45.3	
20	Combined	39.2	2.610
21	Baghouse	45.2	2.583
21	Cyclone	43.8	
21	Combined	43.2	

Table G.10: Results of Modified Rigden's Voids and Specific Gravity Testing for Plant No. 10			
Sample Description		Results of Testing	
Sample No.	Type Sample	% Voids in Compacted Dust	Specific Gravity
1	Baghouse	49.7	
2	Baghouse	50.8	
3	Baghouse	46.4	
4	Baghouse	47.8	
5	Baghouse	46.5	
6	Baghouse	48.1	
7	Baghouse		
8	Baghouse	48.6	2.886
9	Baghouse	47.1	
10	Baghouse	52.4	
11	Baghouse	47.7	2.769
12	Baghouse	48.8	2.776
13	Baghouse	52.0	
14	Baghouse	49.2	
15	Baghouse	47.2	
16	Baghouse	46.5	
17	Baghouse	46.9	
18	Baghouse	46.3	
19	Baghouse	49.1	
20	Baghouse	47.1	
21	Baghouse	45.3	2.815
22	Baghouse	44.4	
23	Baghouse	47.8	
24	Baghouse	46.3	2.777

Table G.11: Results of Modified Rigden's Voids and Specific Gravity Testing for Plant No. 11

Sample Description		Results of Testing	
Sample No.	Type Sample	% Voids in Compacted Dust	Specific Gravity
1	Baghouse	45.9	
2	Baghouse	43.6	
3	Baghouse	52.7	
4	Baghouse	51.5	
5	Baghouse	52.0	
6	Baghouse	52.8	
7	Baghouse	50.5	
8	Baghouse	50.8	
9	Baghouse	52.5	
10	Baghouse	52.4	
11	Baghouse	55.3	
12	Baghouse	49.9	
13	Baghouse	47.3	
14	Baghouse	52.0	
15	Baghouse	51.8	
16	Baghouse	58.8	
17	Baghouse	53.4	
18	Baghouse	58.5	
19	Baghouse	53.3	
20	Baghouse	49.7	
21	Baghouse	47.0	
22	Baghouse	50.3	
23	Baghouse	49.4	
24	Baghouse	51.1	

Table G.12: Results of Modified Rigden's Voids and Specific Gravity Testing for Plant No. 12

Sample Description		Results of Testing	
Sample No.	Type Sample	% Voids in Compacted Dust	Specific Gravity
1	Baghouse		
2	Baghouse	42.4	
3	Baghouse		
4	Baghouse	43.0	2.688
5	Baghouse	42.7	
6	Baghouse	45.4	
7	Baghouse	44.3	2.720
8	Baghouse	41.4	2.666
9	Baghouse	41.0	
10	Baghouse	41.9	
11	Baghouse	43.3	
12	Baghouse	42.2	
13	Baghouse	43.3	2.711
14	Baghouse	44.1	2.745
15	Baghouse	44.6	
16	Baghouse		
17	Baghouse	43.5	
18	Baghouse		
19	Baghouse	44.9	
20	Baghouse	42.9	
21	Baghouse	45.3	
22	Baghouse	43.3	
23	Baghouse	39.3	
24	Baghouse	39.4	

Table G.13: Results of Modified Rigden's Voids and Specific Gravity Testing for Plant No. 13			
Sample Description		Results of Testing	
Sample No.	Type Sample	% Voids in Compacted Dust	Specific Gravity
1	Baghouse	43.4	
1	Combined	41.0	
2	Baghouse	44.2	
2	Combined	40.0	
3	Baghouse	47.4	
3	Combined	43.8	
4	Baghouse	45.4	
4	Combined	42.6	
5	Baghouse	44.8	
5	Combined	42.3	
6	Baghouse	43.9	
6	Combined	44.5	
7	Baghouse	45.0	
7	Combined	44.2	
8	Baghouse	45.2	
8	Combined	42.8	
9	Baghouse	44.5	
9	Combined		
10	Baghouse	46.6	
10	Combined	42.6	
11	Baghouse	45.0	
11	Combined	52.5	
12	Baghouse	46.0	
12	Combined	48.1	
13	Baghouse	44.2	

Table G.13: Results of Modified Rigden's Voids and Specific Gravity Testing for Plant No. 13

Sample Description		Results of Testing	
Sample No.	Type Sample	% Voids in Compacted Dust	Specific Gravity
13	Combined	43.2	
14	Baghouse	45.6	
14	Combined	43.0	2.733
15	Baghouse	44.8	
15	Combined	42.4	
16	Baghouse	43.1	
16	Combined	41.1	
17	Baghouse	45.6	
17	Combined	43.6	
18	Baghouse	43.0	
18	Combined	43.8	
19	Baghouse	45.5	2.703
19	Combined	43.9	
20	Baghouse	45.3	
20	Combined	43.4	
21	Baghouse	44.6	2.702
21	Combined	44.8	
22	Baghouse	44.7	
22	Combined	41.9	
23	Baghouse	45.9	
23	Combined	43.1	
24	Baghouse	43.8	
24	Combined	40.0	

Table G.14: Results of Modified Rigden's Voids and Specific Gravity Testing for Plant No. 14

Sample Description		Results of Testing	
Sample No.	Type Sample	% Voids in Compacted Dust	Specific Gravity
1	Baghouse	48.2	
2	Baghouse		
3	Baghouse		
4	Baghouse	48.4	
5	Baghouse	49.5	2.628
6	Baghouse		
7	Baghouse	45.9	
8	Baghouse		
9	Baghouse	48.9	
10	Baghouse	47.5	
11	Baghouse	49.9	
12	Baghouse	45.0	2.721
13	Baghouse	49.4	
14	Baghouse	45.6	
15	Baghouse	43.8	2.685
16	Baghouse	45.3	
17	Baghouse	48.5	
18	Baghouse	50.2	
19	Baghouse		
20	Baghouse		
21	Baghouse	45.9	
22	Baghouse		
23	Baghouse	43.8	2.774
24	Baghouse	48.2	2.748

Table G.15: Results of Modified Rigden's Voids and Specific Gravity Testing for Plant No. 15

Sample Description		Results of Testing	
Sample No.	Type Sample	% Voids in Compacted Dust	Specific Gravity
1	Baghouse	51.5	2.779
2	Baghouse	51.7	
3	Baghouse	53.8	
4	Baghouse	50.7	
5	Baghouse	51.9	2.664
6	Baghouse	51.8	
7	Baghouse	50.1	
8	Baghouse	47.7	
9	Baghouse	51.1	
10	Baghouse	46.7	2.759
11	Baghouse	55.4	2.754
12	Baghouse	52.5	
13	Baghouse	52.9	
14	Baghouse	55.3	
15	Baghouse	52.9	
16	Baghouse	50.1	
17	Baghouse		2.763
18	Baghouse	51.9	
19	Baghouse		
20	Baghouse	52.2	
21	Baghouse	49.4	
22	Baghouse	53.4	
23	Baghouse	56.2	
24	Baghouse	52.3	

Table G.16: Results of Modified Rigden's Voids and Specific Gravity Testing for Plant No. 16

Sample Description		Results of Testing	
Sample No.	Type Sample	% Voids in Compacted Dust	Specific Gravity
1	Baghouse	56.3	2.824
2	Baghouse	57.4	
3	Baghouse	55.9	
4	Baghouse	55.0	
5	Baghouse	56.7	2.628
6	Baghouse		
7	Baghouse	54.3	
8	Baghouse	55.8	
9	Baghouse	56.6	
10	Baghouse	56.6	2.829
11	Baghouse	56.1	2.738
12	Baghouse	58.4	
13	Baghouse	56.8	
14	Baghouse	56.4	
15	Baghouse	58.2	
16	Baghouse		
17	Baghouse	56.7	
18	Baghouse	57.2	2.868

Table G.17: Results of Modified Rigden's Voids and Specific Gravity Testing for Plant No. 17

Sample Description		Results of Testing	
Sample No.	Type Sample	% Voids in Compacted Dust	Specific Gravity
1	Baghouse	51.4	
2	Baghouse	51.0	
3	Baghouse	58.3	
4	Baghouse	52.4	
5	Baghouse	50.2	2.628
6	Baghouse	50.0	
7	Baghouse	49.8	
8	Baghouse	55.0	
9	Baghouse	52.5	
10	Baghouse	53.7	
11	Baghouse	53.1	
12	Baghouse	51.4	
13	Baghouse	60.7	
14	Baghouse	53.8	2.700
15	Baghouse	54.2	
16	Baghouse	52.2	
17	Baghouse	55.7	
18	Baghouse	50.1	
19	Baghouse	46.4	
20	Baghouse	52.1	
21	Baghouse	50.6	
22	Baghouse	51.5	
23	Baghouse		
24	Baghouse	51.8	

Table G.18: Results of Modified Rigden's Voids and Specific Gravity Testing for Plant No. 18

Sample Description		Results of Testing	
Sample No.	Type Sample	% Voids in Compacted Dust	Specific Gravity
1	Baghouse	46.6	
2	Baghouse	46.1	2.774
3	Baghouse	47.4	
4	Baghouse		
5	Baghouse	48.5	
6	Baghouse	50.7	
7	Baghouse		
8	Baghouse	48.9	
9	Baghouse	47.7	
10	Baghouse	48.7	
11	Baghouse	46.7	
12	Baghouse		
13	Baghouse	50.7	2.785
14	Baghouse		
15	Baghouse	49.8	
16	Baghouse	49.6	
17	Baghouse	52.9	
18	Baghouse	49.1	
19	Baghouse	47.4	
20	Baghouse	47.1	2.664
21	Baghouse		
22	Baghouse		

Appendix H: Results of Mortar Testing

Table H.1: Results of Laboratory Testing of Asphalt Binder/Baghouse Fines Mortars

Binder-Fine Combination	F/A Ratio	Original Mortar					TFOT Aged Material		PAV Aged Material			
		SP, °C	BV @ 135°C, cP	BV @ 175°C, cP	DSR @ 64 °C		DSR @ 64 °C		DSR @ 22 °C		BBR @ -18 °C	
					G*, kPa	δ	G*, kPa	δ	G*,kPa	δ	S, Mpa	m, slope
AC1F1	0.2	57.6	1567	296	3.350	84.2	6.374	80.2	8989	48.1	589	0.317
	0.3	61.9	3687	683	4.989	83.3	10.265	80.4	13419	47.5	879	0.305
	0.4	69.9	11172	1825	7.647	83.3	15.248	79.6	21438	45.4	1046	0.271
	0.5	82.1	42933	5800	13.544	81.8	21.073	78.9	25205	44.6	1291	0.282
AC2F1	0.2	56.7	1367	233	2.975	85.2	5.486	82.6	11782	41.4	835	0.272
	0.3	62.2	3258	642	4.323	85.5	8.074	82.9	8623	44.8	1116	0.259
	0.4	70.6	8833	1658	5.986	85.2	11.251	82.4	27693	39.7	1423	0.250
	0.5	80.0	31783	5133	7.470	84.9	12.554	82.4	23698	41.6	1687	0.254
AC1F2	0.2	52.8	1133	242	2.537	84.3	4.680	80.7	9065	46.4	540	0.325
	0.3	55.6	1950	358	3.577	84.1	7.244	79.9	13417	45.6	781	0.316
	0.4	60.0	3562	683	4.556	84.4	10.290	79.6	15724	45.1	1075	0.288
	0.5	66.7	7579	1571	6.390	83.7	15.495	78.5	26357	43.2	1302	0.276
AC2F2	0.2	55.6	875	200	2.456	85.1	4.970	81.8	9623	40.8	456	0.248
	0.3	58.9	1491	325	3.444	85.2	8.035	80.7	15798	37.2	717	0.251
	0.4	62.2	2875	582	4.489	85.3	8.821	81.1	15774	39.5	1198	0.235

Table H.1: Results of Laboratory Testing of Asphalt Binder/Baghouse Fines Mortars

Binder-Fine Combination	F/A Ratio	Original Mortar					TFOT Aged Material		PAV Aged Material			
		SP, °C	BV @ 135°C, cP	BV @ 175°C, cP	DSR @ 64 °C		DSR @ 64 °C		DSR @ 22 °C		BBR @ -18 °C	
					G*, kPa	δ	G*, kPa	δ	G*,kPa	δ	S, Mpa	m, slope
AC2F2	0.5	66.1	6233	1421	5.364	85.2	12.047	81.0	27846	38.5	1491	0.211
AC1F3	0.2	52.2	1200	237	2.432	83.9	5.044	80.5	8338.2	47.9	516	0.319
	0.3	57.8	2500	491	3.671	83.8						
	0.4	63.9	5525	939	5.196	84.1						
	0.5	69.4	17958	2697	6.503	83.7	13.491	79.7	19212	47.3	1223	0.272
AC2F3	0.2	53.9	1127	246	2.522	85.4	3.948	82.2	10962	41.3	694	0.266
	0.3	58.3	2058	391	3.370	85.6						
	0.4	64.4	5158	875	4.203	4.216						
	0.5	71.7	19617	2925	5.360	85.5	10.524	82.4	27412	40.4	1332	0.252
AC1F4	0.2	53.3	1092	241	2.573	84.4	5.998	79.2	8677	47.0	637	0.303
	0.3	55.6	2025	408	3.400	84.3						
	0.4	61.7	3896	672	4.663	84.2						
	0.5	68.3	8483	1866	5.967	83.5	11.369	79.6	17816	45.6	1097	0.261
AC2F4	0.2	55.6	896	246	2.518	84.7	5.801	80.9	12232	39.5	854	0.262
	0.3	58.9	1679	387	4.383	85.1						

Table H.1: Results of Laboratory Testing of Asphalt Binder/Baghouse Fines Mortars

Binder-Fine Combination	F/A Ratio	Original Mortar					TFOT Aged Material		PAV Aged Material			
		SP, °C	BV @ 135°C, cP	BV @ 175°C, cP	DSR @ 64 °C		DSR @ 64 °C		DSR @ 22 °C		BBR @ -18 °C	
					G*, kPa	δ	G*, kPa	δ	G*,kPa	δ	S, Mpa	m, slope
AC2F4	0.4	62.8	3525	946	4.527	84.9						
	0.5	71.7	8758	2367	6.175	84.8	13.803	80.4	24364	37.8	1204	0.233
AC1F5	0.2	58.9	2162	421	3.168	83.4	6.281	80.5	9077	49.0	677	0.334
	0.3	66.7	7907	1133	4.428	83.8	8.184	80.7	11120	49.8	887	0.268
	0.4	87.2	26383	3108	6.260	83.2	11.657	80.1	10125	50.3	1079	0.312
	0.5	117.8	195933	23267	7.750	83.2	13.920	80.0	12038	50.8	1155	0.255
AC2F5	0.2	60.0	2108	404	2.964	85.3	5.316	82.3	12209	42.2	817	0.232
	0.3	75.0	10654	1866	3.869	85.4	7.066	82.8	14188	43.6	1173	0.239
	0.4	105.6	73467	7775	5.402	84.7	7.713	83.1	16618	45.9	1381	0.247
	0.5	137.8	n/a	171567	7.471	83.5	7.936	83.6	13587	53.3	1730	0.250
AC1F6	0.2	55.6	1208	271	2.687	83.9						
	0.3	57.2	2341	521	3.441	84.1	7.277	79.9	12835	45.9	906	0.298
	0.4	61.7	5142	871	4.641	84.3	14.109	77.3	17342	44.8	1064	0.269
	0.5	73.9	12942	2082	6.453	83.3						
AC2F6	0.2	55.6	996	430	2.379	85.5						

Table H.1: Results of Laboratory Testing of Asphalt Binder/Baghouse Fines Mortars												
Binder-Fine Combination	F/A Ratio	Original Mortar					TFOT Aged Material		PAV Aged Material			
		SP, °C	BV @ 135°C, cP	BV @ 175°C, cP	DSR @ 64 °C		DSR @ 64 °C		DSR @ 22 °C		BBR @ -18 °C	
					G*, kPa	δ	G*, kPa	δ	G*,kPa	δ	S, Mpa	m, slope
AC2F6	0.3	61.1	2154	462	3.180	85.4	6.862	81.5	16279	39.7	1122	0.239
	0.4	66.1	5025	1033	4.489	85.1	10.445	81.0	19128	39.3	1469	0.235
	0.5	73.9	16663	2791	6.109	85.0						
AC1F7	0.2	56.7	979	254	2.646	85.4						
	0.3	62.2	2781	525	4.232	84.0	9.270	79.4	13016	47.1	955	0.286
	0.4	68.3	6137	1183	5.529	84.0	12.019	79.7	13030	49.2	1213	0.283
	0.5	78.9	16820	3250	6.786	84.8						
AC2F7	0.2	55.6	1316	258	2.656	84.0						
	0.3	61.7	2604	521	3.990	85.1	8.299	81.5	14109	42.3	1114	0.248
	0.4	65.0	5737	1391	5.320	85.2	10.457	81.8	15921	42.8	1413	0.235
	0.5	75.0	17280	3320	7.436	83.7						
AC1F8	0.2	52.7	912.5	212.5	2.643	83.6						
	0.3	55.6	1700	329	3.016	84.1	7.075	80.2	13502	46.2	863	0.299
	0.4	58.3	2900	587	4.373	83.9	9.627	79.9	18226	44.8	1128	0.283
	0.5	63.9	4071	904	5.617	86.4						

Table H.1: Results of Laboratory Testing of Asphalt Binder/Baghouse Fines Mortars

Binder-Fine Combination	F/A Ratio	Original Mortar					TFOT Aged Material		PAV Aged Material			
		SP, °C	BV @ 135°C, cP	BV @ 175°C, cP	DSR @ 64 °C		DSR @ 64 °C		DSR @ 22 °C		BBR @ -18 °C	
					G*, kPa	δ	G*, kPa	δ	G*,kPa	δ	S, Mpa	m, slope
AC2F8	0.2	51.7	808	221	2.357	87.0						
	0.3	57.8	1379	313	3.211	85.2	6.481	81.5	14364	40.8	1021	0.240
	0.4	61.1	2233	579	4.171	85.2	9.400	81.1	22466	39.1	1349	0.245
	0.5	61.7	4217	937	5.162	86.8						
AC1F9	0.2	51.1	912	208	2.538	84.4	6.310	78.5	6616	47.2	514	0.309
	0.3	56.1	1975	442	4.113	83.9	7.860	79.0	10299	46.2	757	0.284
	0.4	58.3	3750	692	5.307	83.7	11.730	78.3	14834	45.6	993	0.277
	0.5	64.4	10114	1595	6.559	83.2	13.438	78.3	24445	41.9	1046	0.254
AC2F9	0.2	51.7	829	188	2.015	85.6	4.852	81.4	11858	40.4	679	0.258
	0.3	55.6	1750	388	3.496	85.1	7.501	80.6	19695	37.8	989	0.243
	0.4	58.9	3746	708	4.537	84.8	10.723	80.6	21713	38.7	1312	0.224
	0.5	64.4	7591	1354	6.078	83.9	13.346	80.0	19306	39.6	1405	.241
AC1F10	0.2	53.3	1104	250	2.799	83.8						
	0.3	58.3	2529	516	3.871	84.1	9.183	78.8	11602	47.4	871	0.298
	0.4	66.7	5662	1237	5.418	84.1	14.415	78.2	11776	47.9	1205	0.279

Table H.1: Results of Laboratory Testing of Asphalt Binder/Baghouse Fines Mortars												
Binder-Fine Combination	F/A Ratio	Original Mortar					TFOT Aged Material		PAV Aged Material			
		SP, °C	BV @ 135°C, cP	BV @ 175°C, cP	DSR @ 64 °C		DSR @ 64 °C		DSR @ 22 °C		BBR @ -18 °C	
					G*, kPa	δ	G*, kPa	δ	G*,kPa	δ	S, Mpa	m, slope
AC1F10	0.5	75.6	16416	4016	6.884	83.3						
AC2F10	0.2	55.6	1137	292	2.585	85.0						
	0.3	60.6	2271	491	3.582	85.3	8.433	80.6	12870	42.9	1135	0.247
	0.4	67.2	5662	1371	4.602	85.4	12.276	80.8	14276	42.8	1490	0.223
	0.5	75.6	14467	3842	5.910	85.0						